



UNIVERSITEIT VAN PRETORIA  
UNIVERSITY OF PRETORIA  
YUNIBESITHI YA PRETORIA

**Isolation of antiplasmodial naphthylisoquinoline  
alkaloids from *Ancistrocladus sp.* through bioassay-  
guided fractionation**

by

**MIANDA MUTOMBO Sephora**

Submitted in partial fulfillment of the requirements for the degree

**MAGISTER SCIENTIAE**

In the Faculty of Natural & Agricultural Sciences

**UNIVERSITY OF PRETORIA**

**PRETORIA**

Supervisor: Prof. V. J. Maharaj

Co-supervisor: Prof. G. Bringmann

November 2019

# Declaration

I, **MIANDA MUTOMBO Sephora** declare that the thesis/dissertation, which I hereby submit for the degree MSc chemistry at the University of Pretoria, is my own work and has not previously been submitted by me for a degree at this or any other tertiary institution.

Signature: 

Date: 11 November 2019

## Acknowledgements

I would like to express my gratitude and appreciation to my supervisors Prof. V.J. Maharaj and Prof. G. Bringmann, from the University of Pretoria and University of Würzburg, respectively for their support, patience, time, ideas, and scientific contributions to the present work. Thank you very much for the opportunity you gave me to learn from your expertise.

This work would not have been a success without the funding from the BEBUC Scholarship System, as well as the fUNIKIN (Förderverein Uni Kinshasa e.V.) nonprofit organization and the National Research Foundation (NRF). I here express my appreciation for their financial support.

To Severin Muyisa, I present my gratitude for his scientific advice during the course of this work. I also thank Prof. K. Ndjoko for her scientific advice. I thank all the members of the Bioprospecting group (A. Thakur, B. Tembeni, B. Mzondo, N.K Khorommbi, L. Kruger, C. Ezeofor, F. Katele) in the Department of Chemistry at the University of Pretoria for the time we spent together, many fruitful discussions, and memorable moments. Special thanks to Dr. Mamoalosi Selepe for her help with NMR and LC-MS SPE-NMR and providing me with the necessary training on the use of the equipment. I thank Madelien Wooding for analysis of the samples on the UPLC QTOF MS. I thank Dr. Phanankosi Moyo for the training he provided me on the antiplasmodial bioassaying. Special thanks to Mr. Blaise Kimbadi Lombe from the University of Würzburg for collecting the plant samples, measuring ECD spectra, his help with structure elucidation, and for scientific advice.

I am thankful for the love, encouragement, and moral support from my father Mutombo, my mother Tshala, my brothers (JL. Tshimanga, N. Ilunga, S. Bakupa, L. Mutombo), sisters (A. Muadi, A. Nyakunoba, E. Tshala), and my best friend Eleuthere R. Lukelu.

A very special thanks to Mrs. Anna Weisensel for her words of encouragement and support. C. Nkanga, JC. Kabangu, N. Ngalula, H. Mbuyi, E. Mpoyi, E. Mbikayi, D. Kiliwa, and D. Dinanga ... thank you guys for the time we laughed together.

Above all, I thank the almighty God for life, health, and strength He gave me to bring this work to a completion.

## Summary

*Ancistrocladus* is the only genus in the Ancistrocladaceae family and together with the closely related Dioncophyllaceae, they produce naphthylisoquinoline (NIQ) alkaloids. This class of compounds exhibits a very interesting large spectrum of bioactivities. Some of these compounds have shown very promising antiplasmodial activity. Leaves of an as yet unidentified *Ancistrocladus* sp collected in the region of Bonsolerive (Northwestern part of DRC), were investigated for their antiplasmodial activity. They were air dried at room temperature and ground. The ground plant material was extracted sequentially with *n*-hexane, dichloromethane, ethyl acetate, methanol, and water. Five extracts were obtained and all, except for the *n*-hexane extract, were assayed for their antiplasmodial activity using the Malaria SYBR Green I based assay. The results of the antiplasmodial screening of extracts showed that the methanol extract was the most active one (100 % inhibition at 10 and 20 µg/mL) and was thus chosen for further research. UPLC QTOF MS was used to chemically profile the sequentially extracted material and to identify naphthylisoquinoline alkaloids in the extracts.

The methanol extract was fractionated using silica gel column chromatography to produce 18 fractions. TLC and UPLC QTOF MS were used to target fractions mainly containing naphthylisoquinoline alkaloids and based on this, five fractions were selected for screening against *Plasmodium falciparum* NF54 strains. They all exhibited good antiplasmodial activity (> 95 % inhibition at 5 and 10 µg/mL). One fraction was further fractionated using preparative HPLC and four sub-fractions collected. They were screened against *P. falciparum* NF54 strains. One sub-fraction showed an excellent activity with more than 82 % inhibition at 1 µg/mL.

Three compounds were isolated from the active fractions and one compound from a non-screened fraction using preparative HPLC and LC-MS-SPE-NMR. Through NMR and ECD, the structures of three compounds were fully elucidated as ealamine A (**43**), ancistrocladinium A (**44**) and ancistrocyclinone A (**45**). The structure of one compound was elucidated with only the relative configuration determined (compound **46**). The presence of ealamine A (**43**), which is a 7,8'-coupled hybrid-type NIQ (*R* configured at C-3 with oxygen function at C-6), in this plant material has a geo- and chemotaxonomic

importance. Such NIQs are mostly present in *Ancistrocladus* plants from the Northwestern Congo Basin.

The results of antiplasmodial screening of compounds revealed that ancistrocladinium A (**44**) and ealamine A (**43**) showed good activity ( $IC_{50} < 10 \mu M$ ) against the chloroquine-sensitive (NF54) and chloroquine-resistant (K1 and Indochina clones W2) strains with no cross-resistance towards drug resistant *P. falciparum* parasites (RI values  $< 1$ ). This study reports for the first time the activity of ancistrocladinium A and ealamine A against the W2 strain of *P. falciparum*. Ancistrocyclinone A and compound **46** showed no or only minimal antiplasmodial activity. The inhibitory potential of ancistrocladinium A (**44**) and ealamine A (**43**) were less effective than that of some NIQs previously isolated from other *Ancistrocladus* species. Further studies will be carried beyond the scope of this work to isolate and identify additional NIQs for the purpose of identification of the species (understanding the NIQs pattern of the species) and identification of more potent antiplasmodial NIQs.

# Table of contents

Declaration .....	ii
Acknowledgements .....	iii
Summary .....	iv
List of figures .....	ix
List of tables .....	xiii
Abbreviations.....	xiv
Supplementary data .....	xvii
Chapter 1 .....	1
General introduction .....	1
1.1 Natural products as a source of medicines .....	1
1.2 Background to malaria and the parasite life cycle .....	3
1.3 Plants used to treat malaria based on traditional knowledge .....	5
1.4 Natural products research in malaria therapy .....	7
1.5 Current approved treatments of malaria .....	12
1.6 Problem statement and justification .....	13
1.7 Goal and objectives .....	15
1.8 References .....	16
Chapter 2 .....	22
Isolation and structural elucidation of naphthylisoquinoline alkaloids from an as yet unidentified <i>Ancistrocladus</i> species .....	22
2.1 Background to Ancistrocladaceae .....	22
2.1.1 Geographic distribution and classification .....	22
2.1.2 Botany .....	23
2.1.3 Traditional uses of <i>Ancistrocladus</i> sp. ....	24
2.2 Naphthylisoquinoline alkaloids and their isolation and identification .....	25
2.2.1 Structural types and nomenclature .....	25
2.2.2 Extraction and purification of NIQs .....	27
2.2.3 Structure elucidation using NMR .....	28
2.2.4 Electronic circular dichroism (ECD) spectroscopy .....	28
2.2.5 Oxidative degradation .....	30
2.2.6 Biosynthesis .....	31
2.2.7 Naphthylisoquinoline alkaloids and antiplasmodial activity .....	33

2.3 Methodology .....	34
2.3.1 Plant material .....	34
2.3.2 Processing and extraction .....	35
2.3.3 Fractionation using silica gel column chromatography .....	37
2.3.4 HPLC purification and analysis .....	37
2.3.4.1 High-performance liquid chromatography (HPLC) .....	37
2.3.4.2 Hyphenated liquid chromatography - mass spectrometry - solid-phase extraction – nuclear magnetic resonance (LC-MS-SPE-NMR) .....	38
2.3.4.3 Chemical profiling using UPLC-QTOF-MS .....	40
2.3.4.4 NMR analysis .....	41
2.3.4.5 ECD measurements .....	41
2.3.5 Antiplasmodial screening .....	41
2.4 Results and discussion .....	42
2.4.1 Plant material .....	42
2.4.2 Extraction .....	42
2.4.3 Bioassaying of extracts .....	43
2.4.4 Ultra-performance liquid chromatography – quadrupole time-of-flight – mass spectrometry (UPLC-QTOF-MS) analysis of extracts .....	44
2.4.5 Fractionation and bioassaying of selected fractions .....	49
2.4.6 Isolation of compounds .....	53
2.4.6.1 Purification of Fraction 2 (F <sub>2</sub> ) .....	53
2.4.6.2 Purification of Fraction 5 (F <sub>5</sub> ) .....	57
2.4.6.3 Purification of Fraction 1 (F <sub>1</sub> ) .....	60
2.4.6.4 Purification of Fraction 6 (F <sub>6</sub> ) .....	61
2.4.6.5 Purification of Fraction 7 (F <sub>7</sub> ) .....	62
2.4.7 Structure elucidation of the pure NIQs .....	63
2.4.8 Antiplasmodial screening of compounds .....	81
2.5 Conclusion .....	83
2.6 References .....	85
Chapter 3 .....	94
Experimental section .....	94
3.1 Materials .....	94
3.2 Extraction process .....	95
3.3 UPLC-QTOF-MS analysis .....	96
3.4 Silica gel column and thin-layer-chromatography .....	97
3.5 Isolation of compounds using HPLC .....	97

3.6 Isolation of a compound using LC-MS-SPE-NMR .....	100
3.7 Antiplasmodial screening .....	100
3.8 Structure elucidation .....	102
3.8.1 Ealamine A (43) .....	102
3.8.2 Ancistrocladinium A (44) .....	103
3.8.3 Ancistrocyclinone A (45) .....	104
3.8.4 Compound 46 .....	105
3.9 References .....	106
Chapter 4 .....	107
General conclusion .....	107
Supplementary data .....	110



# List of figures

## Chapter 1

- Figure 1.1** Examples of compounds based on natural products used in modern medicine: morphine (1), aspirin (2), penicillin G (3), paclitaxel (4), dronabinol (5), and cannabidiol (6) ..... 3
- Figure 1.2** *Plasmodium* life cycle: parasite stages in human and mosquito *Anopheles*, Winzele, E.A. .... 5
- Figure 1.3** Structures of 3-acetoxy-5,7-dihydroxycarvotacetone (7), guaianolide (8), caesalminine A (9), fagoronine (10), acetylvismione D (11), ineupatorolide A (12), and 5',6'-dihydrousambarensine (13), few examples of identified antimalarial compounds from plants ..... 10
- Figure 1.4** Structures of quinine (14), chloroquine (15), primaquine (16), amodiaquine (17), and mefloquine (18) used in malaria treatment ..... 11
- Figure 1.5** Structures of artemisinin (19), artemether (20), arteether (21), and artesunate (22) ..... 12
- Figure 1.6** Map of malaria distribution around the world showing the urge burden of the disease carried by sub-Saharan Africa ..... 14

## Chapter 2

- Figure 2.1** Ancistrocladaceae sites in tropical Africa and in South and Southeast Asia ..... 23
- Figure 2.2** (A) Fully developed flower of *A. ikela* at anthesis; (B) Inflorescence of *A. congolensis*; (C) Leaves and inflorescences of *A. ikela* ..... 24
- Figure 2.3** Atom numbering in NIQs ..... 25
- Figure 2.4** Structures of naphthylisoquinoline alkaloids showing different coupling types: 6-O-methylancistectorine A<sub>3</sub> (23), ancistrotectorine C (24), ancistrolkokine G (25), ancistroheynine B (26), ancistrocongoline D (27), ancistroheynine A (28), dioncophyllinol B (29), ancisheynine (30), and shuangancistrotectorine A (31) ..... 26
- Figure 2.5** Ancistrolkokine A<sub>2</sub>, used here as an example to show the use of NOE interactions (red arrows) to determine relative configuration at the stereogenic centers (Me-1 and H-3) and at the axis (interactions between H<sub>eq</sub>-4 and H-7' and between H<sub>ax</sub>-4 and H-1') ..... 28
- Figure 2.6** Comparison of ECD spectra of ancistectorine A<sub>2</sub> (33a) and its atropo-diastereomer 5-*epi*-ancistectorine A<sub>2</sub> (33b), showing how their curves are opposite to each other; (B) Absolute configuration at the central axis of

	jozimine A <sub>2</sub> ( <b>34</b> ) assigned by comparison of its ECD spectrum (solid line, red) with that of shuangancistroretorine A ( <b>31</b> , see Figure 2.4) (dotted line, black); (C) Absolute configuration at the central axis of <b>31</b> assigned by comparison of its experimental ECD spectrum (solid line, black) with the curve calculated for <i>P,M,P</i> -configuration .....	29
<b>Figure 2.7</b>	Structures of ancistroretorine A <sub>2</sub> ( <b>33a</b> ), 5- <i>epi</i> -ancistroretorine A <sub>2</sub> ( <b>33b</b> ), shuangancistroretorine A ( <b>31</b> ) (the structure has been repeated for comparison purpose with jozimine A <sub>2</sub> ), and jozimine A <sub>2</sub> ( <b>34</b> ) .....	30
<b>Figure 2.8</b>	Scheme of ruthenium-mediated oxidative degradation of the isoquinoline moiety of NIQs and schematic chromatogram of the resulting amino acids after Mosher-type derivatization. (i) MeOH, SOCl <sub>2</sub> ; (ii) '(R)-MTPA-Cl', NEt <sub>3</sub> .....	31
<b>Figure 2.9</b>	Biosynthetic pathways to naphthylisoquinoline alkaloids with ancistrocladidine ( <b>35</b> ), ancistrocladine ( <b>36</b> ), and dioncophylline A ( <b>37</b> ) as examples .....	32
<b>Figure 2.10</b>	Structures of <i>N</i> -methylancistroretorine A <sub>1</sub> ( <b>38</b> ), dioncophylline C ( <b>39</b> ), dioncopeltine A ( <b>40</b> ), dioncophyllacine A ( <b>41</b> ), and ancistrobarterine A ( <b>42</b> ), some NIQ compounds with excellent antiplasmodial activities ...	34
<b>Figure 2.11</b>	Flow diagram for sequential extraction of leaf material of <i>Ancistrocladus</i> .....	36
<b>Figure 2.12</b>	Flow diagram for purification of the MeOH extract, the structures of the compounds are shown in Figure 2.13 .....	39
<b>Figure 2.13</b>	Structures of ealamine A ( <b>43</b> ), ancistrocladinium A ( <b>44</b> ), ancistrocyclinone A ( <b>45</b> ), and compound <b>46</b> .....	40
<b>Figure 2.14</b>	ESI positive-mode BPI chromatograms of leaves of <i>Ancistrocladus sp.</i> extracted sequentially with DCM, EtOAc, MeOH, and water .....	47
<b>Figure 2.15</b>	Structures of korupensamine E ( <b>47</b> ), korupensamine D ( <b>48</b> ), ancistrocladinium B ( <b>49</b> ), 6- <i>O</i> -methylhamatinine ( <b>50</b> ), ancistroretoriline A ( <b>51</b> ), and ancistrobertsonine C ( <b>52</b> ) .....	48
<b>Figure 2.16</b>	Selected section of the ESI positive-mode BPI chromatograms of five fractions (F <sub>2</sub> , F <sub>4</sub> , F <sub>5</sub> , F <sub>6</sub> , and F <sub>7</sub> ), which showed mainly the presence of NIQs .....	50
<b>Figure 2.17</b>	ESI positive-mode BPI chromatogram of F <sub>2</sub> . This fraction was resolved by HPLC-MS for isolation of compounds .....	54
<b>Figure 2.18</b>	ESI positive-mode BPI chromatograms of Fractions F <sub>2</sub> SF <sub>1</sub> , F <sub>2</sub> SF <sub>2</sub> , F <sub>2</sub> SF <sub>3</sub> , and F <sub>2</sub> SF <sub>4</sub> ; the part from 0 to 6 min has been removed from the chromatogram because there were no peaks .....	55
<b>Figure 2.19</b>	(A) LC-UV <sub>max</sub> plot SPE-NMR chromatogram; (B) ESI positive-mode BPI chromatogram of Subfraction F <sub>2</sub> SF <sub>1</sub> .....	57

<b>Figure 2.20</b>	HPLC-UV <sub>max</sub> plot chromatogram of Fraction 5 collected from silica gel column chromatography of MeOH extract. A total of twelve subfractions were collected .....	58
<b>Figure 2.21</b>	ESI positive-mode BPI chromatogram of Fraction F <sub>5</sub> SF <sub>5</sub> .....	59
<b>Figure 2.22</b>	LC-UV <sub>max</sub> plot chromatogram of Subfraction 5 from LC-MS-SPE-NMR .....	60
<b>Figure 2.23</b>	HPLC-UV <sub>max</sub> plot chromatogram of Fraction F <sub>1</sub> (AU = Absorbance Units) .....	60
<b>Figure 2.24</b>	HPLC-UV <sub>max</sub> chromatogram of Fraction F <sub>6</sub> .....	61
<b>Figure 2.25</b>	HPLC-UV <sub>max</sub> plot chromatogram of Fraction F <sub>7</sub> .....	62
<b>Figure 2.26</b>	(A) Selected HMBC correlations; (B) Selected NOE interactions showing the configuration at the axis in the compound <b>43</b> ; (C) Structure and absolute configuration of the isolated product <b>43</b> ; (D) ECD spectra of <b>43</b> in red and the reference, ealamine A, which had previously been isolated in Prof. G. Bringmann's laboratory in black showing that they were virtually identical .....	65
<b>Figure 2.27</b>	ESI positive-mode BPI chromatogram of compound <b>44</b> (ancistrocladinium A) isolated from Fractions F <sub>1</sub> , F <sub>5</sub> , and F <sub>6</sub> .....	68
<b>Figure 2.28</b>	(A) Selected HMBC correlations; (B) Structure of ancistrocladinium A ( <b>44</b> ) .....	69
<b>Figure 2.29</b>	Comparison of ECD spectra of isolated compound <b>44</b> and ancistrocladinium A (reference) previously isolated in Prof. G. Bringmann's laboratory. The two spectra were superimposable, which, in combination with the other spectral findings, confirmed that the two compounds were identical .....	70
<b>Figure 2.30</b>	(A) HPLC-UV <sub>max</sub> chromatogram of standard ancistrocladinium A; (B) HPLC-UV <sub>max</sub> chromatogram of compound <b>44</b> ; (C) HPLC-UV <sub>max</sub> chromatogram of mixture of compound <b>44</b> and ancistrocladinium A .....	71
<b>Figure 2.31</b>	DRC map showing collection sites of <i>Ancistrocladus</i> species, from which ealamine A (blue and red pentagon) and ancistrocladinium A (red pentagon) had been previously isolated. The green diamond shows the collection site of the plant material investigated in this study .....	73
<b>Figure 2.32</b>	ESI positive-mode BPI chromatogram of compound <b>45</b> isolated from Fraction 1 collected from silica gel column chromatography of the MeOH extract .....	74
<b>Figure 2.33</b>	Selected NOE (red arrows) and HMBC (blue arrows) correlations of ancistrocyclinone A ( <b>45</b> ) .....	75

<b>Figure 2.34</b>	Comparison of the ECD spectra of the isolated ancistrocyclinone A ( <b>45</b> ) in red and the one previously isolated in Prof. G. Bringmann's laboratory in black (Reference) .....	77
<b>Figure 2.35</b>	Structure of ancistrocyclinone A ( <b>45</b> ) .....	77
<b>Figure 2.36</b>	(A) Selected HMBC correlations; (B) Selected NOE interactions; (C) The two possible enantiomeric structures of compound <b>46/ent-46</b> ; (D) Selected NOE interactions in ancistrolikokine C <sub>2</sub> ( <b>47</b> ) .....	79

## List of tables

### Chapter 2

<b>Table 2.1</b>	<i>In vitro</i> activity of the four extracts against asexual NF54 <i>P. falciparum</i> parasites, tested at concentrations of 20 and 10 µg/mL, using the SYBR Green I assay. Data are from three independent biological replicates, performed in technical triplicates (n = 3) .....	43
<b>Table 2.2</b>	Comparison of the chemical profiles of the DCM, EtOAc, and MeOH extracts .....	48
<b>Table 2.3</b>	Summary of <i>m/z</i> values detected in the Fractions F <sub>2</sub> , F <sub>4</sub> , F <sub>5</sub> , F <sub>6</sub> , and F <sub>7</sub> and compared to the parent MeOH extract .....	52
<b>Table 2.4</b>	<i>In vitro</i> activity of the five fractions collected from column chromatography against asexual NF54 <i>P. falciparum</i> parasites at test concentrations of 10 and 5 µg/mL. Data were from three independent biological replicates, performed in technical triplicates (n = 3) .....	53
<b>Table 2.5</b>	<i>In vitro</i> activity of the four subfractions collected by HPLC-MS of Fraction 2 from column chromatography of the MeOH extract against asexual NF54 <i>P. falciparum</i> parasites, at test concentrations of 5 and 1 µg/mL. Data are from three independent biological replicates, performed in technical triplicates (n = 3) .....	56
<b>Table 2.6</b>	<sup>1</sup> H, <sup>13</sup> C NMR, HMBC, and COSY data of the isolated ealamine A ( <b>43</b> ) .....	66
<b>Table 2.7</b>	Comparison of <sup>1</sup> H and <sup>13</sup> C NMR data of ancistrocladinium A ( <b>44</b> ) in CD <sub>3</sub> OD and the published <sup>1</sup> H and <sup>13</sup> C data in CD <sub>3</sub> OD .....	71
<b>Table 2.8</b>	Comparison of the <sup>1</sup> H and <sup>13</sup> C NMR data of isolated ancistrocyclinone A ( <b>45</b> ) in CD <sub>3</sub> COCD <sub>3</sub> and <sup>1</sup> H and <sup>13</sup> C NMR literature data .....	75
<b>Table 2.9</b>	<sup>1</sup> H, <sup>13</sup> C NMR, HMBC, and NOESY data of compound <b>46</b> .....	80
<b>Table 2.10</b>	<i>In vitro</i> activity of three isolated compounds against asexual NF54 <i>P. falciparum</i> parasites, obtained at concentrations of 1 and 5 µg/mL. Data were from a single independent biological technical repeat, performed in technical triplicates, ± SD .....	81
<b>Table 2.11</b>	Dose-response results of ancistrocladinium A ( <b>44</b> ), ealamine A ( <b>43</b> ), and chloroquine, screened for the IC <sub>50</sub> values for their activities against asexual parasites using the SYBR Green I based assay. Results were representative of a single independent biological replicate, n = 1, each performed as technical triplicates .....	83

## Abbreviations

$^{13}\text{C}$ NMR	Carbon 13 nuclear magnetic resonance
$^1\text{H}$ NMR	Proton nuclear magnetic resonance
<i>A. ealaensis</i>	<i>Ancistrocladus ealaensis</i>
<i>A. congolensis</i>	<i>Ancistrocladus congolensis</i>
<i>A. ileboensis</i>	<i>Ancistrocladus ileboensis</i>
<i>A. likoko</i>	<i>Ancistrocladus likoko</i>
ACT	Artemisinin-based combination therapies
AD	Anno Domini (After date of Christ's birth)
AU	Absorbance units
BC	Before Christ
BPI	Base peak ion
calcd	Calculated
$\text{CDCl}_3$	Deuterated chloroform
$\text{CD}_3\text{COCD}_3$	Deuterated acetone
$\text{CD}_3\text{OD}$	Deuterated methanol
cm	Centimeter
COSY	Correlation spectroscopy
DCM	Dichloromethane
dddH <sub>2</sub> O	Triple distilled water
DMSO	Dimethyl sulfoxide
DNA	Deoxyribonucleic acid
DRC	Democratic Republic of the Congo
ECD	Electronic circular dichroism
EDTA	Ethylenediamine tetraacetic acid
ESI	Electrospray ionization
EtOAc	Ethyl acetate
g	Gram
GPS	Global positioning system

h	Hour
H <sub>ax</sub>	Axial proton
H <sub>eq</sub>	Equatorial proton
HEPES	4-(2-Hydroxyethyl)-1-piperazineethanesulfonic acid
HMBC	Heteronuclear multiple bond correlation
HPLC	High-performance liquid chromatography
HPLC-MS	High-performance liquid chromatography mass spectrometry
HPLC-UV	High-performance liquid chromatography ultraviolet
HTS	High-throughput Screening
Hz	Hertz
iFit	Isotopic fit value
iRBC	Infected red blood cell
km	Kilometer
L	Liter
LC-MS-SPE-NMR	Liquid chromatography - mass spectrometry - solid phase extraction - nuclear magnetic resonance
Me	Methyl
MeCN	Acetonitrile
MeCOMe	Acetone
MeOH	Methanol
mAU	Milli-absorbance units
mg	Milligram
MHz	Megahertz
min	Minute
mL	Milliliter
mM	Millimolar
mm	Millimeter
MS	Mass spectrometry
<i>m/z</i>	Mass to charge ratio
NIQ	Naphthylisoquinoline

nM	Nanomolar
nm	Nanometer
NMR	Nuclear magnetic resonance
NOE	Nuclear Overhauser effect
NOESY	Nuclear Overhauser effect spectrometry
NP	Natural product
<i>P. falciparum</i>	<i>Plasmodium falciparum</i>
<i>P. knowlesi</i>	<i>Plasmodium knowlesi</i>
<i>P. malariae</i>	<i>Plasmodium malariae</i>
<i>P. ovale</i>	<i>Plasmodium ovale</i>
<i>P. vivax</i>	<i>Plasmodium vivax</i>
PDA	Photodiode array
ppm	Parts per million
Qda	Quadrupole Dalton
QTOF	Quadrupole time of flight
RI	Resistance index
RPMI	Roswell Park Memorial Institute
SD	Standard deviation
SEM	Standard error of mean
SPE	Solid phase extraction
TFA	Trifluoroacetic acid
TLC	Thin-layer-chromatography
T <sub>R</sub>	Retention time
μl	Microliter
μM	Micromolar
μm	Micrometer
UPLC	Ultra-performance liquid chromatography
UPLC-QTOF-MS	Ultra-performance liquid chromatography quadrupole time of flight mass spectrometry
UV	Ultraviolet
V	Volt



## Supplementary data

<b>Supplementary data 1</b>	$^1\text{H}$ NMR spectrum of compound <b>43</b> (ealamine A) in $\text{CDCl}_3$ .....	110
<b>Supplementary data 2</b>	NOESY spectrum of compound <b>43</b> (ealamine A) in $\text{CDCl}_3$ .....	110
<b>Supplementary data 3</b>	$^{13}\text{C}$ NMR spectrum of compound <b>43</b> (ealamine A) in $\text{CDCl}_3$ .....	111
<b>Supplementary data 4</b>	Dept 135 spectrum of compound <b>43</b> (ealamine A) in $\text{CDCl}_3$ .....	111
<b>Supplementary data 5</b>	COSY spectrum of compound <b>43</b> (ealamine A) in $\text{CDCl}_3$ .....	112
<b>Supplementary data 6</b>	HMBC spectrum of compound <b>43</b> (ealamine A) in $\text{CDCl}_3$ .....	112
<b>Supplementary data 7</b>	HSQC spectrum of compound <b>43</b> (ealamine A) in $\text{CDCl}_3$ .....	113
<b>Supplementary data 8</b>	MS/MS chromatogram of compound <b>43</b> (ealamine A) in the subfraction $\text{F}_4\text{SF}_5$ .....	113
<b>Supplementary data 9</b>	$^1\text{H}$ NMR spectrum of compound <b>44</b> (ancistrocladinium A) in $\text{CD}_3\text{OD}$ .....	114
<b>Supplementary data 10</b>	COSY spectrum of compound <b>44</b> (ancistrocladinium A) in $\text{CD}_3\text{OD}$ .....	114
<b>Supplementary data 11</b>	$^{13}\text{C}$ NMR spectrum of compound <b>44</b> (ancistrocladinium A) in $\text{CD}_3\text{OD}$ .....	115
<b>Supplementary data 12</b>	Dept 135 spectrum of compound <b>44</b> (ancistrocladinium A) in $\text{CD}_3\text{OD}$ .....	115
<b>Supplementary data 13</b>	HMBC spectrum of compound <b>44</b> (ancistrocladinium A) in $\text{CD}_3\text{OD}$ .....	116

<b>Supplementary data 14</b>	HSQC spectrum of compound <b>44</b> (ancistrocladinium A) in CD <sub>3</sub> OD .....	116
<b>Supplementary data 15</b>	MS/MS data of compound <b>44</b> (ancistrocladinium A) .....	117
<b>Supplementary data 16</b>	IR spectrum of compound <b>44</b> (ancistrocladinium A) ....	118
<b>Supplementary data 17</b>	<sup>1</sup> H NMR spectrum of compound <b>45</b> (ancistrocyclinone A) in CD <sub>3</sub> COCD <sub>3</sub> (solvent-suppression mode) .....	119
<b>Supplementary data 18</b>	COSY spectrum of compound <b>45</b> (ancistrocyclinone A) in CD <sub>3</sub> COCD <sub>3</sub> .....	119
<b>Supplementary data 19</b>	<sup>13</sup> C NMR spectrum of compound <b>45</b> (ancistrocyclinone A) in CD <sub>3</sub> COCD <sub>3</sub> .....	120
<b>Supplementary data 20</b>	HMBC spectrum of compound <b>45</b> (ancistrocyclinone A) in CD <sub>3</sub> COCD <sub>3</sub> .....	120
<b>Supplementary data 21</b>	HSQC spectrum of compound <b>45</b> (ancistrocyclinone A) in CD <sub>3</sub> COCD <sub>3</sub> .....	121
<b>Supplementary data 22</b>	NOESY spectrum of compound <b>45</b> (ancistrocyclinone A) in CD <sub>3</sub> COCD <sub>3</sub> .....	121
<b>Supplementary data 23</b>	MS/MS chromatogram of compound <b>45</b> (ancistrocyclinone A) .....	122
<b>Supplementary data 24</b>	IR spectrum of compound <b>45</b> (ancistrocyclinone A) ....	123
<b>Supplementary data 25</b>	<sup>1</sup> H NMR spectrum of compound <b>46</b> in CD <sub>3</sub> OD .....	124
<b>Supplementary data 26</b>	<sup>13</sup> C NMR spectrum of compound <b>46</b> in CD <sub>3</sub> OD .....	124
<b>Supplementary data 27</b>	HMBC spectrum of compound <b>46</b> in CD <sub>3</sub> OD .....	125
<b>Supplementary data 28</b>	HSQC spectrum of compound <b>46</b> in CD <sub>3</sub> OD .....	125
<b>Supplementary data 29</b>	NOESY spectrum of compound <b>46</b> in CD <sub>3</sub> OD .....	126
<b>Supplementary data 30</b>	MS/MS chromatogram of compound <b>46</b> .....	126
<b>Supplementary data 31</b>	IR spectrum of compound <b>46</b> .....	127

# Chapter 1

## General introduction

### 1.1 Natural products as a source of medicines

Since the dawn of time, natural products (NP) have been a great source of active ingredients in the treatment of diseases. Indeed, they have provided a tremendous library of bioactive compounds with high structural and chemical diversities. Natural products are considered to be the best source of leads and therapeutics, while at least 80 % of the world's population uses plants as alternative therapies as estimated by the World Health Organization (WHO).<sup>[1-4]</sup>

There is a long history in the use of NP in medicine. It dates back to the Egyptian pharmaceutical document called Eber Papyrus from 2900 B.C., which records more than 700 medicines from plants used as infusions, gargles, pills, ointments. From Mesopotamia, *Cupressus sempervirens* (cupress) and *Commiphora* species (myrrh) oils were recorded on clay tablets written in cuneiform from 2600 B.C., and they are still used today against inflammation, coughs, and colds. There are records on the use of NP in China as well, such as: Materia Medica with 52 prescriptions (1100 B.C.), Shennong Herbal with 365 medicines (~ 100 B.C.), and Tang Herbal with 850 medicines (659 A.D.). In Greece, records on medicinal herbs were documented by Dioscorides (100 A.D.) and Theophrastus (~300 B.C.).<sup>[5]</sup>

NP from other sources such as microbial sources were also used in folklore medicine. The charcoal of steamed fungus *Piptoporus betulinus* was used as antiseptic and disinfectant. The Caribbean *Agaricus campestris* was used to soothe throat cancer when stewed in milk. From marine sources, among few examples, in the Aran Islands, *Porphyra umbilicalis* was used for easy digestion and the decoction was given to cows to relieve their springtime constipations.<sup>[5]</sup>

However, over the years, natural products were used in an empirical manner as the active ingredients in traditional medicines were not identified. Medicinal plants, being the main source of NP at that time, were used as a result of trial and error. It was the

work of Anton von Störck and William Withering that laid the foundations of rational clinical investigation of medicinal herbs in the 18<sup>th</sup> century. The beginning of the 19<sup>th</sup> century marked the starting of rational drug discovery from plants with the work of Friedrich Sertürner (a German apothecary assistant), who isolated morphine (**1**) from *Papaver somniferum* L. and published a comprehensive article on his work. In the following decades, many active ingredients, mainly alkaloids, were, isolated from medicinal plants. Due to this, medicinal plants, constituted the basis for the discovery of the early drugs. Thereafter, chemical synthesis was used to produce natural and natural-derived compounds with the best-known example being acetylsalicylic acid (Aspirin, **2**), derived from salicin, which was isolated from the bark of *Salix alba* L. The discovery of penicillin (**3**) by Fleming in 1929 from the fungus *Penicillium notatum*, laid a foundation of a new era of drug discovery in pharmaceutical industries. In fact, the use of pure compounds replaced more and more the use of extracts and semi-purified compounds.<sup>[1, 5, 6]</sup>

Natural products drove pharmaceutical discoveries over decades. However, many pharmaceutical industries scaled back their program on NP and shifted to synthetic chemistry and high-throughput screening (HTS) because of the complexity of natural products-based drug discovery. Unfortunately, the expected results were not obtained as revealed by the declining numbers of drugs that reached the market.<sup>[1, 7]</sup> This led to the interest in drug discovery from NP being revitalized and indeed, of 1073 new compounds approved between 1981 and 2010, only 36 % were from pure synthesis and more than half were based on natural products. Further, 19 drugs related to NP were approved between 2005 and 2010, from which seven were NP, two derived from NP and ten were semi-synthetic.<sup>[1-3, 6, 8-12]</sup> The field of anti-cancer agents is the best example of natural-products derived compounds found in modern pharmacotherapy, e.g., paclitaxel (**4**) used in breast cancer was isolated from *Taxus brevifolia* (Pacific Yew), vincristine and vinblastine were discovered in *Catharanthus roseus* (L.) G. Don.<sup>[1, 8, 13]</sup> There are also approved mixtures of compounds such as: Veregen<sup>TM</sup>, which are catechins isolated from green tea, and used in genital warts in topical application, Sativex<sup>®</sup>, a mixture of dronabinol (**5**), and cannabidiol (**6**) produced by the *Cannabis* plant and used to relieve pains, etc.<sup>[8]</sup>

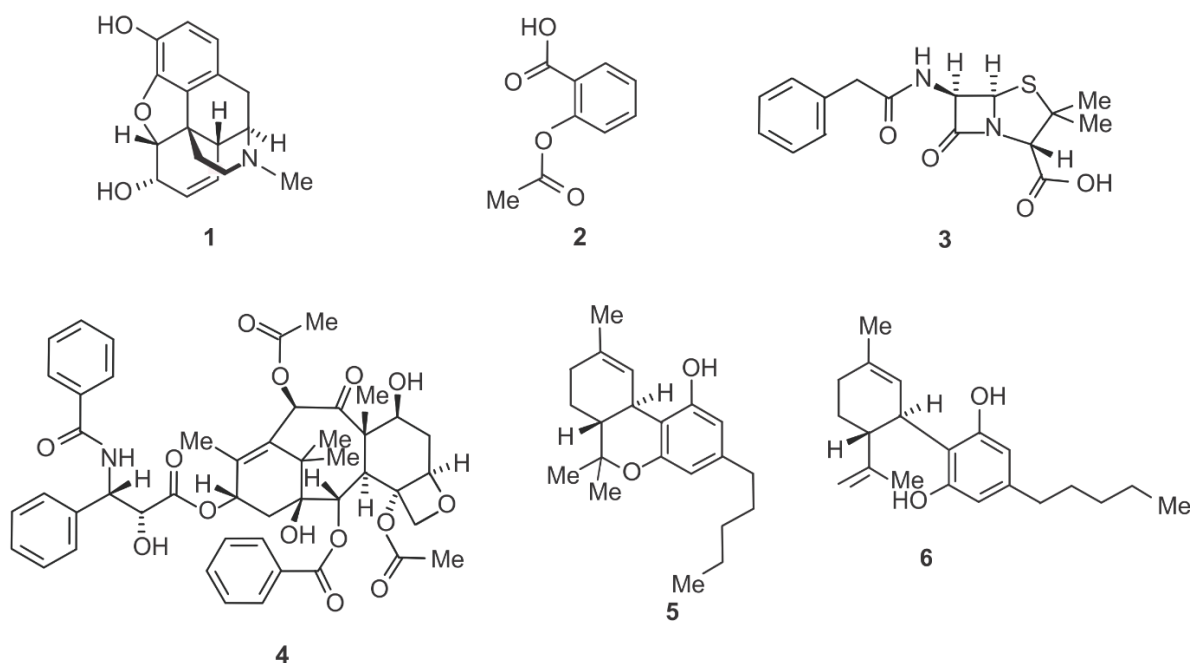


**Figure 1.1:** Examples of compounds based on natural products used in modern medicine: morphine (1), aspirin (2), penicillin G (3), paclitaxel (4), dronabinol (5), and cannabidiol (6).

## 1.2 Background to malaria and the parasite life cycle

Malaria is an infectious disease caused by parasites of the genus *Plasmodium*, of which five species are known to be responsible for the disease: *P. falciparum*, *P. vivax*, *P. malariae*, *P. ovale*, and *P. knowlesi*.<sup>[14, 15]</sup>

*P. falciparum* is the predominant species found in tropical and subtropical areas of Africa, Central and South America, and Southeast Asia. *P. malariae* is less frequent than *P. falciparum* but has the same geographical distribution. *P. vivax* and *P. ovale* have complementary geographical locations with sometimes overlaps. *P. ovale* is found primarily in sub-Saharan Africa and *P. vivax* in Central and South America, India, and Southeast Asia.<sup>[16]</sup>

Most serious malaria illnesses and deaths worldwide are due to infection with *P. falciparum* though severe malaria caused by *P. vivax* has also been reported.<sup>[17]</sup>

The parasites comprise a complex life cycle occurring in two hosts, the human host and the *Anopheles* mosquito (Figure 1.2). Through a bite of feeding *Anopheles*

mosquitoes, with the saliva, sporozoites are injected into humans. These sporozoites infect liver cells and develop into schizonts – the pre-erythrocytic stage, which contains merozoites. When the schizont matures, it ruptures and releases merozoites into the blood stream and these infect erythrocytes, forming trophozoites. The latter develop and later release another batch of erythrocyte-infecting merozoites, this constituting the erythrocytic stage. The synchronized release of merozoites from erythrocytes results in the type of fever that characterizes the disease. However, there is a portion of merozoites in erythrocytes that matures through five distinctive stages into gametocytes (sexual forms of the parasites), male and female. The gametocytes are the only stage of parasites that will continue the development in the mosquito if taken from the blood by a feeding mosquito. Therefore, they will go through molecular and cellular changes inside the mosquito until they reach the stage of sporozoites, which can again infect a human. However, in *P. vivax* and *P. ovale*, some merozoites in hepatocytes turn into hypnozoites, a form that remains dormant for months or even years. Once they become active again, they develop into schizonts, which cause relapses in infected people in most cases – this constitutes the exo-erythrocytic stage.<sup>[18, 19]</sup>

The traditional classification of antimalarial drugs is based on the stages of the parasite life cycle targeted by the drug. They are classified into blood schizonticides (drugs acting on the asexual intraerythrocytic stage of the parasite), tissue schizonticides (acting on the hepatic schizont stage), hypnozoiticides (acting on the hypnozoites), and gametocytocides (drugs killing gametocytes).<sup>[20-22]</sup>

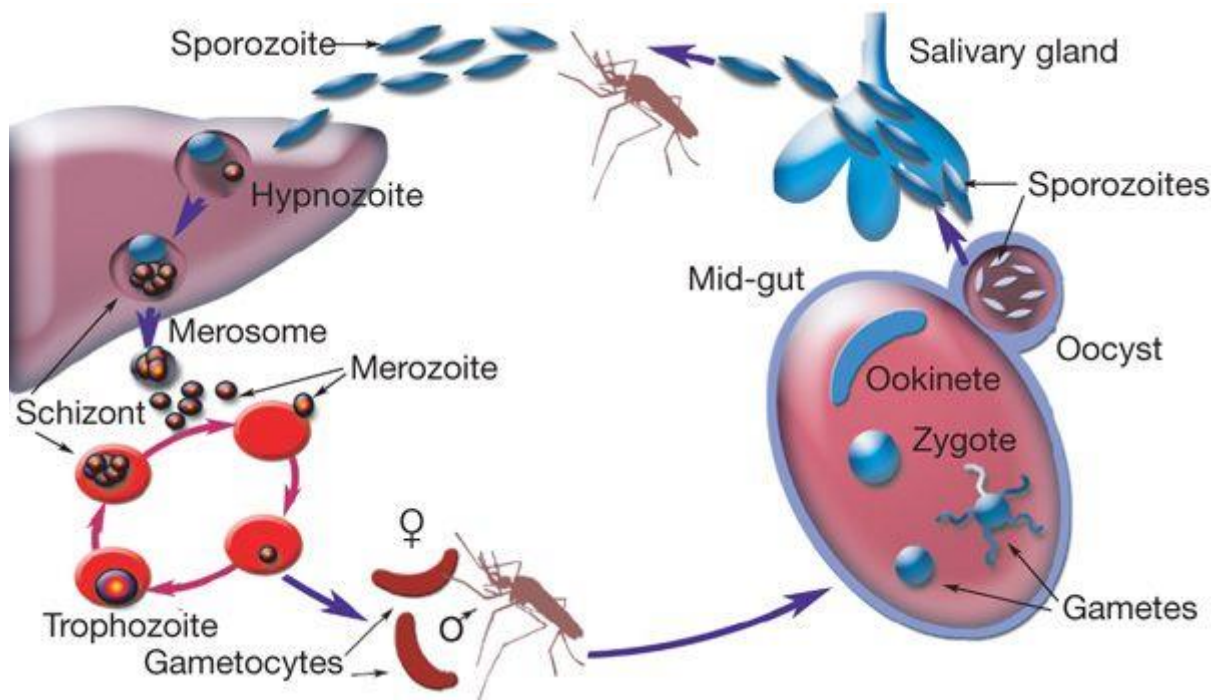


**Figure 1.2:** *Plasmodium* life cycle: parasite stages in human and mosquito *Anopheles*, Winzele, E.A.<sup>[23]</sup>

### 1.3 Plants used to treat malaria based on traditional knowledge

It has been highlighted that plants have played an important role in the fight against diseases. In the case of malaria, communities from affected regions continue to use traditional medicines to treat the disease. More than 1200 plant species from 160 families are documented for their uses in the treatment of fever and malaria.<sup>[24]</sup>

In Ethiopia, a review article published by Alebie et al. (2017), reports 200 medicinal plant species from 71 botanical families traditionally used in the treatment of malaria. *Allium sativum*, *Carica papaya*, *Clerodendrum myricoides*, *Dodonaea angustifolia*, *Vernonia amygdalina*, *Croton macrostachyus*, *Aloe* sp., *Lepidium sativum*, *Justicia schimperiana*, *Phytolacca dodecandra*, *Melia azedarach*, *Azadirachta indica*, *Brucea antidysenteric*, *Tamarindus indica*, *Calpurnia aurea*, *Eucalyptus globulus*, *Salvadora persica*, *Carissa spinarum*, *Ajuga integrifolia*, *Artemisia afra*, *Moringa stenopetala*, and *Ruta chalepensis* were the most commonly utilized species. The most common methods of preparation were decoctions, concoctions, infusions, chewing/eating and pounding, with water as the solvent utilized in most cases.<sup>[25, 26]</sup>

In the Sahel region of Burkina Faso, from an ethnobotanical survey conducted by Bonkian et al. (2017), in the region, 42 plants species belonging to 25 families were identified as being used in the traditional treatment of malaria. The most commonly utilized species were *Guiera senegalensis* J.F. Gmel., *Combretum micranthum* G. Don., *Momordica balsamina* L., *Lannea velutina* A. Rich., *Cassia sieberiana* DC., *Citrus limon* (L.) Osbeck, *Bauhinia rufescens* Lam., *Azadirachta indica* A. Juss., and *Eucalyptus camaldulensis* Dehnh. Leaves were the most commonly consumed part of the plant (57.1 %), while water decoction was the main preparation method (78.5 %) with oral administration.<sup>[27]</sup>

In Sukka Local Government Area of Enugu State, the Southeastern part of Nigeria, an ethnobotanical survey was conducted by Odoh et al. (2018), on the use of medicinal plant by local traditional healers in the treatment of malaria. The survey identified 50 plant species from 30 botanical families utilized in the traditional treatment of malaria. *Azadirachta indica*, *Mangifera indica*, *Carica papaya*, *Cymbopogon citratus*, and *Psidium guajava* were the most commonly used plant species. The solvent mainly consumed was water, yet sometimes a mixture of water/ethanol was utilized. The methods of preparation were decoction and maceration.<sup>[24]</sup>

In Vaupes Medio, Colombia, an ethnobotanical survey conducted by Ramírez and Blair (2017), spotted 41 plants used by traditional healers for malaria treatment. In this study, 35 plants were identified to the species level, five to the genus and one to the family. Among them, *Abuta grandifolia*, *Aspidosperma excelsum*, *Matisia cf. glandifera*, and *Pleonotoma jasminifolia* were the mostly utilized. Decoction in water was the only preparation consumed by the populations and the stem bark the mostly consumed part of the plants.<sup>[4]</sup>

In South Africa, malaria transmission is restricted to the Northeastern part of the country (Limpopo, Mpumalanga and KwaZulu-Natal) and some medicinal plants been reported for their consumption in traditional treatment of malaria by communities of these regions.<sup>[28-30]</sup> Among numerous examples, the powdered bark and roots of *Acacia xanthoploea* Benth were utilized by the Zulus in emetic to treat malaria and in prophylaxis;<sup>[29]</sup> infusions of the leaves of *Solanum nigrum* L. and *Lippia javanica* (Burm. f.) Spreng were used by the Vhavenda as a remedy for malaria and dysentery, and as a prophylactic against malaria, respectively.<sup>[28]</sup>



In the Democratic Republic of the Congo (DRC), an ethnopharmacological survey conducted by Kasali et al. (2014), in the city of Bukavu (eastern part of the country), identified 40 plant species belonging to 27 botanical families consumed in folk medicine to treat malaria. The plant part mostly used was leaves (60 %) with water representing the solvent mainly utilized (77.5 %). Decoction was the main method of formulation (47.5 %) and all preparations consumed in oral administration (100 %). Plant species commonly used by interviewed traditional healers were: *Artemisia annua* L., *Carica papaya* L., *Cinchona ledgeriana* Moes., *Cymbopogon citratus* (DC) Stapf, *Melia azedarach* L., *Tithonia diversifolia* (Hem) A. Cray., *Eucalyptus globulus* L., and *Catharanthus roseus* (L.) G. Don.<sup>[31]</sup> Another ethnopharmacological survey was conducted in the city of Butembo (eastern part of the country) by Kasali et al. (2014). The results identified 46 plant species belonging to 25 families used by traditional healers to treat malaria, while 85 % of preparation methods were decoction and water the main solvent for formulation (91.3 %). In addition 67.4 % of the plant parts utilized were leaves. However, more than half of the plant species that were used in Bukavu were consumed in Butembo as well.<sup>[32]</sup> The local communities of Kinshasa (western part of the country) also utilized medicinal plants to treat fever, pain or malaria. Among species used were *Garcinia kola* Heckel, *Morinda morindoides* (Baker) Milne-Redhead, *Vernonia amygdalina* Oliv., and *Cassia occidentalis* L.<sup>[33, 34]</sup>

This study focuses on *Ancistrocladus* species from DRC, for which there is limited recorded and published information on the traditional use of this genus for the treatment of malaria. Nevertheless it remains a species of high interest due to the promising antiplasmodial activities of a range of isolated and characterized NIQs.

#### **1.4 Natural products research in malaria therapy**

NP have also played a great role in the drug discovery of antimalarial compounds.<sup>[35]</sup> In search for medicines to cure malaria, many researchers have screened several plants as part of screening campaigns. Some of these have been medicinal plants trying to substantiate traditional uses. Okpekon et al. screened 77 plant extracts prepared from 17 medicinal plants used in the Ivory Coast traditional medicine against malaria and other parasitic diseases. Of these, eleven out of the 17 species were used against malaria in folk medicine. However, extracts obtained from only two plants

(*Anogeissus leiocarpus* and *Terminalia glaucescens*), of the eleven used against malaria by traditional healers, showed strong antiplasmodial activity with IC<sub>50</sub> values below 5 µg/mL, while the other species showed an average antiplasmodial activity (IC<sub>50</sub> between 5 and 20 µg/mL) against the chloroquine-resistant FCB1 strain of *P. falciparum*. However, two species (*Afrormosia laxiflora* and *Aframomum sceptrum*) used against other parasitic diseases by traditional healers exhibited significant antiplasmodial activity with IC<sub>50</sub> values below 5 µg/mL.<sup>[36]</sup> Of the 33 medicinal plants of Central West Ivory Coast examined by Zirihi et al., eight showed antiplasmodial activity against *P. falciparum* chloroquine-resistant FCB1/Colombia strain with IC<sub>50</sub> ranging from 2.3 to 13.7 µg/mL with the stem bark extracts of *Funtumia elastica* (IC<sub>50</sub> = 3.3 µg/mL), and *Fagara macrophylla* (IC<sub>50</sub> = 2.3 µg/mL), and the root bark extract of *Rauvolfia vomitoria* (IC<sub>50</sub> = 2.5 µg/mL) being of particular interest because of the low toxicity.<sup>[37]</sup> Simonsen et al. screened ethanolic extracts of 47 species used to treat malaria and fever in folk medicine in India against the *P. falciparum* 3D7 strain and only 23 species showed some antiplasmodial activity with an inhibition of more than 80 % at 100 µg/mL, and 50 % at 50 µg/mL. *Ailanthus excels* Roxb., *Cocculus pendulus* (J.R. and G. Forst) Diels, and *Casearia elliptica* Willd showed more than 80 % inhibition at 12.5 µg/mL.<sup>[38]</sup> From 48 Brazilian plants investigated for their antimalarial activity, *Vernonia brasiliiana*, *Eupatorium squalidum*, *Acanthospermum australe*, *Esenbeckia febrifuga*, *Lisianthus speciosus*, and *Tachia guianensis* showed 40-50 % inhibition activity against *P. berghei in vivo* when administered to infected mice at up to 1.0 g/kg for 4 days, while *V. brasiliiana* exhibited about 50 % inhibition of *P. falciparum in vitro* at 40 ng/mL.<sup>[39]</sup> From 190 plants from five different ecosystems of Madagascar screened by Rasoanaivo et al. against *P. falciparum*, 39 showed activity with IC<sub>50</sub> below 5 µg/mL, while nine had IC<sub>50</sub> between 5 and 7.5 µg/mL.<sup>[40]</sup> From 14 plants (from Venda and northern KwaZulu-Natal) screened by Prozesky et al. against a chloroquine-resistant (PfUP1) strain of *P. falciparum*, nine displayed activity at IC<sub>50</sub> below 5 µg/mL with dichloromethane stem bark extracts of *Ozoroa engleri* R.A. Fernandes and *Balanites maughamii* Sprague (IC<sub>50</sub> 1.70 and 1.94 µg/mL, respectively) being the most active extracts. Moreover, extracts prepared from over 134 species collected throughout South Africa were screened against the D10 strain of *P. falciparum*. Of 66 species that displayed IC<sub>50</sub> below 10 µg/mL, 23 species had IC<sub>50</sub> below 5 µg/mL.<sup>[30]</sup> Extracts (20) prepared from nine medicinal plants used in Kinshasa (DRC) were screened against *P. falciparum*. The whole plant of *Euphorbia*

*hirta* (DCM and EtOH extracts), *Phyllanthus nuriri* (DCM extract), *Cryptolepis sanguinolenta* (EtOH extract), the stem bark of *Garcinia kola* (DCM and EtOH extracts), and the leaves of *Cassia occidentalis* (DCM extract) displayed more than 80 % inhibition of the parasite growth at 6 µg/mL.<sup>[33]</sup>

More than just screening extracts, researchers have been involved in bioassay-guided fractionation and phytochemical investigation of several medicinal plants used in the traditional treatment of malaria. This led to the identification of several structural class of compounds with potent antimalarial activities (alkaloids, chalcones, thienopyrimidinones, quinolones, hexahydroquinolines, flavonoids, quinazolines, quinazolinone derivatives, acridines, enaminones, and terpenic compounds).<sup>[41-43]</sup> Just to mention a few examples (Figure 1.3) of antiplasmodial compounds: 3-acetoxy-5,7-dihydroxycarvotacetone (**7**), a monoterpene that was isolated from *Sphaeranthus bullatus* Mattf., exhibited antiplasmodial activity with IC<sub>50</sub> values of 2.5 µM on D6 and 2.8 µM on W2 strains. A guaianolide (**8**), which is a sesquiterpene discovered in *Eupatorium perfoliatum* L., exhibited activity against *P. falciparum* K1 strains with an IC<sub>50</sub> value of 2.0 µM. Caesalminine A (**9**), a diterpene produced by the seeds of *Caesalpinia minax* Hance, showed activity against *P. falciparum* K1 strains with an IC<sub>50</sub> value of 0.4 µM.<sup>[9]</sup> Fagoronine (**10**), an indole alkaloid found in *Fagara zanthoxyloides*, inhibited growth of *P. falciparum* at an IC<sub>50</sub> of 0.018 µg/mL (0.051 µM). Acetylvismione D (**11**), a quinone isolated from *Psorospermum glaberrimum*, showed activity against *P. falciparum* W2 strains with an IC<sub>50</sub> value of 0.12 µM.<sup>[44, 45]</sup> Ineupatorolide A (**12**), a terpene produced by *Carpesium rosulatum*, exhibited excellent activity against *P. falciparum* D10 strain with an IC<sub>50</sub> of 0.019 µM and *in vivo* activity against *P. berghei* showing blood schizontocidal activity with a significant mean survival time comparable to that of chloroquine (5 mg·kg<sup>-1</sup>·day<sup>-1</sup>) in a 4-day early infection, and in a repository evaluation, and in established infection at doses 2, 5 and 10 mg·kg<sup>-1</sup>·day<sup>-1</sup>. 5',6'-Dihydrousambarensine (**13**), a bis-indole alkaloid discovered in *Strychnos spp.*, showed activity against *P. falciparum* W2 strain with an IC<sub>50</sub> of 0.032 µM.<sup>[46, 47]</sup>

Another interesting class of compounds are naphthylisoquinoline alkaloids, which have shown very attractive antiplasmodial activities both *in vitro* and *in vivo*, ranging from moderate to excellent activity with some compounds having *in vitro* IC<sub>50</sub> in the nanomolar range.<sup>[48]</sup> These compounds are discussed in Chapter 2.

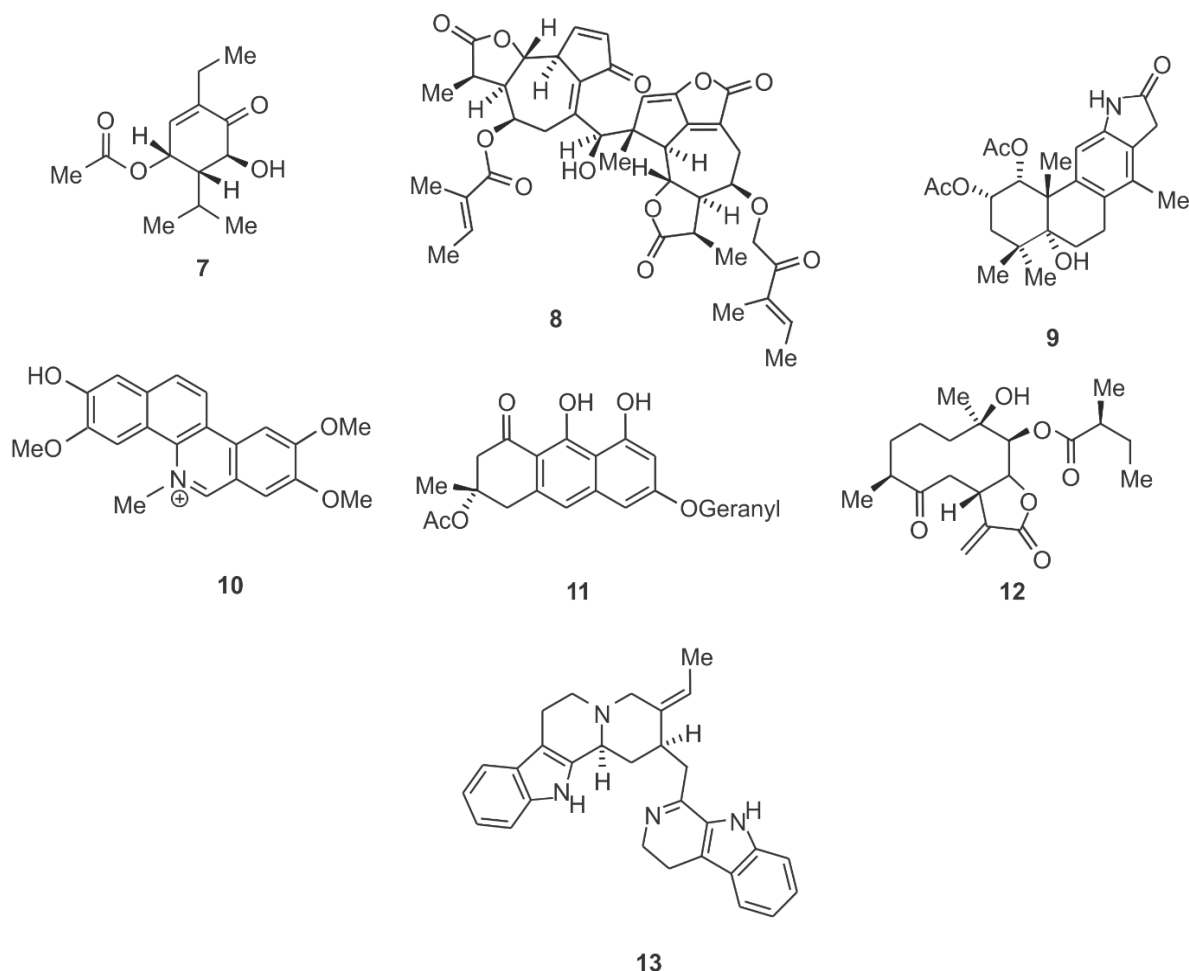


**Figure 1.3:** Structures of 3-acetoxy-5,7-dihydroxycarvotacetone (**7**), guaianolide (**8**), caesalminine A (**9**), fagoronine (**10**), acetylvismione D (**11**), ineupatorolide A (**12**), and 5',6'-dihydrousambarensine (**13**), few examples of identified antimalarial compounds from plants.

One of the major successful discoveries in the antimalarial drug research and development from natural products is that of quinine from the *Cinchona* species. The Incas of South America used barks of various species of *Cinchona* to treat tropical fever. These species were then introduced in Europe in the 1630s and later established as a valuable treatment for malaria. They were drunk as a ground powder mixed with a liquid (usually wine). In 1820, the active ingredient of *Cinchona*, quinine, was isolated by Joseph Caventou and Pierre Pelletier.<sup>[35, 49-51]</sup> After further research and development, derivatives of quinine (**14**) such as chloroquine (**15**), primaquine (**16**), amodiaquine (**17**), and mefloquine (**18**) were synthesized and used for the treatment of malaria (Figure 1.4). For years, chloroquine was successfully used to treat malaria and the victory over malaria was almost reached in the late 1960s.<sup>[52]</sup> Unfortunately,

the parasite developed resistance to chloroquine and malaria could not be eradicated as the resistance to chloroquine spread over almost all malaria endemic areas. Chloroquine became increasingly ineffective, leading to the need for new, effective, and affordable drugs to treat malaria.<sup>[52]</sup>

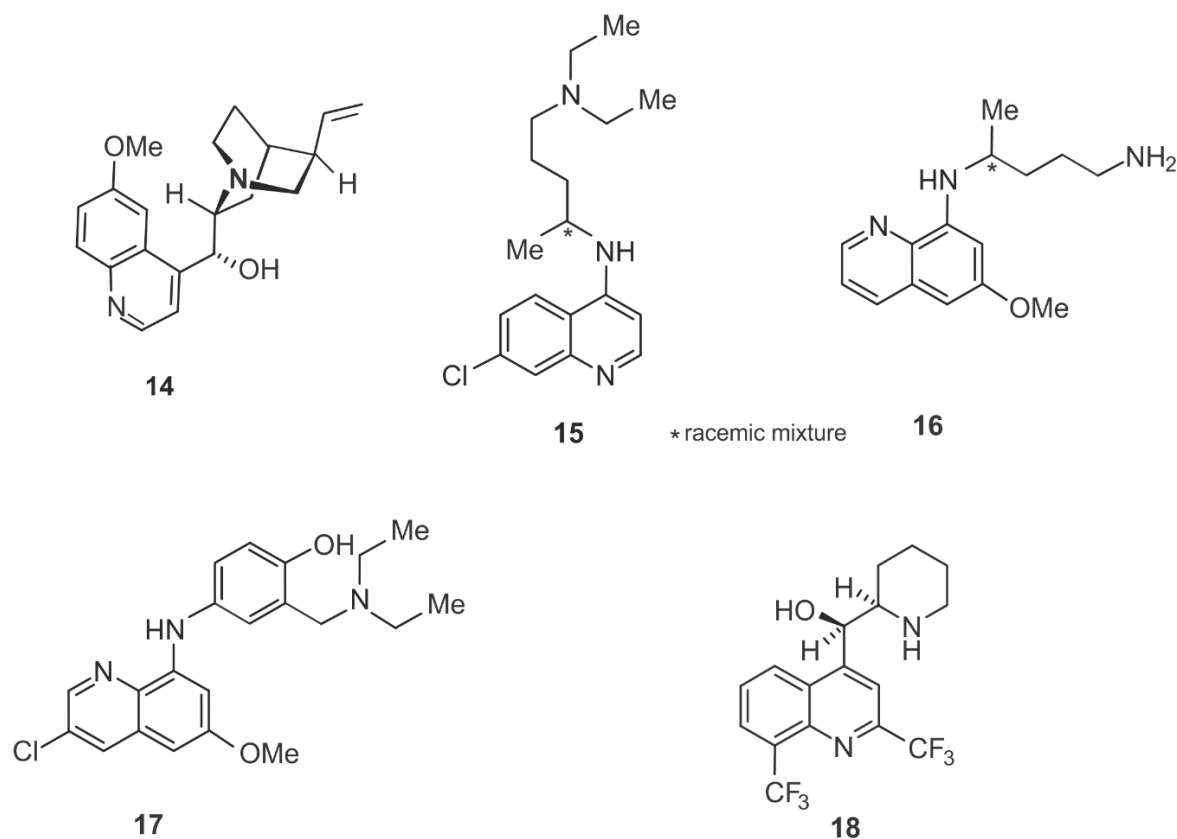


**Figure 1.4:** Structures of quinine (**14**), chloroquine (**15**), primaquine (**16**), amodiaquine (**17**), and mefloquine (**18**) used in malaria treatment.

In the 1960s, during the Vietnam-US war, many Vietnamese soldiers suffered from severe malaria because of the parasites resistance to drugs. The North-Vietnamese government made a request to find effective antimalarial drugs that overcome resistance. This led China to run a project named “Project 523” involving 60 research organizations and more than 500 scientists aiming at finding new antimalarial drugs. One of the many programs under the “Project 523” was the screening of medicinal plants used in the Chinese traditional medicine. A breakthrough came from the herb *Artemisia annua*, which was used to treat febrile illnesses as mentioned in an ancient Chinese publication thought to be from AD 341. Under the screening campaign, Chinese scientists screened more than 100 recipes from well-recorded traditional

Chinese medicine and folk medicines. *Artemisia* was well known for its antimalarial activity, subsequently, a systematic bioassay guided screenings of *Artemisia annua* confirmed the activity of the alcoholic extracts against *Plasmodium falciparum* in 1971.<sup>[50, 53-55]</sup> Thereafter, artemisinin (**19**), the active principle, was isolated in 1972 and the structure elucidated in 1976.<sup>[56]</sup> This compound served as lead for development of several derivatives, artemether (**20**), arteether (**21**), and artesunate (**22**), which are currently used in the combination therapy for the first-line treatment.<sup>[57]</sup>

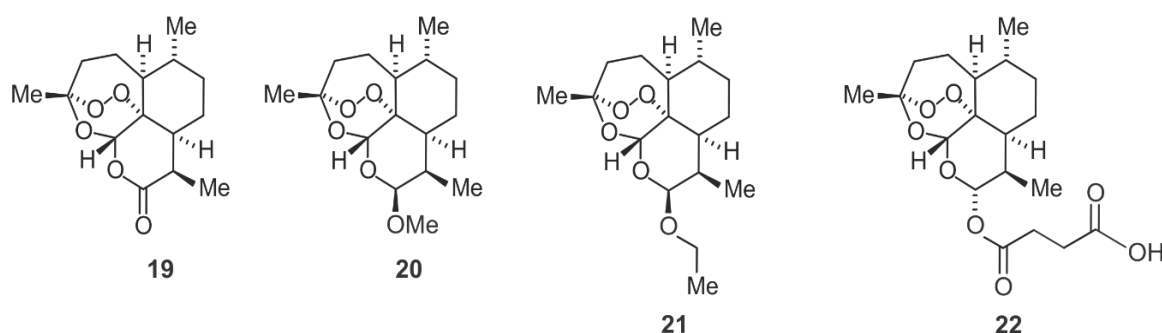


**Figure 1.5:** Structures of artemisinin (**19**), artemether (**20**), arteether (**21**), and artesunate (**22**).

Based on the effectiveness and success of quinine and artemisinin derivatives, NP, mainly from plants, are valuable tools that can actively participate in the fight against malaria.<sup>[58]</sup>

### 1.5 Current approved treatments of malaria

Uncomplicated malaria infection due to *P. falciparum* is treated by artemisinin-based combination therapies (ACTs), which combine two active principles having different modes of action. The following options are recommended by the WHO according to the proven effectiveness of each in the region: artemether + lumefantrine, artesunate + amodiaquine, artesunate + mefloquine, artesunate + sulfadoxine-pyrimethamine, artesunate + pyronaridine, and dihydroartemisin + piperazine. ACTs are also used in non-*falciparum* malaria illnesses though for radical cure of *vivax* infection, chloroquine + primaquine remains the treatment of choice in most regions in case of chloroquine-sensitive infection.<sup>[51, 52]</sup>

Parenteral artesunate and quinine are recommended in case of complicated *falciparum* malaria,<sup>[51, 52, 59]</sup> with artesunate being the best option. The latter acts more rapidly than quinine as evidenced by a significant reduction of mortality in adults and children with severe malaria when treated with artesunate compared to quinine in Southeast Asia and Africa.<sup>[59]</sup>

## **1.6 Problem statement and justification**

Malaria has been successfully eliminated from Europe and North America but remains a public-health problem in sub-Saharan Africa as shown in Figure 1.6.<sup>[60]</sup> According to the World Health Organization (WHO) 2017 report, 216 million cases of malaria and 445 000 malaria deaths have been reported worldwide in 2016, while 80 % of the global malaria occurs in 15 countries of sub-Saharan Africa.<sup>[61]</sup>

However, in these region of sub-Saharan Africa, the early 2000 years marked a turning point in multilateral engagement to malaria control. Therefore, since 2000, the malaria mortality rate has significantly dropped as a result of multiple approaches, namely, indoor residual spraying, insecticide-treated bed nets, and artemisinin-based combination therapy.<sup>[18, 62, 63]</sup>

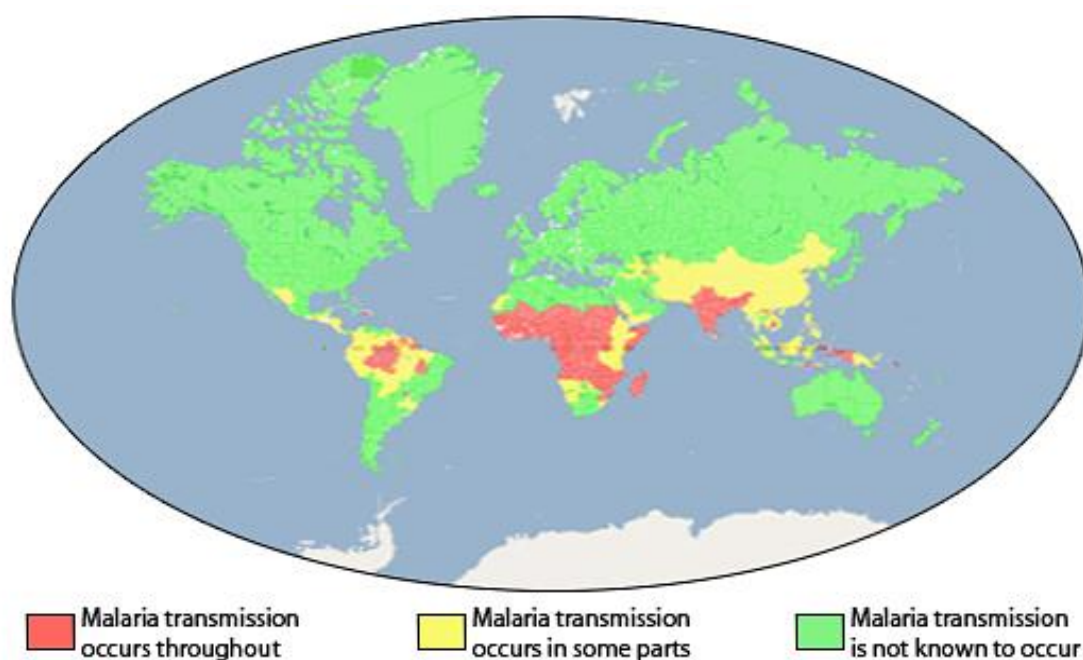


**Figure 1.6:** Map of malaria distribution around the world showing the urge burden of the disease carried by sub-Saharan Africa.<sup>[60]</sup>

Artemisinin-based combination therapy (ACT) is a first-line treatment for uncomplicated *falciparum* malaria in all endemic regions. However, artemisinin resistance and decreased sensitivity of its partner drugs towards *Plasmodium falciparum* has been reported in Southeast Asia, and even cases of ACT treatment failures have been recorded.<sup>[52, 59, 62, 64-69]</sup> Studies have shown that *Plasmodium falciparum* antimalarial drug resistance tends to start from Southeast Asia or South America, which are regions of low-transmission settings, before spreading out to high-transmission regions in sub-Saharan Africa. This is the route followed by chloroquine and later on sulfadoxine-pyrimethamine resistances.<sup>[62]</sup> Else, it has been established that drugs play an important role in malaria control as they may be used in a preventive way or as efficient treatment to rapidly heal malaria, thus, preventing the progression to severe malaria, and limiting development of gametocytes, hence blocking transmission to mosquitoes.<sup>[52]</sup> Therefore, the emergence of *falciparum* resistance to artemisinins and altered sensitivities to its partners in this region of Southeast Asia is of great concern in malaria control and elimination. This indicates that, to prevent any emergence of public health disaster, new drugs able to overcome resistance are needed.<sup>[9, 43, 70]</sup>

*Ancistrocladus* species are well known as a rich source of naphthylisoquinoline alkaloids, a class of compounds with potent antiplasmodial activity.<sup>[40]</sup> Further, some



of the naphthylisoquinoline alkaloids have shown activity against the liver stage, others against the pathogenic blood stage, and some against the gametocytes stages of *P. falciparum* and/or *P. berghei*.<sup>[71-74]</sup>

This study investigates the potential of a new collection of *Ancistrocladus* species through the identification of antiplasmodial naphthylisoquinoline alkaloids as “hit” compounds for further development.

### 1.7 Goal and objectives

The aim of this work is to investigate the antiplasmodial activity through biological screening of extracts from an as yet unidentified *Ancistrocladus* sp, collected in the region Bonsolerive, in the Democratic Republic of the Congo, against asexual chloroquine-sensitive *P. falciparum* strains as well as the isolation and structure elucidation of the active naphthylisoquinoline alkaloids with additional bioassaying against chloroquine-resistant *P. falciparum* strains.

The specific objectives are:

- i. Preparation of extracts using solvents suitable for NIQs isolation through sequential extraction of the plant material, which was collected and air-dried in the DRC.
- ii. Determination of the *in vitro* antiplasmodial activity of extracts against asexual chloroquine-sensitive *P. falciparum* strains NF54.
- iii. Selection of the most active extract based on set criteria and bioassay guided fractionation of the selected extract.
- iv. Isolation of active compound(s) using chromatographic technics (preparative high-performance liquid chromatography, hyphenated liquid chromatography - mass spectrometry - solid phase extraction - nuclear magnetic resonance).
- v. Elucidation of structures of isolated compounds using mass spectrometry, nuclear magnetic resonance, infrared spectra, and electronic circular dichroism.
- vi. Determination of the bioactivity of isolated compound(s) against *P. falciparum* NF54, K1 and W2 strains using the SYBR-Green I based assay.

The **Chapter 2** provides:

- i. Further background to isolation, structure elucidation challenges of naphthylisoquinoline alkaloids,
- ii. A summary of the methodology followed in this study,
- iii. The results of the collection, extraction, isolation, antiplasmodial bioassaying and structure elucidation of naphthylisoquinoline alkaloids from an as yet unidentified *Ancistrocladus* species.

The **Chapter 3** presents the Experimental Section.

The **Chapter 4** discusses the concluding remarks of this work.

## 1.8 References

- [1] A. G. Atanasov, B. Waltenberger, E.-M. Pferschy-Wenzig, T. Linder, C. Wawrosch, P. Uhrin, V. Temml, L. Wang, S. Schwaiger, E. H. Heiss, J. M. Rollinger, D. Schuster, J. M. Breuss, V. Bochkov, M. D. Mihovilovic, B. Kopp, R. Bauer, V. M. Dirsch, H. Stuppner: **Discovery and resupply of pharmacologically active plant-derived natural products: a review.** *Biotechnol. Adv.* **2015**, *33*, 1582-1614.
- [2] A. L. Harvey: **Natural products in drug discovery.** *Drug Discov. Today* **2008**, *13*, 894-901.
- [3] B. Shen: **A new golden age of natural products drug discovery.** *Cell* **2015**, *163*, 1297-1300.
- [4] O. Ramírez, S. Blair: **Ethnobotany of medicinal plants used to treat malaria by traditional healers from ten indigenous Colombian communities located in Vaupes Medio.** *Biodiversity Int. J.* **2017**, *1*, 00022.
- [5] D. A. Dias, S. Urban, U. Roessner: **A historical overview of natural products in drug discovery.** *Metabolites* **2012**, *2*, 303.
- [6] M. S. Butler: **The role of natural product chemistry in drug discovery.** *J. Nat. Prod.* **2004**, *67*, 2141-2153.
- [7] B. David, J.-L. Wolfender, D. A. Dias: **The pharmaceutical industry and natural products: historical status and new trends.** *Phytochem. Rev.* **2015**, *14*, 299-315.
- [8] B. B. Mishra, V. K. Tiwari: **Natural products: an evolving role in future drug discovery.** *Eur. J. Med. Chem.* **2011**, *46*, 4769-4807.
- [9] C. Beaufay, J. Bero, J. Quetin-Leclercq: **Antimalarial terpenic compounds isolated from plants used in traditional medicine (2010 - july 2016).** In *Nat. Antimicrob. Agents*, Springer **2018**, pp. 247-268.
- [10] L. Paloque, A. Triastuti, G. Bourdy, M. Haddad: **Insecticidal and antimalarial properties of plants: a review.** In *Nat. Antimicrob. Agents*, Springer, **2018**, pp. 215-245.

- [11] D. G. I. Kingston: **Modern natural products drug discovery and its relevance to biodiversity conservation**. *J. Nat. Prod.* **2011**, *74*, 496-511.
- [12] J. W. Scannell, A. Blanckley, H. Boldon, B. Warrington: **Diagnosing the decline in pharmaceutical R&D efficiency**. *Nat. Rev. Drug Discov.* **2012**, *11*, 191.
- [13] M. C. McCowen, M. E. Callender, J. F. Lawlis Junior: **Fumagillin (H-3), a new antibiotic with amebicidal properties**. *Science*, **1951**, pp. 202-203.
- [14] K. A. Cullen, P. M. Arguin: **Malaria surveillance - united states, 2012**. *Morbidity and Mortality Weekly Report: Surveillance Summaries* **2014**, *63*, 1-22.
- [15] A. Pain, U. Böhme, A. E. Berry, K. Mungall, R. D. Finn, A. P. Jackson, T. Mourier, J. Mistry, E. M. Pasini, M. A. Aslett, S. Balasubramaniam, K. Borgwardt, K. Brooks, C. Carret, T. J. Carver, I. Cherevach, T. Chillingworth, T. G. Clark, M. R. Galinski, N. Hall, D. Harper, D. Harris, H. Hauser, A. Ivens, C. S. Janssen, T. Keane, N. Larke, S. Lapp, M. Marti, S. Moule, I. M. Meyer, D. Ormond, N. Peters, M. Sanders, S. Sanders, T. J. Sargeant, M. Simmonds, F. Smith, R. Squares, S. Thurston, A. R. Tivey, D. Walker, B. White, E. Zuiderwijk, C. Churcher, M. A. Quail, A. F. Cowman, C. M. R. Turner, M. A. Rajandream, C. H. M. Kocken, A. W. Thomas, C. I. Newbold, B. G. Barrell, M. Berriman: **The genome of the simian and human malaria parasite *Plasmodium knowlesi***. *Nature* **2008**, *455*, 799.
- [16] Centers for Disease Control and Prevention: **Malaria. 2017, December 29**.
- [17] B. Genton, V. D'Acromont, L. Rare, K. Baea, J. C. Reeder, M. P. Alpers, I. Müller: ***Plasmodium vivax* and mixed infections are associated with severe malaria in children: a prospective cohort study from Papua New Guinea**. *PLOS Med.* **2008**, *5*, e127.
- [18] J. Reader, M. Botha, A. Theron, S. B. Lauterbach, C. Rossouw, D. Engelbrecht, M. Wepener, A. Smit, D. Leroy, D. Mancama, T. L. Coetzer, L.-M. Birkholtz: **Nowhere to hide: interrogating different metabolic parameters of *Plasmodium falciparum* gametocytes in a transmission blocking drug discovery pipeline towards malaria elimination**. *Malar. J.* **2015**, *14*, 213.
- [19] H. P. Rang, M. M. Dale: **Rang and Dale's pharmacology**. 7th ed. ed., Elsevier/Churchill Livingstone, Edinburgh, **2012**.
- [20] I. M. Opsenica, M. Tot, L. Gomba, J. E. Nuss, R. J. Sciotti, S. Bavari, J. C. Burnett, B. A. Šolaja: **4-Amino-7-chloroquinolines: probing ligand efficiency provides *Botulinum* neurotoxin serotype a light chain inhibitors with significant antiprotozoal activity**. *J. Med. Chem.* **2013**, *56*, 5860-5871.
- [21] M. Delves, D. Plouffe, C. Scheurer, S. Meister, S. Wittlin, E. A. Winzeler, R. E. Sinden, D. Leroy: **The activities of current antimalarial drugs on the life cycle stages of *Plasmodium*: a comparative study with human and rodent parasites**. *PLOS Med.* **2012**, *9*, e1001169.
- [22] M. Schlitzer: **Malaria chemotherapeutics part I: history of antimalarial drug development, currently used therapeutics, and drugs in clinical development**. *ChemMedChem* **2007**, *2*, 944-986.
- [23] E. A. Winzeler: **Malaria research in the post-genomic era**. *Nature* **2008**, *455*, 751.
- [24] U. E. Odoh, P. F. Uzor, C. L. Eze, T. C. Akunne, C. M. Onyegbulam, P. O. Osadebe: **Medicinal plants used by the people of Nsukka local government area, south-eastern Nigeria for the treatment of malaria: an ethnobotanical survey**. *J. Ethnopharmacol.* **2018**, *218*, 1-15.

- [25] S. Suleman, T. B. Tufa, D. Kebebe, S. Belew, Y. Mekonnen, F. Gashe, S. Mussa, E. Wynendaele, L. Duchateau, B. De Spiegeleer: **Treatment of malaria and related symptoms using traditional herbal medicine in Ethiopia.** *J. Ethnopharmacol.* **2018**, *213*, 262-279.
- [26] G. Alebie, B. Urga, A. Worku: **Systematic review on traditional medicinal plants used for the treatment of malaria in Ethiopia: trends and perspectives.** *Malar. J.* **2017**, *16*, 307.
- [27] L. N. Bonkian, R. S. Yerbanga, M. Traoré, T. Lefevre, I. Sangaré, T. Ouédraogo, O. Traoré, J. B. Ouédraogo, T. R. Guiguemdé: **Plants against malaria and mosquitoes in Sahel region of Burkina Faso: an ethno-botanical survey.** *Int. J. Herb. Med.* **2017**, *5(3)*, 82-87.
- [28] D. E. N. Mabogo: **The ethnobotany of the Vhavenda.** University of Pretoria **1990**.
- [29] E. A. Prozesky, J. J. M. Meyer, A. I. Louw: **In vitro antiplasmodial activity and cytotoxicity of ethnobotanically selected South African plants.** *J. Ethnopharmacol.* **2001**, *76*, 239-245.
- [30] P. Pillay, V. J. Maharaj, P. J. Smith: **Investigating South African plants as a source of new antimalarial drugs.** *J. Ethnopharmacol.* **2008**, *119*, 438-454.
- [31] F. Kasali, A. Mahano, D. Nyakabwa, N. Kadima, F. Misakabu, D. Tshibangu, K. Ngbolua, P. Mpiana: **Ethnopharmacological survey of medicinal plants used against malaria in Bukavu city (DR Congo).** *Eur. J. Med. Plants* **2014**, *4*, 29.
- [32] F. Kasali, A. Mahano, N. Kadima, P. Mpiana, K. Ngbolua, T. Tshibangu: **Ethnopharmacological survey of medicinal plants used against malaria in Butembo city (DR Congo).** *J. Adv. Botany Zool.* **2014**, *1*.
- [33] L. Tona, N. P. Ngimbi, M. Tsakala, K. Mesia, K. Cimanga, S. Apers, T. De Bruyne, L. Pieters, J. Totté, A. J. Vlietinck: **Antimalarial activity of 20 crude extracts from nine African medicinal plants used in Kinshasa, Congo.** *J. Ethnopharmacol.* **1999**, *68*, 193-203.
- [34] L. Tona, R. K. Cimanga, K. Mesia, C. T. Musuamba, T. D. Bruyne, S. Apers, N. Hernans, S. Van Miert, L. Pieters, J. Totté, A. J. Vlietinck: **In vitro antiplasmodial activity of extracts and fractions from seven medicinal plants used in the Democratic Republic of Congo.** *J. Ethnopharmacol.* **2004**, *93*, 27-32.
- [35] J. D. Phillipson: **Phytochemistry and medicinal plants.** *Phytochemistry* **2001**, *56*, 237-243.
- [36] T. Okpekon, S. Yolou, C. Gleye, F. Roblot, P. Loiseau, C. Bories, P. Grellier, F. Frappier, A. Laurens, R. Hocquemiller: **Antiparasitic activities of medicinal plants used in Ivory Coast.** *J. Ethnopharmacol.* **2004**, *90*, 91-97.
- [37] G. N. Zirihi, L. Mambu, F. Guédé-Guina, B. Bodo, P. Grellier: **In vitro antiplasmodial activity and cytotoxicity of 33 West African plants used for treatment of malaria.** *J. Ethnopharmacol.* **2005**, *98*, 281-285.
- [38] H. T. Simonsen, J. B. Nordskjold, U. W. Smitt, U. Nyman, P. Palpu, P. Joshi, G. Varughese: **In vitro screening of Indian medicinal plants for antiplasmodial activity.** *J. Ethnopharmacol.* **2001**, *74*, 195-204.
- [39] L. H. Carvalho, M. G. Brandão, D. Santos-Filho, J. L. Lopes, A. U. Krettli: **Antimalarial activity of crude extracts from Brazilian plants studied in vivo in Plasmodium berghei-infected mice and in vitro against Plasmodium falciparum in culture.** *Braz. J. Med. Biol. Res.* **1991**, *24*, 1113-1123.

- [40] K. Kaur, M. Jain, T. Kaur, R. Jain: **Antimalarials from nature**. *Bioorg. Med. Chem.* **2009**, *17*, 3229-3256.
- [41] M. H. Bule, I. Ahmed, F. Maqbool, M. A. Zia: **Quinazolinone derivatives as a potential class of compounds in malaria drug discovery**. *Int. J. Pharmacol.* **2017**, *13*, 818-831.
- [42] M. Rudrapal, D. Chetia: **Plant flavonoids as potential source of future antimalarial leads**. *Syst. Rev. in Pharmacy* **2017**, *8*, 13.
- [43] M. Vanaerschot, L. Lucantoni, T. Li, J. M. Combrinck, A. Ruecker, T. S. Kumar, K. Rubiano, P. E. Ferreira, G. Siciliano, S. Gulati: **Hexahydroquinolines are antimalarial candidates with potent blood-stage and transmission-blocking activity**. *Nat. Microbiol.* **2017**, *2*, 1403.
- [44] F. Ntie-Kang, P. A. Onguéné, L. L. Lifongo, J. C. Ndom, W. Sippl, L. M. a. Mbaze: **The potential of anti-malarial compounds derived from African medicinal plants, part II: a pharmacological evaluation of non-alkaloids and non-terpenoids**. *Malar. J.* **2014**, *13*, 81.
- [45] P. A. Onguéné, F. Ntie-Kang, L. L. Lifongo, J. C. Ndom, W. Sippl, L. M. a. Mbaze: **The potential of anti-malarial compounds derived from African medicinal plants. Part I: a pharmacological evaluation of alkaloids and terpenoids**. *Malar. J.* **2013**, *12*, 449.
- [46] A. B. Oliveira, M. F. Dolabela, F. C. Braga, R. L. R. P. Jácome, F. P. Varotti, M. M. Póvoa: **Plant-derived antimalarial agents: new leads and efficient phytomedicines. Part I. Alkaloids**. *An. Acad. Bras. Ciênc.* **2009**, *81*, 715-740.
- [47] R. Batista, A. De Jesus Silva Júnior, A. B. De Oliveira: **Plant-derived antimalarial agents: new leads and efficient phytomedicines. Part II. Non-alkaloidal natural products**. *Molecules* **2009**, *14*, 3037.
- [48] G. Bringmann, S. K. Bischof, S. Müller, T. Gulder, C. Winter, A. Stich, H. Moll, M. Kaiser, R. Brun, J. Dreher, K. Baumann: **QSAR guided synthesis of simplified antiplasmodial analogs of naphthylisoquinoline alkaloids**. *Eur. J. Med. Chem.* **2010**, *45*, 5370-5383.
- [49] E. Leete: **Biosynthesis of quinine and related alkaloids**. *Acc. Chem. Res.* **1969**, *2*, 59-64.
- [50] S. Tagboto, S. Townson: **Antiparasitic properties of medicinal plants and other naturally occurring products**. *Adv. Parasitol.* **2001**, *50*, 199-295.
- [51] J. Achan, A. O. Talisuna, A. Erhart, A. Yeka, J. K. Tibenderana, F. N. Baliraine, P. J. Rosenthal, U. D'Alessandro: **Quinine, an old anti-malarial drug in a modern world: role in the treatment of malaria**. *Malar. J.* **2011**, *10*, 144.
- [52] L. Cui, S. Mharakurwa, D. Ndiaye, P. K. Rathod, P. J. Rosenthal: **Antimalarial drug resistance: literature review and activities and findings of the ICEMR network**. *Am. J. Trop. Med. Hyg.* **2015**, *93*, 57-68.
- [53] Z. Guo: **Artemisinin anti-malarial drugs in China**. *Acta Pharm. Sin. B.* **2016**, *6*, 115-124.
- [54] D. Klayman, **Qinghaosu (artemisinin): an antimalarial drug from China**. *Science* **1985**, *228*, 1049-1055.
- [55] J. Chao, Y. Dai, R. Verpoorte, W. Lam, Y.-C. Cheng, L.-H. Pao, W. Zhang, S. Chen: **Major achievements of evidence-based traditional Chinese medicine in treating major diseases**. *Biochem. Pharmacol.* **2017**, *139*, 94-104.
- [56] M. A. Avery, K. M. Muraleedharan, P. V. Desai, A. K. Bandyopadhyaya, M. M. Furtado, B. L. Tekwani: **Structure - activity relationships of the antimalarial**

- agent artemisinin. **8. Design, synthesis, and comfa studies toward the development of artemisinin-based drugs against leishmaniasis and malaria.** *J. Med. Chem.* **2003**, *46*, 4244-4258.
- [57] P. Trigg: **Qinghaosu (artemisinin) as an antimalarial drug.** *Econ. Med. Plant Res.* **1989**, *3*, 19-55.
- [58] P. J. Rosenthal: **Antimalarial drug discovery: old and new approaches.** *J. Exp. Biol.* **2003**, *206*, 3735-3744.
- [59] A. P. Phyo, K. K. Win, A. M. Thu, L. L. Swe, H. Htike, C. Beau, K. Sriprawat, M. Winterberg, S. Proux, M. Imwong, E. A. Ashley, F. Nosten: **Poor response to artesunate treatment in two patients with severe malaria on the Thai–Myanmar border.** *Malar. J.* **2018**, *17*, 30.
- [60] Centers for Disease Control and Prevention: **Where malaria occurs.** **2017, March 17.**
- [61] World Health Organization: **Malaria.** **2018.**
- [62] D. Menard, A. Dondorp: **Antimalarial drug resistance: a threat to malaria elimination.** *Cold Spring Harb. Perspect. Med.* **2017**, *7*.
- [63] S. Bhatt, D. J. Weiss, E. Cameron, D. Bisanzio, B. Mappin, U. Dalrymple, K. E. Battle, C. L. Moyes, A. Henry, P. A. Eckhoff, E. A. Wenger, O. Briët, M. A. Penny, T. A. Smith, A. Bennett, J. Yukich, T. P. Eisele, J. T. Griffin, C. A. Fergus, M. Lynch, F. Lindgren, J. M. Cohen, C. L. J. Murray, D. L. Smith, S. I. Hay, R. E. Cibulskis, P. W. Gething: **The effect of malaria control on *Plasmodium falciparum* in Africa between 2000 and 2015.** *Nature* **2015**, *526*, 207.
- [64] K. M. Tun, M. Imwong, K. M. Lwin, A. A. Win, T. M. Hlaing, T. Hlaing, K. Lin, M. P. Kyaw, K. Plewes, M. A. Faiz, M. Dhorda, P. Y. Cheah, S. Pukrittayakamee, E. A. Ashley, T. J. C. Anderson, S. Nair, M. McDew-White, J. A. Flegg, E. P. M. Grist, P. Guerin, R. J. Maude, F. Smithuis, A. M. Dondorp, N. P. J. Day, F. Nosten, N. J. White, C. J. Woodrow: **Spread of artemisinin-resistant *Plasmodium falciparum* in Myanmar: a cross-sectional survey of the K13 molecular marker.** *Lancet Infect. Dis.* **2015**, *15*, 415-421.
- [65] H. A. Antony, S. C. Parija: **Antimalarial drug resistance: an overview.** *Trop. Parasitol.* **2016**, *6*, 30-41.
- [66] R. Leang, W. R. J. Taylor, D. M. Bouth, L. Song, J. Tarning, M. C. Char, S. Kim, B. Witkowski, V. Duru, A. Domergue, N. Khim, P. Ringwald, D. Menard: **Evidence of *Plasmodium falciparum* malaria multidrug resistance to artemisinin and piperazine in Western Cambodia: dihydroartemisinin-piperazine open-label multicenter clinical assessment.** *Antimicrob. Agents Chemother.* **2015**, *59*, 4719-4726.
- [67] D. Menard, F. Ariey: **Towards real-time monitoring of artemisinin resistance.** *Lancet Infect. Dis.* **2015**, *15*, 367-368.
- [68] C. H. Sibley: **Tracking artemisinin resistance in *Plasmodium falciparum*.** *Lancet Infect. Dis.* **2013**, *13*, 999-1000.
- [69] L. Tilley, J. Straimer, N. F. Gnädig, S. A. Ralph, D. A. Fidock: **Artemisinin action and resistance in *Plasmodium falciparum*.** *Trends Parasitol.* **2016**, *32*, 682-696.
- [70] K. Katsuno, J. N. Burrows, K. Duncan, R. H. van Huijsduijnen, T. Kaneko, K. Kita, C. E. Mowbray, D. Schmatz, P. Warner, B. T. Slingsby: **Hit and lead criteria in drug discovery for infectious diseases of the developing world.** *Nat. Rev. Drug Discov.* **2015**, *14*, 751.
- [71] B. K. Lombe, T. Bruhn, D. Feineis, V. Mudogo, R. Brun, G. Bringmann: **Antiprotozoal spirombandakamines A<sub>1</sub> and A<sub>2</sub>, fused**

- naphthylisoquinoline dimers from a Congolese *Ancistrocladus* plant. *Org. Lett.* **2017**, *19*, 6740-6743.
- [72] B. K. Lombe, T. Bruhn, D. Feineis, V. Mudogo, R. Brun, G. Bringmann: **Cyclombandakamines A<sub>1</sub> and A<sub>2</sub>, oxygen-bridged naphthylisoquinoline dimers from a Congolese *Ancistrocladus* liana.** *Org. Lett.* **2017**, *19*, 1342-1345.
- [73] B. K. Lombe, D. Feineis, V. Mudogo, R. Brun, S. Awale, G. Bringmann: **Michellamines A<sub>6</sub> and A<sub>7</sub>, and further mono- and dimeric naphthylisoquinoline alkaloids from a Congolese *Ancistrocladus* liana and their antiausterity activities against pancreatic cancer cells.** *RSC Adv.* **2018**, *8*, 5243-5254.
- [74] D. T. Tshitenge, D. Feineis, V. Mudogo, M. Kaiser, R. Brun, E.-J. Seo, T. Efferth, G. Bringmann: **Mbandakamine-type naphthylisoquinoline dimers and related alkaloids from the Central African liana *Ancistrocladus ealaensis* with antiparasitic and antileukemic activities.** *J. Nat. Prod.* **2018**, *81*, 918-933.

## Chapter 2

# Isolation and structural elucidation of naphthylisoquinoline alkaloids from an as yet unidentified *Ancistrocladus* species

### 2.1 Background to Ancistrocladaceae

#### 2.1.1 Geographic distribution and classification

The Ancistrocladaceae are a small monogeneric family classified in the Caryophyllales. They grow mainly in the evergreen forest of South and Southeast Asia, and of tropical Africa<sup>[1-3]</sup> (Figure 2.1). *Ancistrocladus* Wall is the only genus belonging to in this family, which has 19 species that have so far been accepted botanically, with 13 from Africa and six from Asia.<sup>[4-6]</sup> They are found in primary, secondary, and seasonal inundated riverside forests, along roadsides, swamps, in cultivated, and other disturbed areas.<sup>[3]</sup> Four species have been described from the rain forest of the Democratic Republic of the Congo (DRC). These are *A. ealaensis* J. Léonard, *A. congolensis* J. Léonard, *A. likoko* J. Léonard, and *A. ileboensis* Heubl, Mudogo & G. Bringmann. However, it is still probable that the number of species or sub-species from DRC may be more than four.<sup>[7, 8]</sup> The reason for this assumption is the fact that many samples of yet unidentified *Ancistrocladus* species have been collected and chemically investigated from different locations of the Congolese rain forest such as the region of the town Ikela,<sup>[9]</sup> vicinity of the village Yafunga,<sup>[7]</sup> and near the town of Mbandaka,<sup>[10]</sup> with sometimes new morphological features and/or chemical patterns.



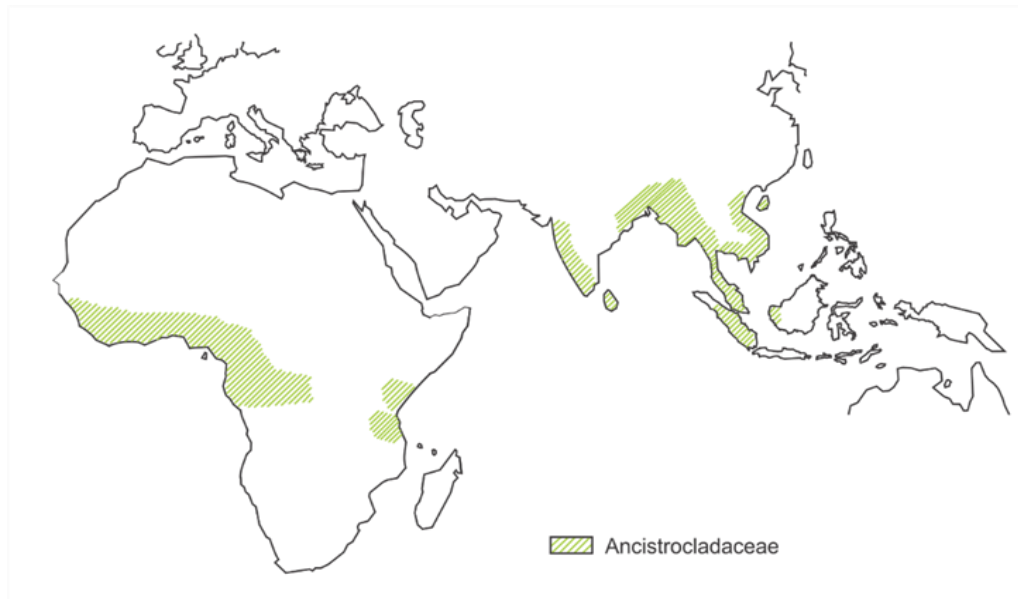


**Figure 2.1:** Ancistrocladaceae sites in tropical Africa and in South and Southeast Asia.

### 2.1.2 Botany

All *Ancistrocladus* species are woody lianas. They start their growth as a self-supporting, monopodial sapling, and then turn to a sympodial liana that climbs by means of woody hooks, recurved to spiraling.<sup>[3, 8]</sup>

The leaves are simple, alternate, entire, and spiraled. They have, on both surfaces, cone-like depressions, and minute epidermal pits containing one trichome each, which secretes a waxy exudate. The pits are sometimes found on sepals as well. The latter are four to five and imbricate. The leaves and sepals bear various other forms of glands. The petals are four to five, mostly imbricate in bud or convolute, and connate at their bases or very shortly coherent. They may be white, yellow, orange, or pink to red. The inflorescences are bracteates, indeterminate, usually pedunculated, and several flowered. The flowers are usually 5 to 12 mm wide, actinomorphic, and bisexual. With regards to fruits and seeds, the nuts are dry indehiscent, and the seeds relatively large, solitary, and deeply ruminant<sup>[3]</sup> (Figure 2.2).



**Figure 2.2:** (A) Fully developed flower of *A. ikela* at anthesis; (B) Inflorescence of *A. congolensis*; (C) Leaves and inflorescences of *A. ikela*.

### 2.1.3 Traditional uses of *Ancistrocladus* sp.

Some traditional usages of species from the Ancistrocladaceae family have been reported. Indeed, *Ancistrocladus* species are used in the traditional medicine of some countries in West Africa, and of South and Southeast Asia for the treatment of malaria, dysentery, leprosy, fever, and measles.<sup>[11]</sup> *Ancistrocladus tectorius* is used in Malaysia, Thailand, and China to treat malaria, dysentery, parasite infections, and venomous-bite snakes.<sup>[12, 13]</sup> *Ancistrocladus abbreviatus* is used for the treatment of measles and fevers.<sup>[11]</sup>

The *Ancistrocladus* species growing in the Yangole region (DRC) is used by the local community as a source of water by hunters and farmers (personal communication of the collector). They cut open the liana and drink the water that runs out.

## 2.2 Naphthylisoquinoline alkaloids and their isolation and identification

### 2.2.1 Structural types and nomenclature

Structurally, naphthylisoquinoline (NIQ) alkaloids are built up from a naphthalene and an isoquinoline moiety, linked *via* a C,C- or N,C-biaryl axis. The isoquinoline part can either be di-, or tetrahydrogenated, or fully aromatic. Due to bulky *ortho*-substituents, most of these compounds display the phenomenon of atropisomerism. The several possibilities of the position of the biaryl axis between the two moieties, the oxygen substitution pattern, the stereocenters in the isoquinoline portion, and the site of dimerization lead to a great structural variability within this class of compounds.<sup>[14]</sup> So far, 5,1'- [like e.g. 6-O-methylancistectorine A<sub>3</sub> (**23**)], 5,3'- [like e.g. ancistrotectorine C (**24**)], 5,8'- [like e.g. ancistrolikokine G (**25**)], 7,1'- [like e.g. ancistrocongoline D (**27**)], 7,3'- [like e.g. ancistroheynine B (**26**)], 7,6'- [like e.g. dioncophyllinol B (**29**)], 7,8'- [like e.g. ancistroheynine A (**28**)], N,8'- [like e.g. ancisheynine (**30**)], and N,6'-coupled naphthylisoquinoline alkaloids have been isolated<sup>[12, 15]</sup> (for the structures, see Figure 2.4). Ancistrocladaceae-type alkaloids are oxygenated at C-6 and S-configured at C-3, while Dioncophyllaceae-type compounds lack an oxygen at C-6 and are R-configured at C-3. Yet, hybrid compounds, which have a combination of these characteristics, have also been isolated.<sup>[16, 17]</sup> Furthermore, dimers with up to three consecutive stereogenic biaryl axis [shuangancistrotectorine A (**31**)] have been isolated, as well as oxidized naphthylisoquinoline alkaloids.<sup>[11]</sup>

For reasons of better comparison among NIQs of different coupling types, the atom numbering in the naphthalene part does not strictly follow the IUPAC rules, but throughout attributes a 2-methyl-4,5-dioxy substitution pattern to the naphthalene, regardless of the site of the axis<sup>[18]</sup> (see Figure 2.3).

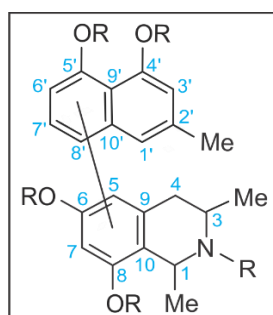


**Figure 2.3:** Atom numbering in NIQs.

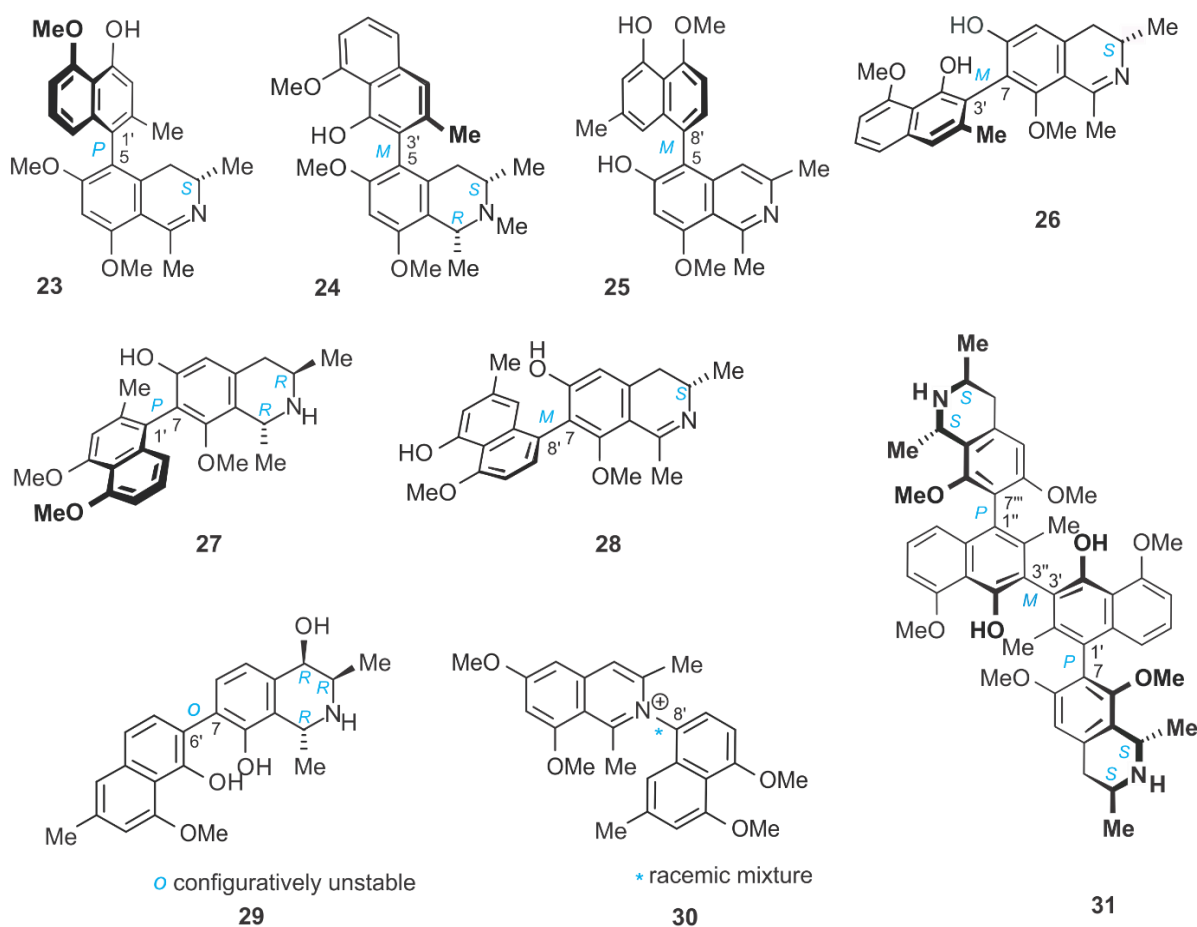


**Figure 2.4:** Structures of naphthylisoquinoline alkaloids showing different coupling types: 6-O-methylancistectorine A<sub>3</sub> (**23**), ancistrotectorine C (**24**), ancistrollokine G (**25**), ancistroheynine B (**26**), ancistrocongoline D (**27**), ancistroheynine A (**28**), dioncophyllinol B (**29**), ancisheynine (**30**), and shuangancistrotectorine A (**31**).

In order to avoid lengthy rational nomenclature, trivial names are given to naphthylisoquinoline alkaloids. Thus, the name may refer to the species, from which the compound was isolated (e.g. ancistrotanzanine A from *Ancistrocladus tanzaniensis*),<sup>[19]</sup> or it might be related to the site where the species that provided the compound occurs (e.g. mbandakamine A, obtained from an unidentified *Ancistrocladus* species collected near Mbandaka),<sup>[20]</sup> or it corresponds to some structural features explained with a word from another language (e.g. the dimer shuangancistrotectorine A, derived from the word “*shuang*” in Chinese, which means “pair”, or “couple”).<sup>[21]</sup>

Mass spectrometry (MS), infrared spectroscopy (IR), ultraviolet spectroscopy (UV), X-ray crystallography, combustion analysis, and nuclear magnetic resonance (NMR) are techniques used to determine the structure of isolated NIQs. The most important tool for their structure elucidation is, however, NMR spectroscopy. Moreover, the determination of their full absolute stereostructures requires additional techniques and methods such as electronic circular dichroism spectroscopy (ECD) and oxidative degradation.

### 2.2.2 Extraction and purification of NIQs

Several solvents and conditions are reported for the selective extraction of NIQs. In general, NIQs are extracted from dry ground plant materials using DCM, MeOH, 95 % EtOH, DCM/MeOH (1:1 or 6:4), DCM/NH<sub>3</sub>, or acidified water (2 % HCl) after defatting the extract with petroleum ether. In some cases, the organic extracts obtained with the mentioned solvents were treated with HCl, then basified with concentrated aqueous ammonia, and the resulting sediments were partitioned between CHCl<sub>3</sub>/H<sub>2</sub>O, or *n*-BuOH/H<sub>2</sub>O, or DCM/H<sub>2</sub>O. In other cases, the extracts obtained with organic solvents were suspended in buffered (NaHCO<sub>3</sub>) H<sub>2</sub>O or H<sub>2</sub>O/MeOH, and then perfused with CHCl<sub>3</sub> or DCM.<sup>[11, 22, 23]</sup>

NIQs are purified mostly by preparative HPLC using (A) MeCN/H<sub>2</sub>O (9:1) + 0.05 % TFA and (B) H<sub>2</sub>O/MeCN (9:1) + 0.05 % TFA, or (A) MeOH/H<sub>2</sub>O (9:1) + 0.05 % TFA and (B) H<sub>2</sub>O/MeOH (9:1) + 0.05 % TFA using isocratic or gradient methods, depending on the resolution of the separation on a reverse-phase column. In some cases, chiral stationary phase columns are needed to separate stereoisomers. However, column chromatography on silica gel, preparative TLC, fast centrifugal partition chromatography (FCPC), high-speed countercurrent chromatography (HSCCC), cation-exchange chromatography (Amberlyst-15), multilayer counter current chromatography (MLCCC), and recrystallization from MeOH:H<sub>2</sub>O, acetone or *n*-hexane:*i*-propanol have also been used in the purification of NIQs. For their detection on TLC, UV at 256 and 360 nm, or Dragendorff's reagent were utilized.<sup>[16, 17, 21, 24-28]</sup> The solvent system CHCl<sub>3</sub>/MeOH (19:1) has been reported for its usage for TLC (silica gel) analysis of these compounds.<sup>[16]</sup>

### 2.2.3 Structure elucidation using NMR

NMR spectroscopy is useful for the determination of the coupling position, the relative configuration, the degree of saturation in the isoquinoline moiety, and the O-substitution patterns. To mention just a few structural features that are obtained from  $^1\text{H}$  NMR: the splitting pattern of the signals of the methyl groups at C-1 and C-3 (0.8 – 1.7 ppm) with the presence or absence of a quartet (H at position 1), multiplet (H at position 3), and two diastereotopic protons, reveal the degree of saturation of the isoquinoline moiety. Furthermore, the chemical shifts of singlets ( $\delta$  3.1 – 4.1 ppm) integrating for 3H (O-Me) and the splitting pattern of aromatic protons provide hints at the coupling position. The relative configuration of the two methyl groups at C-1 and C-3 are confirmed by nuclear Overhauser enhancement (NOE) and rotating-frame Overhauser enhancement (ROE) spectroscopies, as well as the chemical shift of H-3. When the signal of H-3 appears at  $\delta > 3$  ppm, the relative configuration is *trans*, while its *cis* isomer has  $\delta < 3$  ppm. Moreover, the relative configuration at the axis can also be deduced from NOE interactions of H-1 and/or Me-1 with aromatic protons of the naphthalene moiety or the two diastereotopic protons at C-4 with aromatic protons of the naphthalene moiety (Figure 2.5).<sup>[11, 14, 18, 29]</sup>

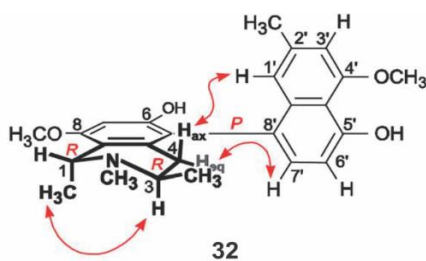


**Figure 2.5:** Ancistrolidikokine A<sub>2</sub>, used here as an example to show the use of NOE interactions (red arrows) to determine relative configuration at the stereogenic centers (Me-1 and H-3) and at the axis (interactions between H<sub>eq</sub>-4 and H-7' and between H<sub>ax</sub>-4 and H-1').<sup>[1]</sup>

### 2.2.4 Electronic circular dichroism (ECD) spectroscopy

Circular dichroism spectroscopy is an important tool for the determination of the configuration at the axis, and in the case of NIQs, electronic circular dichroism (ECD)

is the chiroptical method used because they have a distinct chromophore. Opposite enantiomers give mirror-imaged ECD spectra (Figure 2.6.A). Hence, the axial configuration can be established by comparing the ECD curve with the one of a known compound which must be structurally related and must have the same coupling type in the case of NIQs (Figure 2.6.B). In cases where there is no compound with a structural resemblance, the configuration can then be established by the quantum-chemical calculation of the ECD spectrum and comparison of the calculated curve with the experimentally measured one<sup>[30-32]</sup> (Figure 2.6.C).

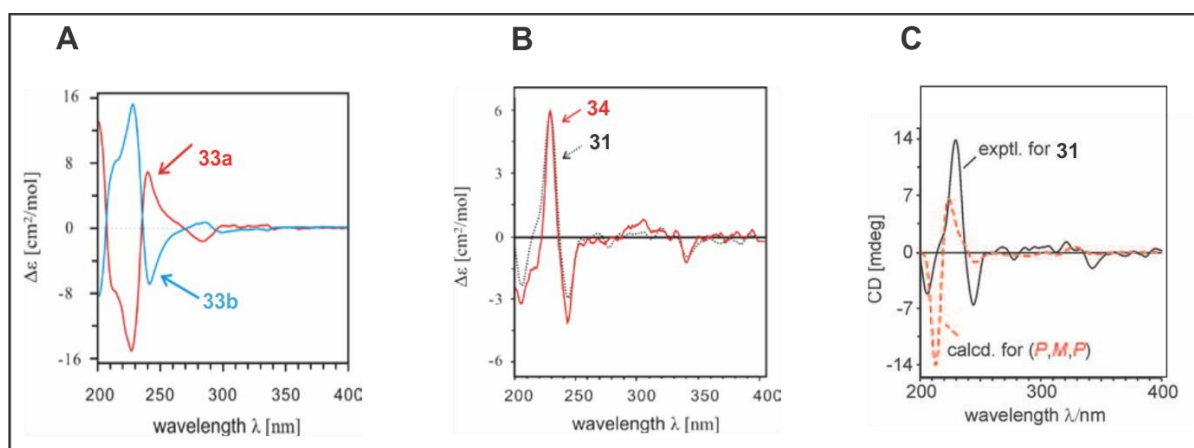


**Figure 2.6:** (A) Comparison of ECD spectra of ancistectorine A<sub>2</sub> (**33a**) and its atropo-diastereomer 5-*epi*-ancistectorine A<sub>2</sub> (**33b**), showing how their curves are opposite to each other;<sup>[9]</sup> (B) Absolute configuration at the central axis of jozimine A<sub>2</sub> (**34**) assigned by comparison of its ECD spectrum (solid line, red) with that of shuangancistroretectorine A (**31**, see Figure 2.4) (dotted line, black);<sup>[9]</sup> (C) Absolute configuration at the central axis of **31** assigned by comparison of its experimental ECD spectrum (solid line, black) with the curve calculated for *P,M,P*-configuration.<sup>[21]</sup>

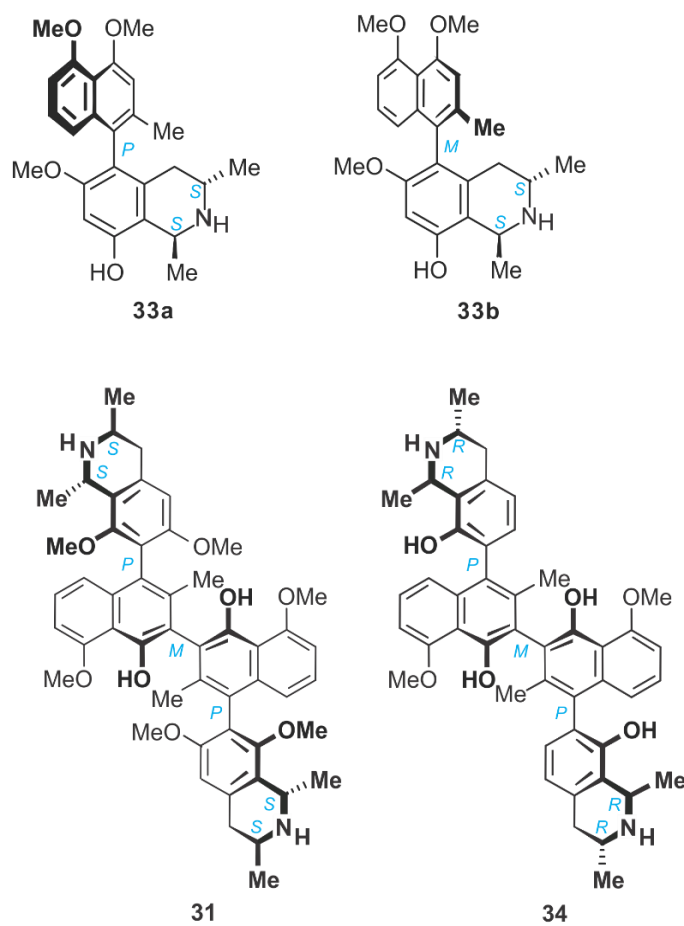


**Figure 2.7:** Structures of ancistectorine A<sub>2</sub> (**33a**), 5-*epi*-ancistectorine A<sub>2</sub> (**33b**), shuangancistroretorine A (**31**) (the structure has been repeated for comparison purpose with jozimine A<sub>2</sub>), and jozimine A<sub>2</sub> (**34**).

### 2.2.5 Oxidative degradation

To determine the absolute configuration at the stereocenters C-1 and C-3 of NIQs, a ruthenium-mediated oxidative degradation resulting in simple and easy-to-analyze amino acids, alanine (Ala) and 3-aminobutyric acid (ABA) has been developed by Prof. G. Bringmann's research group in Würzburg.<sup>[33, 34]</sup> Treatment of 1,3-dimethyldi- and tetrahydroisoquinolines with NaIO<sub>4</sub> and catalytic amounts of ruthenium trichloride leads to the formation of alanine and 3-aminobutyric acid (Figure 2.8). They carry the information about the absolute configuration as C-1 and C-3, respectively, which can be determined after conversion of the amino acids obtained to their methyl esters and Mosher-type derivatization with the acid chloride of *S*- $\alpha$ -methoxy- $\alpha$ -



trifluoromethylphenylacetic acid (i.e with (R)-MTPA-Cl) by gas chromatography with mass-selective detection (GC-MSD), and comparison with standard amino acid derivatives of known configuration. For *cis*-configured 1,3-dimethyltetrahydroisoquinoline NIQs, however, only the configuration at C-3 can be reliably determined because of a rapid oxidation of C-1 which convert the *cis*-configured NIQ to its corresponding dihydroisoquinoline. Thus, the degradation produces only 3-aminobuturic acid from C-3 and very little or not alanine from C-1. This is explained by the fact that the strictly equatorial position of H-1 in *trans*-configured NIQs gives them a strong resistance to oxidative dihydroisoquinoline formation, while in the case of *cis*-configured alkaloids, the imine formation that precedes the C-N cleavage reaction occurs so rapidly and hence destroys the stereochemical information at C-1 by producing the corresponding dihydroisoquinoline. Therefore, the absolute configuration at C-1 can then only be deduced from its relative configuration to C-3 as obtained from NMR.<sup>[33, 34]</sup>

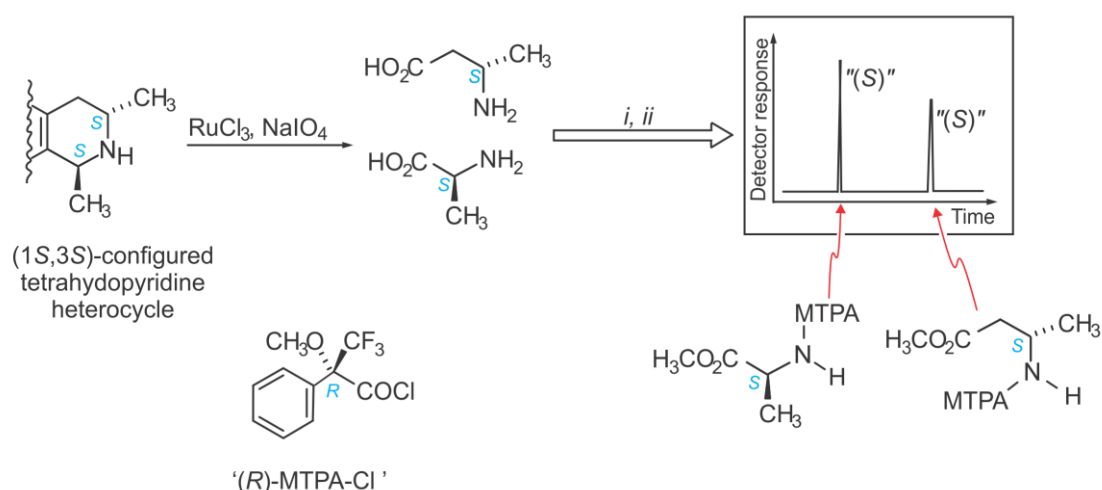


**Figure 2.8:** Scheme of ruthenium-mediated oxidative degradation of the isoquinoline moiety of NIQs and schematic chromatogram of the resulting amino acids after Mosher-type derivatization. (i) MeOH, SOCl<sub>2</sub>; (ii) '(R)-MTPA-Cl', NEt<sub>3</sub>.<sup>[34]</sup>

## 2.2.6 Biosynthesis

NIQs are built up from acetate units.<sup>[35]</sup> Both of the two moieties (the naphthalene portion and the isoquinoline part) follow an acetate-malonate biosynthetic pathway

being each formed from six acetate units via the same  $\beta$ -pentaketo precursor. Hence, they are both formed by cyclization, divergently, by a second aldol condensation in the case of the naphthalene and by nitrogen incorporation in the case of the isoquinoline moiety. Thereafter, through oxidative phenolic biaryl coupling, the two moieties are connected to provide the complete NIQ molecule. Several metabolic transformations (oxidation, reduction, O- or N-methylation, and, in some cases, dimerization) provide all of the structurally so diverse NIQs (Figure 2.9).<sup>[9, 36]</sup>

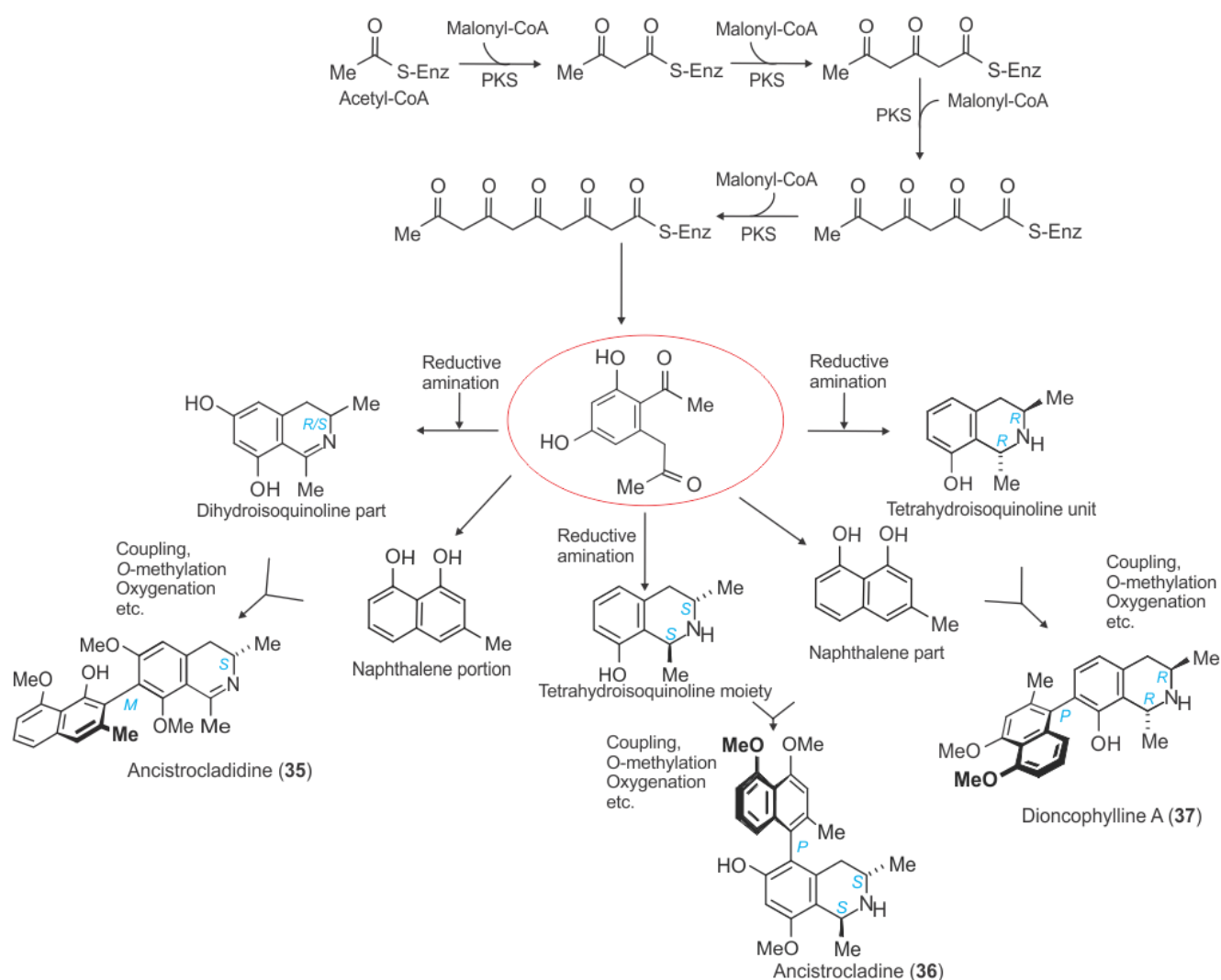


**Figure 2.9:** Biosynthetic pathways to naphthylisoquinoline alkaloids with ancistrocladine (**35**), ancistrocladine (**36**), and dioncophylline A (**37**) as examples.<sup>[11]</sup>

## 2.2.7 Naphthylisoquinoline alkaloids and antiplasmodial activity

Naphthylisoquinoline alkaloids have shown an attractive spectrum of biological activities including antileishmanial, antitrypanosomal,<sup>[37]</sup> antimicrobial,<sup>[38]</sup> fungicidal,<sup>[39]</sup> anti-HIV,<sup>[40]</sup> antileukemic,<sup>[5, 41]</sup> and spasmolytic<sup>[2]</sup> potencies, with all these findings being results of extensive research of Prof. G. Bringmann's group at the University of Würzburg in collaboration with their partners.

Furthermore, many NIQs have shown antiplasmodial activity, ranging from moderate to excellent activity; the structures of some of them are shown in Figure 2.10.

*N*-methylancistectorine A<sub>1</sub> (**38**), ancistectorine A<sub>2</sub> (**33a**, see Figure 2.7), and 5-*epi*-ancistectorine A<sub>2</sub> (**33b**, see Figure 2.7) were reported to have strong antiplasmodial activity against the resistant *P. falciparum* K1 strains with respective IC<sub>50</sub> values of 0.08, 0.07, and 0.03 μM. They were assayed together with chloroquine as a standard and were three to seven times more active than chloroquine.<sup>[42]</sup>

Jozimine A<sub>2</sub> (**34**, see Figure 2.7), which was isolated from an *Ancistrocladus* species collected in the DRC, in the region of the town Ikela, exhibited an excellent antiplasmodial activity against *P. falciparum* NF54 strains with IC<sub>50</sub> value of 1.4 nM, once again more active than the standard used in the assay, chloroquine (IC<sub>50</sub> value 3 nM).<sup>[17]</sup>

Moreover, *Triphyophyllum peltatum* (Dioncophyllaceae) provided two excellent active NIQs, dioncophylline C (**39**), and dioncopeltine A (**40**). They both showed strong potency against NF54 strains of *P. falciparum*, with IC<sub>50</sub> values of 0.04 and 0.05 μM, respectively.<sup>[2, 43]</sup> Further, these two compounds have shown activity against *P. berghei* (ANKA) both *in vitro* (IC<sub>50</sub> values 0.04 μM and 0.1 μM, respectively) and *in vivo* (they both cured infected mice almost completely after oral treatment with 50 mg/kg of body weight per day for four days without noticeable toxic effects).<sup>[43-45]</sup>

Dioncophylline A (**37**, see Figure 2.9) and dioncophyllacine A (**41**), discovered in *T. peltatum*, showed excellent potency against exoerythrocytic stages of *P. berghei* (ANKA) with 67.5 % and 41.9 % inhibition at 26.5 μM, respectively. Ancistrobarterine A (**42**), found in *Ancistrocladus barteri*, exhibited strong activity with 51.6 % inhibition at 24.0 μM, while the standard, primaquine, within the same assay showed 62.1 % inhibition at 96.4 μM.<sup>[46, 47]</sup>



### 2.3.2 Processing and extraction

The leaves were air-dried at room temperature in trays and then pulverized. Powdered leaves (320 g) were extracted three times in an Erlenmeyer flask with continuous stirring for 12 h with *n*-hexane and with filtration between each extraction. The solvent was evaporated in a rotary evaporator yielding a total of 6.37g of *n*-hexane extract. The resulting Residue 1 (as labeled in Figure 2.11) was air-dried at room temperature, transferred to an Erlenmeyer flask, and extracted three times with dichloromethane (DCM) under constant agitation for 12 h. The solution was filtered to provide the Residue 2 and filtrate. The latter was dried under reduced pressure to yield 7.19 g of DCM extract. Residue 2 was likewise treated and further extracted three times with ethyl acetate. The separation of the filtrate and Residue 3 provided 0.98 g of the dry ethyl acetate extract after evaporation of the solvent. The process was repeated on the Residue 3 with MeOH and then water yielding 29.6 g and 5.84 g of respective dry extracts.

All extracts, except for the *n*-hexane extract, which contained non-polar compounds, were screened for their antiplasmodial activity. The MeOH extract showed the best activity (100 % inhibition at 20 and 10 µg/mL) and was used to pursue the fractionation.

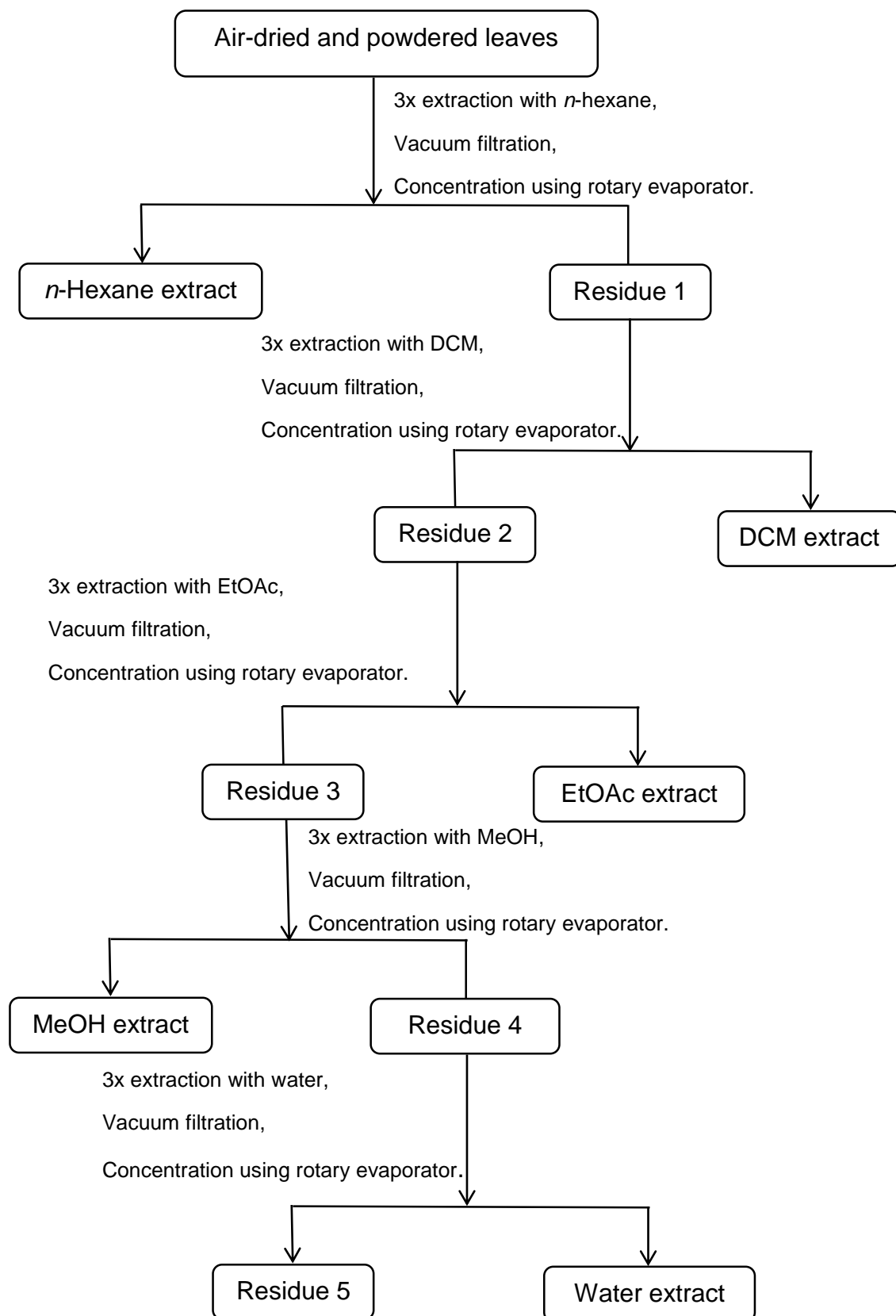


**Figure 2.11:** Flow diagram for sequential extraction of leaf material of *Ancistrocladus*.

### 2.3.3 Fractionation using silica gel column chromatography

The MeOH extract (13.0 g) was fractionated by column chromatography using silica gel treated with 0.1 % triethylamine. The column was first eluted with 100% DCM followed by gradually increasing the polarity with 5 % MeOH in DCM and going up to 25 % of MeOH in 5% increments. Further, the elution was done with 100 % MeCOMe followed by 10 % MeOH in MeCOMe and increasing to 20 % of MeOH in MeCOMe. Finally, the column was washed with mixture of MeCOMe, MeOH, and water (70:20:10). The separation provided 24 fractions, which were analyzed by TLC. Four different solvent systems were used for TLC analysis. These were DCM/MeOH (19:1), DCM/MeOH (18:2), DCM/MeOH (17:3), and DCM/MeOH/formic acid (16:3:1). The TLC plates were visualized under UV at 256 and 366 nm, then stained by spraying with Dragendorff's reagent. Fractions 1 to 4, 7 and 8, 9 and 10, and finally 11 and 12, were combined separately based on the similarity of their TLC profiles. A total of 18 fractions were finally obtained labeled as F<sub>1</sub> to F<sub>18</sub>.

The fractions (F<sub>2</sub>, F<sub>4</sub> to F<sub>7</sub>) containing mainly NIQs as determined through their UPLC-QTOF-MS profiles were screened for their antiplasmodial activity. They all exhibited good activity (> 95 % inhibition at 10 and 5 µg/mL) and were all considered for purification through HPLC and LC-MS-SPE-NMR.

### 2.3.4 HPLC purification and analysis

#### 2.3.4.1 High-performance liquid chromatography (HPLC)

Fraction 2 (F<sub>2</sub>, 50 mg), as shown in Figure 2.12, was resolved by using mass directed purification by preparative HPLC (Waters system 2998 with QDa mass spectrometer detector) on an XBridge Prep C<sub>18</sub> column using the solvents A = H<sub>2</sub>O + 0.1 % NH<sub>4</sub>OH and B = MeCN. This separation gave four semi-pure subfractions that were collected based on their molecular ion mass in electrospray positive mode. The constitution of one compound in Subfraction 3, **46**, was elucidated and its relative configuration determined by using NMR and MS (see Section 2.4.6).

Fractions F<sub>1</sub> (37 mg), F<sub>5</sub> (128 mg), and F<sub>7</sub> (127 mg) were purified by HPLC (Waters 600 system) on a Phenomenex C<sub>18</sub> column using the solvents A = H<sub>2</sub>O/MeCN (9:1) +

0.05 % TFA and B = H<sub>2</sub>O/MeCN (1:9) + 0.05 % TFA in a gradient mode. The collection was done manually based on the UV absorbance of the compounds as they eluted.

The purification of F<sub>1</sub> provided two pure compounds: ancistrocyclinone A (**45**, see Figure 2.13), retention time (RT): 17.2 min, and ancistrocladinium A (**44**, see Figure 2.13), RT: 30.5 min, and three other subfractions. Their structures were determined by using NMR, MS, and ECD spectra. The separation of F<sub>5</sub> resulted in eleven subfractions and one pure compound, which was identified as ancistrocladinium A (**44**) by its NMR, MS, and UV spectra. The purification of F<sub>7</sub> resulted in eleven subfractions, which were analyzed by MS and NMR and were found to be still most complex mixtures.

F<sub>6</sub> (400 mg) was purified by preparative HPLC (Waters system 2767) on an XBridge Prep C<sub>18</sub> column using the solvents A = H<sub>2</sub>O + 0.05 % TFA and B = MeCN + 0.05 % TFA in a gradient mode. The separation resulted in 19 subfractions and one pure compound. They were collected based on their UV absorbance as the compounds eluted. The pure compound was identified as ancistrocladinium A (**44**) by <sup>1</sup>H NMR, MS, and UV spectra.

#### **2.3.4.2 Hyphenated liquid chromatography - mass spectrometry - solid-phase extraction – nuclear magnetic resonance (LC-MS-SPE-NMR)**

Subfraction 5 (24 mg) obtained from semi-preparative HPLC of F<sub>5</sub> (F<sub>5</sub>SF<sub>5</sub>, see Figure 2.12) was further resolved by LC-MS-SPE-NMR (Agilent Technologies 1200 Infinity Series) using 45 % of MeOH in H<sub>2</sub>O containing 0.1 % TFA (isocratic) (flow: 0.5 mL/min) on a reversed phase to give compound **43** (ealamine A, see Figure 2.13) described in Section 2.4.6 (1.6 mg, RT: 20.6 min).



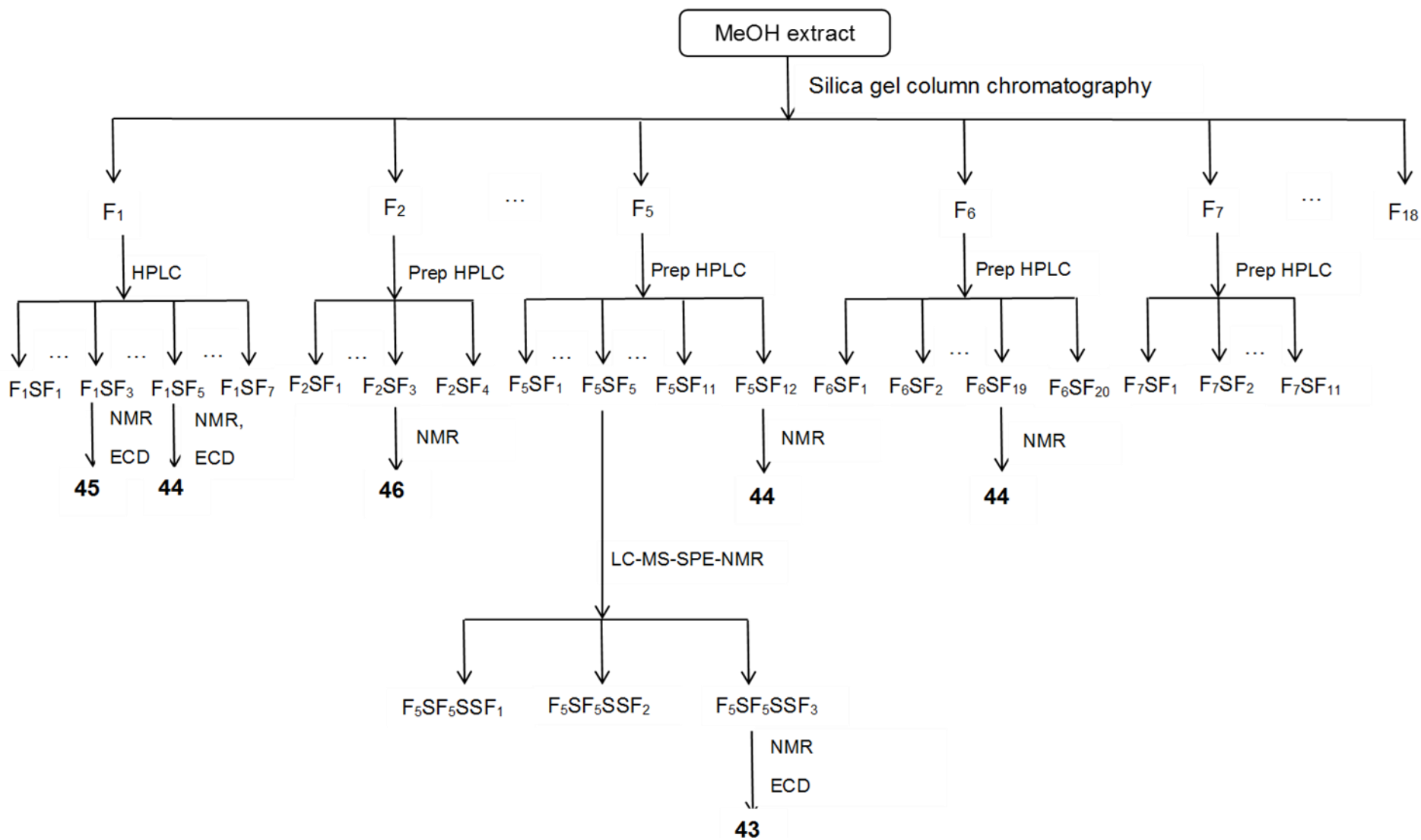


**Figure 2.12:** Flow diagram for purification of the MeOH extract, the structures of the compounds are shown in Figure 2.13.

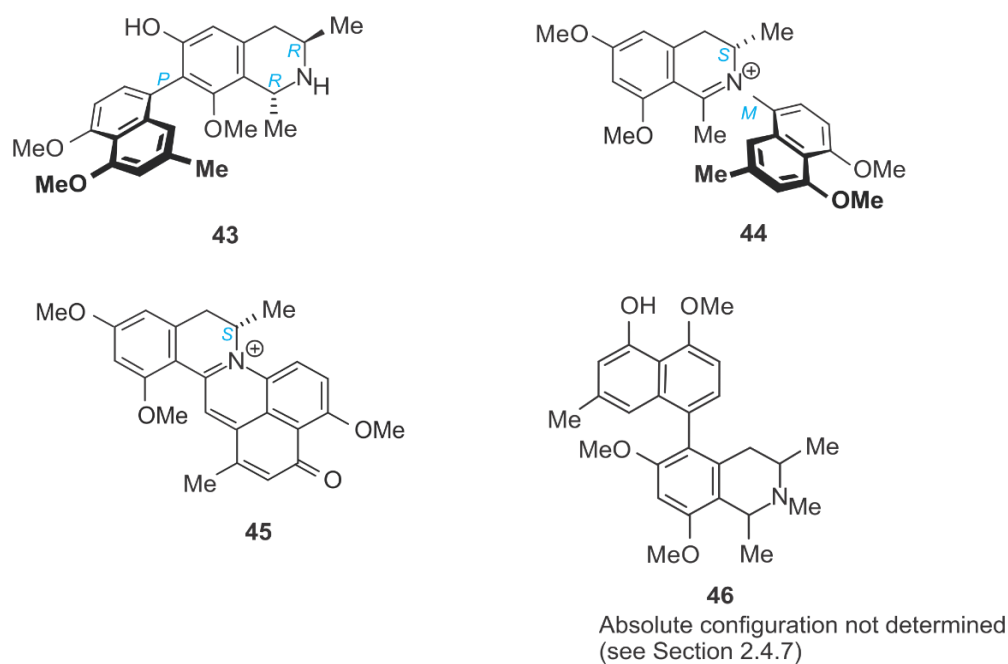


**Figure 2.13:** Structures of ealamine A (**43**), ancistrocladinium A (**44**), ancistrocycalinone A (**45**), and compound **46**.

### 2.3.4.3 Chemical profiling using UPLC-QTOF-MS

The samples (extracts, fractions, and compounds) were run on the ultra-performance liquid chromatography (UPLC), which was performed on a Waters Acquity UPLC System equipped with a binary solvent delivery system and an autosampler, a Waters BEH C<sub>18</sub> (2.1 mm x 100 mm, 1.7 μm) column using the following solvents: A = H<sub>2</sub>O + 0.1 % formic acid and B = MeOH + 0.1 % formic acid with a flow rate of 0.3 mL/min and injection volume of 5 μl. UPLC for Subfractions F<sub>2</sub>SF<sub>1-4</sub> was performed on a Waters Acquity BEH C<sub>18</sub> column (2.1 mm x 150 mm, 1.7 μm) using the following solvents: A = H<sub>2</sub>O + 0.1 % ammonium hydroxide, and B = MeCN. The flow rate was 0.3 mL/min and the injection volume 1 μl. The separated compounds were analyzed by a QTOF mass spectrometer, which was run in electrospray ionization positive mode. NIQs were identified by generating the respective molecular formula from MassLynx V 4.1 and comparison of the *m/z* value with that of published NIQs.

#### **2.3.4.4 NMR analysis**

NMR data were recorded on a Bruker Avance III 400 MHz and 500 MHz Spectrometers equipped with a Prodigy Probe. Compounds were dissolved in suitable deuterated solvents (250 µl for 500 MHz and 500 µl for 400 MHz instruments) and placed in NMR tubes for measurement. Data were processed using the TopSpin 3.5pl7 software from Bruker.

#### **2.3.4.5 ECD measurements**

The electronic circular dichroism spectra were recorded on a J-715 spectropolarimeter (JASCO) at room temperature in Prof. G. Bringmann's laboratory at the University of Würzburg. A standard cell (0.02 cm) and spectrophotometric-grade MeOH were used.

#### **2.3.5 Antiplasmodial screening**

Extracts, fractions, and compounds were screened using the Malaria SYBR Green I based assay. SYBR Green I is a fluorescent nucleic-acid intercalating dye that interacts with DNA. As erythrocytes lack DNA, *Plasmodium* parasite proliferation can be directly monitored in their intra-erythrocytic environment through detecting and monitoring DNA replication. Therefore, a correlation between DNA content (SYBR Green I signal) and parasitemia can be used to monitor a decrease in parasitemia as a measure of inhibition of parasite proliferation.<sup>[48]</sup>

The screening and training was done at the Department of Biochemistry by Dr. Dina Coertzen and Dr. Phanankosi Moyo, respectively, in Prof. Lyn-Marie Birkholtz' research group, University of Pretoria. The detailed method used for screening is described in the Chapter 3.

## 2.4 Results and discussion

### 2.4.1 Plant material

The leaf material of *Ancistrocladus* species was collected by B.K. Lombe, near the village of Bonsolerve in the DRC and is yet unidentified. The delimitation of species of the genus *Ancistrocladus* Wall. may be regarded as problematic because the taxa do not flower frequently and are rare. Due to this, the identification of *Ancistrocladus* species requires tedious work, which considers morphological features, phylogenetic relationships, genetic variability, and naphthylisoquinoline alkaloid patterns. The latter may provide a chemotaxonomical demarcation between species and sub-species.<sup>[8, 49]</sup> The chemical investigation of this plant material, for which the identification of naphthylisoquinoline alkaloids with antiplasmodial activity, would also contribute towards the identification of the species by comparing the chemical patterns with the ones of other species collected in the same region.<sup>[7]</sup>

### 2.4.2 Extraction

The leaves were air-dried at room temperature and ground in Kinshasa (DRC) at the University of Kinshasa before dispatch to Pretoria.

Sequential extraction was done on the dried ground leaves using different solvents, starting with the non-polar *n*-hexane followed by increasing the polarity of the solvents consisting of DCM, EtOAc, MeOH, and water. The extraction yields for *n*-hexane, DCM, EtOAc, MeOH, and water extracts were 1.98 % (6.37 g), 2.24 % (7.19 g), 0.3 % (0.98 g), 9.25 % (29.6 g), and 1.8 % (5.84 g), respectively, based on the dry weight of the extracted plant material. The highest extraction yield was through the use of MeOH indicating that the plants were rich in polar compounds, which was the main purpose to achieve the highest concentration of the NIQs.

### 2.4.3 Bioassaying of extracts

The classification criteria activity for plant extracts against *P. falciparum* used in this study was based on the one published by Moyo *et al* (2016) for dual-point screening of early-stage leads.<sup>[50]</sup> The classification used was as follows:

- a. **Good activity:**  
> 70% inhibition at 20 µg/mL and > 50% inhibition at 10 µg/mL
- b. **Moderate activity:**  
> 70% inhibition at 20 µg/mL and < 50% inhibition at 10 µg/mL  
< 70% inhibition at 20 µg/mL and > 50% inhibition at 10 µg/mL  
50 to 70% inhibition at 20 µg/mL and < 50% inhibition at 10 µg/mL
- c. **No or minimal activity:**  
< 50% inhibition at 20 µg/mL and < 50% inhibition at 10 µg/mL

The extracts, except for the *n*-hexane extract, were screened against *Plasmodium falciparum* NF54 strains at 10 and 20 µg/mL, the results are shown in Table 2.1. The DCM extract showed no or only minimal activity based on the criteria with 3.5 % at 20 µg/mL and 6.3 % at 10 µg/mL. The water and EtOAc extracts showed moderate activity with 43.4 % and 58.4 % at 20 µg/mL, and 42.4 % and 47.6 % 10 µg/mL, respectively. The MeOH extract showed good activity with 100 % inhibition at both 20 and 10 µg/mL (Table 2.1).

**Table 2.1:** *In vitro* activity of the four extracts against asexual NF54 *P. falciparum* parasites, tested at concentrations of 20 and 10 µg/mL, using the SYBR Green I assay. Data are from three independent biological replicates, performed in technical triplicates (n = 3).

Extracts	Asexual proliferation (% inhibition)	
	20 µg/mL	10 µg/mL
DCM	3.5	6.3
EtOAc	58.4	47.6
MeOH	106.4	104.4
Water	43.4	42.4

Based on the classification criteria the MeOH extract was selected for further fractionation.

#### 2.4.4 Ultra-performance liquid chromatography – quadrupole time-of-flight – mass spectrometry (UPLC-QTOF-MS) analysis of extracts

In order to tentatively identify the compounds present in the extracts screened against *P. falciparum*, they were analyzed by UPLC-QTOF-MS.

The ESI positive-mode UPLC-MS chromatograms of the four extracts are shown in Figure 2.14. A comparison of the chromatograms showed that the compounds in the water extract were mainly distributed in the non-polar region between 10 and 18 min, while those in the DCM, EtOAc, and MeOH extracts mainly eluted between 6 and 9 min in a 20-min run time method, showing that medium polar compounds were present in all these solvents. However, some compounds with their corresponding peaks were present in the non-polar region between 13 and 17 min of the chromatograms of EtOAc and MeOH. These findings were somewhat unusual as one would have expected peaks in the water extract to be in the polar section (between 0 and 6 min approximately) with the same for the MeOH extract, while for EtOAc extract, peaks are expected in the polar and non-polar (from 0 to around 15 min), while for DCM they were expected in the non-polar region (between 8 and 18 min approximately). This could be explained by the fact that, since the extracts were analyzed in ESI positive mode, some compounds were not easily ionized in this mode and hence would not be seen on the chromatogram.<sup>[51]</sup> The ESI positive mode was used because NIQs are easily ionized under these conditions.<sup>[52]</sup>

Peaks that eluted from 6.0 min to 8.5 min in DCM, EtOAc, and MeOH extracts were identified as NIQs (see Figure 2.14).

In the DCM extract (Figure 2.14 DCM), peaks identified as NIQs were all monomers. Peak 1, at  $m/z$  394.2015  $[M+H]^+$  (RT: 6.34 min) had a molecular formula of  $C_{24}H_{27}NO_4$ . The latter was typical of NIQs such as a naphthyltetrahydroisoquinoline having two free hydroxy and two methoxy groups (like e.g. korupensamine E, see Figure 2.15)<sup>[23, 41, 42, 53-60]</sup> or being *N*-methylated with three free hydroxy groups and one methoxy (like e.g. korupensamine D, **48**, see Figure 2.15).<sup>[57, 61]</sup> The MS/MS fragmentation of Peak

1 showed a fragment at  $m/z$  380.1261, which indicated a loss of a methyl group. Peak 2, at  $m/z$  422.2324  $[M+H]^+$  (RT: 6.76 min), had a molecular formula of  $C_{26}H_{31}NO_4$ . This formula was in agreement with tetra-*O*-methylated NIQs (like e.g. ancistrosectoriline A, **51**, see Figure 2.15)<sup>[15, 42, 56, 62]</sup> or *N*- and tris-*O*-methylated with one hydroxy group (like e.g. ancistrosectorine C, **24**, see Figure 2.4 ).<sup>[15, 16, 42, 55, 58, 61, 63-65]</sup> Peak 3, at  $m/z$  408.2171  $[M+H]^+$  (RT: 6.84 min), had a molecular formula of  $C_{25}H_{29}NO_4$ . This formula was typical of NIQs such as tris-*O*-methylated naphthyltetrahydroisoquinoline with one free hydroxy group (like e.g. ancistrocladine, **36**, see Figure 2.9) or di-*O*-methylated and *N*-methylated naphthyltetrahydroisoquinoline (like e.g. *N*-methylancistrosectorine A<sub>1</sub>, **38**, see Figure 2.10).<sup>[15, 16, 26, 28, 37, 42, 54, 55, 59, 61-63, 66-70]</sup> Peak 4, at  $m/z$  436.2485  $[M+H]^+$  (RT: 7.78 min), had a molecular formula of  $C_{27}H_{33}NO_4$ . This formula was in agreement with NIQs such as tetra-*O*-methylated and *N*-methylated NIQs (like e.g. ancistrobertsonine C, **52**, see Figure 2.15).<sup>[15, 22, 26, 55, 69]</sup> Peak 5, at  $m/z$  422.2336  $[M+H]^+$  (RT: 7.90 min), had a molecular formula of  $C_{26}H_{31}NO_4$ , just the same as Peak 2, which implied that they had the same general characteristics. However, the fact that they eluted at different retention times indicated that they were structurally different, which could be attributed to differences in the coupling position in the two moieties or the *O*-substitution pattern. Peak 6, at  $m/z$  420.2169  $[M+H]^+$  (RT: 8.23 min), had a molecular formula of  $C_{26}H_{29}NO_4$ . This formula was characteristic of tetra-*O*-methylated NIQs having a dihydroisoquinoline moiety (like e.g. 6-*O*-methylhamatinine, **50**, see Figure 2.15) or NIQs with a formula of  $C_{26}H_{30}NO_4^+$  (in the case of  $m/z$  420.2169  $[M]^+$ ), which would be an *N,C*-coupled naphthyldihydroisoquinoline (like e.g. ancistrocladinium A, **44**, see Figure 2.13).<sup>[19, 37, 56, 63, 71-74]</sup> Peak 7, at  $m/z$  406.2015  $[M+H]^+$  had a molecular formula of  $C_{25}H_{27}NO_4$ . This formula was in agreement with NIQs that were tri-*O*-methylated with one free hydroxy group (like e.g. ancistrobarterine A, **42**, see Figure 2.10)<sup>[4, 5, 15, 19, 22, 23, 26, 46, 55, 63, 75-78]</sup> or with an *N,C*-coupled naphthyldihydroisoquinoline with a molecular formula of  $C_{25}H_{28}NO_4^+$  (in the case of  $m/z$  406.2015  $[M]^+$ ) (like e.g. ancistrocladinium B, **49**, see Figure 2.15).<sup>[73]</sup>

In the EtOAc extract (Figure 2.14 EtOAc) the same  $m/z$  values detected in the DCM extract were present: 394.2014 (Peak 1, 6.23 min), 422.2333 (Peak 2, 6.76 min), 408.2174 (Peak 3, 6.92 min), 436.2490 (Peak 4, 7.77 min), 422.2321 (Peak 5, 7.88 min), and 422.2338 (Peak 6, 8.14 min). The  $m/z$  420.2169 and 406.2015 seen in the DCM extract were not present in the ethyl acetate one.

In the MeOH extract (Figure 2.14 MeOH), most  $m/z$  values detected in the DCM were present as well: 408.2175 (Peak 1, 6.15 min), 394.2017 (Peak 2, 6.29 min), 422.2318 (Peak 4, 6.71 min), 408.2169 (Peak 5, 6.80 min), 422.2320 (Peak 6, 7.86 min), and 420.2183 (Peak 7, 8.20 min). Peak 2 at  $m/z$  378.1699  $[M+H]^+$  (6.60 min) with a molecular formula of  $C_{24}H_{27}NO_3$  in the MeOH extract was not present in the other ones. The latter formula was typical of di-*O*-methylated NIQs with one free hydroxy group and without an oxygen function at C-6 (Dioncophyllaceae-type) (like e.g. dioncophylline A, **37**, see Figure 2.9).<sup>[22, 79-83]</sup>

In the water extract (Figure 2.14 Water), one peak (Peak 1) at  $m/z$  813.5696  $[M+H]^+$  (16.50 min) had a molecular formula of  $C_{50}H_{56}N_2O_8$ , which was in agreement with NIQ dimers (like e.g. shuangancistrotoectrorine A, **31**, see Figure 2.7).<sup>[21]</sup>

Despite the fact that the same  $m/z$  values were found in the DCM, EtOAc, and MeOH extracts (see Table 2.2), it was highly possible that the NIQ compounds present were different between the extracts. The several structural features (coupling sites, oxygen substitution pattern, stereogenic centers C1 and C3, mono- or dimeric structure, degree of saturation of the isoquinoline moiety, possibility of *N*-methylation, etc.) differentiating compounds within the class of NIQs were expected to have also an influence on their polarity. Therefore, as the extraction was sequential with the aforementioned solvents, isomers of different polarity were distributed in the used solvents as per their affinity.

Dioncophyllaceae-type NIQs were clearly present only in the MeOH extract. It could be that they were not present in the other ones or they could have been there in trace quantities. Quite a number of Dioncophyllaceae-type NIQs have shown excellent antiplasmodial activity in the nanomolar range.<sup>[2, 43, 44, 84]</sup> Their presence in the MeOH extract could have contributed to the antiplasmodial activity of the extract. This partially explained why the MeOH extract showed the best activity.



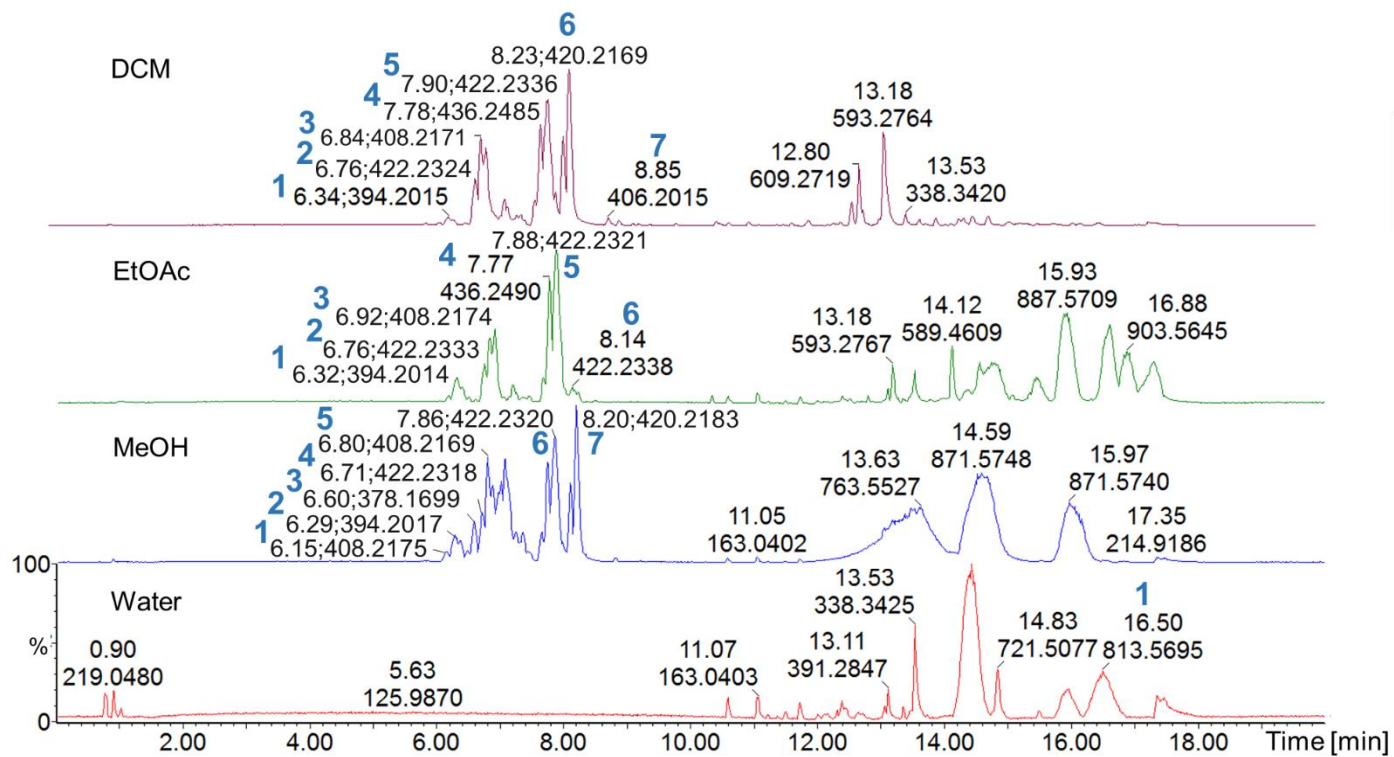


**Figure 2.14:** ESI positive-mode BPI chromatograms of leaves of *Ancistrocladus sp.* extracted sequentially with DCM, EtOAc, MeOH, and water.

**Table 2.2:** Comparison of the chemical profiles of the DCM, EtOAc, and MeOH extracts.

Measured [M+H] <sup>+</sup> or [M] <sup>+</sup> <i>m/z</i>	Formula of possible structure	Examples of possible compound	DCM	EtOAc	MeOH
378.1699	C <sub>24</sub> H <sub>27</sub> NO <sub>3</sub>	Dioncophylline A ( <b>37</b> )	Absent*	Absent*	Present
394.2014	C <sub>24</sub> H <sub>27</sub> NO <sub>4</sub>	Korupensamine E ( <b>47</b> ), Korupensamine D ( <b>48</b> )	Present	Present	Present
406.2015	C <sub>25</sub> H <sub>27</sub> NO <sub>4</sub> or C <sub>25</sub> H <sub>28</sub> NO <sub>4</sub> <sup>+</sup>	Ancistrobarterine A ( <b>42</b> ), Ancistrocladinium B ( <b>49</b> )	Present	Absent*	Absent*
408.2174	C <sub>25</sub> H <sub>29</sub> NO <sub>4</sub>	Ancistrocladine ( <b>36</b> ), <i>N</i> -Methylancistectorine A <sub>1</sub> ( <b>38</b> )	Present	Present	Present
420.2169	C <sub>26</sub> H <sub>29</sub> NO <sub>4</sub> or C <sub>26</sub> H <sub>30</sub> NO <sub>4</sub> <sup>+</sup>	6- <i>O</i> -Methylhamatinine ( <b>50</b> ), Ancistrocladinium A ( <b>44</b> )	Present	Absent*	Present
422.2333	C <sub>26</sub> H <sub>31</sub> NO <sub>4</sub>	Ancistrotectoriline A ( <b>51</b> ), Ancistrotectorine C ( <b>24</b> )	Present	Present	Present
436.2490	C <sub>27</sub> H <sub>33</sub> NO <sub>4</sub>	Ancistrobertsonine C ( <b>52</b> )	Present	Present	Absent*

\* Maybe present in trace quantities.

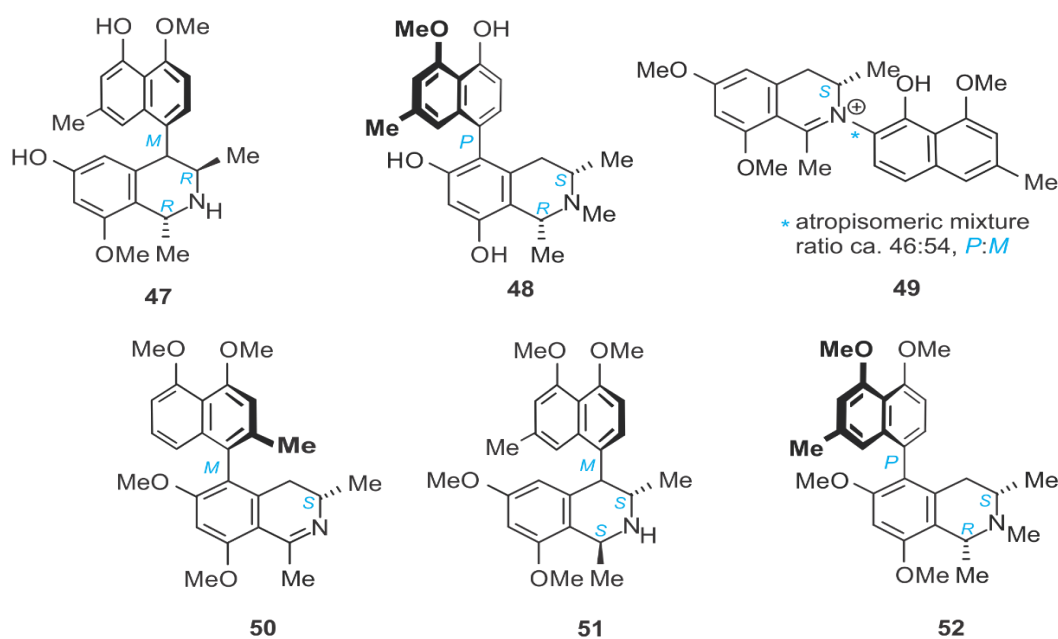


**Figure 2.15:** Structures of korupensamine E (**47**), korupensamine D (**48**), ancistrocladinium B (**49**), 6-*O*-methylhamatinine (**50**), ancistrotectoriline A (**51**), and ancistrobertsonine C (**52**).

#### 2.4.5 Fractionation and bioassaying of selected fractions

In order to isolate and identify the active compound(s) responsible for the potent activity observed for the MeOH extract, 13.0 g was subjected to column chromatography using silica gel treated with 0.1 % triethylamine for the separation of the NIQs. Collection was done in small quantities (100 mL per fraction), while monitoring with TLC. Fractions with similar TLC profiles were combined and hence 24 fractions were obtained. After further analysis by TLC, the first four fractions were combined, likewise the seventh and eighth fractions, the ninth and tenth fractions were mixed, and the eleventh and twelfth fractions were combined. This led to 18 fractions labeled as F<sub>1</sub> (149.2 mg), F<sub>2</sub> (50.0 mg), F<sub>3</sub> (4.72 mg), F<sub>4</sub> (160 mg), F<sub>5</sub> (232 mg), F<sub>6</sub> (854 mg), F<sub>7</sub> (836 mg), F<sub>8</sub> (1.01 g), F<sub>9</sub> (206 mg), F<sub>10</sub> (798 mg), F<sub>11</sub> (203 mg), F<sub>12</sub> (238 mg), F<sub>13</sub> (323 mg), F<sub>14</sub> (376 mg), F<sub>15</sub> (1.61 g), F<sub>16</sub> (127 mg), F<sub>17</sub> (1.08 g), and F<sub>18</sub> (3.79 g).

As the screening process could be tedious and time consuming, only fractions that contained NIQs were subjected for antiplasmodial screening. The fractions labeled as F<sub>2</sub>, F<sub>4</sub>, F<sub>5</sub>, F<sub>6</sub>, and F<sub>7</sub> showed a positive reaction with Dragendorff's reagent on TLC (orange spot) and were further analyzed using UPLC-QTOF-MS. The chromatographic profiles for fractions F<sub>2</sub>, F<sub>4</sub>, F<sub>5</sub>, F<sub>6</sub>, and F<sub>7</sub> are shown in Figure 2.16.

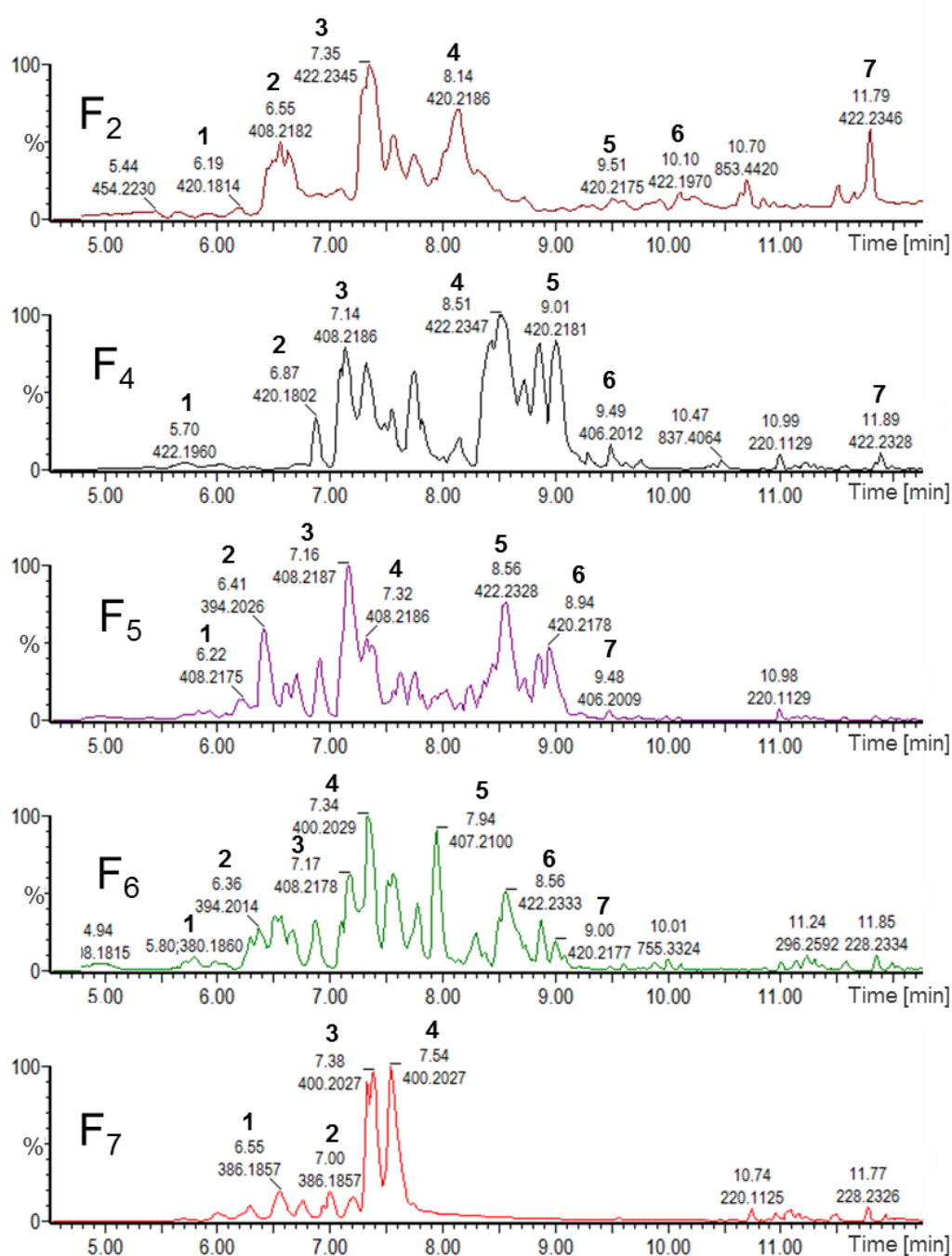


**Figure 2.16:** Selected section of the ESI positive-mode BPI chromatograms of five fractions (F<sub>2</sub>, F<sub>4</sub>, F<sub>5</sub>, F<sub>6</sub>, and F<sub>7</sub>), which showed mainly the presence of NIQs.

The analysis of the five fractions by UPLC-QTOF-MS revealed that the fractionation was successful as these all had different chemical profiles though some compounds with common *m/z* values were present between different fractions (see Table 2.3).

F<sub>2</sub> showed peaks at  $m/z$  420.1814 (Peak 1, 6.19 min, C<sub>26</sub>H<sub>29</sub>NO<sub>4</sub>), 408.2182 (Peak 2, 6.55 min, C<sub>25</sub>H<sub>29</sub>NO<sub>4</sub>), 422.2345 (Peak 3, 7.35 min, C<sub>26</sub>H<sub>31</sub>NO<sub>4</sub>), 420.2185 (Peak 4, 8.14 min, C<sub>26</sub>H<sub>29</sub>NO<sub>4</sub>), 420.2175 (Peak 5, 9.51 min, C<sub>26</sub>H<sub>29</sub>NO<sub>4</sub>), 422.1970 (Peak 6, 10.10 min, C<sub>26</sub>H<sub>31</sub>NO<sub>4</sub>), and 422.2346 (Peak 7, 11.79 min, C<sub>26</sub>H<sub>31</sub>NO<sub>4</sub>), which were discussed earlier, in Section 2.4.3, for the analysis of extracts.

F<sub>4</sub> showed peaks at  $m/z$  422.1980 (Peak 1, 5.70 min, C<sub>26</sub>H<sub>31</sub>NO<sub>4</sub>), 420.1802 (Peak 2, 6.87 min, C<sub>26</sub>H<sub>29</sub>NO<sub>4</sub>), 408.2185 (Peak 3, 7.14 min, C<sub>25</sub>H<sub>29</sub>NO<sub>4</sub>), 422.2347 (Peak 4, 8.51 min, C<sub>26</sub>H<sub>31</sub>NO<sub>4</sub>), 420.2181 (Peak 5, 9.01 min, C<sub>26</sub>H<sub>29</sub>NO<sub>4</sub>), 406.2012 (Peak 6, 9.49 min, C<sub>25</sub>H<sub>27</sub>NO<sub>4</sub> or C<sub>25</sub>H<sub>28</sub>NO<sub>4</sub><sup>+</sup>), and 422.232 (Peak 7, 11.89 min, C<sub>26</sub>H<sub>31</sub>NO<sub>4</sub>), which were examined, in Section 2.4.3, for the analysis of extracts.

F<sub>5</sub> showed peaks at  $m/z$  408.2175 (Peak 1, 6.22 min, C<sub>25</sub>H<sub>29</sub>NO<sub>4</sub>), 394.2026 (Peak 2, 6.41 min, C<sub>24</sub>H<sub>27</sub>NO<sub>4</sub>), 408.2187 (Peak 3, 7.16 min, C<sub>25</sub>H<sub>29</sub>NO<sub>4</sub>), 408.2186 (Peak 4, 7.32 min, C<sub>25</sub>H<sub>29</sub>NO<sub>4</sub>), 422.2328 (Peak 5, 8.56, C<sub>26</sub>H<sub>31</sub>NO<sub>4</sub>), 420.2178 (Peak 6, 8.94 min, C<sub>26</sub>H<sub>29</sub>NO<sub>4</sub> or C<sub>26</sub>H<sub>30</sub>NO<sub>4</sub><sup>+</sup>), and 406.2009 (Peak 7, 9.48 min, C<sub>25</sub>H<sub>27</sub>NO<sub>4</sub> or C<sub>25</sub>H<sub>28</sub>NO<sub>4</sub><sup>+</sup>), which were discussed earlier, in Section 2.4.3, for the analysis of extracts too.

F<sub>6</sub> showed peaks at  $m/z$  394.2014 (Peak 2, 6.36 min, C<sub>24</sub>H<sub>27</sub>NO<sub>4</sub>), 408.2178 (Peak 3, 7.17 min, C<sub>25</sub>H<sub>29</sub>NO<sub>4</sub>), 422.2333 (Peak 6, 8.56 min, C<sub>26</sub>H<sub>31</sub>NO<sub>4</sub>), and 420.2171 (Peak 7, 9.00 min, C<sub>26</sub>H<sub>29</sub>NO<sub>4</sub> or C<sub>26</sub>H<sub>30</sub>NO<sub>4</sub><sup>+</sup>), which again were examined earlier, in Section 2.4.3, for the analysis of extracts. However, F<sub>6</sub> showed some additional  $m/z$  values that had not been detected in the MeOH extract. Peak 1, at  $m/z$  380.1860 [M+H]<sup>+</sup> had a molecular formula of C<sub>23</sub>H<sub>25</sub>NO<sub>4</sub> and was typical of monomeric mono-*O*-methylated NIQs with three free hydroxy groups or *N*-methylated with four free hydroxy groups.<sup>[57, 85-87]</sup> For Peak 4, at  $m/z$  400.2029 [M+H]<sup>+</sup> (7.34 min), the molecular formula C<sub>10</sub>H<sub>22</sub>N<sub>15</sub>O<sub>3</sub> generated by the instrument had iFit percentage of 45.64 %, which was unlikely the correct formula. Further, this  $m/z$  had not yet been reported for NIQs. This pointed to the fact that it could be an unusual naphthylisoquinoline alkaloid, maybe a pentacyclic *N,C*-coupled with aromatic isoquinoline moiety.<sup>[88]</sup> For Peak 5, at  $m/z$  407.2100 (7.94 min), the molecular formula C<sub>23</sub>H<sub>27</sub>N<sub>4</sub>O<sub>3</sub> generated by the instrument had an iFit percentage of 74.18 % and was thus improbably the correct formula. Further, the  $m/z$  being an odd number, while it was run in positive mode, showed that it was a compound that did not contain nitrogen unless it was a case of a diprotonated naphthylisoquinoline dimer [M+2]<sup>2+</sup>, which would have had two nitrogen atoms.<sup>[21]</sup>

F<sub>7</sub> showed peaks at *m/z* 400.2027 [M+H]<sup>+</sup> (Peak 3, 7.38 min, and Peak 4, 7.54 min), which was already discussed for Fraction F<sub>6</sub>. For Peaks 1 and 2 at *m/z* 386.1857 [M+H]<sup>+</sup> (6.55 and 7.00 min), the molecular formula C<sub>8</sub>H<sub>24</sub>N<sub>11</sub>O<sub>7</sub> had an iFit percentage of 63.99 % and thus was not likely to be the correct formula. This *m/z* value had as yet not been reported for NIQs, again pointing to the fact that the two peaks might be unusual NIQs. The difference of 14 mass units between those two values (*m/z* 400.2027 compared to *m/z* 386.1857) was indicative that the compounds at *m/z* 386.1857 had one methyl less than the compounds at *m/z* 400.2027.

**Table 2.3:** Summary of *m/z* values detected in the Fractions F<sub>2</sub>, F<sub>4</sub>, F<sub>5</sub>, F<sub>6</sub>, and F<sub>7</sub> and compared to the parent MeOH extract.

<i>m/z</i> (molecular formula)	MeOH extract	F <sub>2</sub>	F <sub>4</sub>	F <sub>5</sub>	F <sub>6</sub>	F <sub>7</sub>
380.1860 (C <sub>23</sub> H <sub>25</sub> NO <sub>4</sub> )	Absent	Absent	Absent	Absent	Present	Absent
386.1857*	Absent	Absent	Absent	Absent	Absent	Present
394.2026 (C <sub>24</sub> H <sub>27</sub> NO <sub>4</sub> )	Present	Absent	Absent	Present	Present	Absent
400.2027*	Absent	Absent	Absent	Absent	Present	Present
406.2009 (C <sub>25</sub> H <sub>27</sub> NO <sub>4</sub> or C <sub>25</sub> H <sub>28</sub> NO <sub>4</sub> <sup>+</sup> )	Absent	Absent	Present	Present	Absent	Absent
407.2100*	Absent	Absent	Absent	Absent	Present	Absent
408.2178 (C <sub>25</sub> H <sub>29</sub> NO <sub>4</sub> )	Present	Present	Present	Present	Present	Absent
420.2175 (C <sub>26</sub> H <sub>29</sub> NO <sub>4</sub> or C <sub>26</sub> H <sub>30</sub> NO <sub>4</sub> <sup>+</sup> )	Present	Present	Present	Present	Present	Absent
422.2346 (C <sub>26</sub> H <sub>31</sub> NO <sub>4</sub> )	Present	Present	Present	Present	Present	Absent

\*The correct molecular formula was not generated.

The UPLC-QTOF-MS chromatogram of the five screened fractions revealed some *m/z* values that had not been detected in the parent MeOH extract (see Table 2.3). This indicated that their ionization and hence their expression were suppressed in the extract or that the separation was not good and they were therefore co-eluting with

other compounds. For some *m/z* values, the molecular formulas were not deduced from the instrument. This implied that the compounds needed to be isolated and analyzed by NMR to permit their possible identification.

Based on the analysis results, all five fractions were screened against asexual *P. falciparum* NF54 strains in a dual-point assay at 10 and 5 µg/mL. The classification criteria were the same as the one used for plant extracts as mentioned earlier (Section 2.4.2, bioassaying). All five fractions showed good activities with more than 95 % inhibition at both concentrations (Table 2.4).

**Table 2.4:** *In vitro* activity of the five fractions collected from column chromatography against asexual NF54 *P. falciparum* parasites at test concentrations of 10 and 5 µg/mL. Data were from three independent biological replicates, performed in technical triplicates (n = 3).

Fraction number	Asexual proliferation (% inhibition)	
	10 µg/mL	5 µg/mL
Fraction 2	97.02 ± 0.21	97.16 ± 0.92
Fraction 4	96.12 ± 0.49	96.72 ± 0.56
Fraction 5	95.27 ± 0.34	96.55 ± 0.45
Fraction 6	99.17 ± 2.47	96.84 ± 0.31
Fraction 7	98.28 ± 1.58	98.00 ± 1.04

Since the antiplasmodial activity of all the fractions were similar, it was difficult to select the most active fraction for further purification. All five were subjected to chromatographic techniques to purify and isolate the active compounds.

## 2.4.6 Isolation of compounds

### 2.4.6.1 Purification of Fraction 2 (F<sub>2</sub>)

F<sub>2</sub> was resolved by using mass-directed purification preparative HPLC. All *m/z* values in the ESI positive mode corresponding to NIQs [422.1968 (6.15 min), 436.2147 (6.71

min), 408.2180 (7.95 min), 436.2510 (9.39 min), 422.2347 (9.81 min), 436.2503 (10.51 min), 422.2348 (10.96 min), 422.2334 (13.57 min), and 422.2347 (13.81 min)] were targeted and collected. Only the four compounds highlighted in the HPLC-MS chromatogram shown in Figure 2.17 were collected in sufficient quantities to allow further analysis and were labeled as F<sub>2</sub>SF<sub>1</sub> (1.8 mg), F<sub>2</sub>SF<sub>2</sub> (1.3 mg), F<sub>2</sub>SF<sub>3</sub> (3.1 mg), and F<sub>2</sub>SF<sub>4</sub> (1.4 mg).

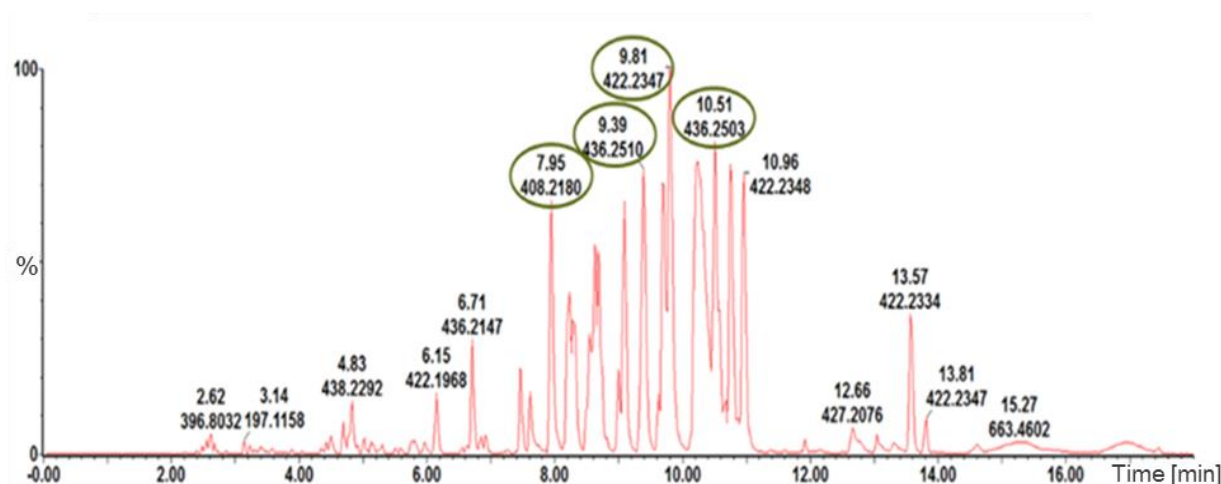


**Figure 2.17:** ESI positive-mode BPI chromatogram of F<sub>2</sub>. This fraction was resolved by HPLC-MS for isolation of compounds.

The four compounds were further analyzed by UPLC-QTOF-MS and the results showed that all were impure (Figure 2.18). They were further investigated by NMR. The <sup>1</sup>H NMR spectra of F<sub>2</sub>SF<sub>1</sub>, F<sub>2</sub>SF<sub>2</sub>, and F<sub>2</sub>SF<sub>4</sub> confirmed that they were still mixtures. However, the NMR of F<sub>2</sub>SF<sub>3</sub> indicated that the compound had only minor impurities, therefore, 1D and 2D NMR were measured and the constitution was elucidated and the relative configuration determined (compound **46**, see Section 2.4.7).



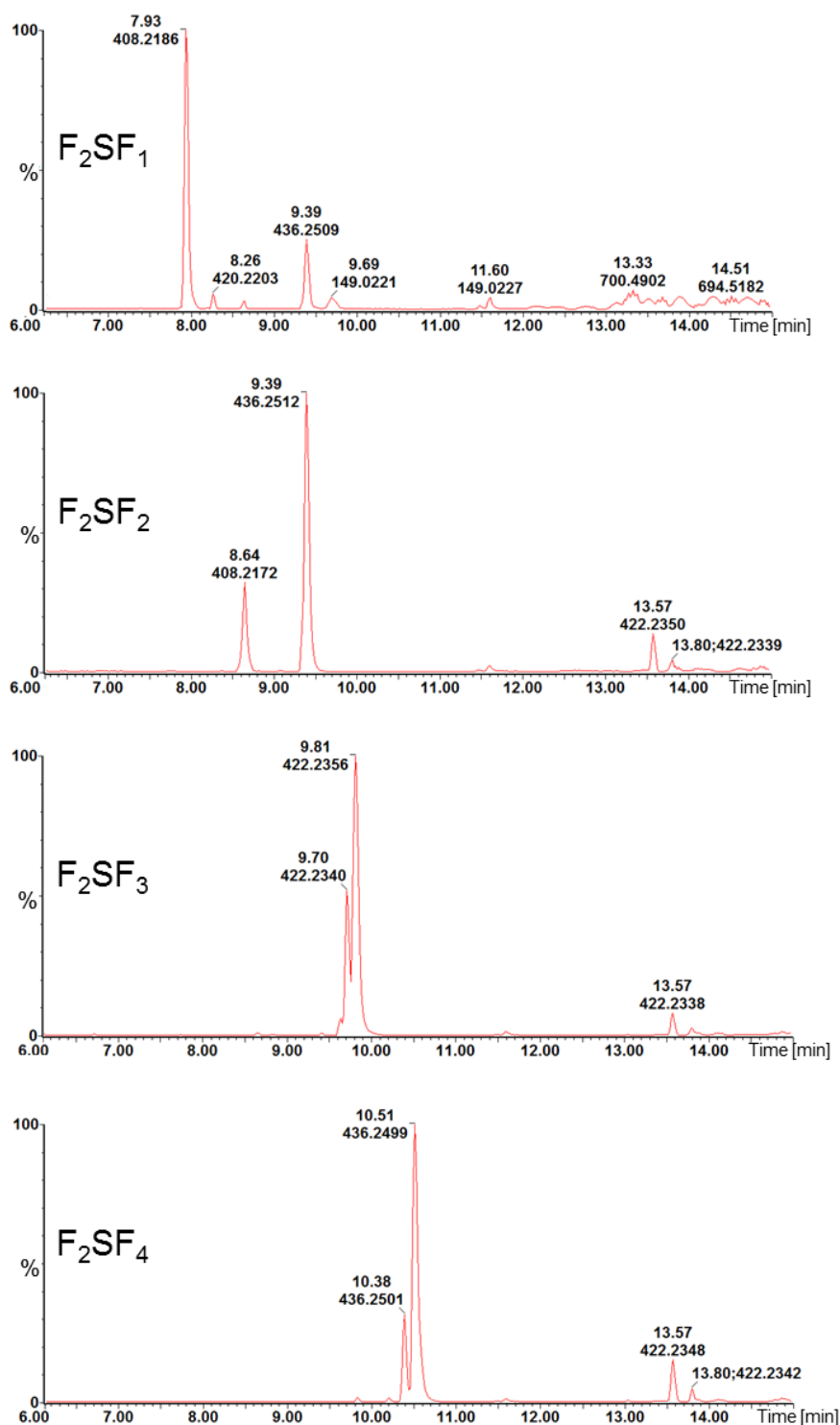


**Figure 2.18:** ESI positive-mode BPI chromatograms of Fractions F<sub>2</sub>SF<sub>1</sub>, F<sub>2</sub>SF<sub>2</sub>, F<sub>2</sub>SF<sub>3</sub>, and F<sub>2</sub>SF<sub>4</sub>; the part from 0 to 6 min has been removed from the chromatogram because there were no peaks.

F<sub>2</sub>SF<sub>1</sub>, F<sub>2</sub>SF<sub>2</sub>, F<sub>2</sub>SF<sub>3</sub>, and F<sub>2</sub>SF<sub>4</sub> were screened against asexual *P. falciparum* NF54 strains in a dual-point assay at concentrations of 5 and 1 µg/mL. Based on the aforementioned classification criteria for biological activity (Section 2.4.2), Fraction

F<sub>2</sub>SF<sub>1</sub> exhibited a good activity (97.97 % inhibition at 5 µg/mL and 82.34 % inhibition at 1 µg/mL), while F<sub>2</sub>SF<sub>2</sub> (15.59 % inhibition at 5 µg/mL and 2.72 % inhibition at 1 µg/mL), F<sub>2</sub>SF<sub>3</sub> (-0.55 % inhibition at 5 µg/mL and -1.02 % inhibition at 1 µg/mL), and F<sub>2</sub>SF<sub>4</sub> (31.85 % inhibition at 5 µg/mL and 5.84 % inhibition at 1 µg/mL) showed no or only minimal activity (Table 2.5).

**Table 2.5:** *In vitro* activity of the four subfractions collected by HPLC-MS of Fraction 2 from column chromatography of the MeOH extract against asexual NF54 *P. falciparum* parasites, at test concentrations of 5 and 1 µg/mL. Data are from three independent biological replicates, performed in technical triplicates (n = 3).

Sub-Fractions	Asexual proliferation (% inhibition)	
	5 µg/mL	1 µg/mL
F <sub>2</sub> SF <sub>1</sub>	97.97 ± 0.62	82.34 ± 5.18
F <sub>2</sub> SF <sub>2</sub>	15.59 ± 7.79	2.72 ± 9.55
F <sub>2</sub> SF <sub>3</sub>	-0.55 ± 12.08	-1.02 ± 9.44
F <sub>2</sub> SF <sub>4</sub>	31.85 ± 6.62	5.84 ± 7.94

The result showed that F<sub>2</sub>SF<sub>1</sub> contained the most active ingredient of F<sub>2</sub>. Due to its limited quantity it was subjected to LC-MS-SPE-NMR, which should permit isolation of the main compounds, through multiple trapping. However, in the process of developing a suitable method for purification based on HPLC-UV (200 – 400 nm), it appeared that the mixture was still highly complex as compared to the one analyzed by UPLC-MS (Figure 2.19). The restricted amount (1.7 mg remained after using 0.1 mg for bioassaying) did not allow for repeated chromatographic runs to resolve and develop an efficient method for the separation of the compounds. The fraction was stored for future repetition of the purification to obtain sufficient quantities of it for further continuation of the research.

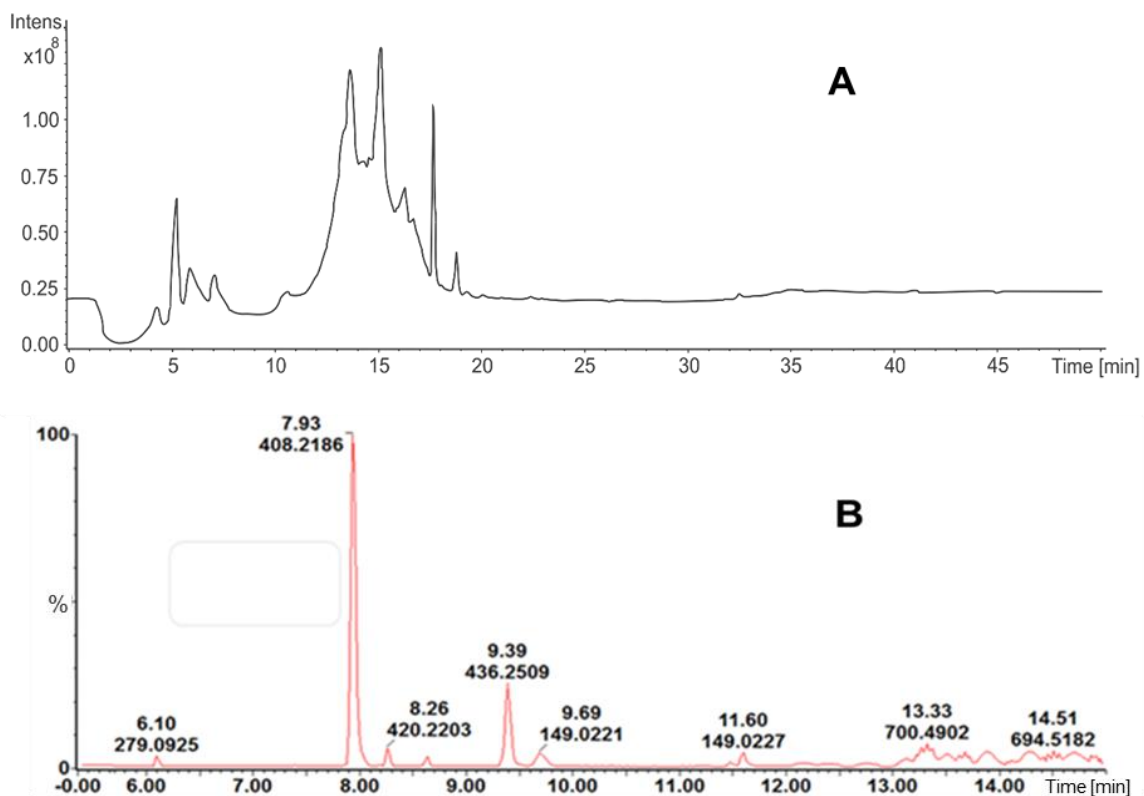


**Figure 2.19:** (A) LC-UV<sub>max</sub> plot SPE-NMR chromatogram; (B) ESI positive-mode BPI chromatogram of Subfraction F<sub>2</sub>SF<sub>1</sub>.

#### 2.4.6.2 Purification of Fraction 5 (F<sub>5</sub>)

Fraction 5 was subjected to purification by semi-preparative HPLC-UV. The separation resulted in twelve subfractions as shown in Figure 2.20, labeled as F<sub>5</sub>SF<sub>1</sub> to 12.

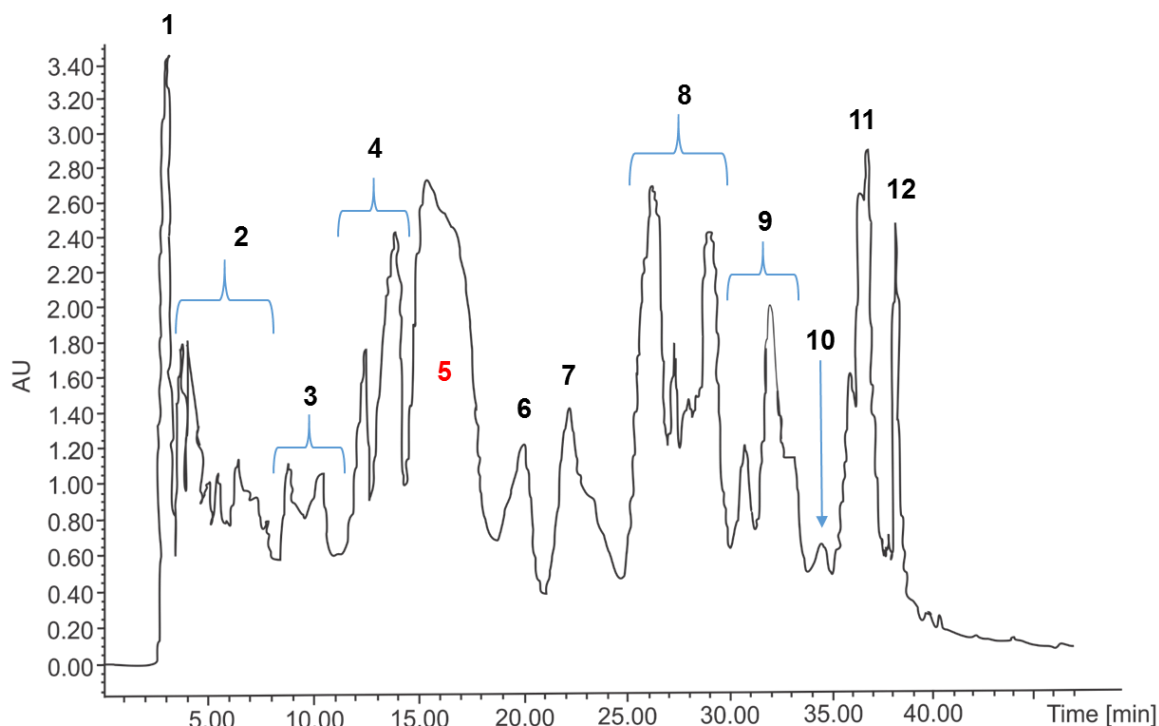


**Figure 2.20:** HPLC-UV<sub>max</sub> plot chromatogram of Fraction 5 collected from silica gel column chromatography of MeOH extract. A total of twelve subfractions were collected.

The subfractions were analyzed by UPLC-QTOF-MS. The latter showed that they were all still mixtures except for the twelfth fraction (Peak 12, labeled as F<sub>5</sub>SF<sub>12</sub>), which was pure though only 0.5 mg was collected. The UV spectrum, <sup>1</sup>H NMR, and LC-MS of this pure compound indicated that it was a known compound, ancistrocladinium A (**44**, see Figure 2.13), which allowed its identification in Fraction 1 (F<sub>1</sub>) as discussed below.

The quantities collected for each subfraction [F<sub>5</sub>SF<sub>1</sub> (5.75 mg), F<sub>5</sub>SF<sub>2</sub> (3.94 mg), F<sub>5</sub>SF<sub>3</sub> (4.99 mg), F<sub>5</sub>SF<sub>4</sub> (4.10 mg), F<sub>5</sub>SF<sub>5</sub> (24.1 mg), F<sub>5</sub>SF<sub>6</sub> (7.34 mg), F<sub>5</sub>SF<sub>7</sub> (4.54 mg), F<sub>5</sub>SF<sub>8</sub> (11.2 mg), F<sub>5</sub>SF<sub>9</sub> (12.4 mg), F<sub>5</sub>SF<sub>10</sub> (2.39 mg), and F<sub>5</sub>SF<sub>11</sub> (4.01 mg)], together with their complexities, did not warrant any further screening against *P. falciparum*.

However, Subfraction 5 (F<sub>5</sub>SF<sub>5</sub>) was considered worthwhile to pursue the purification as it was collected in a reasonable quantity (24.2 mg) and it contained a compound with  $m/z$  [M+H]<sup>+</sup> 408.2400, among the main compounds (see Figure 2.21). This choice was further supported by the following reasons: Quite a number of naphthylisoquinoline alkaloids with  $m/z$  408 [M+H]<sup>+</sup> have been reported to exhibit moderate to very good antiplasmodial activities;<sup>[26, 37, 42, 54, 69, 89, 90]</sup> furthermore, it is

known that a free hydroxy group at position C-8 of NIQs has a positive impact on the antimalarial activity<sup>[91]</sup> and NIQs with an  $m/z$   $[M+H]^+$  408 has at least one free hydroxy group. In addition, the semi-pure subfraction obtained from Fraction 2 ( $F_2SF_1$ ) that showed a good antiplasmodial activity (Table 2.5), contained a compound at  $m/z$   $[M+H]^+$  408.2186 as the main one (shown in Figure 2.18).

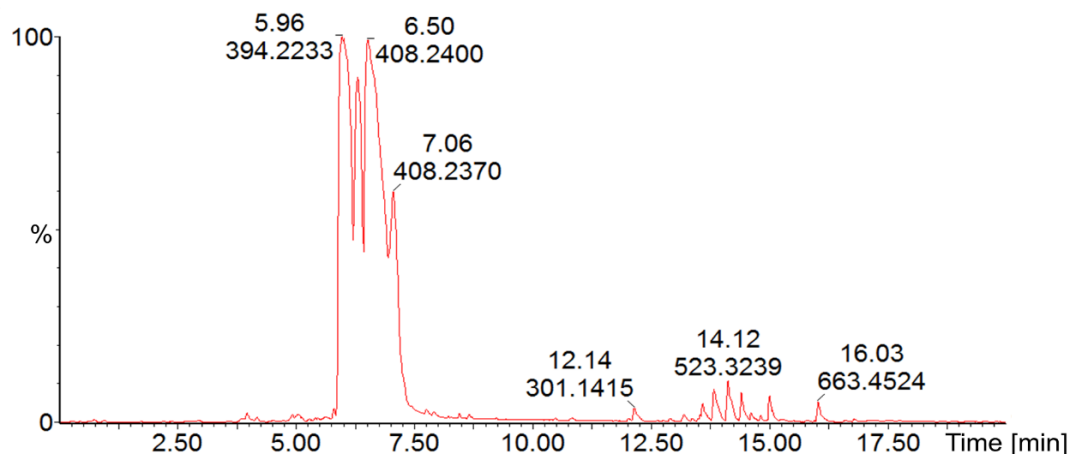


**Figure 2.21:** ESI positive-mode BPI chromatogram of Fraction  $F_5SF_5$ .

Based on the mass spectral data,  $F_5SF_5$  was subjected to purification by hyphenated liquid chromatography – mass spectrometry – solid phase extraction – nuclear magnetic resonance (LC-MS-SPE-NMR). The three peaks labeled in Figure 2.22 were trapped in SPE cartridges through multi-trapping. Peaks 1 and 2 were collected in small quantities of 0.4 and 0.3 mg, respectively. Peak 3 was the targeted compound (at  $m/z$  408.2700) and was collected in pure form and sufficient quantities for further analysis (1.6 mg). It was screened against *P. falciparum* (see Section 2.4.8) and its structure was elucidated by using NMR and ECD as ealamine A (**43**) (see Section 2.4.7, Figure 2.26).

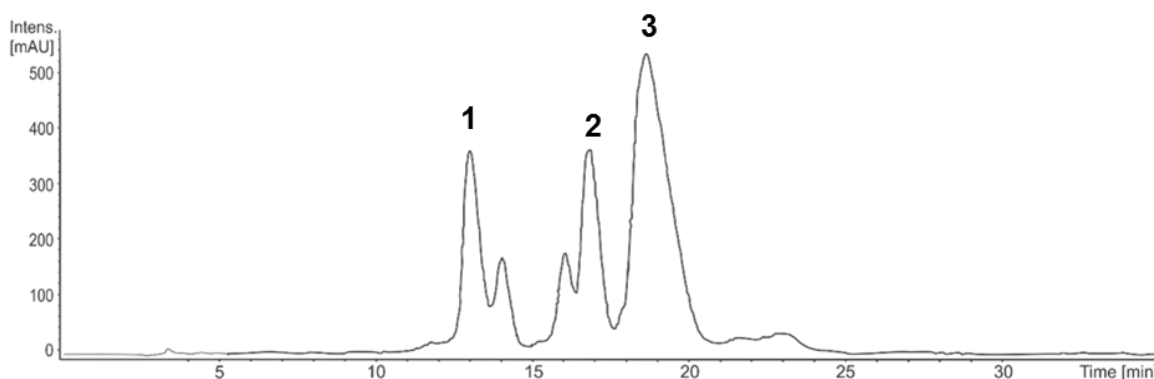


**Figure 2.22:** LC-UV<sub>max</sub> plot chromatogram of Subfraction 5 from LC-MS-SPE-NMR.

### 2.4.6.3 Purification of Fraction 1 (F<sub>1</sub>)

In order to isolate more of the compound **44** (ancistrocladinium A, see Section 2.4.7, Figure 2.28) collected from Fraction F<sub>5</sub> (F<sub>5</sub>SF<sub>12</sub>) for further analysis, other preceding fractions were analyzed by HPLC and the compound was one of the major Peaks in Fraction F<sub>1</sub> (Peak 5, Figure 2.23) as identified by the UV spectrum with maximum absorption at 216, 232, and 335 nm. Based on this, Fraction F<sub>1</sub> was subjected to purification by HPLC connected to a UV detector and Peaks 1 to 5, as labeled in Figure 2.23, were collected manually.

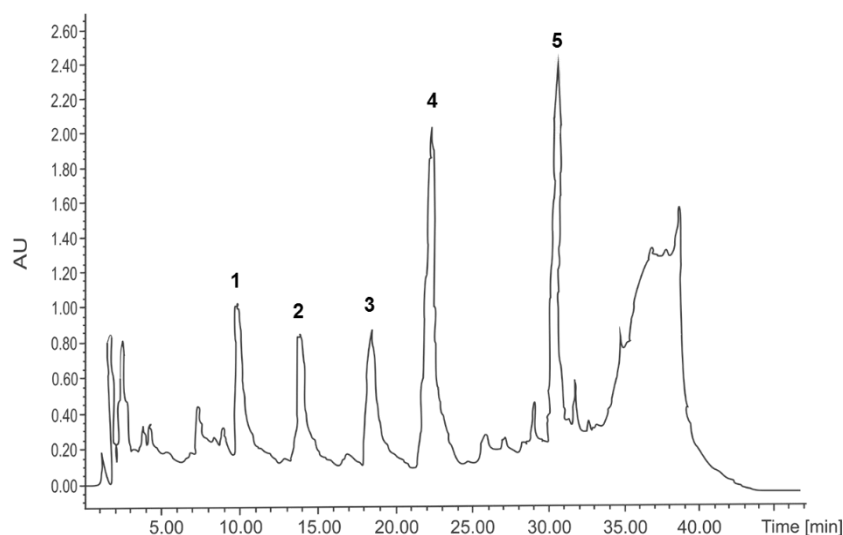


**Figure 2.23:** HPLC-UV<sub>max</sub> plot chromatogram of Fraction F<sub>1</sub> (AU = Absorbance Units).

After analysis of the collected fractions by UPLC-QTOF-MS and <sup>1</sup>H NMR, only Peaks 3 and 5 consisted of pure compounds, while the rest were impure. Peak 5 (1 mg) was

further confirmed to be ancistrocladinium A (**44**) as isolated from F<sub>5</sub>SF<sub>12</sub> based on the *m/z* at 420.2197 and <sup>1</sup>H NMR. Peak 3 (1.9 mg) was an additional compound later identified as ancistrocyclinone A (**45**, see Section 2.4.7, see Figure 2.35).

Fraction F<sub>1</sub> did not give a positive reaction for alkaloids with Dragendorff's reagent on TLC because the NIQs identified have a quaternary nitrogen.

The two compounds were screened against *P. falciparum* (Section 2.4.8) and their structures were elucidated by NMR, MS, and ECD spectroscopy as described in Section 2.4.7.

#### 2.4.6.4 Purification of Fraction 6 (F<sub>6</sub>)

Fraction F<sub>6</sub> was also subjected to purification by preparative HPLC coupled to a UV detector. The peaks were collected in test tubes (about 2 mL/tube) by using a fraction collector, which produced various subfractions. Some of the latter were subsequently combined, providing 20 subfractions (see chromatogram in Figure 2.24).

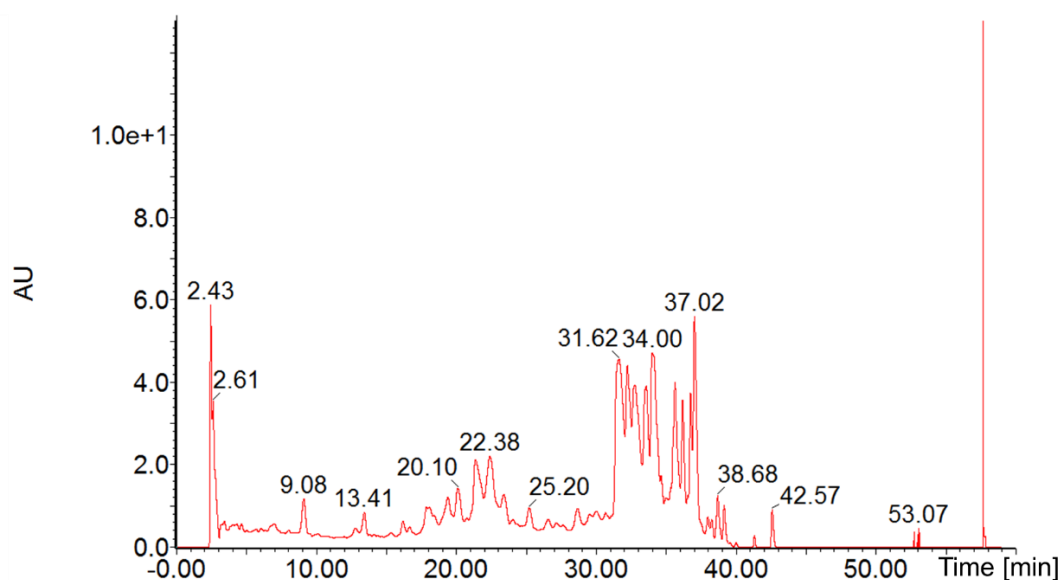


**Figure 2.24:** HPLC-UV<sub>max</sub> chromatogram of Fraction F<sub>6</sub>.

Analysis of those fractions by UPLC-QTOF-MS and <sup>1</sup>H NMR that appeared to be pure based on the collected peaks of the UV chromatogram, only the peak at 42.57 min was confirmed to be pure and was identical to the compound **44** (ancistrocladinium A, see

Figure 2.28) collected from Fractions F<sub>5</sub> (F<sub>5</sub>SF<sub>12</sub>, see Section 2.4.6.2) and F<sub>1</sub> (F<sub>1</sub>SF<sub>5</sub>, see Section 2.4.6.3). The fact that this compound was found in these three different fractions, indicated that it may have been tailing during the fractionation by column chromatography.

#### 2.4.6.5 Purification of Fraction 7 (F<sub>7</sub>)

The purification of Fraction F<sub>7</sub> was also attempted by semi-preparative HPLC. Figure 2.25 shows the UV<sub>max</sub> plot. Eleven time-based subfractions were collected and were analyzed by UPLC-QTOF-MS, which showed that they were still complex mixtures. Due to the complexity and the limited quantities of each subfraction, the purification was not further pursued.

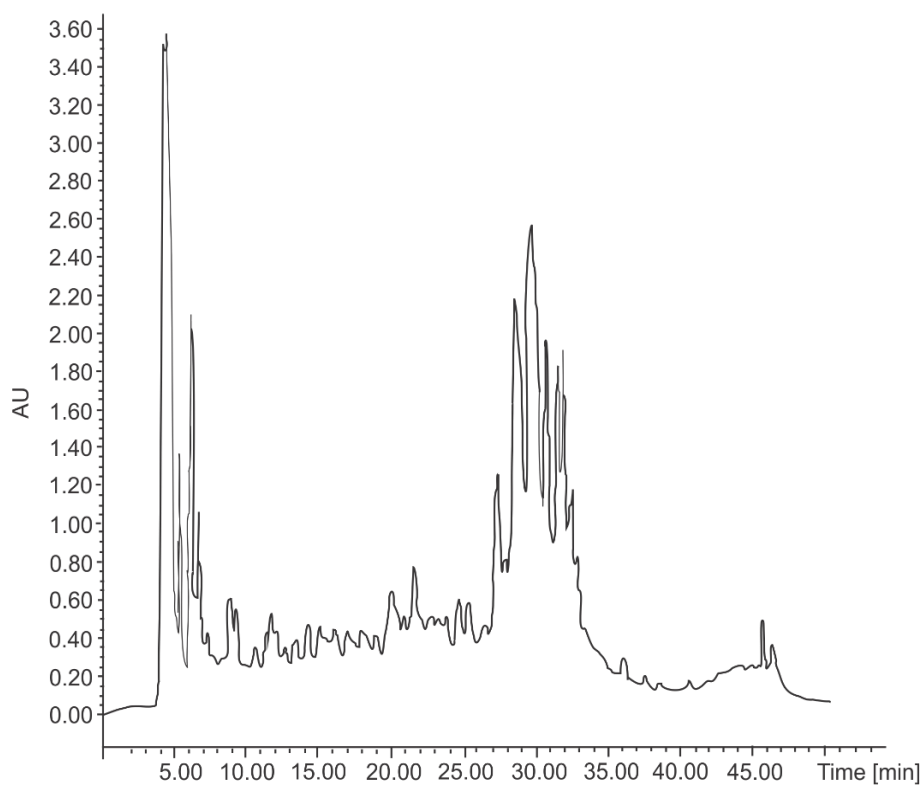


**Figure 2.25:** HPLC-UV<sub>max</sub> plot chromatogram of Fraction F<sub>7</sub>.



### 2.4.7 Structure elucidation of the pure NIQs

Compound **43** (ealamine A) was isolated as a yellow solid weighing 1.6 mg from Fraction F<sub>5</sub> as described earlier in Section 2.4.6.2. It had a molecular formula of C<sub>25</sub>H<sub>29</sub>NO<sub>4</sub>, as deduced from its monoprotonated molecular ion at *m/z* 408.2174 based on the QTOF mass spectrum. The formula was further confirmed by the number of protons in <sup>1</sup>H NMR and of carbon atoms in the <sup>13</sup>C NMR spectrum. Furthermore, the <sup>1</sup>H NMR spectrum suggested that the compound was a naphthyltetrahydroisoquinoline alkaloid as in the aliphatic region the following features were observed: the presence of a quartet, which was assigned to the proton on position H-1 ( $\delta_{\text{H}}$  4.75, 1H), a multiplet assigned to H-3 ( $\delta_{\text{H}}$  3.72, 1H), two diastereotopic protons, H-4<sub>eq</sub> ( $\delta_{\text{H}}$  3.01) and H-4<sub>ax</sub> ( $\delta_{\text{H}}$  3.05), two doublets each integrating for three protons ( $\delta_{\text{H}}$  1.58 and 1.66) characteristic of Me-3 and Me-1.<sup>[7]</sup> These deductions were further supported by COSY correlations between Me-1 and H-1, Me-3 and H-3, and between H-4<sub>ax</sub> and H-3. A singlet present at  $\delta_{\text{H}}$  2.38 and integrating for three protons was characteristic of an aryl-methyl group.<sup>[69]</sup>

Three *O*-methyl groups were identified with two at  $\delta_{\text{H}}$  3.98 and  $\delta_{\text{H}}$  4.00 and further highfield shifted one at  $\delta_{\text{H}}$  3.07 indicating it to be located *ortho* to the axis because the highfield shift was due to the anisotropic effect caused by the naphthalene substituent.<sup>[14, 82]</sup> In the aromatic region, the presence of two signals of *ortho*-coupled protons ( $\delta_{\text{H}}$  6.87 and 7.31, *J* = 7.99 Hz), two of *meta*-coupled protons ( $\delta_{\text{H}}$  6.87 and 7.31, *J* = 0.9 Hz), and one singlet at  $\delta_{\text{H}}$  6.57 revealed that the coupling site of the naphthalene part could be either at C-6' or at C-8'.<sup>[92]</sup> This assumption was supported by the 'normal' chemical shift of Me-2' ( $\delta_{\text{H}}$  2.38), which would be at a higher field if it was close to the axis.<sup>[61]</sup>

The location of the axis at C-8' was confirmed from the fact that one of the signals of *ortho*-coupled protons at  $\delta_{\text{H}}$  6.87 was clearly at position C-6' as HMBC correlations were seen between H-6' and C-5' ( $\delta_{\text{C}}$  158.3) and between OMe-5' and C-5'. The finding that one of the methoxy groups resonated at C-5' ( $\delta_{\text{H}}$  4.00) was based on HMBC interactions between the signals of the protons of that methoxy and C-5', between H-6' and C-5', and between H-7' and C-5' (Figure 2.26.A) as well as the NOE interactions between the signal of the same methoxy and the doublet assigned as H-6'. All carbons connected to protons were deduced from HSQC (Table 2.4).

The DEPT-135 and  $^{13}\text{C}$  NMR measurements further confirmed the presence of one  $\text{CH}_2$ , seven CH groups, six  $\text{CH}_3$  entities, and eleven quaternary carbons.

In the isoquinoline unit, the coupling site was determined to be at position C-7 as deduced from the HMBC correlation of the aromatic proton resonating at 6.57 ppm to C-4, confirming that this proton had to be located at C-5 ( $\delta_{\text{C}}$  110.0). This deduction was further supported by the high-field  $^1\text{H}$  NMR chemical shift ( $\delta_{\text{H}}$  3.07) of the methoxy group at C-8 as it indicated its position *ortho* to the axis.<sup>[70]</sup>

The remaining methoxy group was located to be at C-4' based on the HMBC correlations of the protons of OMe-4' to C-4', while further HMBC interactions were seen between H-1' and the C-4' confirming the position of both that methoxy group at C-4' and the H-1' proton. This assumption was further supported by an NOE interaction between the protons of OMe-4' and H-3'.

The methyl groups at position C-1 and position C-3 were evidenced to be *trans* to each other due to NOE interactions between the protons of Me-1 and H-3 (Figure 2.26.B).

The configuration of the biaryl axis was deduced to be *P* based on long-distance NOE interactions between the protons of Me-1 and H-7'. In order to confirm this assumption, the compound was sent to the laboratory of Prof. G. Bringmann (who is our collaboration partner and the co-supervisor of my work) in Germany (University of Würzburg) for ECD measurements. The ECD spectrum of the compound **43**, measured by Mr. B.K. Lombe, was compared to the one of ealamine A, a compound previously isolated from *A. ealaensis*.<sup>[93]</sup> They were virtually identical (see Figure 2.26.D). The superimposition of the two ECD spectra confirmed the configuration of the isolated compound.

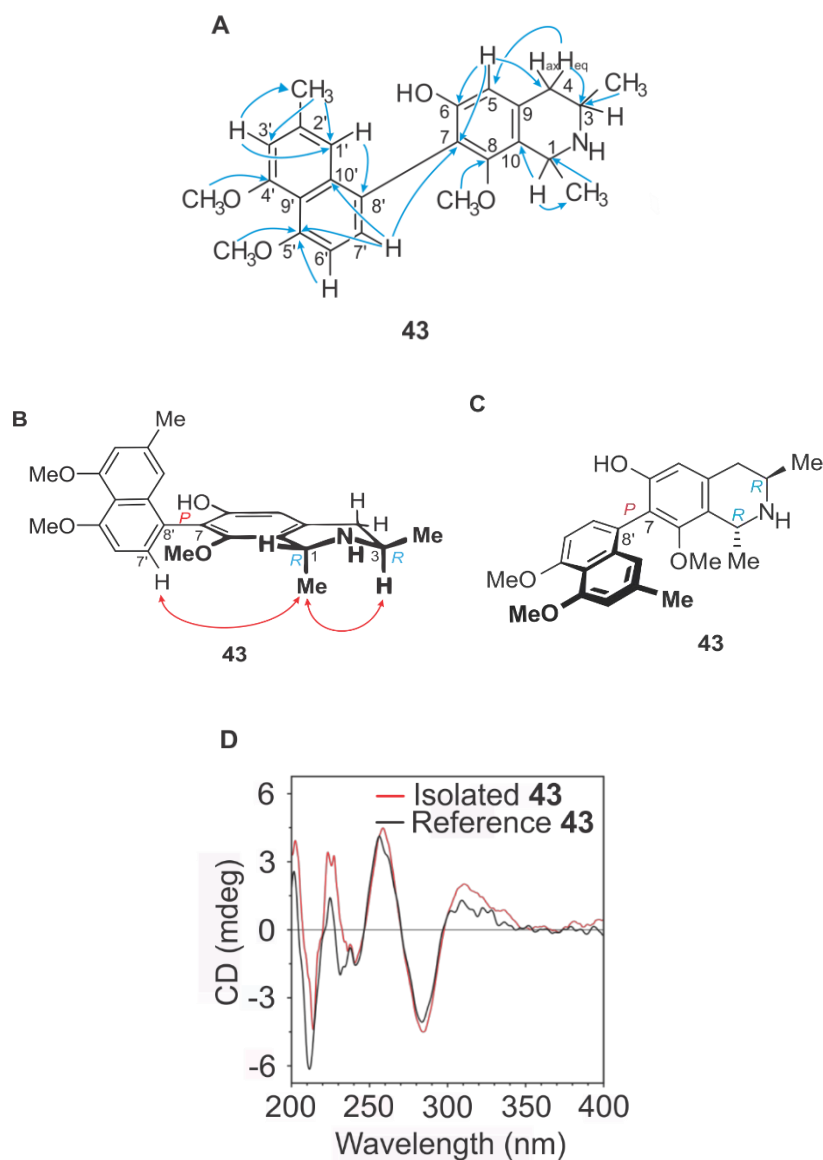


**Figure 2.26:** (A) Selected HMBC correlations; (B) Selected NOE interactions showing the configuration at the axis in the compound **43**; (C) Structure and absolute configuration of the isolated product **43**; (D) ECD spectra of **43** in red and the reference, ealamine A, which had previously been isolated in Prof. G. Bringmann's laboratory<sup>[94]</sup> in black showing that they were virtually identical.

**Table 2.6:**  $^1\text{H}$ ,  $^{13}\text{C}$  NMR, HMBC, and COSY data of the isolated ealamine A (**43**).

Position	$^1\text{H}$ (ppm, $J$ in Hz)	$^{13}\text{C}$ (ppm)	HMBC (H $\rightarrow$ C)	COSY
1	4.75 (1H, $q$ , $J = 6.57$ Hz)	48.5	C-9, C-3, 1-Me	1-Me
3	3.72 (1H, $m$ )	44.1		3-Me
4 <sub>eq</sub>	3.01 (1H, $dd$ , $J = 17.73, 4.20$ Hz)	34.1	C-3, C-5, C-9, C-10	H-4 <sub>ax</sub>
4 <sub>ax</sub>	3.05 (1H, $dd$ , $J = 17.73, 11.56$ Hz)	34.1	C-3, C-10	H-4 <sub>eq</sub> , H-3
5	6.57 (1H, $s$ )	110.0	C-4, C-7, C-6	
6	-	154.3		
7	-	118.9		
8	-	155.8		
9	-	119.2		
10	-	132.4		
1'	6.73 (1H, $d$ , $J = 0.9$ Hz)	109.3	2'-Me, C-4', C-8'	
2'	-	138.6		
3'	6.9 (1H, $s$ )	117.0	2'-Me, C-1', C-9'	2'-Me
4'	-	157.6		
5'	-	158.4		
6'	6.87 (1H, $d$ , $J = 7.99$ Hz)	105.4	C-8', C-10', C-5'	H-7'
7'	7.31 (1H, $d$ , $J = 7.99$ Hz)	130.8	C-7, C-5', C-9'	H-6'
8'	-	116.2		
9'	-	135.9		
10'	-	119.9		
1-Me	1.66 (3H, $d$ , $J = 6.69$ Hz)	19.4	C-1, C-9	H-1
2'-Me	2.38 (3H, $s$ )	22.1	C-1', C-3', C-2'	H-3'
3-Me	1.58 (3H, $d$ , $J = 6.39$ Hz)	19.1	C-4, C-3	H-3
8-OMe	3.07 (3H, $s$ )	60.3	C-8	
4'-OMe	3.98 (3H, $s$ )	56.6	C-4'	
5'-OMe	4.00 (3H, $s$ )	56.5	C-5'	

Ealamine A (**43**) had been previously isolated from the twigs and leaves of *Ancistrocladus ealaensis* J. Léonard and from the leaves of an as yet unidentified *Ancistrocladus* species collected around the village Leeke near the town of Ikela.<sup>[93]</sup> *A. ealaensis* was collected in the Eala region (northwestern part of DRC), while the plant material investigated in this study was collected in the vicinity of the village Bonsolerive (northwestern part of DRC, south of the Eala region). These regions are in the same part of the country (Figure 2.31). This compound, ealamine A (**43**), is among the 7,8'-coupled NIQs that possess *R*-configuration at C-3, which have been rarely detected in *Ancistrocladus* species. Further, such NIQs have so far been identified only in *A. ealaensis* (ten compounds) and in *A. korupensis* from Cameroon (three compounds). In addition, ealamine A (**43**, see Figure 2.28C), being *R*-configured at C-3 and with an oxygen function at C-6, is a hybrid-type NIQs (mixed Ancistrocladaceae- and Dioncophyllaceae-type characteristics in the same compound). This has geo- and chemotaxonomic significance because such types of NIQs are mostly present in the *Ancistrocladus* plants from the Northwestern Congo Basin, while *Ancistrocladus* species from Asia and East Africa exclusively produce Ancistrocladaceae-type NIQs (*S*-configured at C-3 and with an oxygen function at C-6).<sup>[4, 11, 20, 59, 61, 93, 95]</sup>

The compound isolated from Fractions F<sub>1</sub>, F<sub>5</sub>, and F<sub>6</sub> was identified as a known<sup>[73]</sup> *N,C*-coupled naphthylisoquinoline alkaloid, ancistrocladinium A (**44**), based on its UV spectrum, NMR data, and mass spectral analysis. The cationic mass of 420.2197 generated by UPLC-QTOF-MS (Figure 2.27) corresponded to a molecular formula of C<sub>26</sub>H<sub>30</sub>NO<sub>4</sub><sup>+</sup> (calculated mass 420.2175). The latter was further confirmed by the number of protons in <sup>1</sup>H NMR and of carbon atoms in <sup>13</sup>C NMR.

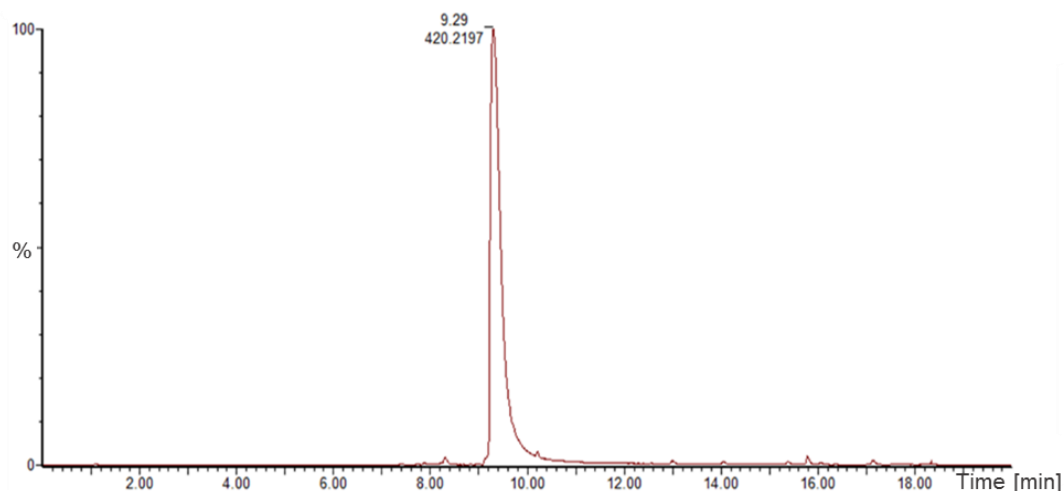


**Figure 2.27:** ESI positive-mode BPI chromatogram of compound **44** (ancistrocladinium A) isolated from Fractions F<sub>1</sub>, F<sub>5</sub>, and F<sub>6</sub>.

The <sup>1</sup>H NMR spectrum showed three methyl groups appearing as one doublet at  $\delta_{\text{H}}$  1.30 and two singlets at  $\delta_{\text{H}}$  2.50 and  $\delta_{\text{H}}$  2.52, one multiplet at  $\delta_{\text{H}}$  4.55, and two diastereotopic protons H-4<sub>eq</sub> at  $\delta_{\text{H}}$  3.13 and H-4<sub>ax</sub>  $\delta_{\text{H}}$  3.83. This hinted at the presence of a dihydroisoquinoline moiety as was further confirmed by the absence of a quartet in the <sup>1</sup>H NMR spectrum in the region  $\delta_{\text{H}}$  4 ppm for H-1 and the chemical shift of C-1 at 177.9 ppm in the <sup>13</sup>C NMR signal indicating the presence of a double bond. In addition, four methoxy groups at  $\delta_{\text{H}}$  3.97,  $\delta_{\text{H}}$  4.00,  $\delta_{\text{H}}$  4.03, and  $\delta_{\text{H}}$  4.04 were observed. All the methoxy signals had normal chemical shifts, which showed that they were all far from the axis.<sup>[73]</sup> The aromatic region showed six protons (Table 2.7) appearing as two doublets and four singlets. The doublets were *ortho*-coupled, as deduced from the presence of H,H-COSY interactions between them ( $\delta_{\text{H}}$  6.97 and  $\delta_{\text{H}}$  7.46), and were located at C-6' and C-7', respectively. One proton ( $\delta_{\text{H}}$  6.98) was located at C-3' ( $\delta_{\text{C}}$  111.1) as deduced from HMBC correlations between H-3' and CH<sub>3</sub>-2', and between H-3' and C-4'. One proton ( $\delta_{\text{H}}$  7.09) was located at C-1' ( $\delta_{\text{C}}$  113.5) as deduced from HMBC correlations between H-1' and CH<sub>3</sub>-2', and between H-1' and C-3', and between H-1' and C-8'. One proton ( $\delta_{\text{H}}$  6.77) was located at C-5 (109.3) as assumed from HMBC correlations between H-5 and C-4 ( $\delta_{\text{C}}$  34.9). The final aromatic proton was located at C-7 as deduced from HBMC correlations between H-7 and C-6. The DEPT-135 confirmed the presence of seven CH<sub>3</sub> groups, one CH<sub>2</sub>, seven CH entities, and eleven quaternary carbons in the molecule. The position of the axis in the naphthalene moiety was deduced from the chemical shift of Me-2' at 2.50 ppm indicating that this methyl

was not close to the axis.<sup>[73]</sup> Further confirmation came from the presence of two *ortho*-coupled protons assigned to be at C-6' and C-7'. In addition, HMBC correlations were seen between H-1' and C-8', between H-6' and C-8', which further confirmed the position of the axis to be at C-8'.

In the isoquinoline moiety, the only possible coupling site was N-2, because aromatic protons were present at C-5 and C-7, while there was one further methoxy at C-6 and another one on C-8 as deduced from HMBC correlations (Figure 2.28.A).

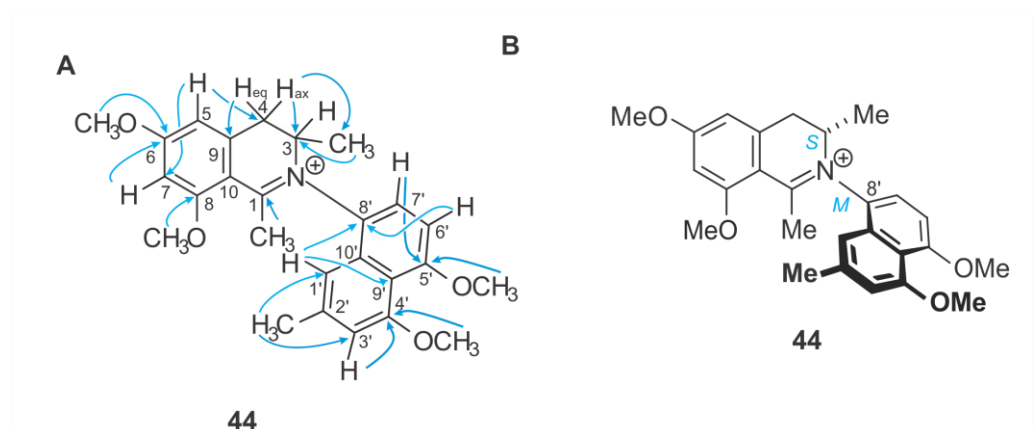


**Figure 2.28:** (A) Selected HMBC correlations; (B) Structure of ancistrocladinium A (**44**).

The ECD measurement of the compound was performed in Prof. G. Bringmann's laboratory at the University of Würzburg. Measurements were done for both the compound **44** and a standard of ancistrocladinium A (Prof. G. Bringmann has a library of NIQ standards, which include ancistrocladinium A). The ECD spectrum of the isolated product (curve in red) was virtually identical to that of ancistrocladinium A (curve in black) previously isolated<sup>[73]</sup> (Figure 2.29).

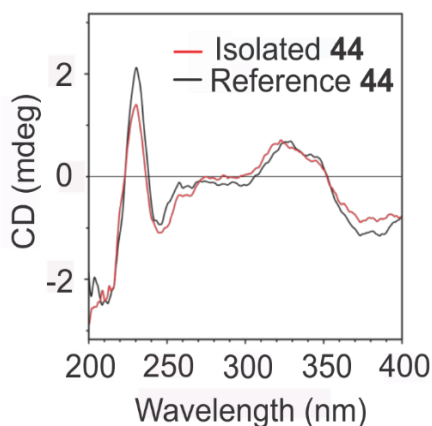


**Figure 2.29:** Comparison of ECD spectra of isolated compound **44** and ancistrocladinium A (reference) previously isolated in Prof. G. Bringmann's laboratory. The two spectra were superimposable, which, in combination with the other spectral findings, confirmed that the two compounds were identical.

An HPLC comparison between compound **44** and a standard sample of ancistrocladinium A undertaken by B.K. Lombe in Prof. G. Bringmann's laboratory showed that the compound **44** and the standard sample of ancistrocladinium A had the same retention time (6.4 min) using the same HPLC conditions (Figures 2.30A and 2.30B). Additionally, when analyzed by HPLC, their peaks co-eluted (Figure 2.30C), providing further confirmation that the isolated compound was ancistrocladinium A (**44**).



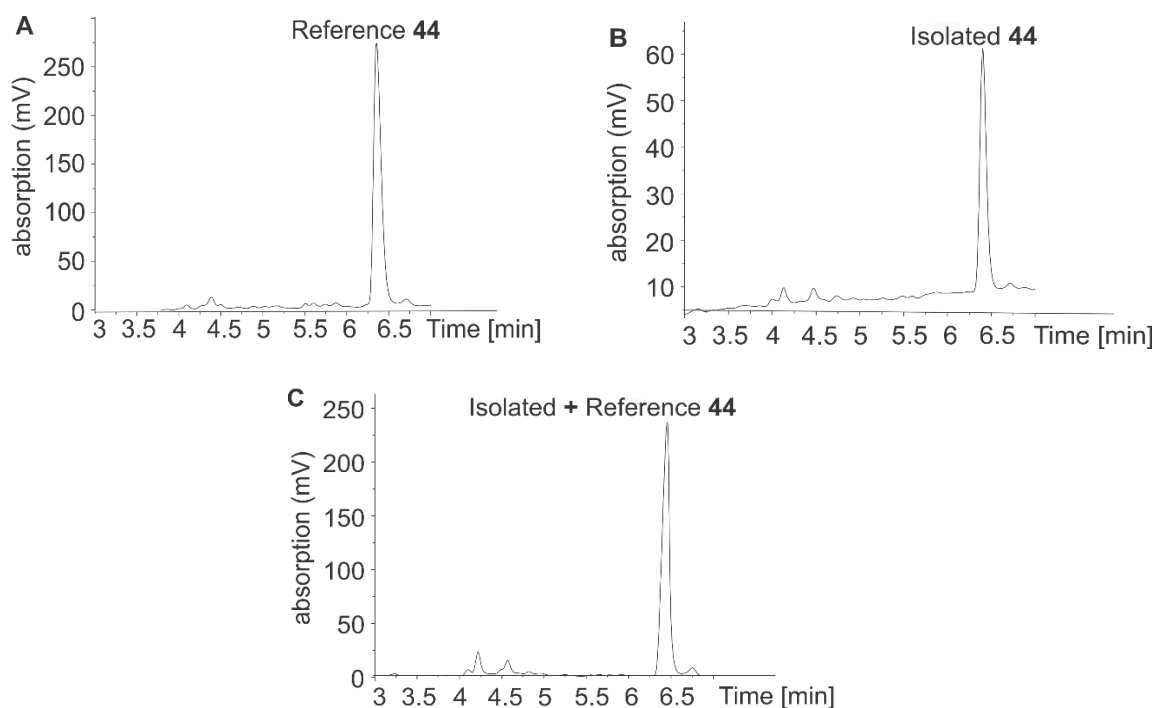


**Figure 2.30:** (A) HPLC-UV<sub>max</sub> chromatogram of standard ancistrocladinium A; (B) HPLC-UV<sub>max</sub> chromatogram of compound **44**; (C) HPLC-UV<sub>max</sub> chromatogram of mixture of compound **44** and ancistrocladinium A.

**Table 2.7:** Comparison of <sup>1</sup>H and <sup>13</sup>C NMR data of ancistrocladinium A (**44**) in CD<sub>3</sub>OD and the published <sup>1</sup>H and <sup>13</sup>C data in CD<sub>3</sub>OD.

<sup>1</sup> H and <sup>13</sup> C data of isolated ancistrocladinium A ( <b>44</b> )			<sup>1</sup> H and <sup>13</sup> C literature data <sup>[73]</sup>	
Position	<sup>1</sup> H (ppm, <i>J</i> in Hz)	<sup>13</sup> C (ppm)	<sup>1</sup> H (ppm, <i>J</i> in Hz)	<sup>13</sup> C (ppm)
1	-	177.9	-	179.6
3	4.25 (1H, <i>m</i> )	59.6	4.25 (1H, <i>m</i> )	61.3
4 <sub>eq</sub>	3.127 (1H, <i>dd</i> , <i>J</i> = 16.8, 2.3 Hz)	35.0	3.13 (1H, <i>dd</i> , <i>J</i> = 17.4, 2.5 Hz)	36.7
4 <sub>ax</sub>	3.833 (1H, <i>dd</i> , <i>J</i> = 16.8, 6.2 Hz)	35.0	3.83 (1H, <i>dd</i> , <i>J</i> = 17.4, 6.2 Hz)	36.7
5	6.77 (1H, <i>s</i> )	109.4	6.77 (1H, <i>s</i> )	111.1
6	-	170.7	-	172.6
7	6.74 (1H, <i>s</i> )	98.9	6.74 (1H, <i>s</i> )	100.7
8	-	166.3	-	168.1
9	-	110.8	-	113.8
10	-	142.2	-	143.9

1'	7.09 (1H, s)	113.5	7.08 (1H, s)	114.8
2'	-	142.0		143.7
3'	6.98 (1H, s)	111.1	6.98 (1H, s)	112.9
4'	-	159.9		161.5
5'	-	161.0		162.7
6'	6.97 (1H, d, $J = 7.9$ Hz)	104.8	6.97 (1H, d, $J = 8.5$ Hz)	106.6
7'	7.46 (1H, d, $J = 7.9$ Hz)	127.2	7.46 (1H, d, $J = 8.5$ Hz)	128.9
8'	-	118.0	-	119.7
9'	-	130.8	-	133.8
10'	-	129.9	-	131.6
1-Me	2.52 (3H, s)	24.8	2.52 (3H, s)	26.5
2'-Me	2.50 (3H, s)	22.3	2.50 (3H, s)	23.9
3-Me	1.30 (3H, d, $J = 6.81$ Hz)	15.5	1.30 (3H, d, $J = 7.1$ Hz)	17.2
4'-OMe	3.97 (3H, s)	56.9	3.97 (3H, s)	58.9
5'-OMe	4.00 (3H, s)	56.9	4.01 (3H, s)	58.6
6-OMe	4.03 (3H, s)	57.0	4.03 (3H, s)	58.6
8-OMe	4.04 (3H, s)	57.1	4.04 (3H, s)	58.9

Compound **44** (ancistrocladinium A) had for the first time been isolated and described from the leaves of an unidentified *Ancistrocladus* species collected in the habitat Yetoto, in the vicinity of Ikela (northwestern part of DRC)<sup>[73]</sup> a region at a distance from the collection site of the plant material investigated in this study (see Figure 2.31). |

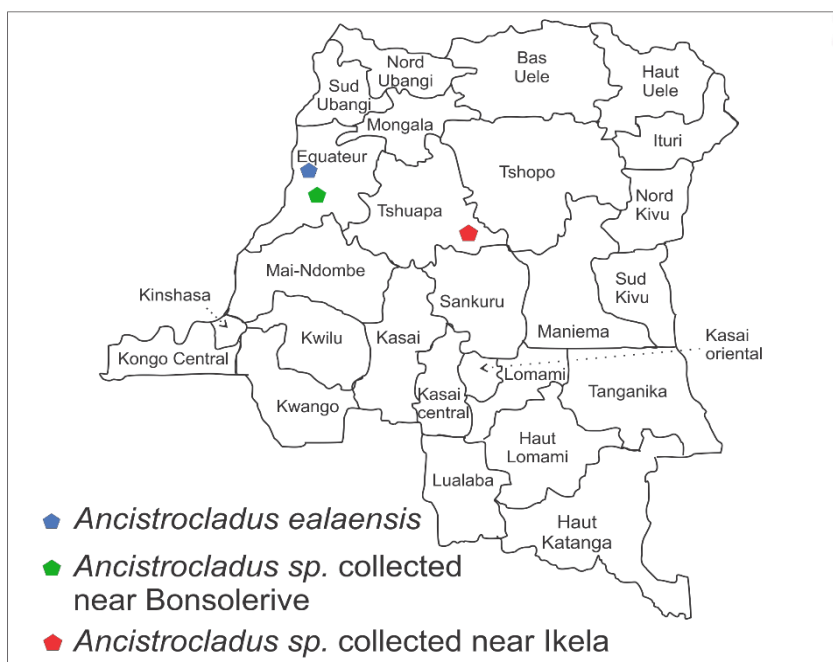


**Figure 2.31:** DRC map showing collection sites of *Ancistrocladus* species, from which ealamine A (blue and red pentagon) and ancistrocladinium A (red pentagon) had been previously isolated. The green diamond shows the collection site of the plant material investigated in this study.

The compound obtained from Fraction F<sub>1</sub> was identified as the known<sup>[88]</sup> *N,C*-coupled naphthylisoquinoline alkaloid, ancistrocyclinone A (**45**) based on its UV spectrum, the NMR data and mass spectral analysis. The cationic mass 402.1745 generated from UPLC-QTOF-MS (Figure 2.32) corresponded to a molecular formula of C<sub>25</sub>H<sub>24</sub>NO<sub>4</sub><sup>+</sup> (calculated mass 402.1705), which was further confirmed by the number of protons in <sup>1</sup>H NMR and of carbon atoms in <sup>13</sup>C NMR.

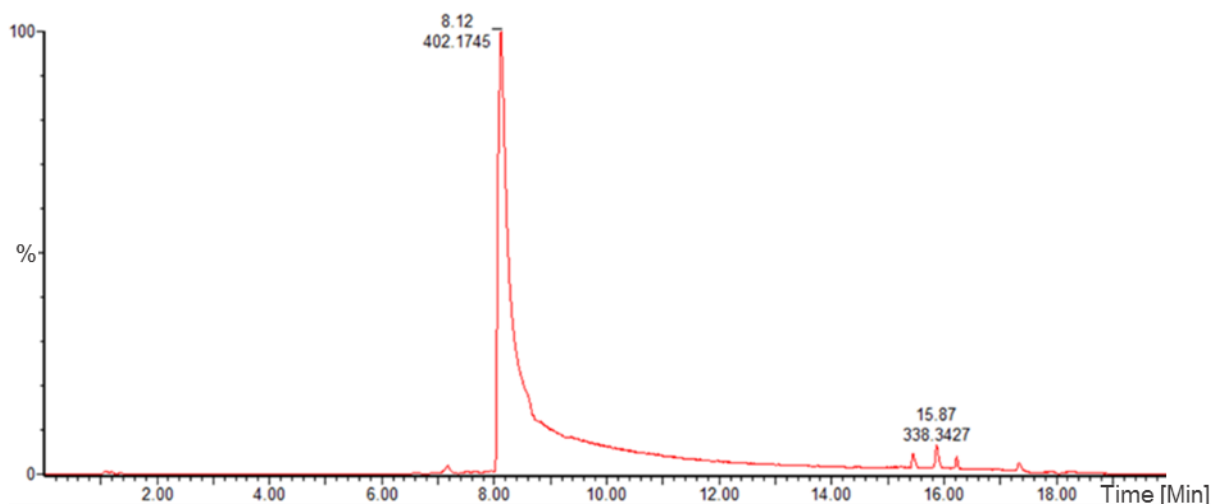


**Figure 2.32:** ESI positive-mode BPI chromatogram of compound **45** isolated from Fraction 1 collected from silica gel column chromatography of the MeOH extract.

$^1\text{H}$  NMR spectrum showed two methyl groups appearing as one doublet at  $\delta_{\text{H}}$  1.58 and one singlet at  $\delta_{\text{H}}$  2.67, one proton appearing as a multiplet at  $\delta_{\text{H}}$  6.22 and two diastereotopic protons H-4<sub>eq</sub> at  $\delta_{\text{H}}$  3.33 and H-4<sub>ax</sub>  $\delta_{\text{H}}$  3.73. This evidenced that the compound was a naphthyldihydroisoquinoline alkaloid. Furthermore, the  $^1\text{H}$  NMR spectrum showed the presence of three methoxy groups in the normal *O*-methyl region at  $\delta_{\text{H}}$  4.04,  $\delta_{\text{H}}$  4.20, and  $\delta_{\text{H}}$  4.25. In the aromatic region, six protons were present, appearing as two doublets and four singlets. One proton was located at position C-5 as deduced from the NOE interactions (Figure 2.33) between H-5 ( $\delta_{\text{H}}$  6.87) and the protons of OMe-6 ( $\delta_{\text{H}}$  4.04), and between H-5 and H-4<sub>eq</sub> ( $\delta_{\text{H}}$  3.33). Final confirmation was achieved through HMBC correlations between H-5 and C-4 (34.0 ppm). One proton was located at C-7 as inferred from NOE interactions between H-7 ( $\delta_{\text{H}}$  6.89) and the protons of OMe-6 and from further NOE interactions between H-7 and the protons of OMe-8 ( $\delta_{\text{H}}$  4.20). Two protons (8.24 and 9.10 ppm) were *ortho*-coupled as revealed by the coupling constant of 8.8 Hz and the H,H-COSY interactions. They were located at positions C-6' and C-7' as further confirmed by NOE interactions between the protons of OMe-5' (4.25 ppm) and H-6' ( $\delta_{\text{H}}$  8.24). All these were in accordance with the data published for ancistrocyclinone A.<sup>[88]</sup> One olefinic proton ( $\delta_{\text{H}}$  9.26 ppm) was assigned at position C-11' as deduced from the HMBC correlations between H-11' and C-2' ( $\delta_{\text{C}}$  144.2) and between H-11' and C-9 ( $\delta_{\text{C}}$  109.4). In addition, HMBC correlations

were seen between H-11' and C-9' ( $\delta_C$  126.1). The position of H-11' was further confirmed by NOE interactions between H-11' and the protons of OMe-2' and between H-11' and the protons of OMe-8. Final confirmation was the presence of H,H-COSY interactions between H-11' and Me-2'. This confirmed C-11' as the bridge of the six-membered ring as in the published compound.<sup>[88]</sup> The rest of the  $^1\text{H}$ ,  $^{13}\text{C}$  NMR data, HMBC correlations, NOE interactions, and COSY interactions confirmed the compound to be identical to the known compound ancistrocyclinone A (**45**, see Figure 2.35).

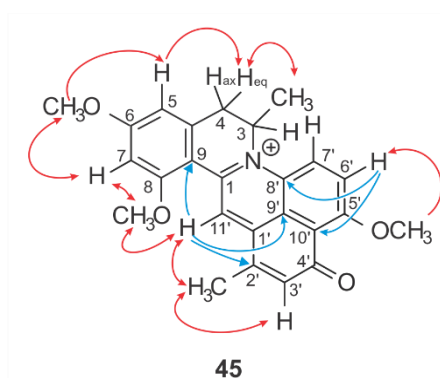


**Figure 2.33:** Selected NOE (red arrows) and HMBC (blue arrows) correlations of ancistrocyclinone A (**45**).

**Table 2.8:** Comparison of the  $^1\text{H}$  and  $^{13}\text{C}$  NMR data of isolated ancistrocyclinone A (**45**) in  $\text{CD}_3\text{COCD}_3$  and  $^1\text{H}$  and  $^{13}\text{C}$  NMR literature data.

$^1\text{H}$ and $^{13}\text{C}$ data of isolated ancistrocyclinone A in $\text{CD}_3\text{COCD}_3$			$^1\text{H}$ and $^{13}\text{C}$ literature data in $\text{CD}_3\text{OD}$ <sup>[88]</sup>	
Position	$^1\text{H}$ (ppm, $J$ in Hz)	$^{13}\text{C}$ (ppm)	$^1\text{H}$ (ppm, $J$ in Hz)	$^{13}\text{C}$ (ppm)
1		148.1		148.6
3	6.22 (1H, $m$ )	54.9	5.98 (1H, $m$ )	55.3
4 <sub>eq</sub>	3.33 (1H, $dd$ , $J = 16.9, 0.7$ Hz)	34.1	3.21 (1H, $dd$ , $J = 16.7, 1.7$ Hz)	34.3
4 <sub>ax</sub>	3.73 (1H, $dd$ , $J = 16.9, 5.4$ Hz)	34.1	3.56 (1H, $dd$ , $J = 16.7, 5.6$ Hz)	34.3
5	6.87 (1H, $s$ )*	108.3	6.80 (1H, $d$ , $J = 2.2$ Hz)	108.4
6	-	167.5	-	168.2
7	6.89 (1H, $s$ )*	99.2	6.82 (1H, $d$ , $J = 2.2$ Hz)	99.5
8	-	162.5	-	162.9

9	-	109.4	-	109.7
10	-	139.3	-	139.4
1'	-	141.4	-	141.0
2'	-	144.2	-	146.0
3'	6.87 (1H, s)*	136.7	6.91 (1H, d, $J = 1.3$ Hz)	136.7
4'	-	182.2	-	184.2
5'	-	163.2	-	163.9
6'	8.24 (1H, d, $J = 8.8$ Hz)	122.5	8.15 (1H, d, $J = 10.0$ Hz)	122.5
7'	9.10 (1H, d, $J = 8.8$ Hz)	126.8	8.93 (1H, d, $J = 10.0$ Hz)	127.4
8'	-	132.5	-	132.8
9'	-	126.2	-	126.4
10'	-	114.9	-	115.1
11'	9.22 (1H, s)	124.3	9.19 (1H, s)	125.0
2'-Me	2.67 (3H, s)*	18.7	2.64 (3H, d, $J = 1.4$ Hz)	18.2
3-Me	1.58 (3H, d, $J = 5.9$ Hz)	16.9	1.50 (3H, d, $J = 6.9$ Hz)	16.7
6-OMe	4.04 (3H, s)	56.7	4.01 (3H, s)	56.7
8-OMe	4.20 (3H, s)	57.3	4.12 (3H, s)	57.2
5'-OMe	4.25 (3H, s)	57.9	4.26 (3H, s)	57.9

\* The doublets are not seen in this case as in the publication maybe because the instrument (Bruker Avarice III 500 MHz Spectrometer) utilized in this study had a lower-field magnet and the deuterated solvent used was different from the one in the publication.

The compound **45** was further analyzed by BK Lombe in Prof. G. Bringmann's laboratory for ECD measurements. The ECD spectrum was compared to the one of ancistrocyclinone A (**45**) previously isolated.<sup>[88]</sup> The two spectra were virtually identical (Figure 2.34) and confirmed that the absolute configuration of the isolated compound was identical with that of ancistrocyclinone A (**45**).

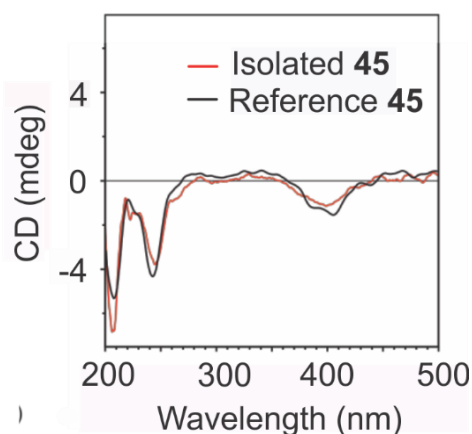


**Figure 2.34:** Comparison of the ECD spectra of the isolated ancistrocyclinone A (**45**) in red and the one previously isolated in Prof. G. Bringmann's laboratory in black (Reference).<sup>[88]</sup>

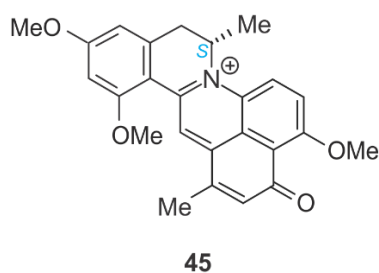


**Figure 2.35:** Structure of ancistrocyclinone A (**45**).

The fourth compound (**46**) was isolated from Fraction F<sub>2</sub>, it was the main compound in Subfraction F<sub>2</sub>SF<sub>3</sub> (yellow solid), with a molecular formula of C<sub>26</sub>H<sub>31</sub>NO<sub>4</sub> as deduced from its monoprotonated molecule at *m/z* 422.2347 from UPLC-QTOF-MS and from the number of protons in <sup>1</sup>H NMR and of the signals in <sup>13</sup>C NMR spectrum.

<sup>1</sup>H NMR indicated that the compound was a naphthyltetrahydroisoquinoline as established by the presence of a quartet at 4.56 ppm (H-1), a multiplet at 3.61 ppm (H-3), and signals of two diastereotopic protons H-4<sub>eq</sub> [ $\delta_{\text{H}}$  2.55 (*J* 17.9 and 4.8 Hz)] and H-4<sub>ax</sub> [ $\delta_{\text{H}}$  2.03 (*J* 17.9 and 11.7 Hz)]. Three signals of methyl groups were present in the spectrum, appearing as two doublets, deduced to be located at positions C-1 ( $\delta_{\text{H}}$  1.54) and C-3 ( $\delta_{\text{H}}$  1.10), and one singlet, characteristic of the aryl-methyl ( $\delta_{\text{H}}$  2.22), situated at C-2' ( $\delta_{\text{C}}$  139.05). A signal of one additional methyl group was seen in the spectrum, as a singlet, and was located on the nitrogen atom based on its chemical shift ( $\delta_{\text{H}}$  2.59). The position was further confirmed by NOE interactions between the

protons of Me-N and Me-3. Further, NOE interactions between the protons of Me-N and Me-1 and between those of Me-N and H-1 confirmed that methyl to be located on the nitrogen atom. Three signals of O-methyl groups were observed, two having normal chemical shifts at  $\delta_{\text{H}}$  3.98 and  $\delta_{\text{H}}$  4.10 and one slightly highfield at  $\delta_{\text{H}}$  3.65 indicating that it was located close to the axis. The aromatic region showed the presence of signals of five protons. Two were *ortho*-coupled ( $\delta_{\text{H}}$  6.92 and  $\delta_{\text{H}}$  7.06), two *meta*-coupled ( $\delta_{\text{H}}$  6.44 and  $\delta_{\text{H}}$  6.63) and one singlet at  $\delta_{\text{H}}$  6.73. This indicated that the coupling site in the naphthalene part could be either at C-6' or C-8', similar to ealamine A (**43**), as described earlier.

The coupling site was deduced to be at C-8' by NOE interactions between H-6' ( $\delta_{\text{H}}$  6.92) and the protons of OMe-5' ( $\delta_{\text{H}}$  4.10). Furthermore, the position of the axis was confirmed by HMBC correlations between H-6' and C-5' and between the protons of OMe-5' and C-5' ( $\delta_{\text{C}}$  157.26). One methoxy ( $\delta_{\text{H}}$  3.65) was located at C-6 as deduced from NOE interactions between H-7 ( $\delta_{\text{H}}$  6.73) and the protons of the O-methyl group at C-6. The third methoxy ( $\delta_{\text{H}}$  3.98) was located at C-8 as deduced from NOE interactions between H-7 and the protons of the O-methyl entity at C-8. This deduction was further confirmed by HMBC correlations between H-7 and C-8 and between the protons of OMe-8 and C-8 ( $\delta_{\text{C}}$  158.22), which pointed to the coupling site in the isoquinoline moiety being C-5. This assumption was further confirmed by HMBC interactions of H-7' ( $\delta_{\text{H}}$  7.06) to C-5 ( $\delta_{\text{C}}$  121.82).

The relative configuration at the stereocenters C-1 and C-3 was deduced to be *trans* from NOE interactions between Me-1 and H-3. Due to limited quantity, the absolute configuration at these stereocenters could not be determined by the published method of ruthenium-mediated oxidative degradation as developed by Prof. G. Bringmann's research group.<sup>[34]</sup>

Furthermore, NOE interactions between H-7' and the H<sub>eq</sub> at C-4 were observed, showing that they were on the same side of the isoquinoline plane. Likewise, the NOE interactions in the series H-4<sub>eq</sub> – H-3 – Me-1 indicated that they were on the same side of the isoquinoline plane. This was corroborated by NOE interactions between H-1' and H-4<sub>ax</sub> (Figure 2.36.B) showing that if the configuration at the stereocenters was 1*R*,3*R* the configuration at the axis would be *P* or if the configuration was 1*S*,3*S*, the configuration at the axis would be *M*.<sup>[7]</sup>



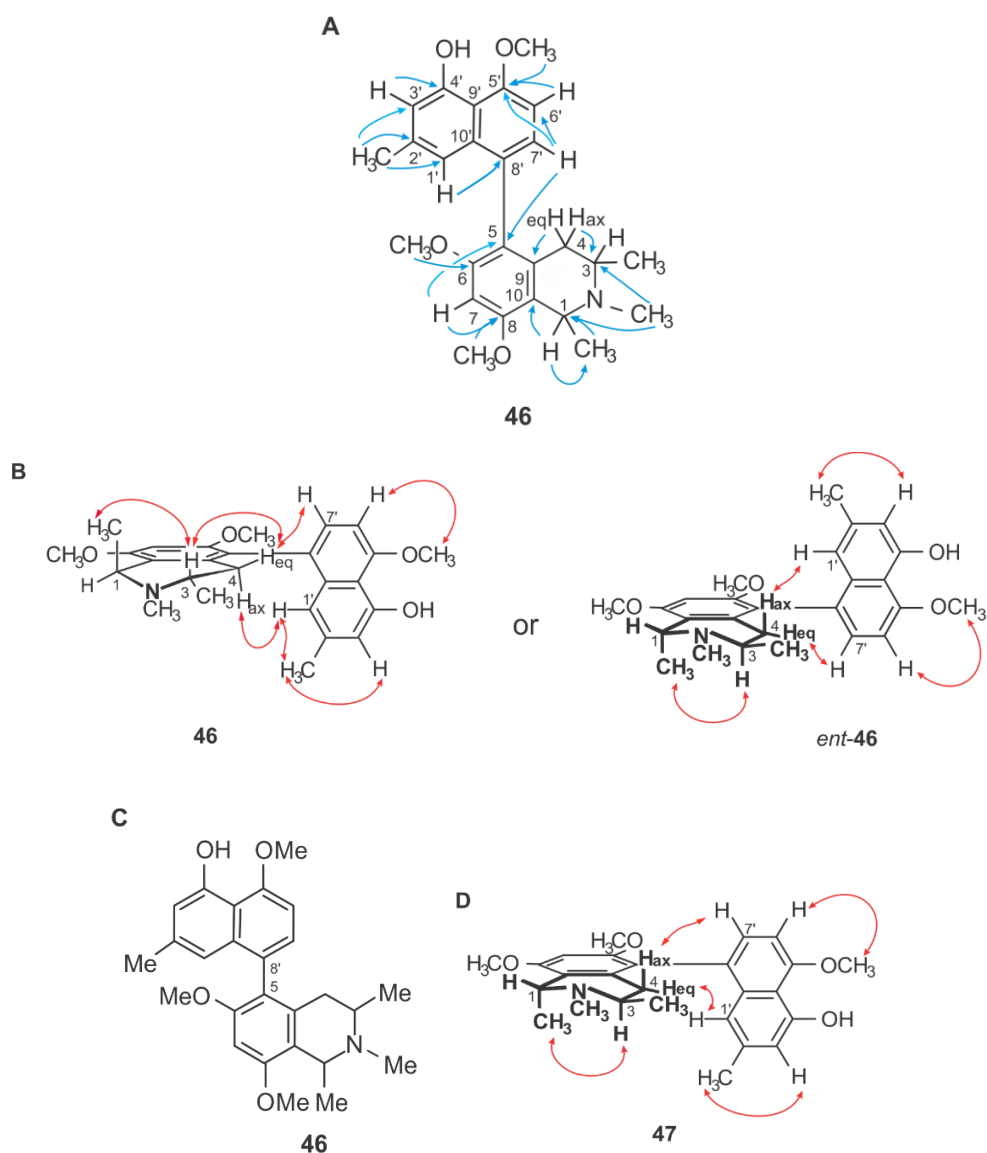


**Figure 2.36:** (A) Selected HMBC correlations; (B) Selected NOE interactions; (C) The two possible enantiomeric structures of compound **46/ent-46**; (D) Selected NOE interactions in ancistrolikokine C<sub>2</sub> (**47**).

The data suggested that this compound was closely related to ancistrolikokine C<sub>2</sub> (**47**). However, ancistrolikokine C<sub>2</sub> (**47**) showed long-range NOE interactions between H-4<sub>eq</sub> and H-1' and between MeO H-4<sub>ax</sub> and H-7', while compound **46** showed long-range NOE interactions between H-4<sub>ax</sub> and H-1' and H-4<sub>eq</sub> and H-7'.<sup>[92]</sup> Since this was contrasting to ancistrolikokine C<sub>2</sub> (*M*), it is possible that this compound could be *P*-configured at the axis. However, this could be only confirmed by ECD analysis, which could not be done due to limited quantity. Since this compound was inactive in the antiplasmodial bioassay (see Section 2.4.6), it did not warrant any further work to determine the absolute configuration.

**Table 2.9:**  $^1\text{H}$ ,  $^{13}\text{C}$  NMR, HMBC, and NOESY data of compound **46**.

Position	$^1\text{H}$ (ppm, $J$ in Hz)	$^{13}\text{C}$ (ppm)	$^3\text{J}$ HMBC (H $\rightarrow$ C)	NOESY
1	4.56 (1H, <i>q</i> , 6.5 Hz)	58.2	1-Me, C-9, C-10	1-Me, N-Me
3	3.61 (1H, <i>m</i> )	49.8		3-Me, 1-Me, H-4 <sub>eq</sub>
4 <sub>eq</sub>	2.55 (1H, <i>dd</i> , $J = 17.9$ , 4.8 Hz)	31.4	C-10, C-9	H-3, H-4 <sub>ax</sub> , H-7'
4 <sub>ax</sub>	2.03 (1H, <i>dd</i> , $J = 17.9$ , 11.7 Hz)	31.4	C-3, C-10	3-Me, H-4 <sub>eq</sub> , H-1'
5	-	121.8		
6	-	159.4		
7	6.73 (1H, <i>s</i> )	95.3	C-5, C-9, C-8	6-OMe, 8-OMe
8	-	158.2		
9	-	116.4		
10	-	133.6		
1'	6.44 (1H, <i>s</i> )	116.4	C-8', 2'-Me, C-9'	H-4 <sub>ax</sub> , 2'-Me
2'	-	139.0		
3'	6.63 (1H, <i>d</i> , 1.22 Hz)	113.0	2'-Me, C-1', C-4'	2'-Me
4'	-	156.1		
5'	-	157.3		
6'	6.92 (1H, <i>d</i> , $J = 7.9$ Hz)	104.5	C-5', C-8', C-9'	H-5'
7'	7.06 (1H, <i>d</i> , $J = 7.9$ Hz)	129.2	C-5, C-10', C-6', C-5'	H-4 <sub>eq</sub>
8'	-	128.3		
9'	-	114.8		
10'	-	137.1		
1-Me	1.54 (3H, <i>d</i> , $J = 6.66$ Hz)	17.9	C-1, C-9	N-Me, H-3, H-1, 8-OMe
2'-Me	2.22 (3H, <i>s</i> )	22.0	C-3', C-2', C-1'	H-1', H-3'
3-Me	1.10 (3H, <i>d</i> , $J = 6.46$ Hz)	17.4	C-4, C-3	H-4 <sub>ax</sub> , N-Me, H-3
N-Me	2.59 (3H, <i>s</i> )	35.7	C-1, C-3,	H-1, 1-Me, 3-Me
6-OMe	3.65 (3H, <i>s</i> )	56.4	C-6	H-7
8-OMe	3.98 (3H, <i>s</i> )	56.2	C-8	H-7, 1-Me
5'-OMe	4.10 (3H, <i>s</i> )	56.8	C-5'	H-6'

## 2.4.8 Antiplasmodial screening of compounds

In order to classify the *in vitro* antiplasmodial activity of compounds as “excellent”, “good”, “moderate”, “low”, and “inactive”, Basco et al. (1994) adopted the following criteria  $IC_{50} < 10 \mu\text{g/mL}$ , “good activity”,  $IC_{50}$  of 10-50  $\mu\text{g/mL}$ , “moderate activity”,  $IC_{50}$  of 50-100  $\mu\text{g/mL}$ , “low activity”, and  $IC_{50} > 100 \mu\text{g/mL}$ , “inactive”.<sup>[96, 97]</sup> Muriithi et al. (2002) expressed the  $IC_{50}$  in  $\mu\text{M}$  and considered the following criteria:  $IC_{50}$  of 1-20  $\mu\text{M}$ , “limited activity”,  $IC_{50} > 100 \mu\text{M}$ , “inactive”,  $IC_{50}$  of 20-60  $\mu\text{M}$ , “low activity”.<sup>[98]</sup> Batista et al. (2009) adopted the following criteria:  $IC_{50} < 1 \mu\text{M}$ , “excellent/potent activity”,  $IC_{50}$  of 1-20  $\mu\text{M}$ , “good activity”,  $IC_{50}$  of 20-100  $\mu\text{M}$ , “moderate activity”,  $IC_{50}$  of 100-200  $\mu\text{M}$ , “low activity”, and  $IC_{50} > 200 \mu\text{M}$ , “inactive”.<sup>[99]</sup>

In this study, the classification criteria considered by Batista et al. (2009)<sup>[99]</sup> is adopted.

Ancistrocyclinone A (**45**), ancistrocladinium A (**44**), and ealamine A (**43**) were selected for screening against asexual *P. falciparum* NF54 strains (chloroquine-sensitive strains) as compound **46** had previously been screened as part of the subfractions ( $F_2SF_3$ ), which did not show any activity. The three compounds were screened in a dual-point assay at concentrations of 1 and 5  $\mu\text{g/mL}$ . The screening results showed that ancistrocladinium A (**44**) and ealamine A (**43**) had good activity as they both had > 50 % inhibition at 5  $\mu\text{g/mL}$  (Table 2.10). Limited or no activity was observed at 1  $\mu\text{g/mL}$ , while ancistrocyclinone A (**45**) did not show any antiplasmodial activity at both test concentrations.

**Table 2.10:** *In vitro* activity of three isolated compounds against asexual NF54 *P. falciparum* parasites, obtained at concentrations of 1 and 5  $\mu\text{g/mL}$ . Data were from a single independent biological technical repeat, performed in technical triplicates,  $\pm$  SD.

Compound	Asexual proliferation (% inhibition)	
	1 $\mu\text{g/mL}$	5 $\mu\text{g/mL}$
Ancistrocladinium A ( <b>44</b> )	13.8	85.1
Ancistrocyclinone A ( <b>45</b> )	0.0	0.0
Ealamine A ( <b>43</b> )	0.0	96.4

The two active compounds were then tested against drug-resistant *P. falciparum* cell lines to determine their IC<sub>50</sub> values. Ancistrocladinium A (**44**) and ealamine A (**43**) showed good activity (Table 2.11) against NF54 with IC<sub>50</sub> values of 4.67 μM and 5.74 μM respectively. They were further screened against the *P. falciparum* K1 (chloroquine-, pyrimethamine-, mefloquine-, and cycloguanil-resistant) and W2 (chloroquine-, quinine-, pyrimethamine-, and cycloguanil-resistant) strains. Ancistrocladinium A (**44**) demonstrated IC<sub>50</sub> values of 3.27 μM against K1 and 4.17 μM against W2, while ealamine A (**43**) displayed IC<sub>50</sub> values of 1.54 μM against K1 and 3.12 μM against W2, which were regarded as being “good” as per the classification criteria of Batista et al. (2009). Even more interesting, they exhibited no cross-resistance towards drug resistant *P. falciparum* parasites with resistance index (RI) values < 1, making them valuable hits for further investigation.<sup>[100]</sup>

The antiplasmodial activity of ancistrocladinium A (**44**) had previously been reported against K1 strains of *P. falciparum* with IC<sub>50</sub> value of 0.60 μM (the IC<sub>50</sub> value of chloroquine in the same assay was 0.128 μM),<sup>[73]</sup> which was classified as moderate as per the classification criteria used in the analysis, while in this assay it showed an IC<sub>50</sub> value of 3.27 μM (IC<sub>50</sub> value of chloroquine in the same assay 0.154 μM). In the current assay, the IC<sub>50</sub> value of **44** against K1 *P. falciparum* was fivefold higher than the one reported,<sup>[73, 74]</sup> while the IC<sub>50</sub> value of chloroquine in the assay presented here was only 1.2 fold higher than the one reported for ancistrocladinium A assay.<sup>[73, 74]</sup> The difference might be because the assays were different, and in addition, conducted in a different environment. Further, we here report for the first time the antiplasmodial activity of ancistrocladinium A (**44**) against the NF54 and W2 strains of *P. falciparum*.

The activity of ealamine A (**43**) against *P. falciparum* K1 and NF54 strains had been reported in the PhD thesis of D.T. Tshitenge with IC<sub>50</sub> values of 1.61 and 6.28 μM (IC<sub>50</sub> values of chloroquine 0.008 and 0.364 μM, respectively).<sup>[94]</sup> The IC<sub>50</sub> values of ealamine A (**43**) obtained in this study against K1 and NF54 strains were in agreement with the ones reported. Further, it is the first time that the activity of ealamine A (**43**) against W2 strains is presented, which is regarded as being good (3.12 μM).

**Table 2.11:** Dose-response results of ancistrocladinium A (**44**), ealamine A (**43**), and chloroquine, screened for the IC<sub>50</sub> values for their activities against asexual parasites using the SYBR Green I based assay. Results were representative of a single independent biological replicate, n = 1, each performed as technical triplicates.

Compound	NF54	K1	RI ( $\frac{K1}{NF54}$ )	W2	RI ( $\frac{W2}{NF54}$ )
	IC <sub>50</sub> (μM)	IC <sub>50</sub> (μM)		IC <sub>50</sub> (μM)	
Chloroquine	0.01 ± 0.003	0.154 ± 0.014	15.4	0.233 ± 0.049	23.3
<b>44</b>	4.67	3.27	0.7	4.17	0.9
<b>43</b>	5.74	1.54	0.3	3.12	0.5

The structures of the two active compounds, ancistrocladinium A (**44**) and ealamine A (**43**, see Figure 2.13), had different coupling types with one being *N*,8'-coupled (ancistrocladinium A, **44**) and the other one 7,8'-coupled (ealamine A, **43**). Additionally, ancistrocladinium A (**44**) had a dihydroisoquinoline moiety, *S*-configuration at C-3, and *M*-configuration at the axis, while ealamine A (**43**) had a tetrahydroisoquinoline moiety, *R*-configuration at C-3, and *P*-configuration at the axis. This complexity in the various possible configurations of NIQs provided a challenge to identify the pharmacophore of NIQs for antiplasmodial activity.

The inhibitory potentials of ancistrocladinium A (**44**) and ealamine A (**43**) were less efficient than those of some NIQs such as dioncophylline C (**39**, see Figure 2.10), which had exhibited excellent activity against *P. falciparum* NF54 strains, with an IC<sub>50</sub> value of 0.04 μM,<sup>[2, 43]</sup> *N*-methylancistectorine A<sub>1</sub> (**38**, see Figure 2.10), ancistectorine A<sub>2</sub> (**33a**, see Figure 2.7), 5-*epi*-ancistectorine A<sub>2</sub> (**33b**, see Figure 2.7), which had shown excellent antiplasmodial activities against *P. falciparum* resistant strains K1 with IC<sub>50</sub> values of 0.08, 0.07, and 0.03 μM, respectively.<sup>[42]</sup>

## 2.5 Conclusion

Leaves of *Ancistrocladus* sp. collected in Bonsolerive (DRC) were extracted with *n*-hexane, DCM, EtOAc, MeOH, and water and their antiplasmodial activities assessed against *Plasmodium falciparum* NF54 strains. The MeOH extract displayed far superior *in vitro* antiplasmodial activity (100 % inhibition at 10 and 20 μg/mL) as compared to

other extracts showing that the more potent compounds were concentrated in it, or maybe only in higher quantities. By UPLC-QTOF-MS analysis, naphthylisoquinoline (NIQ) alkaloids were confirmed to be present in the DCM, EtOAc, and MeOH extracts with most of them having the same  $m/z$  values. However, the significant differences in the antiplasmodial efficacy between these extracts demonstrated that the NIQs present were structurally different. This confirmed that the several features that differentiate NIQs of the same  $m/z$  value have an influence on the biological activity. Nevertheless as the overall goal was to identify NIQs with antiplasmodial activity, the use of UPLC-QTOF-MS was successful in confirming that the MeOH extract, which had the best antiplasmodial activity, did contain NIQs predominately, although as a highly complex mixture.

UPLC-QTOF-MS analysis was again successful in identifying selective fractions mainly containing naphthylisoquinoline alkaloids after the silica gel column chromatography purification of the MeOH extract, which gave 18 fractions. This greatly supported the targeted approach of identifying NIQs as potential antiplasmodial lead compounds and reducing the number of samples for bioassaying. The five fractions that contained NIQs showed good antiplasmodial activity with more than 95 % inhibition both at 10 and 5  $\mu\text{g/mL}$  providing further confirmation that these compounds are responsible for the biological activity.

One of the major obstacles for isolation of NIQs is the complexity of their mixtures due to the various stereochemical possibilities, thereby making purification together with the small quantities of the specific stereoisomers a serious challenge. This was experienced for one of the subfractions ( $F_2SF_1$ ) prepared from the active Fraction 2 ( $F_2$ ) using preparative HPLC, which showed a good antiplasmodial activity with 98 % inhibition at 5  $\mu\text{g/mL}$  and 82 % inhibition at 1  $\mu\text{g/mL}$  against *P. falciparum* NF54. Due to its limited quantities, while UPLC-QTOF-MS and NMR indicated it to still be highly complex, further purification to isolate the active compound did not succeed.

From the remaining active fractions, three compounds were isolated by HPLC and LC-MS-SPE-NMR and with the use of MS, NMR, and ECD spectroscopic techniques the structure of the compounds were elucidated. They were identified as the known alkaloids ealamine A (**43**),<sup>[94]</sup> ancistrocladinium A (**44**),<sup>[73]</sup> and ancistrocyclinone A (**45**).<sup>[88]</sup> The structure of the fourth compound **46** was elucidated to the relative configuration.

Ealamine A (**43**), ancistrocladinium A (**44**), and ancistrocyclinone A (**45**) were assayed against *P. falciparum* NF54, while **46** was not screened because it was identified and its structure elucidated from a subfraction (F<sub>2</sub>SF<sub>3</sub>, see Table 2.5) that showed no or only minimal activity. Ealamine A (**43**) and ancistrocladinium A (**44**) exhibited good antiplasmodial activities and were thereafter screened against *P. falciparum* resistant K1 and W2 strains. They both showed good activities against all these strains (IC<sub>50</sub> < 10 μM) with no cross-resistance between the strains.

## 2.6 References

- [1] S. Fayez, D. Feineis, V. Mudogo, S. Awale, G. Bringmann: **Ancistrolikokines E-H and related 5,8-coupled naphthylisoquinoline alkaloids from the Congolese liana *Ancistrocladus likoko* with antiausterity activities against PANC-1 human pancreatic cancer cells.** *RSC Adv.* **2017**, *7*, 53740-53751.
- [2] G. François, G. Bringmann, J. D. Phillipson, L. Aké Assi, C. Dochez, M. Rübenacker, C. Schneider, M. Wéry, D. C. Warhurst, G. C. Kirby: **Activity of extracts and naphthylisoquinoline alkaloids from *Triphyophyllum peltatum*, *Ancistrocladus abbreviatus* and *A. barteri* against *Plasmodium falciparum* in vitro.** *Phytochemistry* **1994**, *35*, 1461-1464.
- [3] C. M. Taylor, R. E. Gereau, G. M. Walters: **Revision of *Ancistrocladus* Wall. (*Ancistrocladaceae*).** *Ann. Missouri Bot. Gard.* **2005**, *92*, 360-399.
- [4] B. K. Lombe, D. Feineis, V. Mudogo, R. Brun, S. Awale, G. Bringmann: **Michellamines A<sub>6</sub> and A<sub>7</sub>, and further mono- and dimeric naphthylisoquinoline alkaloids from a Congolese *Ancistrocladus* liana and their antiausterity activities against pancreatic cancer cells.** *RSC Adv.* **2018**, *8*, 5243-5254.
- [5] D. T. Tshitenge, D. Feineis, V. Mudogo, M. Kaiser, R. Brun, E.-J. Seo, T. Efferth, G. Bringmann: **Mbandakamine-type naphthylisoquinoline dimers and related alkaloids from the Central African liana *Ancistrocladus ealaensis* with antiparasitic and antileukemic activities.** *J. Nat. Prod.* **2018**, *81*, 918-933.
- [6] J. Li, R. Seupel, T. Bruhn, D. Feineis, M. Kaiser, R. Brun, V. Mudogo, S. Awale, G. Bringmann: **Jozilebomines A and B, naphthylisoquinoline dimers from the Congolese liana *Ancistrocladus ileboensis*, with antiausterity activities against the PANC-1 human pancreatic cancer cell line.** *J. Nat. Prod.* **2017**, *80*, 2807-2817.
- [7] S. M. Kavatsurwa, B. K. Lombe, D. Feineis, D. F. Dibwe, V. Maharaj, S. Awale, G. Bringmann: **Ancistroyafungines A-D, 5,8'- and 5,1'-coupled naphthylisoquinoline alkaloids from a Congolese *Ancistrocladus* species, with antiausterity activities against human PANC-1 pancreatic cancer cells.** *Fitoterapia* **2018**, *130*, 6-16.
- [8] G. Heubl, F. Turini, V. Mudogo, I. Kajahn, G. Bringmann: ***Ancistrocladus ileboensis* (D.R. Congo), a new liana with unique alkaloids.** *Plant Ecol. Evol.* **2010**, *143*, 63-69.

- [9] G. Zhang: **PhD thesis**. Julius-Maximilians-Universität Würzburg **2012**.
- [10] B. K. Lombe, T. Bruhn, D. Feineis, V. Mudogo, R. Brun, G. Bringmann: **Antiprotozoal spirombandakamines A<sub>1</sub> and A<sub>2</sub>, fused naphthylisoquinoline dimers from a Congolese *Ancistrocladus* plant**. *Org. Lett.* **2017**, *19*, 6740-6743.
- [11] S. R. M. Ibrahim, G. A. Mohamed: **Naphthylisoquinoline alkaloids potential drug leads**. *Fitoterapia* **2015**, *106*, 194-225.
- [12] G. Bringmann, R. Seupel, D. Feineis, M. Xu, G. Zhang, M. Kaiser, R. Brun, E.-J. Seo, T. Efferth: **Antileukemic ancistrobenomine B and related 5,1'-coupled naphthylisoquinoline alkaloids from the Chinese liana *Ancistrocladus tectorius***. *Fitoterapia* **2017**, *121*, 76-85.
- [13] G. Bringmann, R. Seupel, D. Feineis, G. Zhang, M. Xu, J. Wu, M. Kaiser, R. Brun, E.-J. Seo, T. Efferth: **Ancistectorine D, a naphthylisoquinoline alkaloid with antiprotozoal and antileukemic activities, and further 5,8'- and 7,1'-linked metabolites from the Chinese liana *Ancistrocladus tectorius***. *Fitoterapia* **2016**, *115*, 1-8.
- [14] G. Bringmann, C. Günther, W. Saeb, J. Mies, R. Brun, L. Aké Assi: **8-O-Methyldioncophyllinol B and revised structures of other 7,6'-coupled naphthylisoquinoline alkaloids from *Triphyophyllum peltatum* (Dioncophyllaceae)**. *Phytochemistry* **2000**, *54*, 337-346.
- [15] C. Jiang, Z.-L. Li, P. Gong, S.-L. Kang, M.-S. Liu, Y.-H. Pei, Y.-K. Jing, H.-M. Hua: **Five novel naphthylisoquinoline alkaloids with growth inhibitory activities against human leukemia cells HL-60, K562 and U937 from stems and leaves of *Ancistrocladus tectorius***. *Fitoterapia* **2013**, *91*, 305-312.
- [16] G. Bringmann, F. Teltschik, M. Schäffer, R. Haller, S. Bär, S. A. Robertson, M. A. Isahakia: **Ancistrobertsonine A and related naphthylisoquinoline alkaloids from *Ancistrocladus robertsoniorum***. *Phytochemistry* **1998**, *47*, 31-35.
- [17] G. Bringmann, G. Zhang, T. Büttner, G. Bauckmann, T. Kupfer, H. Braunschweig, R. Brun, V. Mudogo: **Jozimine A<sub>2</sub>: the first dimeric Dioncophyllaceae-type naphthylisoquinoline alkaloid, with three chiral axes and high antiplasmodial activity**. *Chem.: Eur. J.* **2013**, *19*, 916-923.
- [18] G. Bringmann, M. Rübenacker, T. Geuder, L. Aké Assi: **Dioncophylline B, a naphthylisoquinoline alkaloid with a new coupling type from *Triphyophyllum peltatum***. *Phytochemistry* **1991**, *30*, 3845-3847.
- [19] G. Bringmann, M. Dreyer, J. H. Faber, P. W. Dalsgaard, J. W. Jaroszewski, H. Ndangalasi, F. Mbago, R. Brun, M. Reichert, K. Maksimenka, S. B. Christensen: **Ancistrotanzanine A, the first 5,3'-coupled naphthylisoquinoline alkaloid, and two further, 5,8'-linked related compounds from the newly described species *Ancistrocladus tanzaniensis***. *J. Nat. Prod.* **2003**, *66*, 1159-1165.
- [20] G. Bringmann, B. K. Lombe, C. Steinert, K. Ndjoko Ioset, R. Brun, F. Turini, G. Heubl, V. Mudogo: **Mbandakamines A and B, unsymmetrically coupled dimeric naphthylisoquinoline alkaloids, from a Congolese *Ancistrocladus* species**. *Org. Lett.* **2013**, *15*, 2590-2593.
- [21] M. Xu, T. Bruhn, B. Hertlein, R. Brun, A. Stich, J. Wu, G. Bringmann: **Shuangancistrotectorines A-E, dimeric naphthylisoquinoline alkaloids with three chiral biaryl axes from the Chinese plant *Ancistrocladus tectorius***. *Chem.: Eur. J.* **2010**, *16*, 4206-4216.



- [22] G. Bringmann, F. Pokorny: **The naphthylisoquinoline alkaloids.** in *The Alkaloids*, ed. G. A. Cordell, Academic Press Inc, New York, **1995**, vol. 46, pp. 127-271.
- [23] Z.-Q. Xin, X.-Q. Li, Y. Ye: **Two new naphthylisoquinoline alkaloids from stems and leaves of *Ancistrocladus tectorius* AU - Tang, Chun-Ping.** *Nat. Prod. Res.* **2010**, 24, 989-994.
- [24] F. Bracher, W. J. Eisenreich, J. Mühlbacher, M. Dreyer, G. Bringmann: **Saludimerines A and B, novel-type dimeric alkaloids with stereogenic centers and configurationally semistable biaryl axes.** *J. Org. Chem.* **2004**, 69, 8602-8608.
- [25] A. Karn, A. Mewada, M. Sharon, M. Sharon: **Antimalarial activity of yaoundamine a naphthylisoquinoline alkaloid, extracted from stems of *Ancistrocladus heyneanus*.** *Annals Biol. Sci.* **2014**, 2, 40-44.
- [26] G. Bringmann, F. Teltschik, M. Michel, S. Busemann, M. Rückert, R. Haller, S. Bär, S. A. Robertson, R. Kaminsky: **Ancistrobertsonines B, C, and D as well as 1,2-didehydroancistrobertsonine D from *Ancistrocladus robertsoniorum*.** *Phytochemistry* **1999**, 52, 321-332.
- [27] G. Bringmann, C. Schneider, U. Möhler, R.-M. Pfeifer, R. Götz, L. Aké Assi, E.-M. Peters, K. Peters: **Two atropisomeric *N*-methyldioncophyllines A and *N*-methylphylline, their naphthalene-free heterocyclic moiety, from *Ancistrocladus barteri*.** *Z. Naturforsch. B Chem.* **2003**, 58, 577-584.
- [28] G. Bringmann, R. Zagst, H. Reuscher, L. Aké Assi: **Ancistrobrevine B, the first naphthylisoquinoline alkaloid with a 5,8'-coupling site, and related compounds from *Ancistrocladus abbreviatus*.** *Phytochemistry* **1992**, 31, 4011-4014.
- [29] G. Bringmann, D. Koppler, D. Scheutzow, A. Porzel: **Determination of configuration at the biaryl axes of naphthylisoquinoline alkaloids by long-range NOE effects.** *Magn. Reson. Chem.* **1997**, 35, 297-301.
- [30] G. Bringmann, T. Bruhn, K. Maksimenka, Y. Hemberger: **The assignment of absolute stereostructures through quantum chemical circular dichroism calculations.** *Eur. J. Org. Chem.* **2009**, 2009, 2717-2727.
- [31] G. Bringmann, T. A. M. Gulder, M. Reichert, T. Gulder: **The online assignment of the absolute configuration of natural products: HPLC-CD in combination with quantum chemical CD calculations.** *Chirality* **2008**, 20, 628-642.
- [32] T. Bruhn, A. SchaumLöffel, Y. Hemberger, G. Bringmann: **SpecDis: quantifying the comparison of calculated and experimental electronic circular dichroism spectra.** *Chirality* **2013**, 25, 243-249.
- [33] G. Bringmann, T. Geuder, M. Rübenacker, R. Zagst: **Facile degradation procedure for determination of absolute configuration in 1,3-dimethyltetra- and dihydroisoquinolines.** *Phytochemistry* **1991**, 30, 2067-2070.
- [34] G. Bringmann, R. God, M. Schäffer: **An improved degradation procedure for determination of the absolute configuration in chiral isoquinoline and  $\beta$ -carboline derivatives.** *Phytochemistry* **1996**, 43, 1393-1403.
- [35] G. Bringmann, D. Feineis: **Stress-related polyketide metabolism of Dioncophyllaceae and Ancistrocladaceae.** *J. Exp. Bot.* **2001**, 52, 2015-2022.
- [36] G. Bringmann, J. Mutanyatta-Comar, M. Greb, S. Rüdener, T. F. Noll, A. Irmer: **Biosynthesis of naphthylisoquinoline alkaloids: synthesis**

- and incorporation of an advanced  $^{13}\text{C}_2$ -labeled isoquinoline precursor. *Tetrahedron* **2007**, *63*, 1755-1761.
- [37] G. Bringmann, A. Hamm, C. Günther, M. Michel, R. Brun, V. Mudogo: **Ancistroalaines A and B, two new bioactive naphthylisoquinolines, and related naphthoic acids from *Ancistrocladus ealaensis***. *J. Nat. Prod.* **2000**, *63*, 1465-1470.
- [38] C. Wiart, S. Mogana, S. Khalifah, M. Mahan, S. Ismail, M. Buckle, A. Narayana, M. Sulaiman: **Antimicrobial screening of plants used for traditional medicine in the state of Perak, Peninsular Malaysia**. *Fitoterapia* **2004**, *75*, 68-73.
- [39] G. Bringmann, M. Rübenacker, E. Ammermann, G. Lorenz, L. Aké Assi, G. Bringmann: **Dioncophyllines A and B as fungicides**. *European Patent EP* **1992**, *515*, A1.
- [40] G. Bringmann, C. Steinert, D. Feineis, V. Mudogo, J. Betzin, C. Scheller: **HIV-inhibitory michellamine-type dimeric naphthylisoquinoline alkaloids from the Central African liana *Ancistrocladus congolensis***. *Phytochemistry* **2016**, *128*, 71-81.
- [41] S. Favez, D. Feineis, V. Mudogo, E.-J. Seo, T. Efferth, G. Bringmann: **Ancistrolikokine I and further 5,8'-coupled naphthylisoquinoline alkaloids from the Congolese liana *Ancistrocladus likoko* and their cytotoxic activities against drug-sensitive and multidrug resistant human leukemia cells**. *Fitoterapia* **2018**, *129*, 114-125.
- [42] G. Bringmann, G. Zhang, T. Ölschläger, A. Stich, J. Wu, M. Chatterjee, R. Brun: **Highly selective antiplasmodial naphthylisoquinoline alkaloids from *Ancistrocladus tectorius***. *Phytochemistry* **2013**, *91*, 220-228.
- [43] G. François, G. Timperman, J. Holenz, L. A. Assi, T. Geuder, L. Maes, J. Dubois, M. Hanocq, G. Bringmann: **Naphthylisoquinoline alkaloids exhibit strong growth-inhibiting activities against *Plasmodium falciparum* and *P. berghei* in vitro - structure-activity relationships of dioncophylline C**. *Ann. Trop. Med. Parasitol.* **1996**, *90*, 115-123.
- [44] G. François, G. Bringmann, C. Dochez, C. Schneider, G. Timperman, L. Aké Assi: **Activities of extracts and naphthylisoquinoline alkaloids from *Triphyophyllum peltatum*, *Ancistrocladus abbreviatus* and *Ancistrocladus barteri* against *Plasmodium berghei* (Anka strain) in vitro**. *J. Ethnopharmacol.* **1995**, *46*, 115-120.
- [45] G. François, G. Timperman, W. Eling, L. Aké Assi, J. Holenz, G. Bringmann: **Naphthylisoquinoline alkaloids against malaria: evaluation of the curative potentials of dioncophylline C and dioncopeltine A against *Plasmodium berghei* in vivo**. *Antimicrob. Agents Chemother.* **1997**, *41*, 2533-2539.
- [46] G. Bringmann, C. Schneider, L. Aké Assi: **Ancistrobarterine A: a new "mixed" Ancistrocladaceae/Dioncophyllaceae-type alkaloid from *Ancistrocladus barteri***. *Planta Med.* **1993**, *59*, A620-A621.
- [47] G. François, G. Timperman, T. Steenackers, L. Aké Assi, J. Holenz, G. Bringmann: **In vitro inhibition of liver forms of the rodent malaria parasite *Plasmodium berghei* by naphthylisoquinoline alkaloids - structure-activity relationships of dioncophyllines A and C and ancistrocladine**. *Parasitol. Res.* **1997**, *83*, 673-679.
- [48] J. D. Johnson, R. A. Dennull, L. Gerena, M. Lopez-Sanchez, N. E. Roncal, N. C. Waters: **Assessment and continued validation of the malaria SYBR**

- Green I-based fluorescence assay for use in malaria drug screening.** *Antimicrob. Agents Chemother.* **2007**, *51*, 1926-1933.
- [49] H. Meimberg, H. Rischer, F. G. Turini, V. Chamchumroon, M. Dreyer, M. Sommaro, G. Bringmann, G. Heubl: **Evidence for species differentiation within the *Ancistrocladus tectorius* complex (Ancistrocladaceae) in Southeast Asia: a molecular approach.** *Plant Syst. Evol.* **2010**, *284*, 77-98.
- [50] P. Moyo, M. Botha, S. Nondaba, J. Niemand, V. J. Maharaj, J. N. Eloff, A. I. Louw, L. Birkholtz: ***In vitro* inhibition of *Plasmodium falciparum* early and late stage gametocyte viability by extracts from eight traditionally used South African plant species.** *J. Ethnopharmacol.* **2016**, *185*, 235-242.
- [51] H. Li, W. Yao, Q. Liu, J. Xu, B. Bao, M. Shan, Y. Cao, F. Cheng, A. Ding, L. Zhang: **Application of UHPLC-ESI-Q-TOF-MS to identify multiple constituents in processed products of the herbal medicine Ligustri Lucidi Fructus.** *Molecules* **2017**, *22*, 689.
- [52] G. Bringmann, M. Rückert, J. Schlauer, M. Herderich: **Separation and identification of dimeric naphthylisoquinoline alkaloids by liquid chromatography coupled to electrospray ionization mass spectrometry.** *J. Chromatogr. A* **1998**, *810*, 231-236.
- [53] A. Montagnac, A. H. A. Hadi, F. Remy, M. Païs: **Isoquinoline alkaloids from *Ancistrocladus tectorius*.** *Phytochemistry* **1995**, *39*, 701-704.
- [54] G. Bringmann, M. Wohlfarth, H. Rischer, J. Schlauer, R. Brun: **Extract screening by HPLC coupled to MS-MS, NMR, and CD: a dimeric and three monomeric naphthylisoquinoline alkaloids from *Ancistrocladus griffithii*.** *Phytochemistry* **2002**, *61*, 195-204.
- [55] G. Bringmann, J. Spuziak, J. H. Faber, T. Gulder, I. Kajahn, M. Dreyer, G. Heubl, R. Brun, V. Mudogo: **Six naphthylisoquinoline alkaloids and a related benzopyranone from a Congolese *Ancistrocladus* species related to *Ancistrocladus congolensis*.** *Phytochemistry* **2008**, *69*, 1065-1075.
- [56] M. Unger, M. Dreyer, S. Specker, S. Laug, M. Pelzing, C. Neusüß, U. Holzgrabe, G. Bringmann: **Analytical characterisation of crude extracts from an african *Ancistrocladus* species using high-performance liquid chromatography and capillary electrophoresis coupled to ion trap mass spectrometry.** *Phytochem. Anal.* **2004**, *15*, 21-26.
- [57] Y. F. Hallock, K. P. Manfredi, J. W. Blunt, J. H. Cardellina II, M. Schaeffer, K.-P. Gulden, G. Bringmann, A. Y. Lee, J. Clardy: **Korupensamines A-D, novel antimalarial alkaloids from *Ancistrocladus korupensis*.** *J. Org. Chem.* **1994**, *59*, 6349-6355.
- [58] G. Bringmann, C. Günther, S. Busemann, M. Schäffer, J. D. Olowokudejo, B. I. Alo: **Ancistroguineines A and B as well as ancistrotectorine-naphthylisoquinoline alkaloids from *Ancistrocladus guineensis*.** *Phytochemistry* **1998**, *47*, 37-43.
- [59] G. Bringmann, C. Günther, W. Saeb, J. Mies, A. Wickramasinghe, V. Mudogo, R. Brun: **Ancistolikokines A-C: new 5,8'-coupled naphthylisoquinoline alkaloids from *Ancistrocladus likoko*.** *J. Nat. Prod.* **2000**, *63*, 1333-1337.
- [60] Y. F. Hallock, K. P. Manfredi, J.-R. Dai, J. H. Cardellina II, R. J. Gulakowski, J. B. McMahon, M. Schäffer, M. Stahl, K.-P. Gulden, G. Bringmann, G. François, M. R. Boyd: **Michellamines D-F, new HIV-inhibitory dimeric naphthylisoquinoline alkaloids, and korupensamine E, a new antimalarial monomer, from *Ancistrocladus korupensis*.** *J. Nat. Prod.* **1997**, *60*, 677-683.

- [61] G. Bringmann, K. Messer, R. Brun, V. Mudogo: **Ancistrocongolines A-D, new naphthylisoquinoline alkaloids from *Ancistrocladus congolensis***. *J. Nat. Prod.* **2002**, *65*, 1096-1101.
- [62] C.-P. Tang, Y.-P. Yang, Y. Zhong, Q.-X. Zhong, H.-M. Wu, Y. Ye: **Four new naphthylisoquinoline alkaloids from *Ancistrocladus tectorius***. *J. Nat. Prod.* **2000**, *63*, 1384-1387.
- [63] N. H. Anh, A. Porzel, H. Ripperger, G. Bringmann, M. Schäffer, R. God, T. Van Sung, G. Adam: **Naphthylisoquinoline alkaloids from *Ancistrocladus cochinchinensis***. *Phytochemistry* **1997**, *45*, 1287-1291.
- [64] G. Bringmann, R. Weirich, D. Lisch, L. Aké Assi: **Ancistrobrevine D: an unusual alkaloid from *Ancistrocladus abbreviatus***. *Planta Med.* **1992**, *58*, 703-704.
- [65] N. Ruangrunsi, V. Wongpanich, P. Tantivatana, H. J. Cowe, P. J. Cox, S. Funayama, G. A. Cordell: **Traditional medicinal plants of Thailand, V. Ancistrotectorine, a new naphthalene-isoquinoline alkaloid from *Ancistrocladus tectorius***. *J. Nat. Prod.* **1985**, *48*, 529-535.
- [66] G. Bringmann, L. Kinzinger, T. Ortmann, N. J. D. Souza: **Isoancistrocladine from *Ancistrocladus heyneanus*: the first naturally occurring N-unsubstituted cis-configured naphthyltetrahydroisoquinoline alkaloid**. *Phytochemistry* **1993**, *35*, 259-261.
- [67] G. Bringmann, M. Dreyer, H. Rischer, K. Wolf, H. A. Hadi, R. Brun, H. Meimberg, G. Heubl: **Ancistrobenomine A, the first naphthylisoquinoline oxygenated at Me-3, and Related 5,1'-coupled alkaloids, from the "new" plant species *Ancistrocladus benomensis***. *J. Nat. Prod.* **2004**, *67*, 2058-2062.
- [68] G. Bringmann, R. Zagst, L. Aké Assi: **Ancistrobrevine B: a naphthylisoquinoline alkaloid with a novel coupling type from *Ancistrocladus abbreviatus***. *Planta Med.* **1991**, *57*, A96-A97.
- [69] G. Bringmann, M. Dreyer, J. H. Faber, P. W. Dalsgaard, J. W. Jaroszewski, H. Ndangalasi, F. Mbago, R. Brun, S. B. Christensen: **Ancistrotanzanine C and related 5,1'- and 7,3'-coupled naphthylisoquinoline alkaloids from *Ancistrocladus tanzaniensis***. *J. Nat. Prod.* **2004**, *67*, 743-748.
- [70] G. Bringmann, M. Dreyer, M. Michel, F. S. K. Tayman, R. Brun: **Ancistroheynine B and two further 7,3'-coupled naphthylisoquinoline alkaloids from *Ancistrocladus heyneanus* Wall.** *Phytochemistry* **2004**, *65*, 2903-2907.
- [71] G. Bringmann, W. Saeb, M. Rückert, J. Mies, M. Michel, V. Mudogo, R. Brun: **Ancistrolikokine D, a 5,8'-coupled naphthylisoquinoline alkaloid, and related natural products from *Ancistrocladus likoko***. *Phytochemistry* **2003**, *62*, 631-636.
- [72] G. Bringmann, M. Rückert, W. Saeb, V. Mudogo: **Characterization of metabolites in plant extracts of *Ancistrocladus likoko* by high-performance liquid chromatography coupled on-line with <sup>1</sup>H NMR spectroscopy**. *Magn. Reson. Chem.* **1999**, *37*, 98-102.
- [73] G. Bringmann, I. Kajahn, M. Reichert, S. E. H. Pedersen, J. H. Faber, T. Gulder, R. Brun, S. B. Christensen, A. Ponte-Sucre, H. Moll, G. Heubl, V. Mudogo: **Ancistrocladinium A and B, the first N,C-coupled naphthylidihydroisoquinoline alkaloids, from a Congolese *Ancistrocladus* species**. *J. Org. Chem.* **2006**, *71*, 9348-9356.
- [74] G. Bringmann, B. Hertlein-Amslinger, I. Kajahn, M. Dreyer, R. Brun, H. Moll, A. Stich, K. Ndjoko Ioset, W. Schmitz, L. H. Ngoc: **Phenolic analogs of the N,C-**

- coupled naphthylisoquinoline alkaloid ancistrocladinium A, from *Ancistrocladus cochinchinensis* (Ancistrocladaceae), with improved antiprotozoal activities. *Phytochemistry* **2011**, *72*, 89-93.
- [75] D. Meksuriyen, N. Ruangrungsi, P. Tantivatana, G. A. Cordell: **NMR spectroscopic analysis of ancistrocladidine**. *Phytochemistry* **1990**, *29*, 2750-2752.
- [76] G. Bringmann, F. Pokorny, M. Stäblein, M. Schäffer, L. Aké Assi: **Ancistrobrevine C from *Ancistrocladus abbreviatus*: the first mixed 'Ancistrocladaceae/Dioncophyllaceae-type' naphthylisoquinoline alkaloid**. *Phytochemistry* **1993**, *33*, 1511-1515.
- [77] T. R. Govindachari, P. C. Parthasarathy, T. G. Rajagopalan, H. K. Desai, K. S. Ramachandran, E. Lee: **Absolute configuration of ancistrocladisine and ancistrocladidine**. *J. Chem. Soc., Perkin Trans. 1* **1975**, 2134-2136.
- [78] S. Awale, D. F. Dibwe, C. Balachandran, S. Fayez, D. Feineis, B. K. Lombe, G. Bringmann: **Ancistrolidikone E<sub>3</sub>, a 5,8'-coupled naphthylisoquinoline alkaloid, eliminates the tolerance of cancer cells to nutrition starvation by inhibition of the Akt/mTOR/Autophagy signaling pathway**. *J. Nat. Prod.* **2018**, *81*, 2282-2291.
- [79] G. Bringmann, M. Rübenacker, J. R. Jansen, D. Scheutzow, L. Aké Assi: **On the structure of the Dioncophyllaceae alkaloids dioncophylline A ("triphyphylline") and "O-methyl-triphyphylline"**. *Tetrahedron Lett.* **1990**, *31*, 639-642.
- [80] G. Bringmann, G. François, L. Aké Assi, J. Schlauer: **The alkaloids of *Triphyophyllum peltatum* (Dioncophyllaceae)**. *CHIMIA Int. J. Chem.* **1998**, *52*, 18-28.
- [81] G. Bringmann, A. Irmer, S. Rüdener, J. Mutanyatta-Comar, R. Seupel, D. Feineis: **5'-O-Methyldioncophylline D, a 7,8'-coupled naphthylisoquinoline alkaloid from callus cultures of *Triphyophyllum peltatum*, and its biosynthesis from a late-stage tetrahydroisoquinoline precursor**. *Tetrahedron* **2016**, *72*, 2906-2912.
- [82] G. Bringmann, M. Rübenacker, W. Koch, D. Koppler, T. Ortmann, M. Schäffer, L. Aké Assi: **5'-O-Demethyl-8-O-methyl-7-*epi*-dioncophylline a and its 'regularly' configured atropisomer from *Triphyophyllum peltatum***. *Phytochemistry* **1994**, *36*, 1057-1061.
- [83] J. Li, R. Seupel, D. Feineis, V. Mudogo, M. Kaiser, R. Brun, D. Brännert, M. Chatterjee, E.-J. Seo, T. Efferth, G. Bringmann: **Dioncophyllines C<sub>2</sub>, D<sub>2</sub>, and F, and related naphthylisoquinoline alkaloids from the Congolese liana *Ancistrocladus ileboensis* with potent activities against *Plasmodium falciparum* and against multiple myeloma and leukemia cell lines**. *J. Nat. Prod.* **2017**, *80*, 443-458.
- [84] G. François, G. Bringmann, J. D. Phillipson, M. R. Boyd, L. Aké Assi, C. Schneider, G. Timperman: **Antimalarial naphthylisoquinoline alkaloids and pharmaceutical compositions and medical uses thereof**. Google Patents, **2003**.
- [85] G. Bringmann, M. Rübenacker, P. Vogt, H. Busse, L. Aké Assi, K. Peters, H. G. von Schnering: **Dioncopeltine A and dioncolactone A: alkaloids from *Triphyophyllum peltatum***. *Phytochemistry* **1991**, *30*, 1691-1696.
- [86] G. Bringmann, M. Wenzel, M. Rückert, K. Wolf, S. Busemann, M. Schäffer, L. Aké Assi: **Dioncophyllinol D, the first 4-hydroxylated naphthylisoquinoline**

- alkaloid, from the leaves of *Triphyophyllum peltatum*. *Heterocycles* **1998**, *2*, 985-990.
- [87] S. Fayez, D. Feineis, L. Aké Assi, M. Kaiser, R. Brun, S. Awale, G. Bringmann: **Ancistrobrevines E-J and related naphthylisoquinoline alkaloids from the West African liana *Ancistrocladus abbreviatus* with inhibitory activities against *Plasmodium falciparum* and PANC-1 human pancreatic cancer cells.** *Fitoterapia* **2018**, *131*, 245-259.
- [88] R. Seupel, Y. Hemberger, D. Feineis, M. Xu, E.-J. Seo, T. Efferth, G. Bringmann: **Ancistrocyclinones A and B, unprecedented pentacyclic N,C-coupled naphthylisoquinoline alkaloids, from the Chinese liana *Ancistrocladus tectorius*.** *Org. Biomol. Chem.* **2018**, *16*, 1581-1590.
- [89] K. Kaur, M. Jain, T. Kaur, R. Jain: **Antimalarials from nature.** *Bioorg. Med. Chem.* **2009**, *17*, 3229-3256.
- [90] G. Bringmann, W. Saeb, J. Kraus, R. Brun, G. François: **Jozimine B, a constitutionally unsymmetric, antiplasmodial 'dimer' of the naphthylisoquinoline alkaloid ancistrocladine.** *Tetrahedron* **2000**, *56*, 3523-3531.
- [91] G. Bringmann, S. K. Bischof, S. Müller, T. Gulder, C. Winter, A. Stich, H. Moll, M. Kaiser, R. Brun, J. Dreher, K. Baumann: **QSAR guided synthesis of simplified antiplasmodial analogs of naphthylisoquinoline alkaloids.** *Eur. J. Med. Chem.* **2010**, *45*, 5370-5383.
- [92] S. Fayez, D. Feineis, V. Mudogo, S. Awale, G. Bringmann: **Ancistrolikokines E-H and related 5,8'-coupled naphthylisoquinoline alkaloids from the Congolese liana *Ancistrocladus likoko* with antiausterity activities against PANC-1 human pancreatic cancer cells.** *RSC Adv.* **2017**, *7*, 53740-53751.
- [93] J.-P. Mufusama, D. Feineis, V. Mudogo, M. Kaiser, R. Brun, G. Bringmann: **Antiprotozoal dimeric naphthylisoquinolines, mbandakamines B<sub>3</sub> and B<sub>4</sub>, and related 5,8'-coupled monomeric alkaloids, ikelacongolines A-D, from a Congolese *Ancistrocladus* liana.** *RSC Adv.* **2019**, *9*, 12034-12046.
- [94] D. T. Tshitenge: **PhD thesis.** Julius-Maximilians-Universität Würzburg **2017**.
- [95] T. R. Govindachari, P. C. Parthasarathy: **Ancistrocladine, a new type of isoquinoline alkaloid from *Ancistrocladus heyneanus*.** *Tetrahedron* **1971**, *27*, 1013-1026.
- [96] L. K. Basco, S. Mitaku, A. L. Skaltsounis, N. Ravelomanantsoa, F. Tillequin, M. Koch, J. Le Bras: **In vitro activities of furoquinoline and acridone alkaloids against *Plasmodium falciparum*.** *Antimicrob. Agents Chemother.* **1994**, *38*, 1169-1171.
- [97] M. F. Dolabela, S. G. Oliveira, J. M. Nascimento, J. M. Peres, H. Wagner, M. M. Póvoa, A. B. de Oliveira: **In vitro antiplasmodial activity of extract and constituents from *Esenbeckia febrifuga*, a plant traditionally used to treat malaria in the Brazilian Amazon.** *Phytomedicine* **2008**, *15*, 367-372.
- [98] M. W. Muriithi, W. R. Abraham, J. Addae-Kyereme, I. Scowen, S. L. Croft, P. M. Gitu, H. Kendrick, E. N. M. Njagi, C. W. Wright: **Isolation and in vitro antiplasmodial activities of alkaloids from *Teclea trichocarpa*: in vivo antimalarial activity and X-ray crystal structure of normelicopicine.** *J. Nat. Prod.* **2002**, *65*, 956-959.
- [99] R. Batista, A. De Jesus Silva Júnior, A. B. De Oliveira: **Plant-derived antimalarial agents: new leads and efficient phytomedicines. Part II. Non-alkaloidal natural products.** *Molecules* **2009**, *14*, 3037.

- [100] K. Katsuno, J. N. Burrows, K. Duncan, R. H. van Huijsduijnen, T. Kaneko, K. Kita, C. E. Mowbray, D. Schmatz, P. Warner, B. T. Slingsby: **Hit and lead criteria in drug discovery for infectious diseases of the developing world.** *Nat. Rev. Drug Discov.* **2015**, *14*, 751.

# Chapter 3

## Experimental section

### 3.1 Materials

All solvents, analytical and technical grade, were procured from Merck and Radchem, and used without further treatment. Column chromatography was performed on Merck silica gel 60 (0.063-0.20 mm). Merck silica gel plates 60 F<sub>254</sub> were used for thin-layer-chromatography and they were visualized with Dragendorff's reagent or under UV at 254 and 360 nm (Spectroline<sup>®</sup>, Model ENF-240C/FE, Spectronics Corporation Westbury, New York, USA).

Analytical high-performance liquid chromatography was performed on two instruments: Waters 600 system in combination with UV detection at 210 – 400 nm (Waters 996 Photodiode array (PDA) detector) using a Luna C18 column (4.60 x 250 mm, 5 µm, Phenomenex), and Waters 2767 system equipped with a PDA detector (2998) using an XBridge C18 column (4.6 x 150 mm, 5 µm, Waters). The flow rate in both cases was 1 mL/min.

Purification and isolation of compounds was done on three different HPLC instruments: Waters 600 system equipped with Waters 996 PDA detector using a semi-prep. Luna C<sub>18</sub> column (10.00 x 250 mm, 10 µm, Phenomenex) with a flow rate of 4 or 5 mL/min. Waters 2767 system with PDA (2998) and MS detectors (Waters, Milford, MA, USA) using an XBridge Prep C<sub>18</sub> column (19 x 250 mm, 5 µm, Waters) with a flow rate of 20 mL/min. Waters 2767 system equipped with a PDA (2998) detector and an XBridge Prep C<sub>18</sub> column (19 x 250 mm, 5 µm, Waters) with a flow rate of 17.06 mL/min.

Hyphenated high-performance liquid chromatography - mass spectrometry - solid phase extraction - nuclear magnetic resonance (LC-MS-SPE-NMR) was performed on an Agilent Technologies 1200 Infinity series (Bruker, Germany) equipped with an amaZon SL ion trap instrument (HCT/esquire series), a Bruker NMR-MS interface (BNMI), a Bruker Prospekt II solid-phase extraction system as the interface between the HPLC and the NMR, a SamplePro Tube liquid handler (with a rack of 48 x 2 mL Autosampler vials, 225 mL glass vessel, and a rack of 24 x 3.0 mm NMR tubes).



Ultra-performance liquid chromatography profiling was performed on an Acquity UPLC coupled to a Waters Synapt G2 QTOF mass spectrometer operating in both, positive and negative electrospray ionization (ESI)

The ECD spectra were recorded on a J-715 spectropolarimeter (JASCO) at room temperature. A standard cell (0.02 cm) and spectrophotometric-grade MeOH were used.

Nuclear magnetic resonance spectroscopy:  $^1\text{H}$  NMR (400 MHz, 500 MHz),  $^{13}\text{C}$  NMR (125.75 MHz), and 2D NMR data were recorded at room temperature on Bruker Avarice III 400 MHz and 500 MHz spectrometers. Deuterated solvents were used to dissolve the compounds,  $\text{CD}_3\text{OD}$  (Merck, Switzerland),  $\text{CD}_3\text{COCD}_3$  (Aldrich Chemistry, Sigma-Aldrich, USA), and  $\text{CDCl}_3$  (Aldrich Chemistry, Sigma-Aldrich, USA). The chemical shifts were reported in ppm ( $\delta$ -scale) and the calibrations of the spectra were done by using the trace protons from the deuterated solvents, for  $\text{CD}_3\text{OD} = \delta_{\text{H}} - 3.31$  and  $\delta_{\text{C}} - 49.1$ ,  $\text{CDCl}_3 = \delta_{\text{H}} - 7.26$  and  $\delta_{\text{C}} - 77.16$ , and  $\text{CD}_3\text{COCD}_3 = \delta_{\text{H}} - 2.05$  and  $\delta_{\text{C}} - 29.82$ . The spectra were processed using the TopSpin 3.5pl7 software from Bruker. The coupling constants " $J$ " were given in Hertz (Hz). The signal multiplicity were reported with the corresponding letter in italics as follows: *s* = singlet, *d* = doublet, *dd* = doublet of doublet, *q* = quartet, *m* = multiplet.

### 3.2 Extraction process

Dried ground leaves (320 g) were placed in a 2 L conical flask and 1 L of *n*-hexane was added. The mixture was stirred continuously using a magnetic stirrer for 12 h. The extract was then filtered through filter paper using a Buchner funnel connected to a vacuum pump. The process was repeated twice. All the filtrates were combined, evaporated to dryness in a rotary evaporator, and the extract weighed to calculate the extraction yield. The final residue, after the three successive extractions with *n*-hexane and separation by filtration, was dried in the fume hood, then placed in an Erlenmeyer flask and 1 L of DCM extract was added. The process was conducted under the same conditions, and the resulting DCM extract weighed to determine the yield, while the residue was used to further extract with EtOAc, thereafter with MeOH, and finally with water in the same way. The final residue, after extraction with water, was discarded.

### 3.3 UPLC-QTOF-MS analysis

A Waters Acquity UPLC System equipped with a binary solvent delivery system and an autosampler was used to perform UPLC analysis. A solution of 1 mg/mL of a dried extract, fraction, or pure compound was prepared using either 100 % MeCN, MeOH or a 1:1 mixture of MeCN and water, or of MeOH and water, depending on the solubility of the sample. The solution was centrifuged to remove particles. The separation was performed on a Waters BEH C18 (2.1 mm x 100 mm, 1.7  $\mu$ m column). The mobile phase consisted of solvent A: water + 0.1 % FA (formic acid) and solvent B: MeOH + 0.1 % FA. The gradient used for extracts and fractions was as follows: 0.10 min, 3 % B, 12 min, 100 % B, 16 min, 100 % B, 16.50 min, 3 % B. For pure compounds, the gradient was as follows: 0.10 min, 3 % B, 14 min, 100 % B, 16 min, 100 % B, 16.50 min, 3 % B. The flow rate was, in all cases, 0.3 mL/min, and the injection volume was 5  $\mu$ l. The run time was 20 min. MassLynx V 4.1 software (Waters Inc., Milford, Massachusetts, USA) was used for data acquisition and processing. A Waters Synapt G2 high definition QTOF mass spectrometer equipped with an ESI source was used to acquire positive ion data.

Fraction F<sub>2</sub> and its subfractions collected from prep. HPLC were analyzed on a Waters Acquity UPLC system with MS detector (Waters, Milford, MA, USA). Separation was achieved on an Acquity UPLC BEH C<sub>18</sub> column (2.1 mm x 150 mm, 1.7  $\mu$ m, Waters) maintained at 40 °C. Some preliminary tests were performed prior to setting the conditions to obtain chromatograms with better resolution and short analysis time. The mobile phase consisted of water + 0.1 % NH<sub>4</sub>OH (solvent A) and MeCN (solvent B) at a flow rate of 0.3 mL/min. The gradient elution was executed as follow: 0 min, 5 % B, 1 min, 30 % B, 14 min 90 % B, 16 min, 90 % B, and 16.05 min, 5 % B. The total run time was 18 min and the injection volume was 1.0  $\mu$ l (full-loop injection). Mass spectrometry was operated in a positive-ion electrospray mode and nitrogen (N<sub>2</sub>) was used as the desolvation gas. Data were acquired between 80 and 1200 *m/z*. The following parameters were set: capillary voltages 3500 V; sampling cone voltages 45 V, extraction cone 4 V, source temperature 100 °C, desolvation temperature 450 °C, desolvation gas flow 550 l/h. Masslynx 4.1 software was used to process and obtain all the chromatographic data.

### 3.4 Silica gel column and thin-layer-chromatography

1500 g of Silica Gel 60 (0.063-0.2 mm/70-230 mesh) was mixed with DCM + 0.1 % triethylamine to form a homogeneous slurry suspension in a beaker (stationary phase). The suspension was then poured into a glass column 107 cm of length, which had a diameter of 7 cm and was equipped with a 2 L reservoir. Dried MeOH extract (13.0 g) was redissolved in MeOH and 10 g of Silica Gel 60 was added to the solution. The mixture was stirred with a glass rod and evaporated to dryness in a rotary evaporator. The resulting powder was layered on the column layer bed. The column was first eluted with 100 % DCM followed by gradually increasing the polarity by starting with 5 % of MeOH in DCM to 25 % in 5 % increments of MeOH. Further, the mobile phase was changed to 100 % MeCOMe, then the polarity increased to 10 % of MeOH in MeCOMe, then 20 % of MeOH. The column was washed with a mixture of MeCOMe, MeOH, and water (70:20:10). The separation provided 24 fractions, which were analyzed by TLC. The compounds on the plates were visualized under UV at 254 and 360 nm and the alkaloids were observed as orange spots after spraying with Dragendorff's reagent. Based on the similar TLC profiles, Fractions 1 to 4 were combined, 7 and 8 were mixed, 9 and 10 were combined and likewise 11 and 12, providing 18 final fractions. The TLC plates were developed using the following solvent systems: DCM/MeOH (19:1), DCM/MeOH (18:2), DCM/MeOH (17:3) and DCM/MeOH/FA (16:3:1). Pasteur pipettes (Hirschmann<sup>®</sup>, Hirschmann Laborgeräte GmbH & Co. KG, Germany) were used to spot the samples. The plates were dried using a cold hair dryer before visualization.

### 3.5 Isolation of compounds using HPLC

128 mg of Fraction 5 obtained from column chromatography was dissolved in 1.5 mL HPLC-grade MeOH. The solution was filtered through a 0.22- $\mu$ m membrane (Millipore) to remove any insoluble particles and then subjected to purification by HPLC. The conditions were optimized on an analytical column (Luna C<sub>18</sub> column: 4.60 x 250 mm, 5  $\mu$ m, Phenomenex) for a well-resolved chromatogram before transferring the method to semi-preparative conditions on a Luna C<sub>18</sub> column (10.00 x 250 mm, 10  $\mu$ m, Phenomenex). The mobile phase consisted of water/MeCN (9:1) + 0.05 % TFA (solvent A) and MeCN/water (9:1) + 0.05 % TFA (solvent B). The gradient was as

follows: 0 min, 20 % B, 20 min, 20 % B, 21 min, 30 % B, 31 min, 30 % B, 33 min, 50 % B, 40 min, 80 % B, 45 min, 80 % B, and 47 min, 20 % B. The injection volume was 50  $\mu$ l. The flow rate was 4 mL/min. Data were collected using the Millenium<sup>®</sup> (Waters, Version 4.00) software. The detector connected to the HPLC was PDA (Waters<sup>™</sup> 996). UV<sub>max</sub> plot from 210 to 400 nm was used for the chromatographic runs. The total run time was 50 min and peaks were collected manually as they eluted, providing eleven subfractions and one pure compound [ancistrocladinium A (**44**), see Section 3.8.2].

37.57 mg of Fraction 1 were dissolved in 2 mL MeOH, then filtered on an AcrodiscR Syringe filter (Pall Corporation Acrodisc, Acrodisc 13 mm minispikes with 0.2  $\mu$ m GHP 300/pk). The solution was subjected to purification by HPLC. After an optimized method had been developed on a Luna C18 column (4.60 x 250 mm, 5  $\mu$ m, Phenomenex), the isolation was performed on the same column. The mobile phase consisted of solvent A (water/MeCN 9:1 + 0.05 % TFA) and solvent B (MeCN/water 9:1 + 0.05 % TFA) at a flow rate of 1 mL/min. The gradient eluent was applied as follows: 0 min, 20 % B, 17 min, 30 % B, 28 min, 60 % B, 30 min, 100 % B, 32 min, 100 % B, 33 min, 80 % B, 36 min, 60 % B, and 38 min, 20 % B. The total run time was 50 min and the injection volume was 50  $\mu$ l. A PDA (Waters<sup>™</sup> 996) was used for detection (UV<sub>max</sub> plot 210 – 400 nm) and the peaks were collected manually. Data were treated using Millenium<sup>®</sup> (Waters, Version 4.00) software. The fractions were dried under reduced pressure and the resulting residues analyzed by UPLC-QTOF-MS. Two pure compounds, ancistrocladinium A (**44**, see Section 3.8.2) and ancistrocyclinone A (**45**, see Section 3.8.3), were obtained and submitted for NMR analysis.

50 mg of Fraction 2 were dissolved in 1 mL MeOH. The resulting solution was filtered on AcrodiscR Syringe filters and then subjected to purification by HPLC. The conditions were optimized in order to achieve chromatograms with better resolution in a short analysis time. The separation was achieved on an XBridge Prep C<sub>18</sub> column (19 x 250 mm, 5  $\mu$ m, Waters) maintained at 40 °C. The mobile phase consisted of 0.1% NH<sub>4</sub>OH in water (solvent A) and MeCN (solvent B) at a flow rate of 20 mL/min. The gradient elution was as follows: 0 min, 5 % B, 4 min, 60 % B, 10 min, 85 % B, 13 min, 90 % B, 14 min, 90 % B, and 14.2 min, 5 % B. The total run time was 15 min. The injection volume was 100  $\mu$ L. Data were collected by chromatographic software MassLynx 4.1 (Waters, USA). The preparative HPLC system was interfaced with a QDa mass spectrometer and operated in positive ion mode. The probe temperature was set to

600 °C and the source temperature was 120 °C. The capillary and cone voltages were set to 800 and 10 V, respectively. Data were gathered between 100 and 700 *m/z*. The eluents were collected in 220 tubes (about 2 mL) using a fraction collector placing the target compounds in various fractions, which were subsequently combined and concentrated to give four subfractions. The latter were analyzed by UPLC-QTOF-MS. The constitution of one compound in one subfraction was elucidated (compound **46**, see Section 3.8.4).

400 mg of Fraction 6 were dissolved in 4 mL MeOH. The solution was filtered over an AcrodiscR Syringe filter before subjecting it to purification by HPLC. Chromatographic conditions were optimized on an XBridge C18 column (4.6 mm x 150 mm, 5 µm, Waters). The Waters Prep Calculator software was used to upscale the optimized method to the XBridge Prep C18 column (19 mm x 250 mm, 5 µm, Waters). The mobile phase consisted of water + 0.05 % TFA (Solvent A) and MeCN + 0.05 % TFA (Solvent B) with the flow rate of 17.06 mL/min (obtained from the calculator). The gradient used was as follows: 0 min, 20 % B, 1.67 min, 20 % B, 28.33 min, 30 % B, 46.67 min, 60% B, 50 min, 100 % B, 55 min, 100 % B, and 55.33 min, 20 % B. The total run time was 59 min. The injection volume was 130 µL. Data were collected using MassLynx 4.1 software (Waters, USA). The preparative HPLC system was interfaced with a 2998 PDA detector. The separation provided 19 subfractions and one pure compound, ancistrocladinium A (**44**, see Section 3.8.2).

125 mg of Fraction 7 were dissolved in 1 mL of MeOH and then filtered on an AcrodiscR Syringe filter. The solution was subjected to purification by HPLC. The conditions were optimized on a Luna C<sub>18</sub> column (4.60 mm x 250 mm, 5 µm, Phenomenex) for a well-resolved chromatogram before transferring it to semi-preparative Luna C18 column (10.00 mm x 250 mm, 10 µm, Phenomenex). The fractionation was achieved using the following mobile phase: solvent A (water/MeCN 9:1 + 0.05 % TFA) and solvent B (MeCN/water 9:1 + 0.05 % TFA) at a flow rate of 5 mL/min. The gradient eluent was applied as follows: 0 min, 20 % B, 22 min, 30 % B, 35 min, 60 % B, 37 min, 100 % B, 40 min, 100 % B, 41 min, 80 % B, 43 min, 60 % B, 45 min, 40 % B, and 46 min, 20 % B. The total run time was 50 min and the injection volume was 50 µL. A PDA (Waters™ 996) was used for detection (UV<sub>max</sub> plot 210 – 400 nm) and the peaks were collected manually as they eluted. They were dried under reduced pressure and the resulting residues analyzed by UPLC-QTOF-MS. As all the subfractions were still mixtures, they

were stored. Data were acquired and analyzed using the Millenium® (Waters, Version 4.00) software.

### 3.6 Isolation of a compound using LC-MS-SPE-NMR

The Subfraction 5 (collected from semi-prep HPLC of Fraction 5, between 14.45 - 18.28 min) was further resolved on LC-MS-SPE-NMR. It (24.2 mg) was dissolved in 2 mL HPLC grade MeOH. The solution was filtered on an AcrodiscR Syringe filters. The separation was achieved on an XSelect® HSS T3 (4.6 mm x 150 mm, 5 µm, Waters). The mobile phase consisted of solvent A being water + 0.1 % TFA and solvent B as MeOH. An isocratic method of 45 % MeOH and 55 % of solvent A was used. The flow rate was 0.5 mL/min and the run time was 35 min. The injection volume was 8 µl. The peak detections were done by Bruker Amazon SL mass spectrometer (for LC-MS method) and PDA detector. Through multiple chromatographic runs of the same sample, the peaks of interest were trapped in individual allocated SPE cartridges after the column. The loaded cartridges were dried using pressurized nitrogen gas. 250 µl of deuterated MeCN was used to elute the peaks from the cartridges through the capillaries into the 3 mm NMR tubes in the SamplePro Tube liquid handler. After NMR analysis, the compounds were transferred from the NMR tubes to pre-weighed vials, and the solvents were evaporated to dryness in a vacuum concentrator (acid-resistant CentriVap® Concentrator, LABCONCO, USA). Of the three peaks collected, only one consisted of a pure compound, ealamine A (**43**, see Section 3.8.1), and was kept for bioactivity screening and further analysis for structure elucidation. The remaining two impure compounds were also transferred from NMR tubes into vials for storage. Data were collected using HyStar™ software package.

### 3.7 Antiplasmodial screening

Prior to assaying, the *P. falciparum* parasites were cultivated. They were maintained at 37 °C in human erythrocytes (O<sup>+</sup>) suspended in complete culture medium [RPMI 1640 medium (Sigma-Aldrich) supplemented with 25 mM HEPES (Sigma-Aldrich), 20 mM D-glucose (Sigma-Aldrich), 200 µM hypoxanthine (Sigma-Aldrich), 0.2 % sodium

bicarbonate, 24 µg/mL gentamycin (Sigma-Aldrich) and 0.5 % AlbuMAX II] in an atmosphere of 90 % N<sub>2</sub>, 5 % O<sub>2</sub>, and 5 % CO<sub>2</sub>.<sup>[1, 2]</sup> The culture was then synchronized as described in the literature<sup>[3]</sup> in order to have a culture of *P. falciparum* at the ring-stage, and then centrifuged at 35 rpm for 5 min. The supernatant was discarded and the precipitate - erythrocytes - suspended in a solution of 5 % D-sorbitol for 5 min at room temperature. The suspension was again centrifuged and the supernatant discarded. The pellet was washed 3 times with complete culture medium to remove the remaining sorbitol solution and re-suspended in the medium for parasite growth.

Stock solutions were prepared at 10 mM for compounds and 10 mg/mL for extracts and fractions (dissolved in 40 % DMSO/dddH<sub>2</sub>O). For dual point experiments, solutions at the required concentrations in complete RPMI medium were prepared by dilutions from stock solutions and dispensed into triplicates, while for IC<sub>50</sub> determinations, serial dilutions were made and allocated into triplicates test wells with concentration ranging from 0 to 10<sup>-5</sup> M.

*In vitro* ring-stage intra-erythrocytic *P. falciparum* NF54, K1, or W2 parasite cultures (200 µl at 1 % hematocrit, 1 % parasitemia, level of parasitemia determined by counting under light microscopy approximately 500 erythrocytes on a thin blood smear stained with Giemsa) were treated with extracts, fractions, or compounds at test concentrations. The controls for assays included chloroquine disulphate (1 µM, as the positive control) and complete RPMI medium (as the negative control) and grown for 96 h at 37°C under the 90 % N<sub>2</sub>, 5 % O<sub>2</sub>, and 5 % CO<sub>2</sub> gas mixture in 96-well plates. At the conclusion of the 96 h growth period, equal volumes (100 µl each) of the *P. falciparum* parasite cultures were combined with SYBR Green I lysis buffer (0.2 µl/mL 10 000 x SYBR Green I, Invitrogen, 20 mM Tris, pH 7.5, 5 mM EDTA, 0.008% (w/v) saponin, 0.08% (v/v) Triton X-100). The samples were incubated at 37 °C for 1 h, after which the fluorescence was measured using a GloMax<sup>®</sup>-Explorer detection system with Instinct<sup>®</sup> software (excitation at 485 nm and emission at 538 nm) or a Fluoroskan Ascent<sup>®</sup> FL microplate fluorimeter (Thermo Scientific, excitation at 485 nm and emission at 538 nm). The 'background' fluorescence (i.e. the one measured in the samples derived from chloroquine-treated iRBC samples, in which parasite proliferation was completely inhibited) was subtracted from the total fluorescence measured for each sample to provide a measure of parasite proliferation. Data obtained were analyzed in Excel and sigmoidal dose-response curves were plotted

using GraphPad 5.0 or 6.0. Experiments were always performed in triplicate, for a single biological replicate.

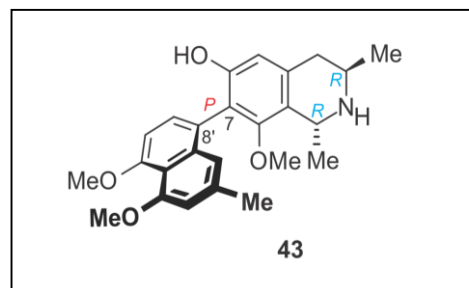
### 3.8 Structure elucidation

#### 3.8.1 Ealamine A (43)

Yellow solid (1.6 mg)

UV (HPLC):  $\lambda_{max}$  ( $\log \epsilon$ ) = 229 (2.54), 307 (0.75) nm.

ECD (MeOH):  $\lambda_{max}$  ( $\Delta \epsilon$ ) = 203 (+3.92), 213 (-4.2), 223 (+3.3), 227 (+3.2), 258 (+4.5), 285 (-4.5), 310 (+1.9) nm



$^1\text{H}$  NMR ( $\text{CDCl}_3$ , 500 MHz):  $\delta_{\text{H}}$  1.58 (3H, *d*,  $^3J = 6.39$  Hz,  $\text{CH}_3$ -3), 1.66 (3H, *d*,  $^3J = 6.69$  Hz,  $\text{CH}_3$ -1), 2.38 (3H, *s*,  $\text{CH}_3$ -2'), 3.01 (1H, *dd*,  $^2J = 17.73$ ,  $^3J = 3.80$ ,  $\text{H}_{\text{eq}}$ -4), 3.05 (1H, *dd*,  $^2J = 17.73$ ,  $^3J = 11.56$ ,  $\text{H}_{\text{ax}}$ -4), 3.07 (3H, *s*,  $\text{OCH}_3$ -8), 3.72 (1H, *m*, H-3), 3.98 (3H, *s*,  $\text{OCH}_3$ -4'), 4.00 (3H, *s*,  $\text{OCH}_3$ -5'), 4.75 (1H, *q*,  $^3J = 6.79$  Hz, H-1), 6.57 (1H, *s*, H-5), 6.73 (1H, *s*, H-1'), 6.86 (1H, *d*,  $^3J = 7.99$  Hz, H-6'), 6.90 (1H, *s*, H-3'), 7.31 (1H, *d*,  $^3J = 7.99$  Hz, H-7').

$^{13}\text{C}$  NMR ( $\text{CDCl}_3$ , 125.76 MHz):  $\delta_{\text{C}}$  19.1 ( $\text{CH}_3$ -3), 19.4 ( $\text{CH}_3$ -1), 22.1 ( $\text{CH}_3$ -2'), 34.1 (C-4), 44.1 (C-3), 48.5 (C-1), 56.5 (5'- $\text{OCH}_3$ ), 56.6 (4'- $\text{OCH}_3$ ), 60.3 (8'- $\text{OCH}_3$ ), 105.4 (C-6'), 109.3 (C-1'), 110.0 (C-5), 116.2 (C-8'), 117.0 (C-3'), 118.9 (C-7), 119.2 (C-9), 119.9 (C-10'), 130.8 (C-7'), 132.4 (C-10), 135.9 (C-9'), 138.6 (C-2'), 154.3 (C-6), 155.8 (C-8), 157.6 (C-4'), 158.4 (C-5').

LC-MS/MS (Q TOF MS ES+):  $m/z$  (%) = 408  $[\text{M}+\text{H}]^+$  (19.2), 391  $[\text{M}-\text{OH}]^+$  (19.2), 376  $[\text{M}-\text{OCH}_3]^+$  (13.6), 202  $[\text{M}-\text{isoquinoline moiety}]^+$  (100).

LC-MS  $m/z$  calcd. for  $\text{C}_{25}\text{H}_{30}\text{NO}_4$   $[\text{M}+\text{H}]^+$  408.2175; found 408.2174.

The spectroscopic data were in agreement with those reported in the literature.<sup>[4]</sup>



### 3.8.2 Ancistrocladinium A (44)

Yellow amorphous powder (2 mg)

UV (HPLC):  $\lambda_{max}$  ( $\log \epsilon$ ) = 216 (0.98), 232 (1.35),  
335 (0.64) nm.

ECD (MeOH):  $\lambda_{max}$  ( $\Delta \epsilon$ ) = 210 (-2.4), 230 (+1.4),  
245 (-1.07), 322 (+0.70) nm.

IR  $\lambda_{max}$  3445, 2981, 1686, 1579, 1454, 1383, 1309, 1283, 1204, 828, 798, 717  $\text{cm}^{-1}$ .

$^1\text{H}$  NMR (500 MHz,  $\text{CD}_3\text{OD}$ ):  $\delta_{\text{H}}$  = 1.30 (3H, *d*,  $^3J$  = 6.81,  $\text{CH}_3$ -3), 2.50 (3H, *s*,  $\text{CH}_3$ -2'), 2.52 (3H, *s*,  $\text{CH}_3$ -1), 3.13 (1H, *dd*,  $^2J$  = 16.8,  $^3J$  = 2.3 Hz,  $\text{H}_{\text{eq}}$ -4), 3.83 (1H, *dd*,  $^2J$  = 16.8,  $^3J$  = 6.2 Hz,  $\text{H}_{\text{ax}}$ -4), 3.97 (3H, *s*,  $\text{OCH}_3$ -4'), 4.00 (3H, *s*,  $\text{OCH}_3$ -5'), 4.03 (3H, *s*,  $\text{OCH}_3$ -6), 4.04 (3H, *s*,  $\text{OCH}_3$ -8), 4.25 (1H, *m*, H-3), 6.74 (1H, *s*, H-7), 6.77 (1H, *s*, H-5), 6.97 (1H, *d*,  $^3J$  = 7.9 Hz, H-6'), 6.98 (1H, *s*, H-3'), 7.09 (1H, *s*, H-1'), 7.46 (1H, *d*,  $^3J$  = 7.9 Hz, H-7') ppm.

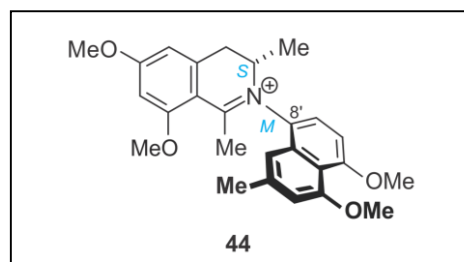
$^{13}\text{C}$  NMR (125.76 MHz,  $\text{CD}_3\text{OD}$ ):  $\delta_{\text{C}}$  = 15.5 (3- $\text{CH}_3$ ), 22.3 (2'- $\text{CH}_3$ ), 24.8 (1- $\text{CH}_3$ ), 35.0 (C-4), 56.9 (5'- $\text{OCH}_3$ ), 56.9 (4'- $\text{OCH}_3$ ), 57.0 (6- $\text{OCH}_3$ ), 57.1 (8- $\text{OCH}_3$ ), 59.6 (C-3), 98.9 (C-7), 104.8 (C-6'), 109.4 (C-5), 110.8 (C-9), 111.1 (C-3'), 113.5 (C-1'), 118.0 (C-8'), 127.2 (C-7'), 129.9 (C-10'), 130.8 (C-9'), 142.0 (C-2'), 142.1 (C-10), 159.8 (C-4'), 161.0 (C-5'), 166.3 (C-8), 170.7 (C-6), 177.9 (C-1) ppm.

LC-MS/MS (2 TOF MS  $\text{ES}^+$ ):  $m/z$  (%) = 420 [ $\text{M}$ ] $^+$  (100), 404 [ $\text{M}-\text{CH}_4$ ] $^+$  (76), 390 (34.4) [ $\text{M}-2\text{CH}_3$ ] $^+$ , 376 [ $\text{M}+\text{H}-3\text{CH}_3$ ] $^+$  (78.4).

LC-MS  $m/z$  calcd. for  $\text{C}_{26}\text{H}_{30}\text{NO}_4^+$  420.2169; found 420.2197.

The spectroscopic data were in agreement with the ones published in the literature.<sup>[5]</sup>

6]

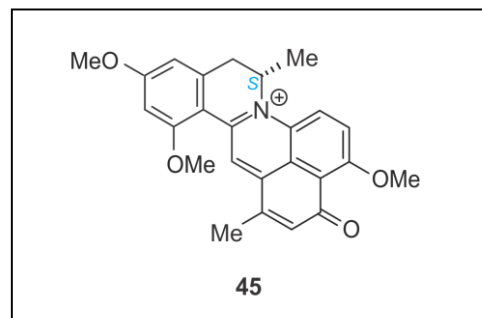


### 3.8.3 Ancistrocyclinone A (45)

Deep red solid (1.9 mg)

UV (HPLC):  $\lambda_{max}$  ( $\log \epsilon$ ) = 237 (0.75), 282 (0.54), 308 (0.95), 376 (0.43) nm.

ECD (MeOH):  $\lambda_{max}$  ( $\Delta \epsilon$ ) = 207 (-6.9), 245 (-3.8), 400 (-1.06) nm.



IR  $\lambda_{max}$  3427, 2924, 2853, 1683, 1585, 1456, 1281, 1140, 1096, 721  $\text{cm}^{-1}$ .

$^1\text{H}$  NMR (500 MHz,  $\text{CD}_3\text{COCD}_3$ ):  $\delta_{\text{H}}$  = 1.58 (3H, *d*,  $^3J$  = 5.9 Hz,  $\text{CH}_3$ -3), 2.67 (3H, *s*,  $\text{CH}_3$ -2'), 3.33 (1H, *dd*,  $^2J$  = 16.9,  $^3J$  = 3.7 Hz,  $\text{H}_{\text{eq}}$ -4), 3.73 (1H, *dd*,  $^2J$  = 16.9,  $^3J$  = 3.1 Hz,  $\text{H}_{\text{ax}}$ -4), 4.04 (3H, *s*,  $\text{OCH}_3$ -6), 4.20 (3H, *s*,  $\text{OCH}_3$ -8), 4.25 (3H, *s*,  $\text{OCH}_3$ -5'), 6.22 (1H, *m*, H-3), 6.87 (2H, *s*, H-5 and H-3'), 6.89 (1H, *s*, H-7), 8.24 (1H, *d*,  $^3J$  = 8.8 Hz, H-6'), 9.10 (1H, *d*,  $^3J$  = 8.8 Hz, H-7'), 9.22 (1H, *s*, H-11') ppm.

$^{13}\text{C}$  NMR (125.75 MHz,  $\text{MeCOMe-}d_6$ ):  $\delta_{\text{C}}$  = 16.9 (3- $\text{CH}_3$ ), 18.7 (2'- $\text{CH}_3$ ), 34.1 (C-4), 54.9 (C-3), 56.7 (6- $\text{OCH}_3$ ), 57.3 (8- $\text{OCH}_3$ ), 57.9 (5'- $\text{OCH}_3$ ), 99.2 (C-7), 108.3 (C-5), 109.4 (C-9), 114.9 (C-10'), 122.5 (C-6'), 124.3 (C-11'), 126.2 (C-9'), 126.8 (C-7'), 132.5 (C-8'), 136.7 (C-3'), 139.3 (C-10), 141.4 (C-1'), 144.2 (C-2'), 148.1 (C-1), 162.5 (C-8), 163.2 (C-5'), 167.5 (C-6), 182.2 (C-4') ppm.

LC-MS/MS (2 TOF MS  $\text{ES}^+$ ):  $m/z$  (%) = 402 (20.8) [ $\text{M}^+$ ], 387 (38.8) [ $\text{M}-\text{CH}_3$ ] $^+$ , 358 (100) [ $\text{M}-\text{OCH}_3-\text{CH}_3$ ] $^+$ , 343 (87.2) [ $\text{M}-2\text{OCH}_3$ ] $^+$ .

LC-MS:  $m/z$  calculated for  $\text{C}_{25}\text{H}_{24}\text{NO}_4^+$  402.1700; found 402.1746.

The spectroscopic data were in agreement with those reported in the literature.<sup>[7]</sup>

### 3.8.4 Compound 46

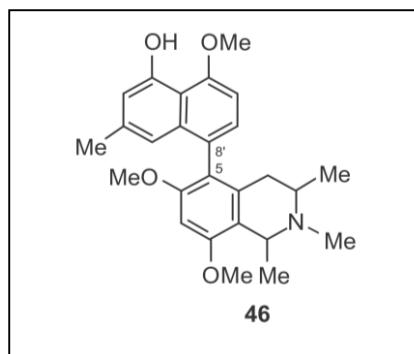
Yellow amorphous solid (3 mg of impure material)

IR  $\lambda_{max}$  3417, 2914, 2853, 2357, 1683, 1609, 1585, 1456, 1204, 1139, 831, 721  $\text{cm}^{-1}$ .

$^1\text{H}$  NMR (500 MHz,  $\text{CD}_3\text{OD}-d_4$ ):  $\delta_{\text{H}} = 1.10$  (3H, *d*,  $^3J = 6.46$  Hz,  $\text{CH}_3$ -3), 1.54 (3H, *d*,  $^3J = 6.66.9$  Hz,  $\text{CH}_3$ -1), 2.03 (1H, *dd*,  $J = 17.9, 11.7$  Hz,  $\text{H}_{\text{eq}}$ -4), 2.22 (3H, *s*,  $\text{CH}_3$ -2'), 2.55 (1H, *dd*,  $J = 17.9, 4.8$  Hz,  $\text{H}_{\text{ax}}$ -4), 2.59 (3H, *s*,  $\text{CH}_3$ -N), 3.61 (1H, *m*, H-3), 3.65 (3H, *s*,  $\text{OCH}_3$ -6), 3.98 (3H, *s*,  $\text{OCH}_3$ -8), 4.10 (3H, *s*,  $\text{OCH}_3$ -5'), 4.56 (1H, *q*,  $J = 6.5$  Hz, H-1), 6.44 (1H, *s*, H-1'), 6.63 (1H, *d*,  $J = 1.22$  Hz, H-3'), 6.73 (1H, *s*, H-7), 6.92 (*d*,  $J = 7.9$  Hz, 1H, H-6'), 7.06 (*d*,  $J = 7.9$  Hz, 1H, H-7') ppm.

$^{13}\text{C}$  NMR (125.75 MHz,  $\text{CD}_3\text{OD}-d_4$ ):  $\delta_{\text{C}} = 17.4$  (3- $\text{CH}_3$ ), 17.9 (1- $\text{CH}_3$ ), 22.0 (2'- $\text{CH}_3$ ), 31.4 (C-4), 35.7 (N- $\text{CH}_3$ ), 49.8 (C-3), 56.2 (8- $\text{OCH}_3$ ), 56.4 (6- $\text{OCH}_3$ ), 56.8 (5'- $\text{OCH}_3$ ), 58.2 (C-1), 95.3 (C-7), 104.5 (C-6'), 113.0 (C-3'), 114.8 (C-9'), 116.4 (C-9), 116.4 (C-1'), 121.8 (C-5), 128.3 (C-8'), 129.2 (C-7'), 133.6 (C-10), 137.1 (C-10'), 139.0 (C-2'), 156.1 (C-4'), 157.3 (C-5'), 158.2 (C-8), 159.4 (C-6) ppm.

LC-MS:  $m/z$  calculated for  $\text{C}_{26}\text{H}_{32}\text{NO}_4^+$  422.2326; found 422.2356.



### 3.9 References

- [1] B. K. Verlinden, J. Niemand, J. Snyman, S. K. Sharma, R. J. Beattie, P. M. Woster, L.-M. Birkholtz: **Discovery of novel alkylated (bis)urea and (bis)thiourea polyamine analogues with potent antimalarial activities.** *J. Med. Chem.* **2011**, *54*, 6624-6633.
- [2] M. Smilkstein, N. Sriwilaijaroen, J. X. Kelly, P. Wilairat, M. Riscoe: **Simple and inexpensive fluorescence-based technique for high-throughput antimalarial drug screening.** *Antimicrob. Agents Chemother.* **2004**, *48*, 1803-1806.
- [3] C. Lambros, J. P. Vanderberg: **Synchronization of *Plasmodium falciparum* erythrocytic stages in culture.** *J. Parasitol.* **1979**, *65*, 418-420.
- [4] D. T. Tshitenge: **PhD thesis.** Julius-Maximilians-Universität Würzburg **2017**.
- [5] G. Bringmann, I. Kajahn, M. Reichert, S. E. H. Pedersen, J. H. Faber, T. Gulder, R. Brun, S. B. Christensen, A. Ponte-Sucre, H. Moll, G. Heubl, V. Mudogo: **Ancistrocladinium A and B, the first N,C-coupled naphthyldihydroisoquinoline alkaloids, from a Congolese *Ancistrocladus* species.** *J. Org. Chem.* **2006**, *71*, 9348-9356.
- [6] G. Zhang: **PhD thesis.** Julius-Maximilians-Universität Würzburg **2012**.
- [7] R. Seupel, Y. Hemberger, D. Feineis, M. Xu, E.-J. Seo, T. Efferth, G. Bringmann: **Ancistrocyclinones A and B, unprecedented pentacyclic N,C-coupled naphthylisoquinoline alkaloids, from the Chinese liana *Ancistrocladus tectorius*.** *Org. Biomol. Chem.* **2018**, *16*, 1581-1590.

## Chapter 4

### General conclusion

The most potent antimalarial drugs (quinine and artemisinin derivatives) are from natural products (medicinal plants) origin, which implies that medicinal plants are a valuable source to consider for new antimalarial drugs with novel mechanism of actions and able to overcome resistance.

As a result of intensive research done by Prof. G. Bringmann and his collaborators on the plant species from the Ancistrocladaceae family and the closely related one, Dioncophyllaceae, extracts and naphthylisoquinoline alkaloid compounds, with interesting antiplasmodial activities against chloroquine-sensitive and chloroquine-resistant strains of *Plasmodium falciparum* and against *P. berghei* *in vitro* and *in vivo*, had been identified.

As part of this study a new collection of leaves of an *Ancistrocladus* species was done by B.K. Lombe in the region Bonsolerve (DRC) and was investigated for its antiplasmodial activity together with the isolation and identification of naphthylisoquinoline alkaloids. The species is yet unidentified.

The plant material was subjected to sequential extraction by using *n*-hexane, DCM, EtOAc, MeOH, and water. The highest extraction yield was through the use of MeOH, which showed that the plant was rich in polar compounds. All extracts, except for the *n*-hexane, were screened against *P. falciparum*. The MeOH extract exhibited the best activity with 100 % inhibition at both concentrations tested (10 and 20 µg/mL) compared to the other ones prepared from a sequential extraction procedure (DCM, EtOAc, and water) indicating that the most active constituents were concentrated in the MeOH extract.

NIQs were confirmed to be present in the DCM, EtOAc, and MeOH extracts, while in the water extract, only one peak corresponding to the *m/z* of NIQs was found through UPLC-QTOF-MS. Preliminary identification of selected NIQ classes were also made

based on the mass spectral analysis. As a result, MeOH extract was chosen for further investigations in order to identify compounds responsible for the activity.

The fractionation of the MeOH extract was carried out by column chromatography using silica gel treated with 0.1 % triethylamine, from which 18 final fractions were collected. TLC and UPLC-QTOF-MS were used to investigate and select fractions containing mainly NIQs for antiplasmodial screening. Five fractions were selected after being investigated by UPLC-QTOF-MS, which revealed that the fractionation was successful as they all had different chemical profiles. In these fractions, NIQs were identified although for some  $m/z$  values, the molecular formula could not be deduced with acceptable iFit values by using the software. These compounds therefore needed to be isolated and investigated by NMR measurements in order to determine the molecular formula. The five fractions were screened against *P. falciparum* NF54 strains and all exhibited good antiplasmodial activity with more than 95 % inhibition at both tested concentrations (10 and 5  $\mu\text{g/mL}$ ). As they all exhibited similar antiplasmodial potency, it was difficult to select the most active ones for further purification and they were all subjected to chromatographic techniques.

Fraction 2 was further resolved by mass-directed preparative HPLC, from which four peaks (subfractions) were collected. Their UPLC-QTOF-MS analysis revealed that they were still mixtures. However, NMR analysis revealed that one peak consisted of a compound with only minor impurities, so that its constitution and relative configuration were elucidated (compound **46**). This alkaloid was similar to ancistrol kokine C<sub>2</sub> (**47**) although it differed from it by the relative configuration at the axis. The four subfractions were all screened against the *P. falciparum* NF54 strain and one of them exhibited a good activity (98 % inhibition at 5  $\mu\text{g/mL}$  and 82 % inhibition at 1  $\mu\text{g/mL}$ ), while the remaining ones showed no or only minimal activity. Due to limited quantities of the active one, the isolation and identification of the active ingredient could not be further pursued.

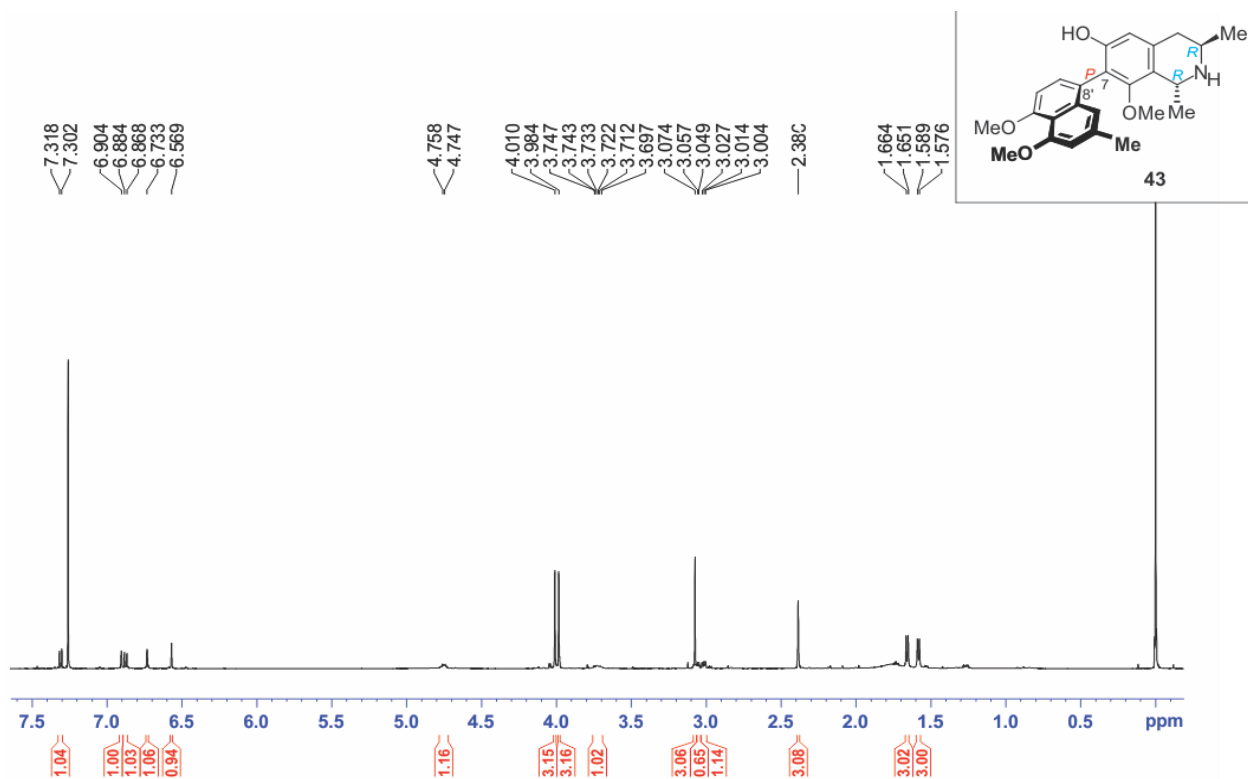
Two compounds were isolated and analyzed (by NMR and ECD spectra) from active fractions (Fractions 5 and 6). These were ealamine A (**44**) and ancistrocladinium A (**45**). One compound was identified in a non-screened fraction (Fraction 1) as ancistrocyclinone A (**46**) through NMR and ECD spectra. In the past, ealamine A (**43**) had been isolated from the twigs and leaves of *Ancistrocladus ealaensis* J. Léonard and from the leaves of a yet unidentified *Ancistrocladus* species collected around the

village Leeke near the town of Ikela. Ancistrocladinium A (**44**) had previously been found in the leaves of a Congolese *Ancistrocladus* species harvested in Yetoto and from stem bark of *Ancistrocladus* species from Yafunga. Ancistrocyclinone A (**45**) had previously been found in the Chinese plant *Ancistrocladus tectorius*.

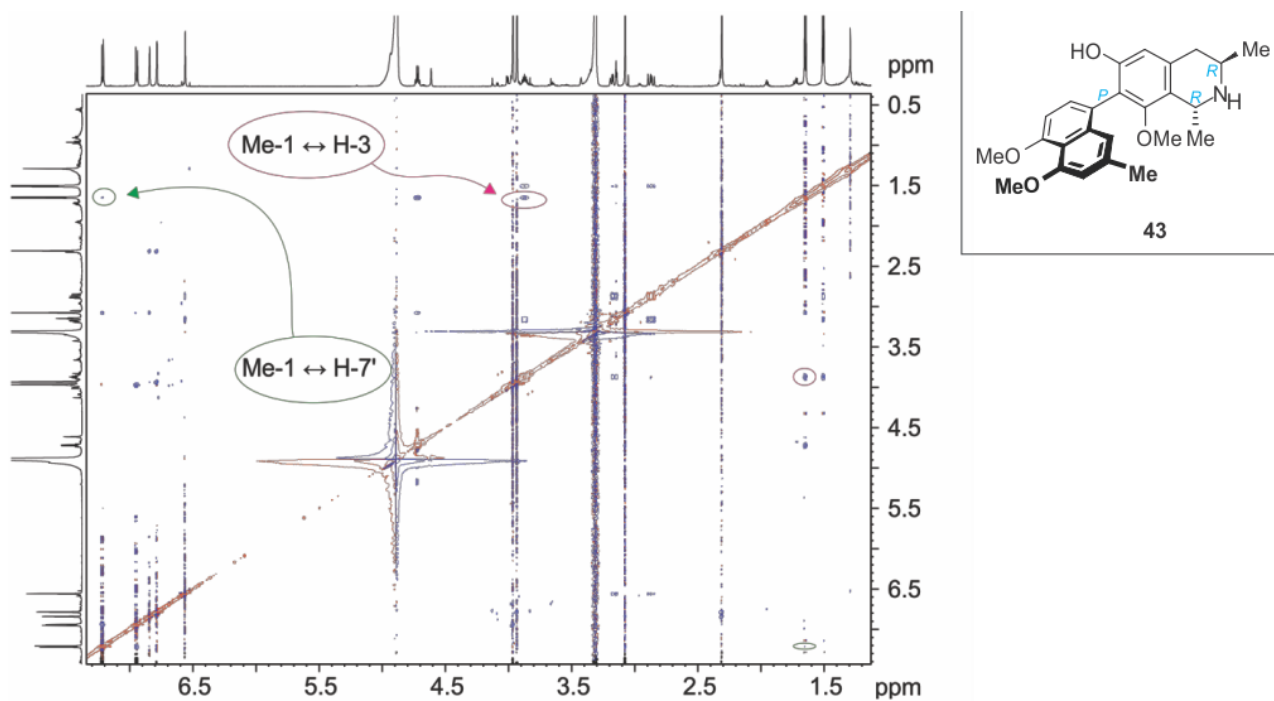
All pure compounds were screened for their antiplasmodial activity. Ealamine A (**43**) and ancistrocladinium A (**44**) showed good activity against *P. falciparum* NF54 strains (IC<sub>50</sub> 5.74 and 4.67 μM, respectively), while ancistrocyclinone A (**45**) was inactive. Ealamine A (**43**) and ancistrocladinium A (**44**) were further screened against K1 and W2 strains of *P. falciparum* and they both showed good activities (IC<sub>50</sub> 1.54 and 3.12; 3.27 and 4.17 μM, respectively). The activity of ancistrocladinium A had only been reported against the K1 strain as moderate based on the set classification criteria, making this the first report on its activity against NF54 and W2 strains with its resistance index being less than 1. Likewise, the potency of ealamine A (**43**) had only been described against NF54 and K1 strains.

The IC<sub>50</sub> values of the isolated compounds were not comparable to those of some NIQs that had shown excellent antiplasmodial activity such as dioncophyllin C (**39**), jozimine A<sub>2</sub> (**34**), and dioncopeltine A (**40**) (IC<sub>50</sub> 0.04 μM, 1.4 nM, and 0.05 μM, respectively). However, the activity of one subfraction (F<sub>2</sub>SF<sub>1</sub>) showed that NIQs with improved activity can still be found in this plant material. Further work will be pursued to identify the additional NIQs from all the active fractions. However, this is often challenging in using the bioassay-guided fractionation process. This is mainly due to the close similarity of structures within the class of NIQs and the number of stereoisomers, making separation into single chemical entities not a trivial task. Another problem is the presence of small quantities of NIQs in the plant material. As the species is yet unidentified, a phytochemical investigation for the isolation of additional NIQs will contribute to the development of NIQ patterns for chemotaxonomic identification purposes.

## Supplementary data

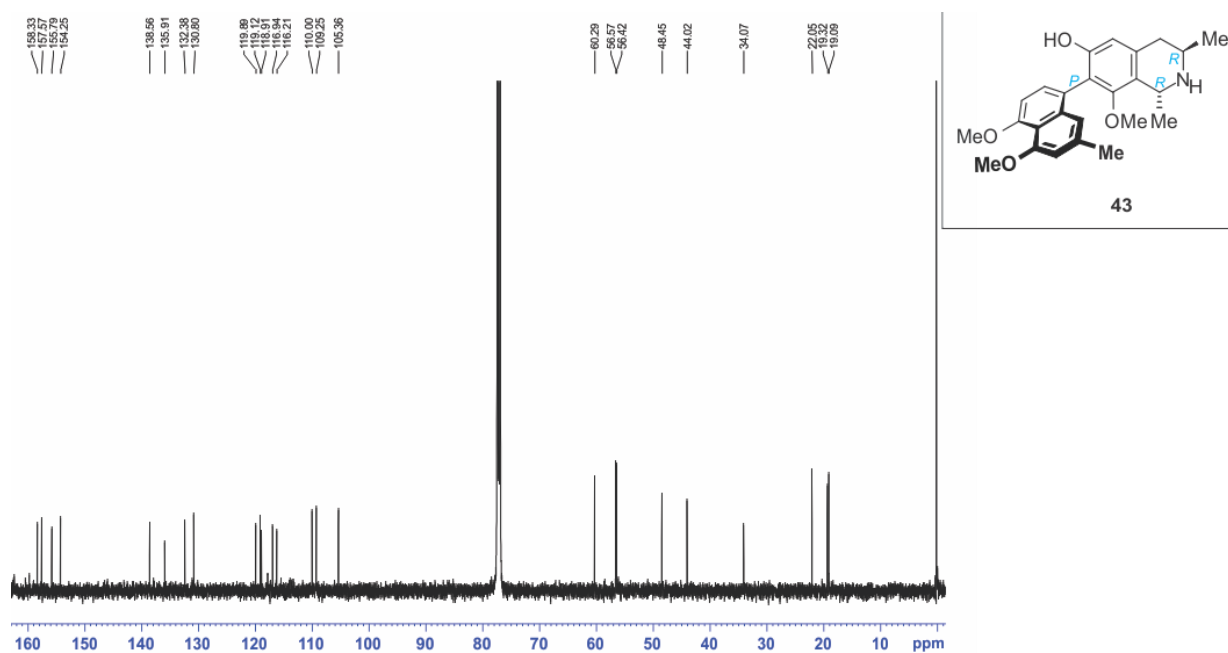


Supplementary data 1:  $^1\text{H}$  NMR spectrum of compound **43** (ealamine A) in  $\text{CDCl}_3$

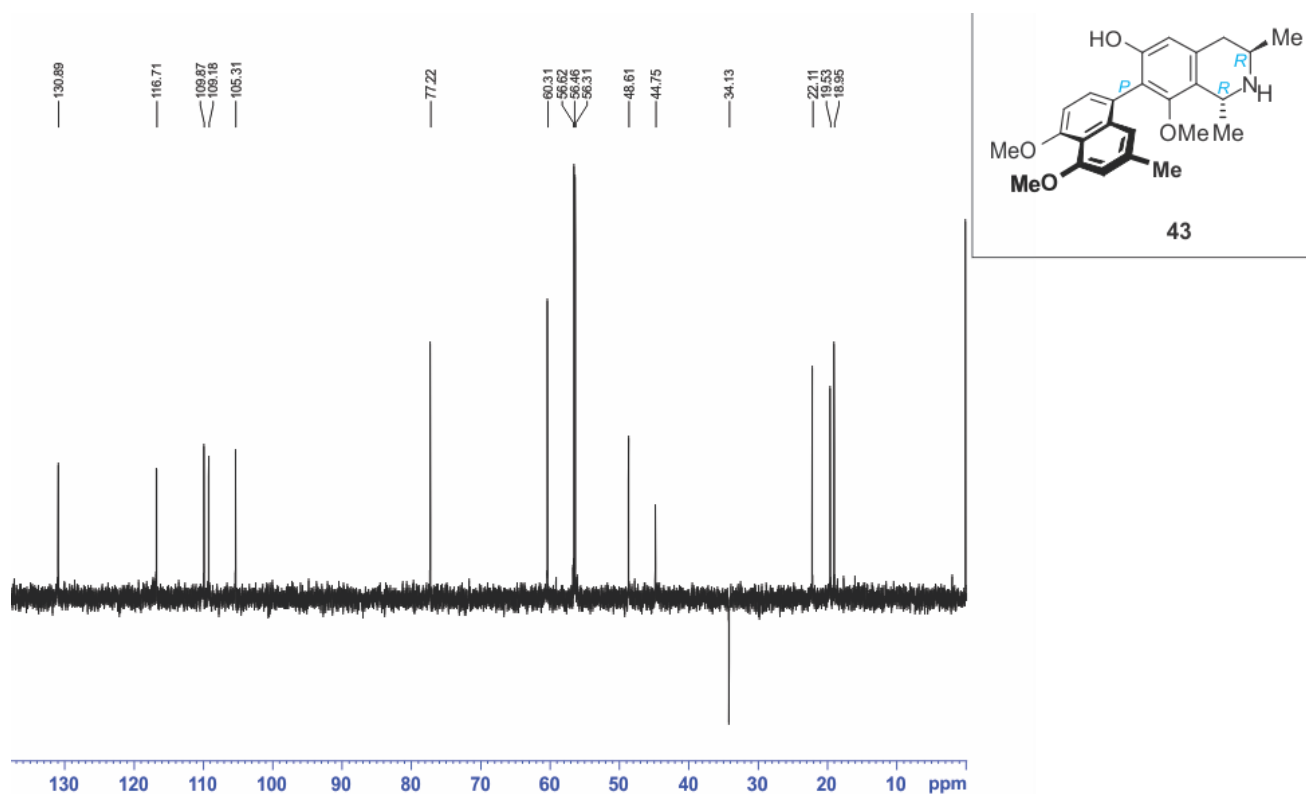


Supplementary data 2: NOESY spectrum of compound **43** (ealamine A) in  $\text{CDCl}_3$

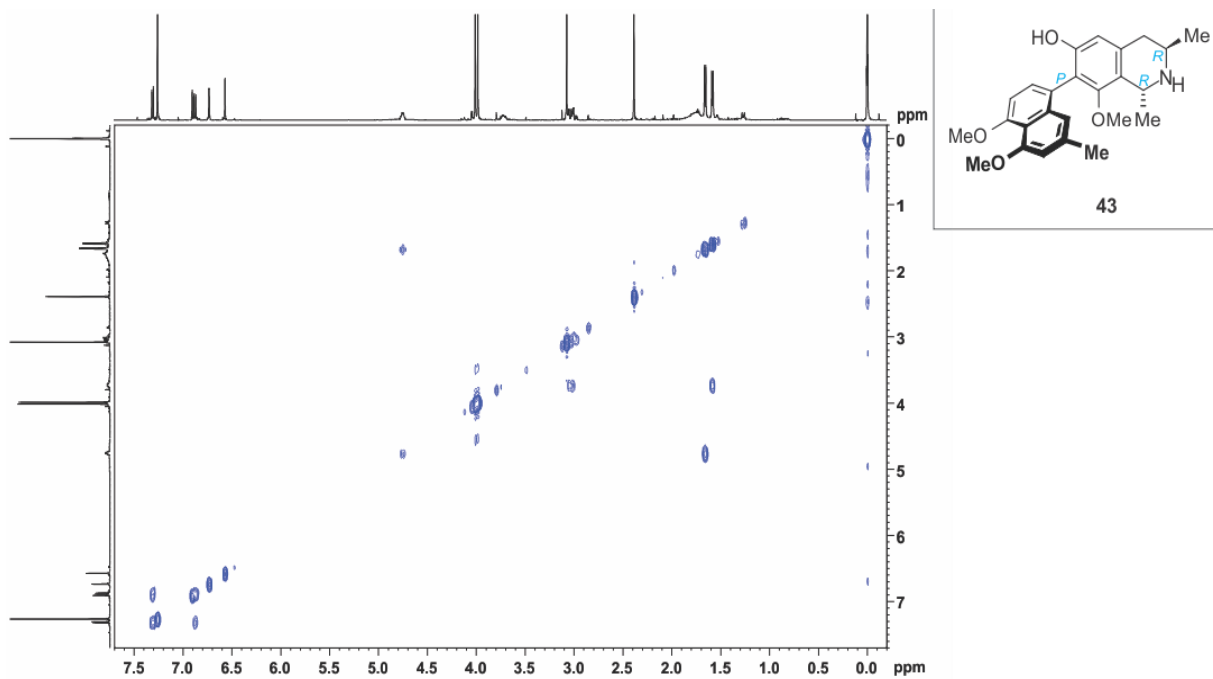




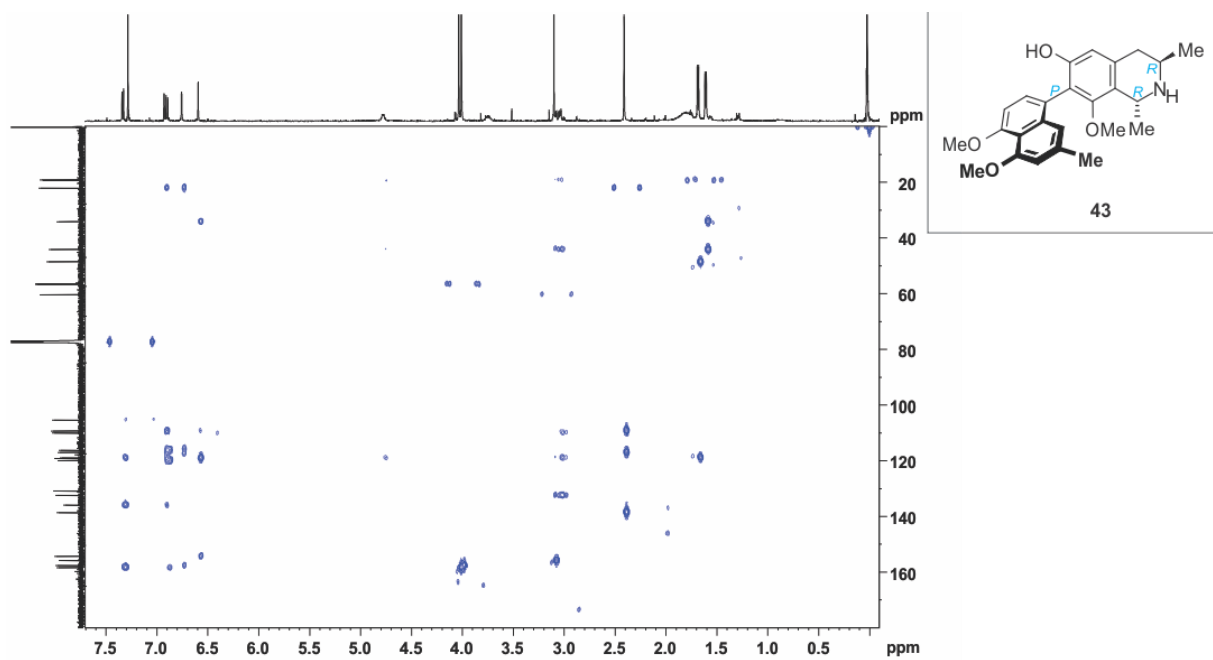
**Supplementary data 3:** <sup>13</sup>C NMR spectrum of compound **43** (ealamine A) in CDCl<sub>3</sub>



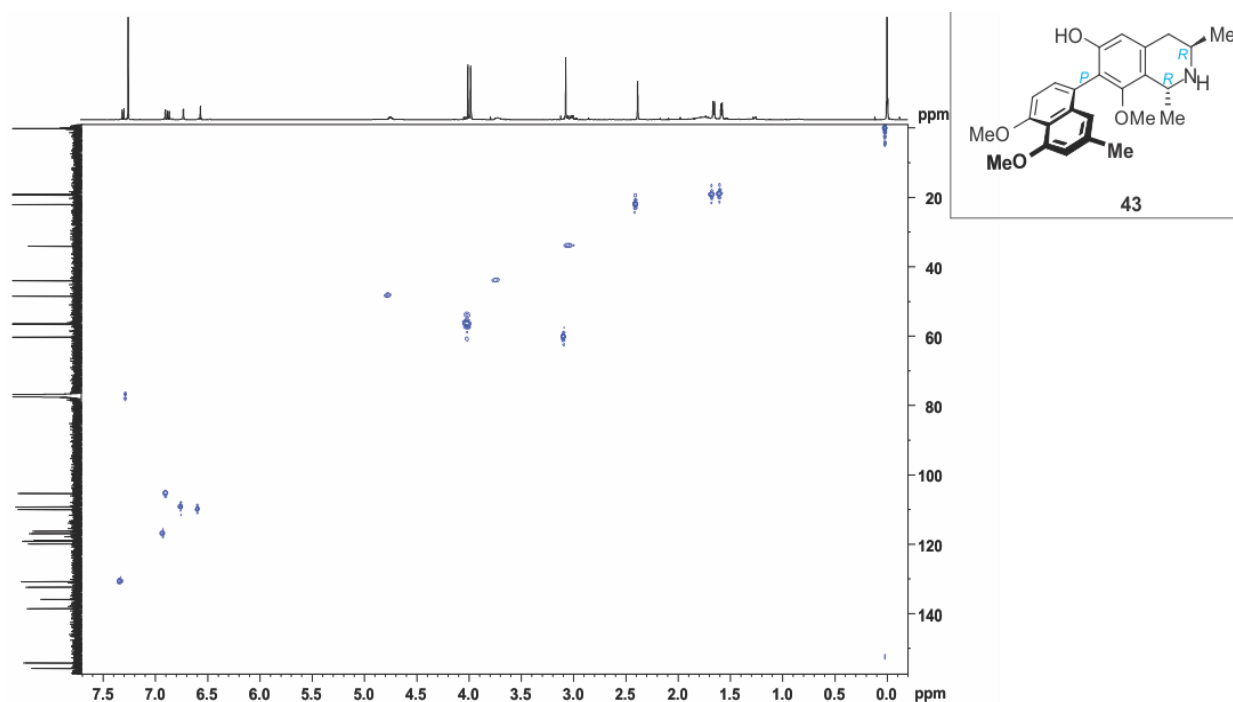
**Supplementary data 4:** Dept 135 spectrum of compound **43** (ealamine A) in CDCl<sub>3</sub>



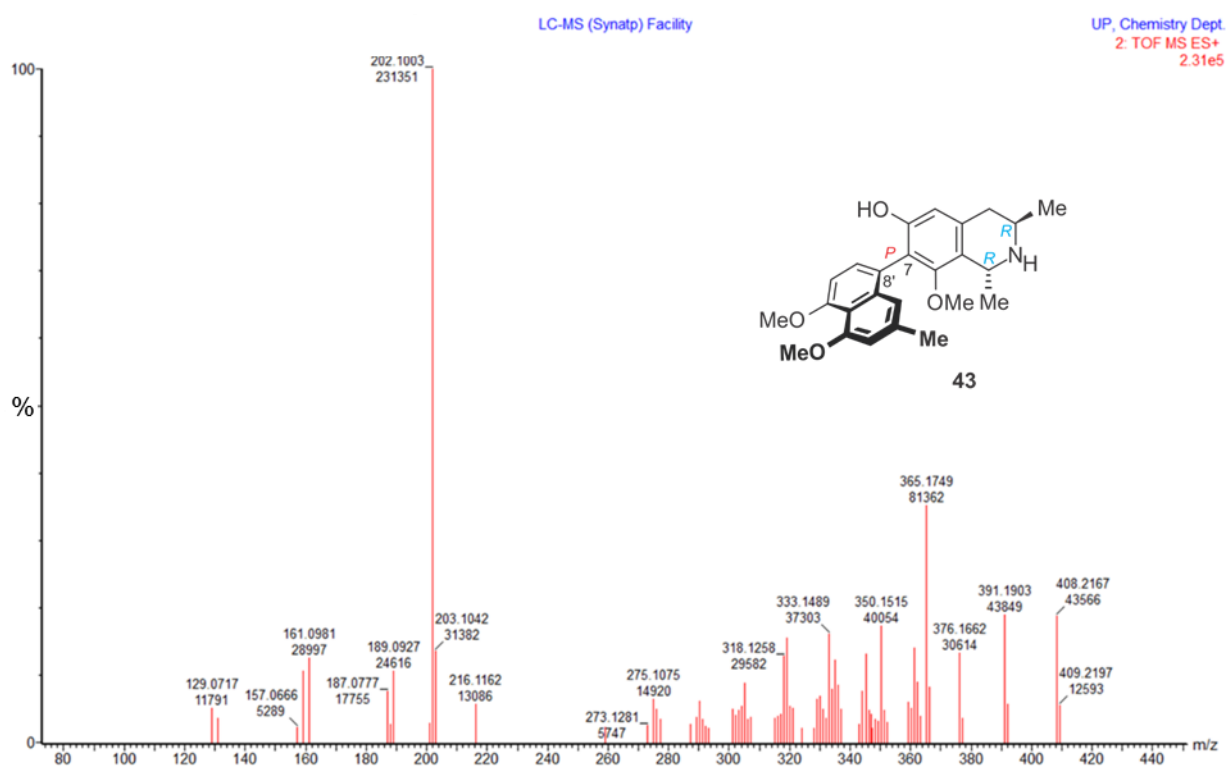
**Supplementary data 5:** COSY spectrum of compound **43** (ealamine A) in CDCl<sub>3</sub>



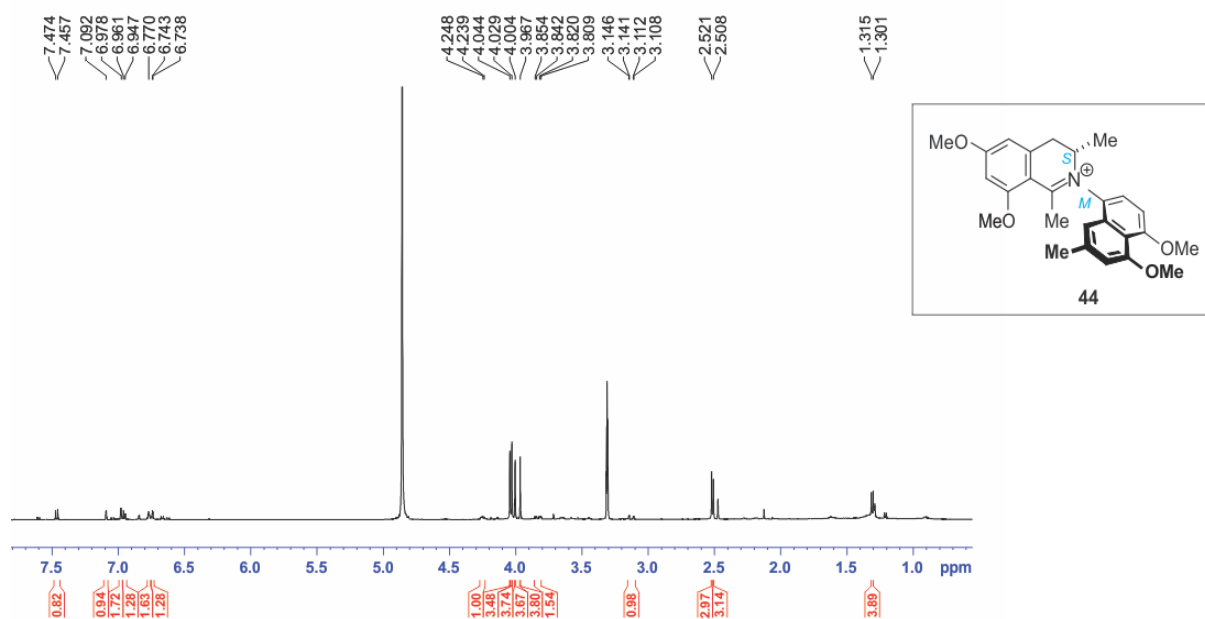
**Supplementary data 6:** HMBC spectrum of compound **43** (ealamine A) in CDCl<sub>3</sub>



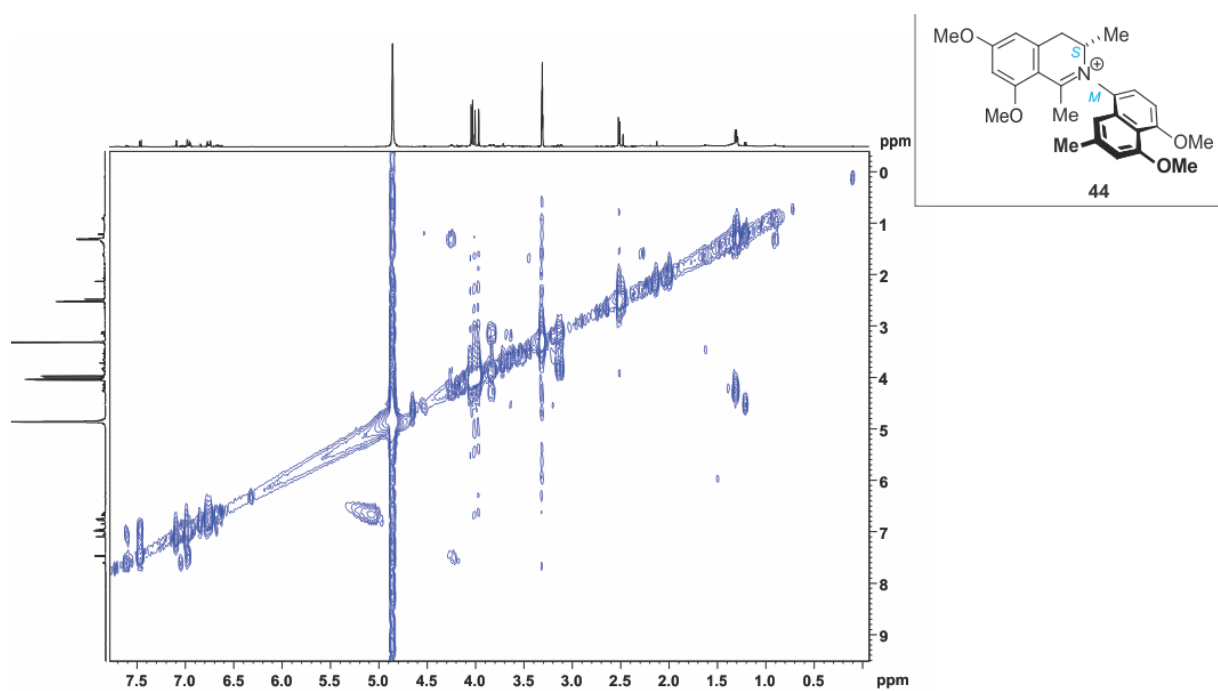
**Supplementary data 7:** HSQC spectrum of compound **43** (ealamine A) in CDCl<sub>3</sub>



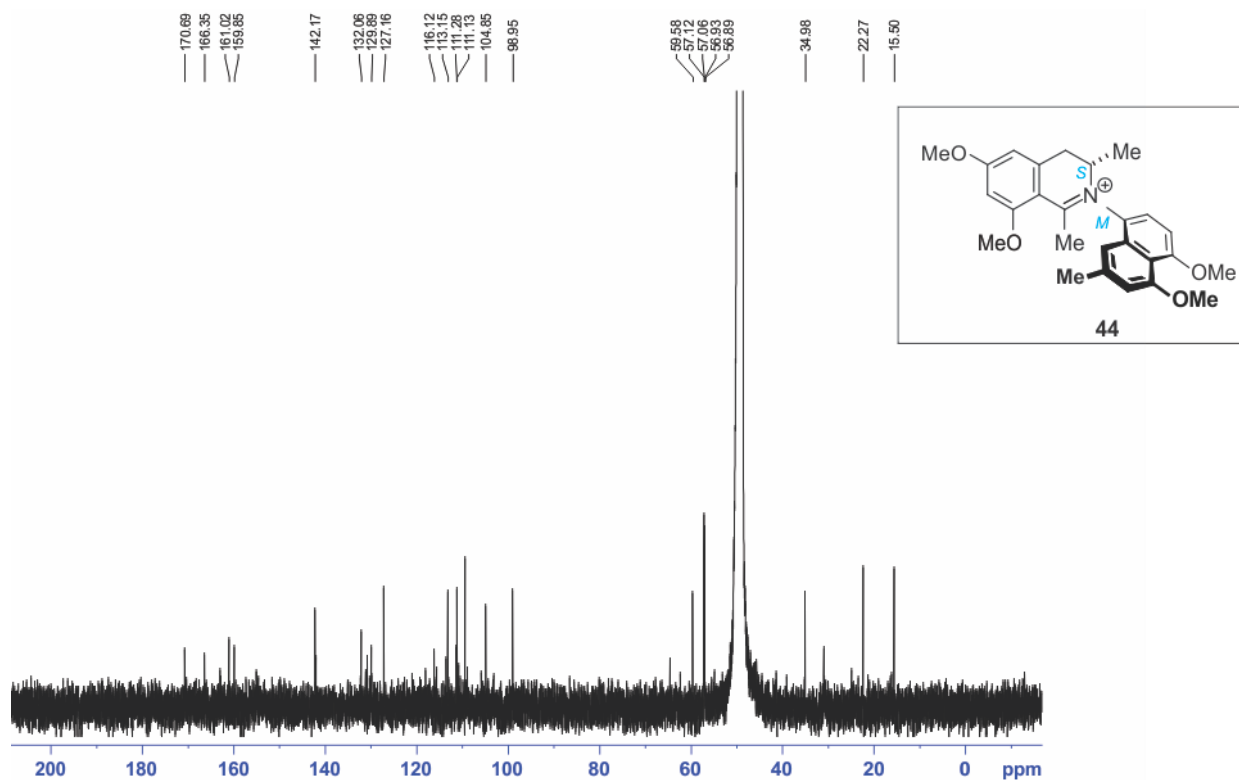
**Supplementary data 8:** MS/MS chromatogram of compound **43** (ealamine A) in the subfraction F<sub>4</sub>SF<sub>5</sub>



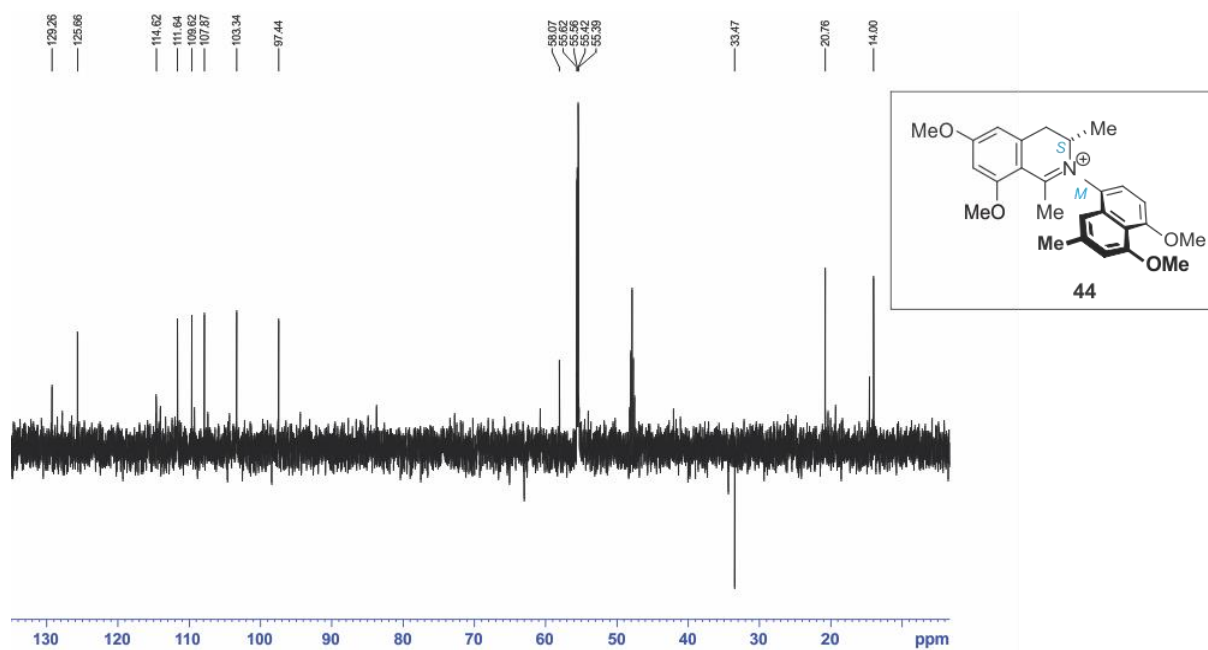
**Supplementary data 9:**  $^1\text{H}$  NMR spectrum of compound **44** (ancistrocladinium A) in  $\text{CD}_3\text{OD}$



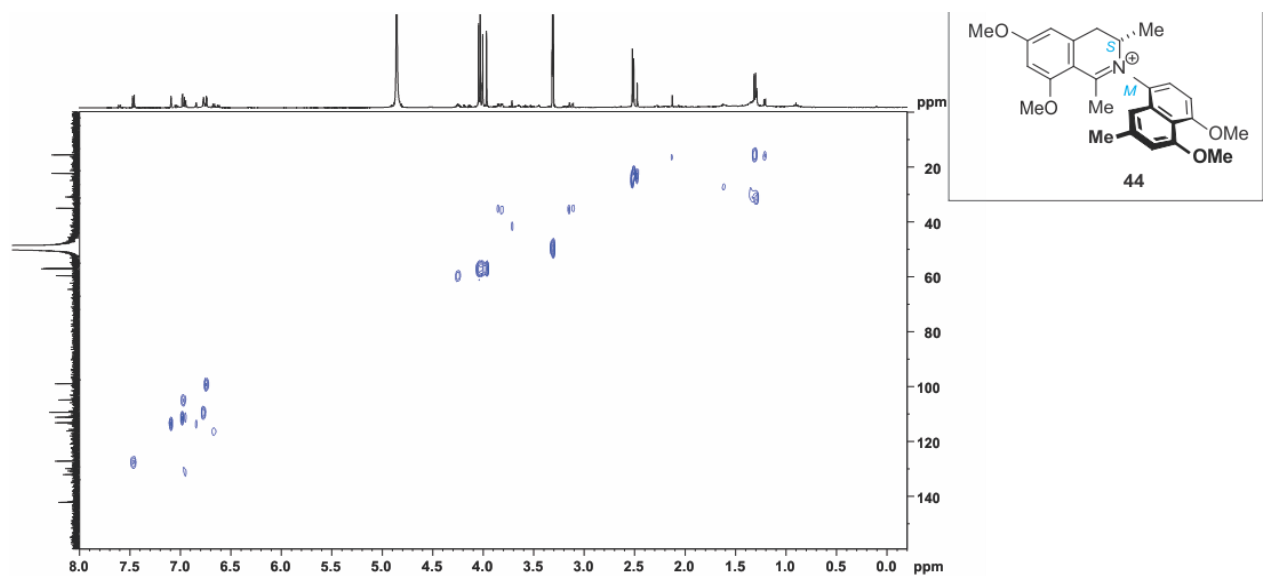
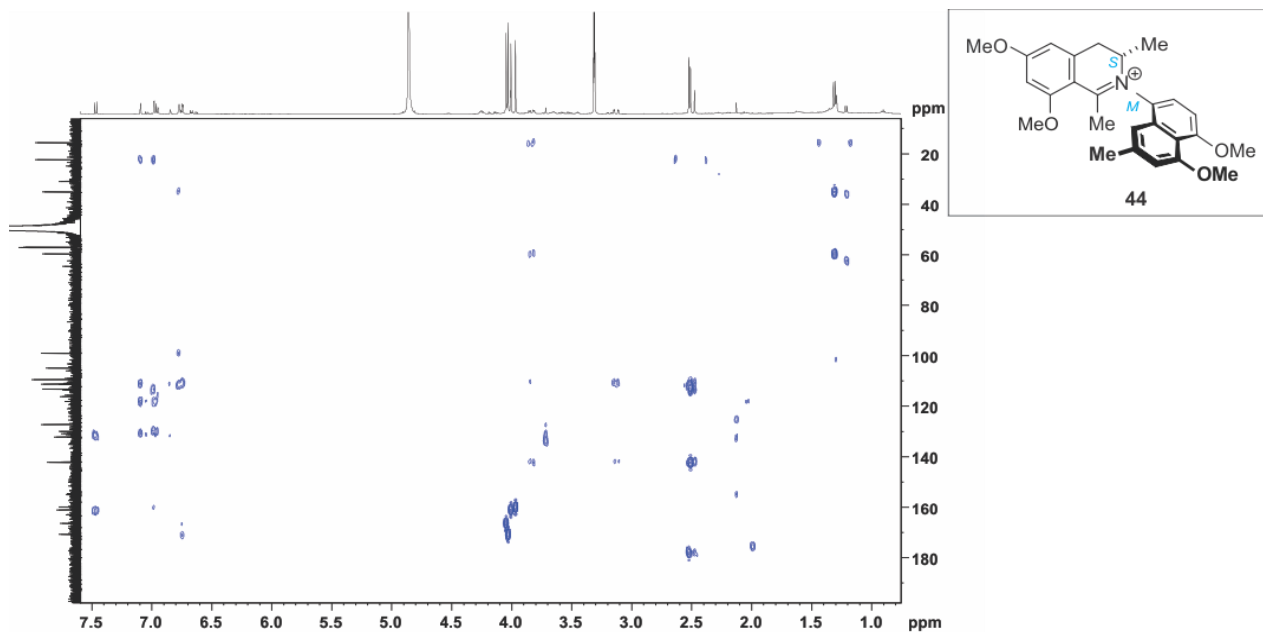
**Supplementary data 10:** COSY spectrum for compound **44** (ancistrocladinium A) in  $\text{CD}_3\text{OD}$

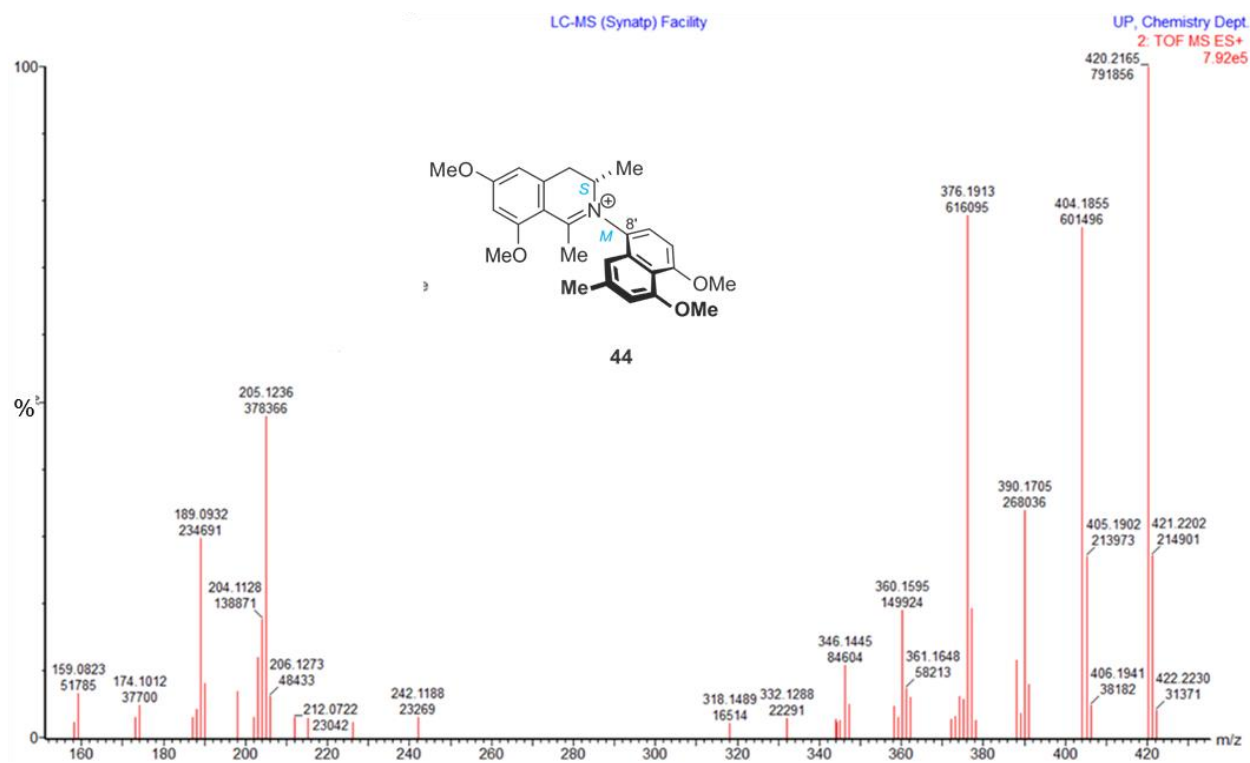


**Supplementary data 11:** <sup>13</sup>C NMR spectrum of compound **44** (ancistrocladinium A) in CD<sub>3</sub>OD

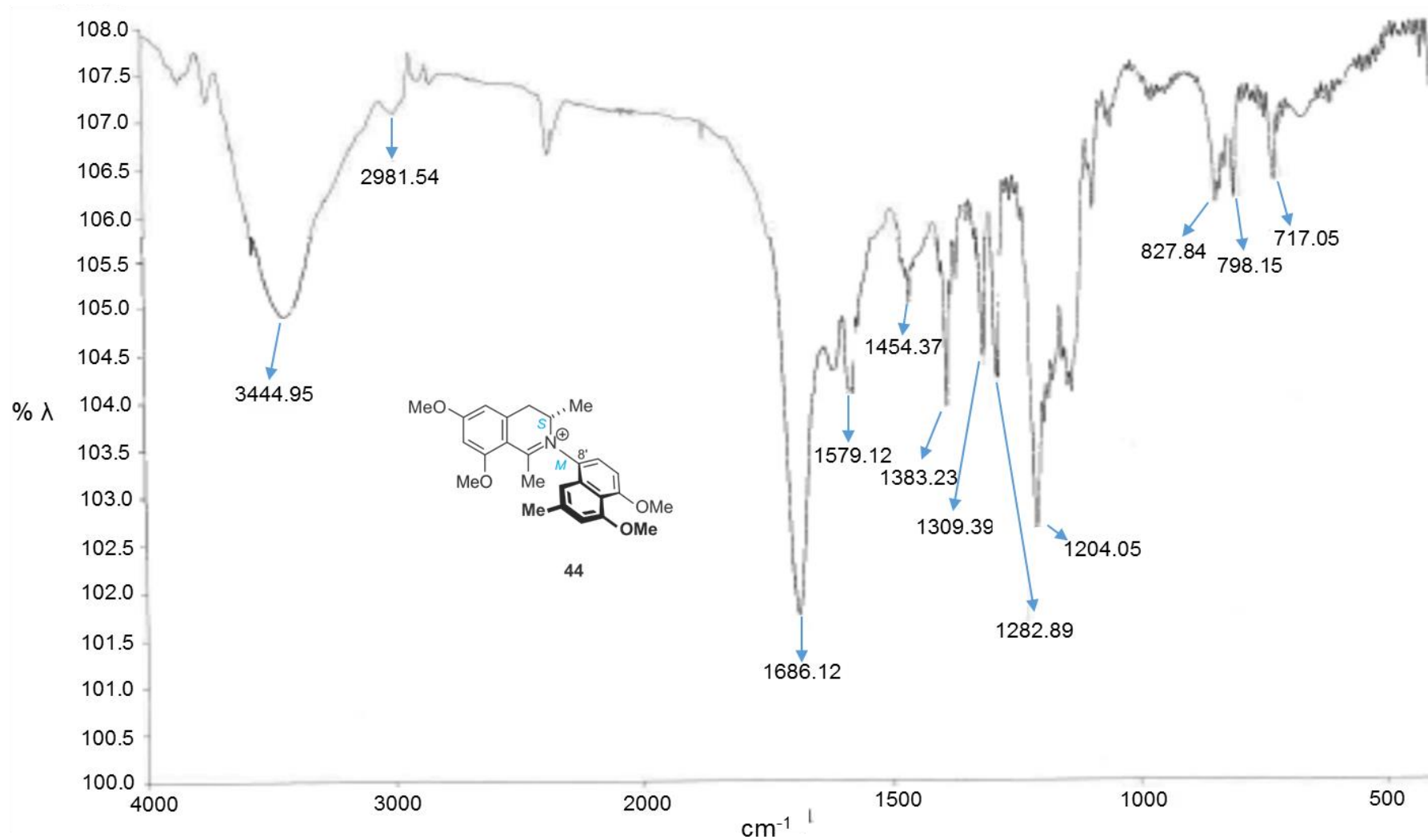


**Supplementary data 12:** Dept 135 spectrum of compound **44** (ancistrocladinium A) in CD<sub>3</sub>OD



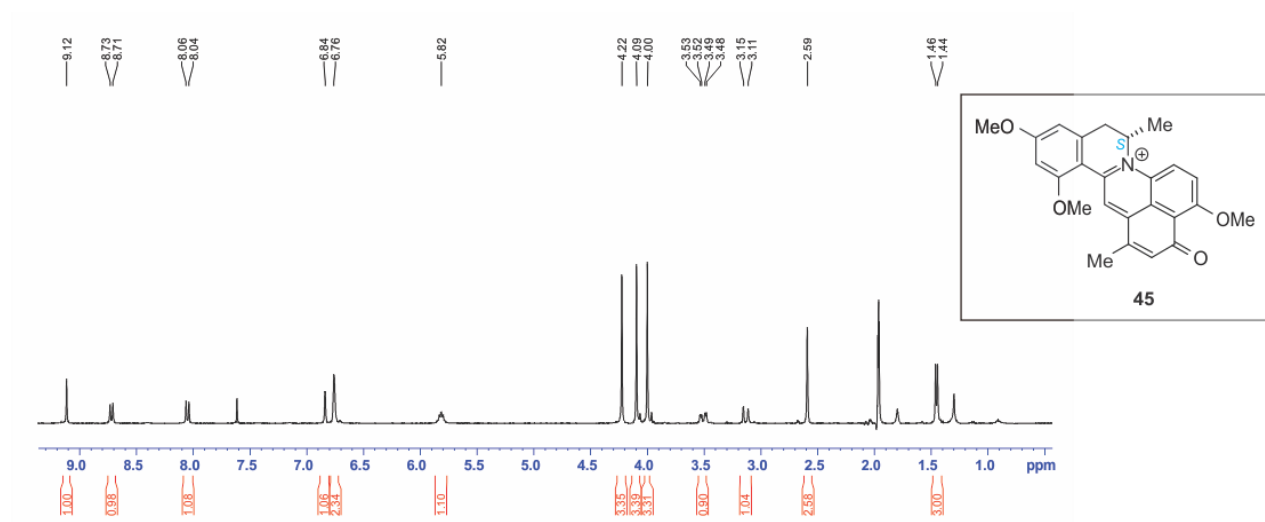


**Supplementary data 15: MS/MS chromatogram of compound 44 (ancistrocladinium A)**

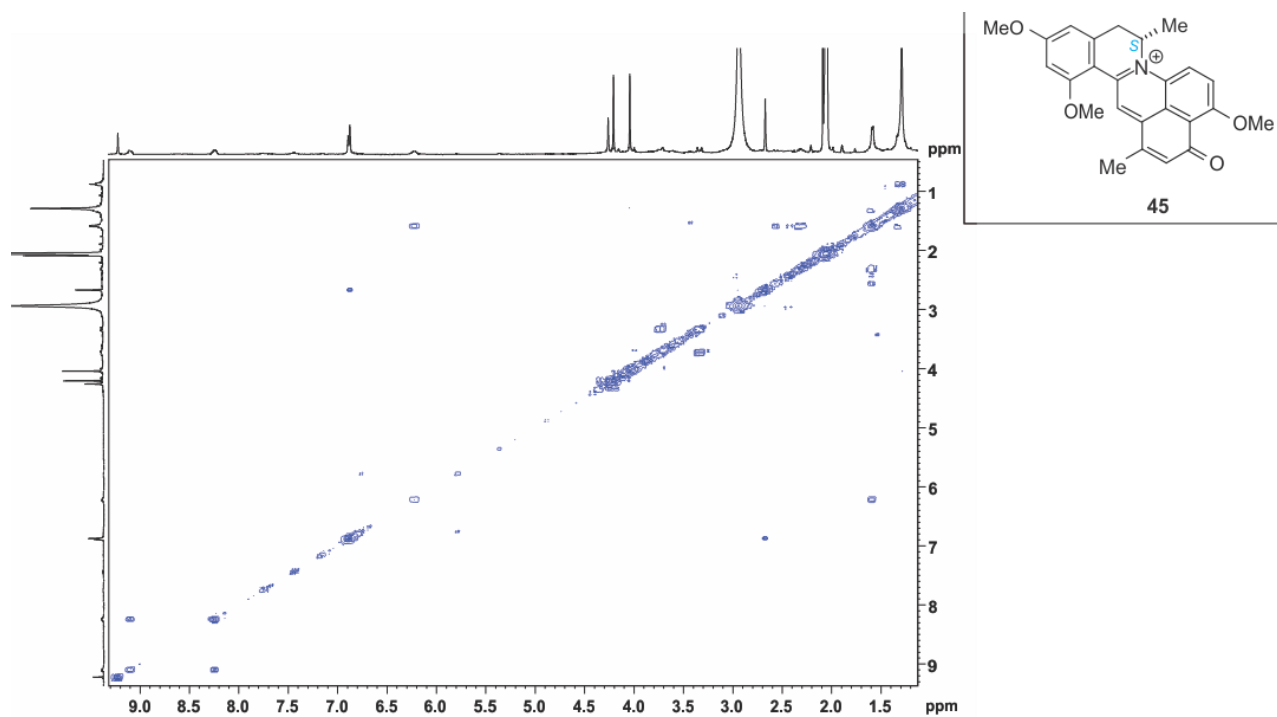


**Supplementary data 16:** IR spectrum of compound **44** (ancistrocladinium A)

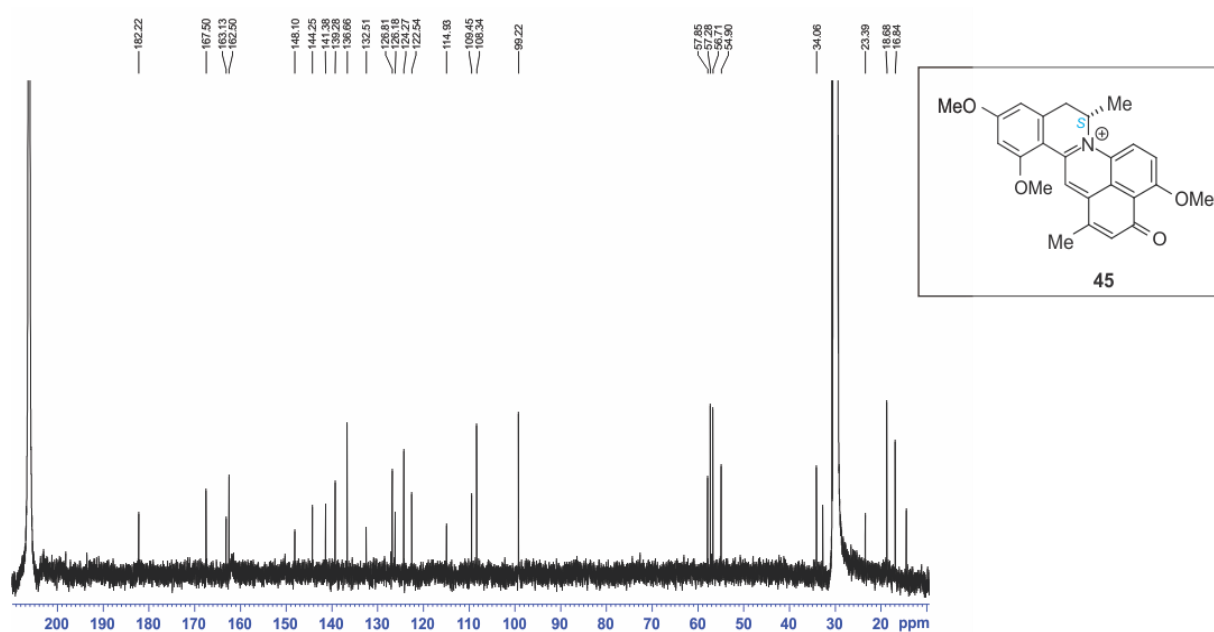




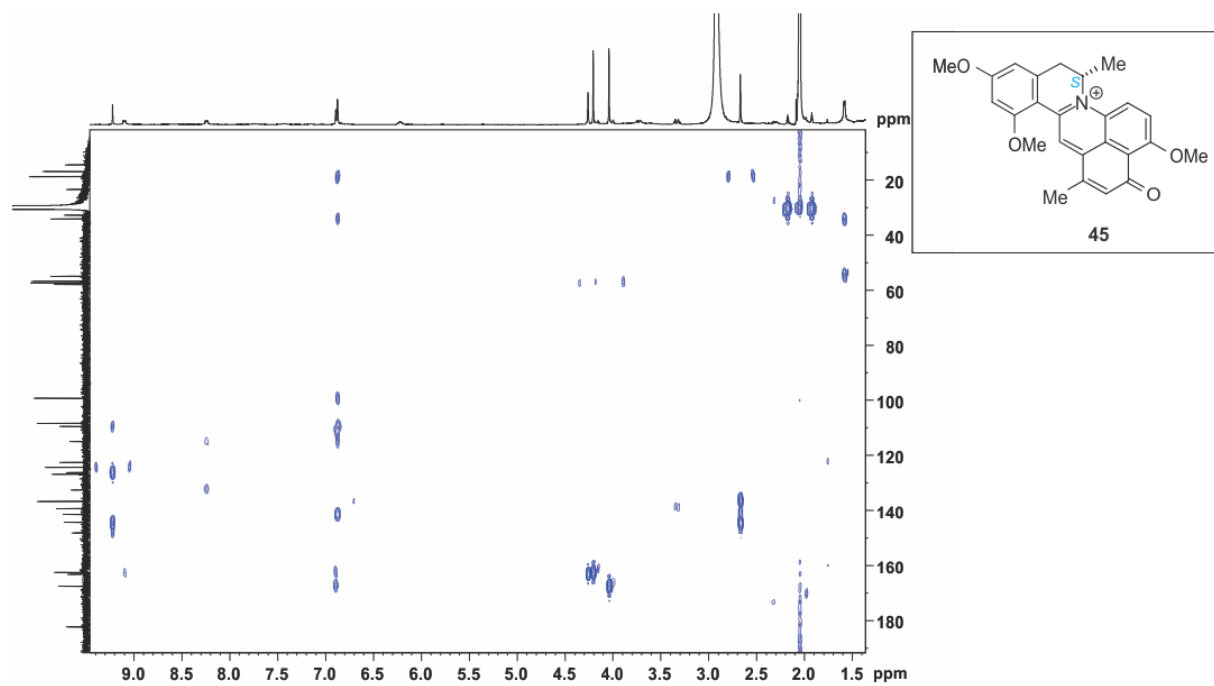
**Supplementary data 17:** <sup>1</sup>H NMR spectrum of compound **45** (ancistrocyclinone A) in CD<sub>3</sub>COCD<sub>3</sub> (solvent-suppression mode)



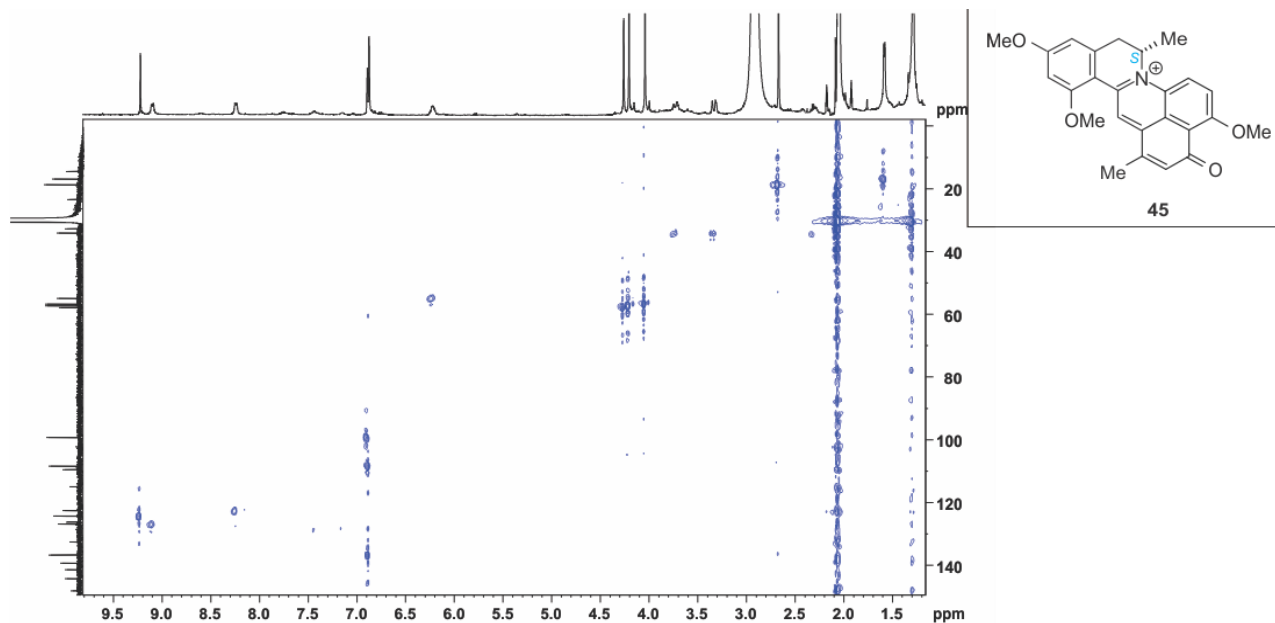
**Supplementary data 18:** COSY spectrum of compound **45** (ancistrocyclinone A) in CD<sub>3</sub>COCD<sub>3</sub>



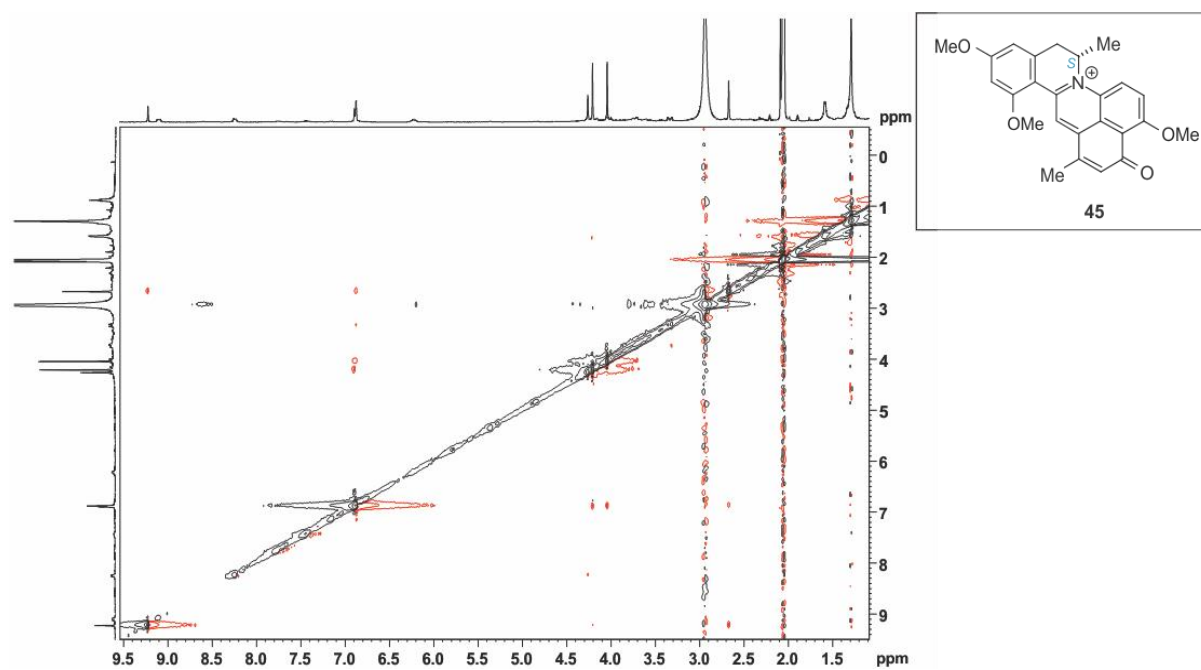
**Supplementary data 19:**  $^{13}\text{C}$  NMR spectrum of compound **45** (ancistrocyclinone A) in  $\text{CD}_3\text{COCD}_3$



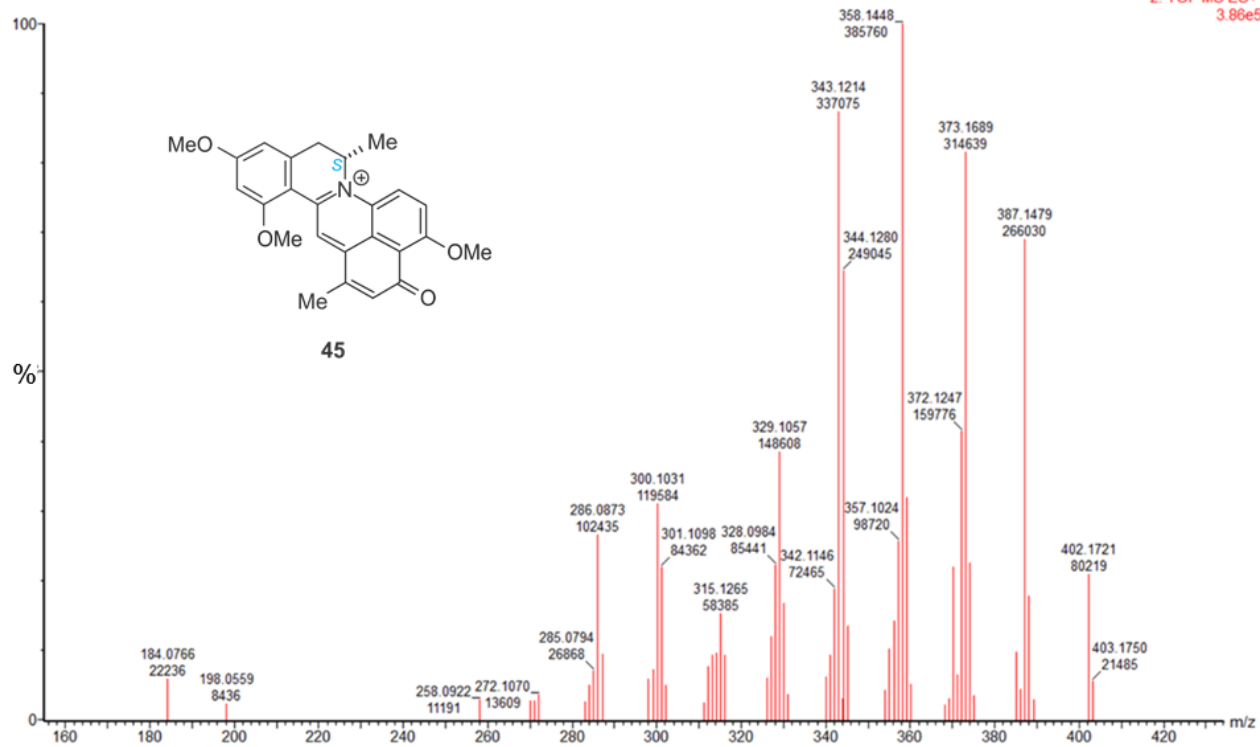
**Supplementary data 20:** HMBC spectrum of compound **45** (ancistrocyclinone A) in  $\text{CD}_3\text{COCD}_3$



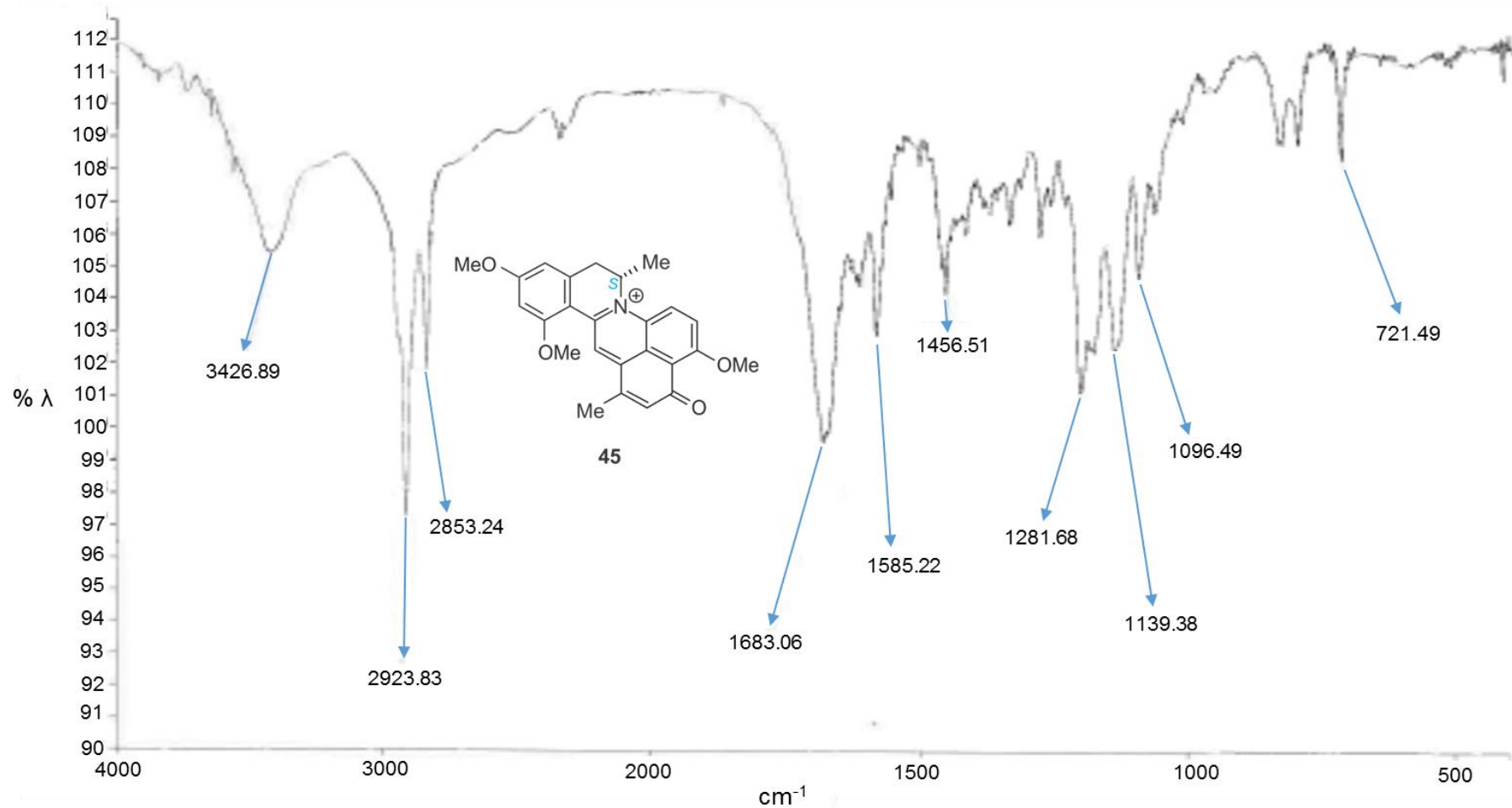
**Supplementary data 21:** HSQC spectrum of compound **45** (ancistrocyclinone A) in CD<sub>3</sub>COCD<sub>3</sub>



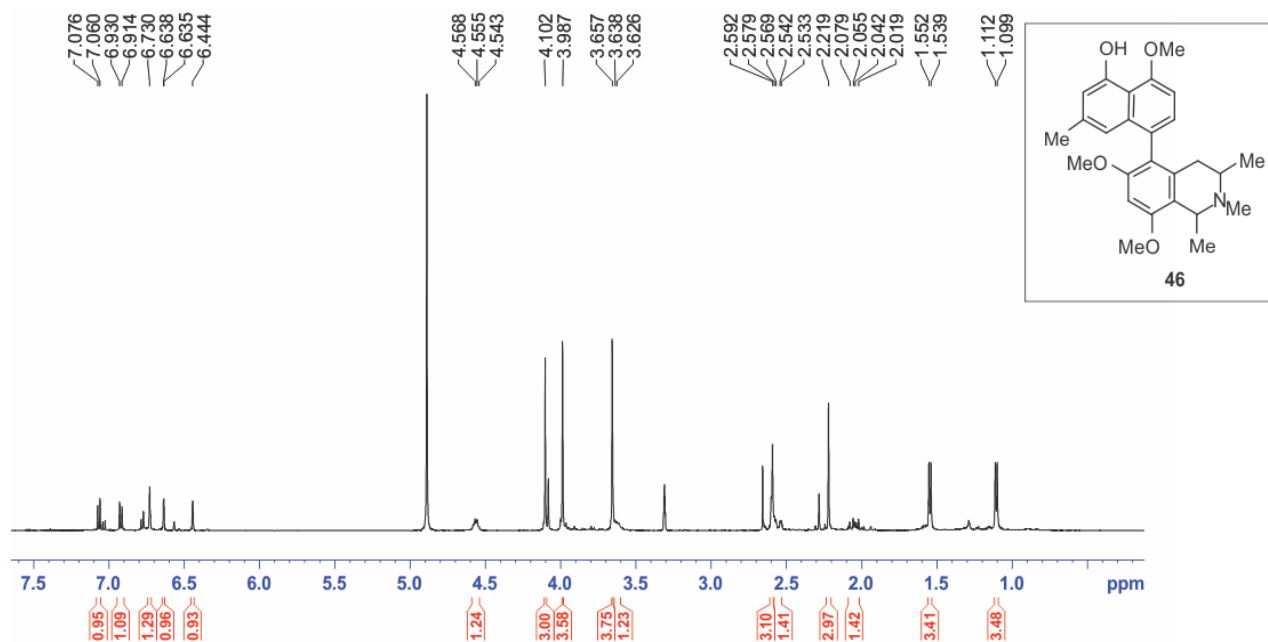
**Supplementary data 22:** NOESY spectrum of compound **45** (ancistrocyclinone A) in CD<sub>3</sub>COCD<sub>3</sub>



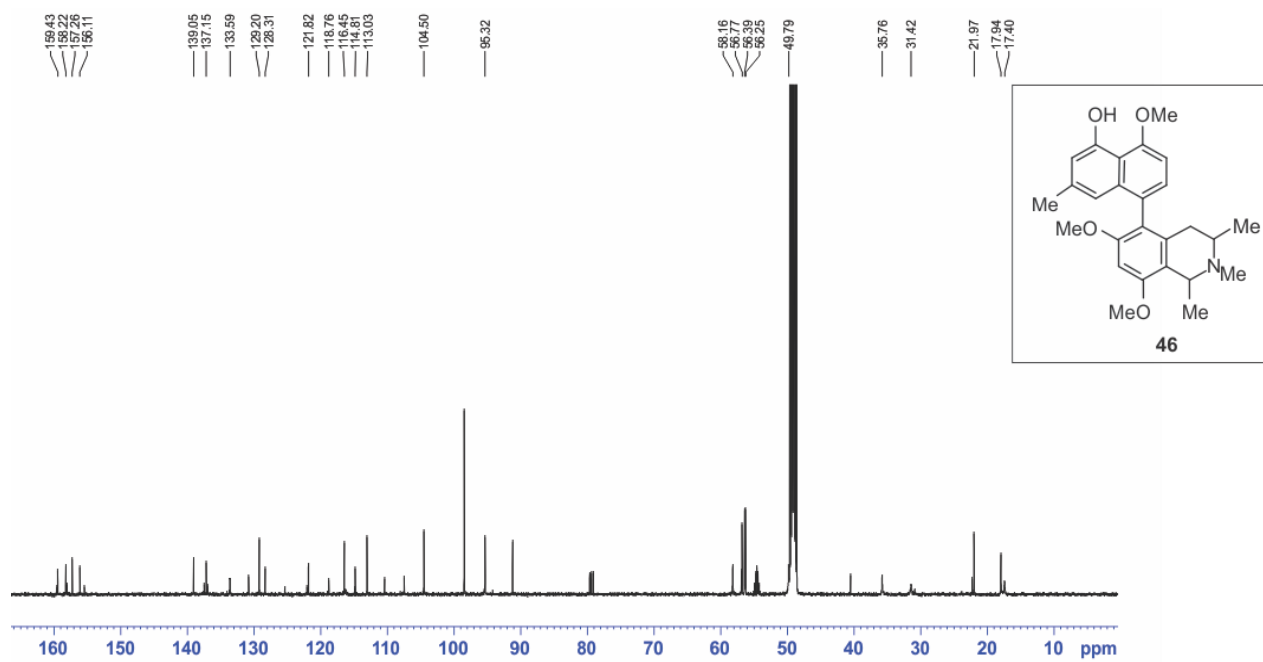
**Supplementary data 23: MS/MS chromatogram of compound 45 (ancistrocycalinone A)**



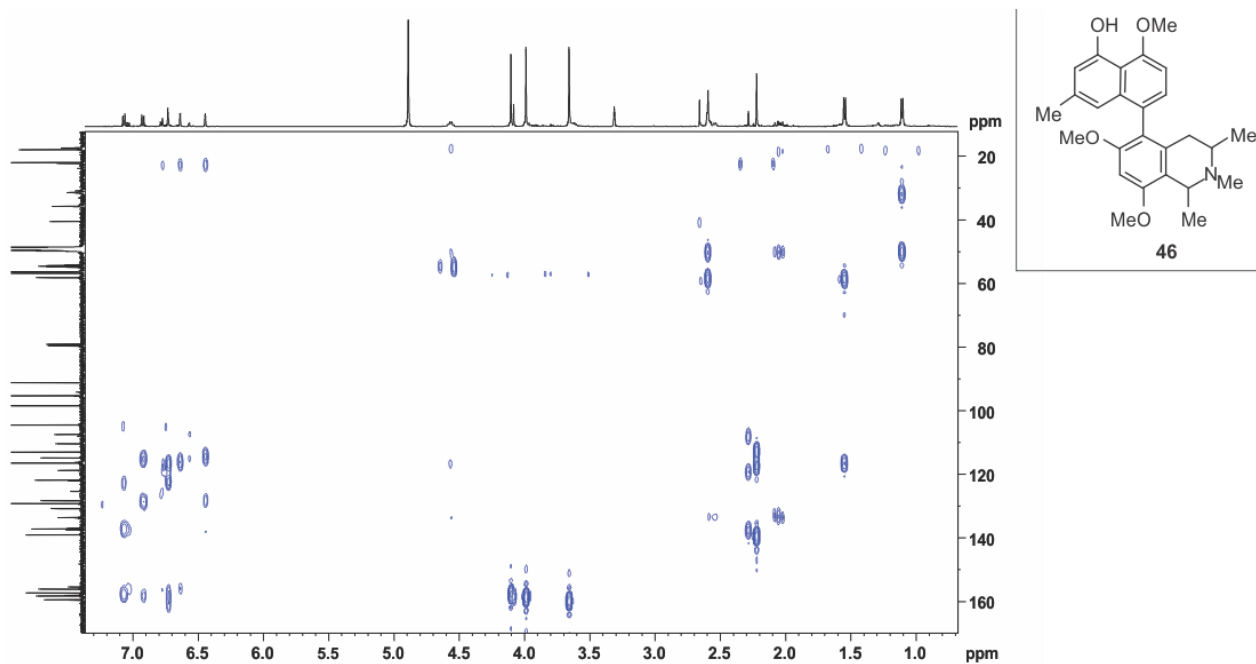
**Supplementary data 24:** IR spectrum of compound **45** (ancistrocyclinone A)



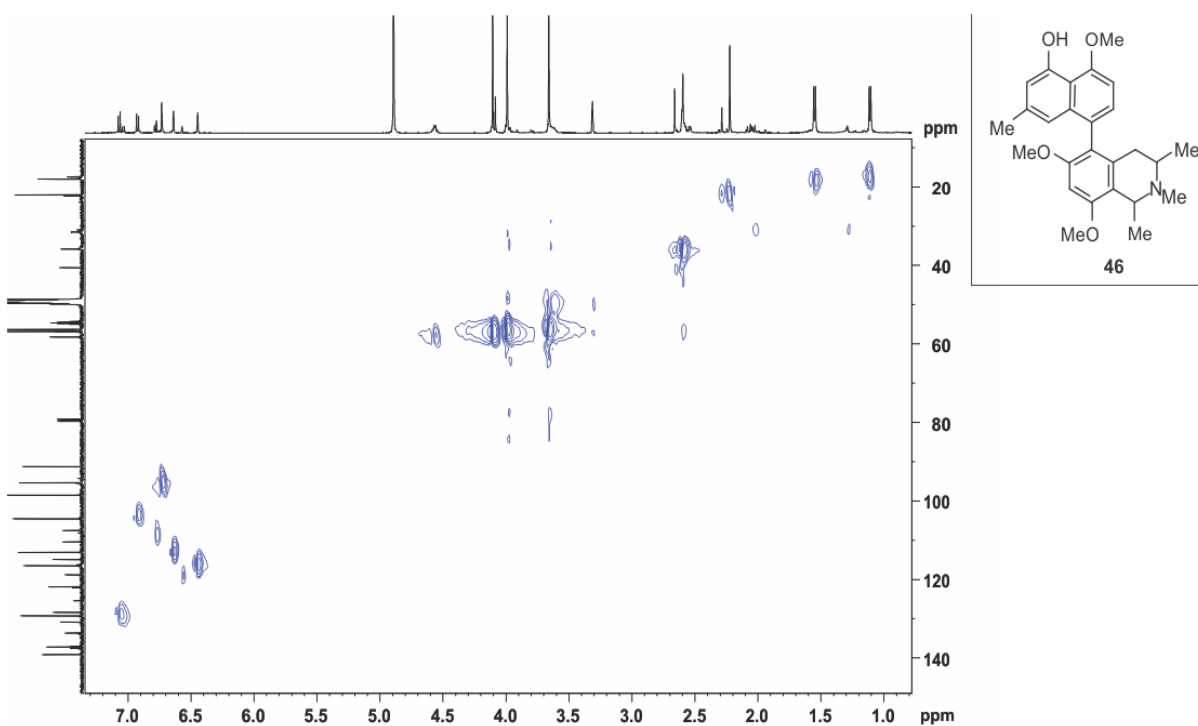
**Supplementary data 25:** <sup>1</sup>H NMR spectrum of compound **46** in CD<sub>3</sub>OD



**Supplementary data 26:** <sup>13</sup>C NMR spectrum of compound **46** in CD<sub>3</sub>OD



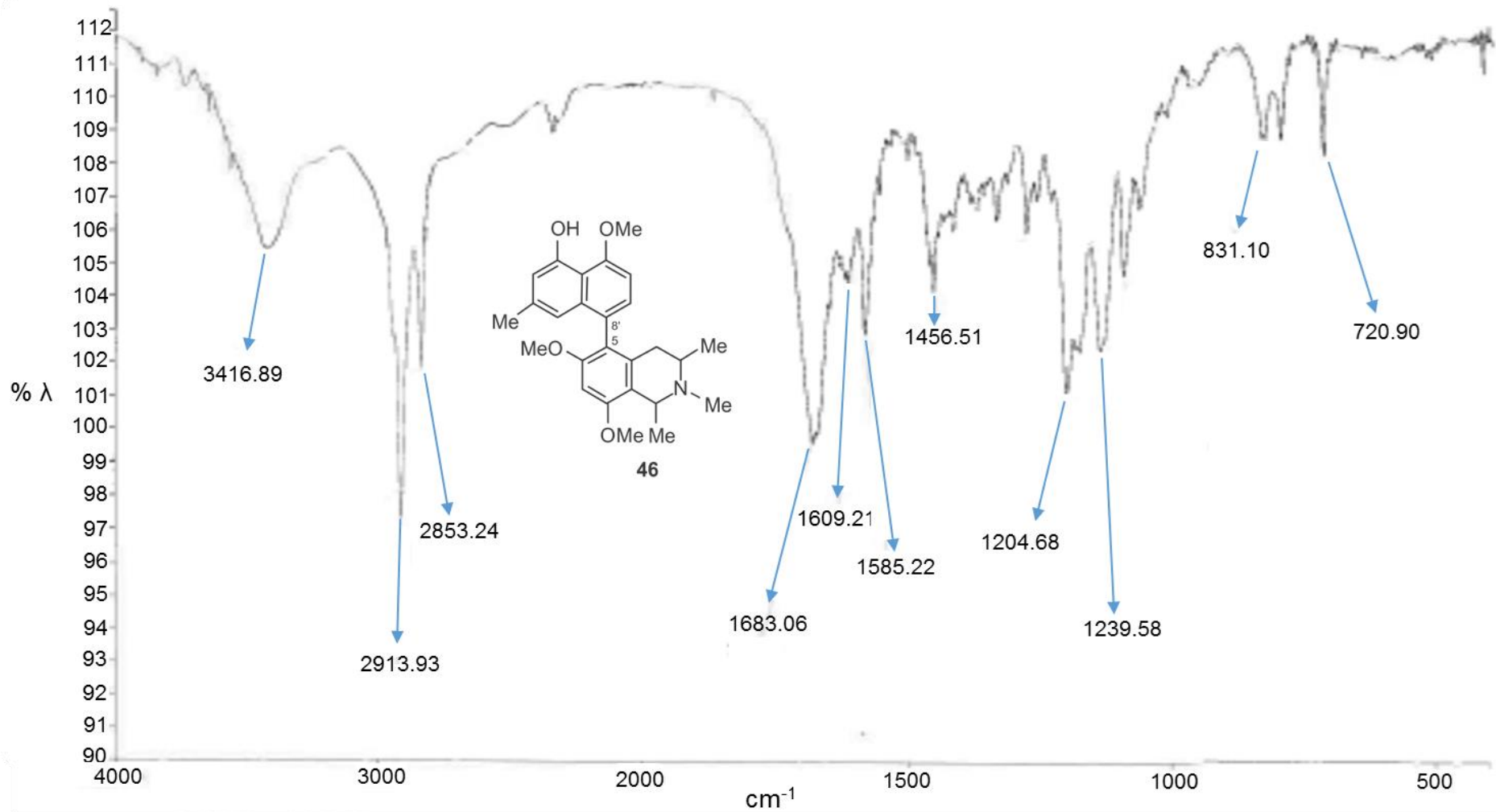
**Supplementary data 27: HMBC spectrum of compound **46** in CD<sub>3</sub>OD**



**Supplementary data 28: HSQC spectrum of compound **46** in CD<sub>3</sub>OD**







Supplementary data 31: IR spectrum of compound 46